THESE DE DOCTORAT DE

Par

Mirian Tiaki KANEIWA KUBO

Thermal process of fruit juices using microwaves: multiphysics modeling and enzyme inactivation

University of São Paulo
"Luiz de Queiroz" College of Agriculture

Thermal process of fruit juices using microwaves: multiphysics modeling and enzyme inactivation

Mirian Tiaki Kaneiwa Kubo

Thesis submitted in fulfillment of the requirements for the joint degree of Doctor in Science. Areas Process and Bioprocess Engineering at ONIRIS, and Food Science and Technology at ESALQ/USP

Nantes
2018

Mirian Tiaki Kaneiwa Kubo
Food Engineer

Thermal process of fruit juices using microwaves: multiphysics modeling and enzyme inactivation

Advisors:
Prof. Dr. **PEDRO ESTEVES DUARTE AUGUSTO**
Prof. Dr. **LIONEL BOILLEREAUX**

Thesis submitted in fulfillment of the requirements for the joint degree of Doctor in Science. Areas Process and Bioprocess Engineering at ONIRIS, and Food Science and Technology at ESALQ/USP

Nantes
2018

2

ACKNOWLEDGEMENTS

I would like to express my sincere gratitude to those who have been part of my journey towards a Doctoral degree. The execution of this work was only possible thanks to several people who, directly or indirectly, helped and supported me.

First, I express my gratefulness to my advisor Prof. Lionel Boillereaux for providing me good autonomy to conduct this research and helping me especially with the Neural Networks and paperwork. I would like to extend my sincere appreciation to Prof. Sébastien Curet for his support especially with COMSOL and with the microwave devices. I would also like to thank Prof. Pedro Augusto for his efforts especially with the inactivation kinetics and paperwork for the double degree, his guidance and his encouragement to think big and work hard since 2005.

I am grateful to the reviewers Prof. Hélène Simonin et Prof. João Borges Laurindo for their time and constructive criticism to examine the thesis. I would also like to thank the examination committee members Prof. Denis Flick and Prof. Francis Courtois for accepting to be part of the jury.

I gratefully acknowledge CNPq for providing me financial support (PhD scholarship, process number 233347/2014-3) and for funding the project number 401004/2014–7.

I also acknowledge FAPESP for the financial help to purchase commercial enzymes during my stay in Brazil (project number 2014/16998-3).

I would like to thank Prof. Marie de Lamballerie for her time to be a member of my *Comité de Suivi de Thèse*.

I would like to thank *Service des Relations Internationales* and *DRED (Direction de la Recherche et des Etudes Doctorales)*, more particularly to Christina Péréon who helped me with the paperwork for the visa and *titre de séjour*.

I would like to thank *Serviço de Pós Graduação* (ESALQ/USP) for the support and guidelines related to the double diploma.

I would also like to express my sincere appreciation to all the members of GPA - ONIRIS (professors, PhD and master students, secretariat staff, engineers, laboratory technicians, interns, temporary employees) for creating a friendly atmosphere. Special thanks are due to

"Prediction is very difficult, especially if it is about the future"

Niels Henrik David Bohr, Nobel laureate in Physics

TABLE OF CONTENTS

ABSTRACT

Thermal process of fruit juices using microwaves: multiphysics modeling and enzyme inactivation

This work aims at studying the use of microwave heating for enzyme inactivation in fruit juices by means of numerical and experimental approaches. In the first part, a study on the dielectric properties of model fruit juices is conducted, evidencing their high dependence on the temperature, frequency and composition of the product. Then in the second part, the inactivation of peroxidase is studied using conventional heating and the data are fitted by a first order kinetic model. In the third and main part of this work, a three-dimensional finite element model is developed to simulate the microwave heating of juices, coupling electromagnetics, heat transfer and fluid flow as well as the peroxidase inactivation kinetics previously determined. As a result, spatial temperature distribution, flow pattern and peroxidase inactivation are obtained. The model is experimentally validated and good agreement is observed, confirming the relevance of the approach. Finally, in the last part, the potential peroxidase reactivations after conventional and microwave heating are assessed and compared. Also, the possible existence of non-thermal effects of microwaves is discussed thanks to additional experimentations. In conclusion, this work shows the large interest of computer simulation as a tool for understanding the multiphysics process of microwave heating for enzyme inactivation, which can be particularly interesting for further design of optimized microwave processing.

Keywords: Microwave heating; Enzyme inactivation; Dielectric properties; Modeling; Peroxidase.

RÉSUMÉ

Traitement thermique micro-onde de jus de fruits: modélisation multiphysique et inactivation enzymatique

Ce travail vise à étudier l'intérêt du chauffage micro-ondes pour l'inactivation des enzymes dans les jus de fruits, à travers des approches numériques et aussi expérimentales. En premier lieu, une étude sur les propriétés diélectriques des jus de fruit modèles est menée, démontrant leur forte sensibilité à la température, à la fréquence et à la composition du produit. Dans une seconde partie, l'inactivation de la peroxydase est étudiée par chauffage conventionnel et les données sont ajustées par un modèle cinétique du premier ordre. Dans la troisième et principale partie de ce travail, un modèle tridimensionnel, résolu par éléments finis, est proposé pour simuler le chauffage par micro-ondes du jus, en couplant électromagnétisme, transfert de chaleur et écoulement, avec la cinétique d'inactivation de la peroxydase précédemment déterminée. Cette simulation permet de prédire la distribution spatiale de la température, le profil d'écoulement et l'inactivation de la peroxydase. L'accord entre le modèle et les expériences est très satisfaisant, ce qui confirme la pertinence de l'approche. Dans la dernière partie, les réactivations de la peroxydase après chauffage conventionnel et micro-ondes sont évaluées et comparées. Enfin, l'éventuelle existence d'effets non thermiques des micro-ondes est discutée via des expériences additionnelles. En conclusion, ces travaux montrent tout l'intérêt de la simulation numérique comme outil de compréhension du processus multiphysique du chauffage par micro-ondes pour l'inactivation des enzymes, ce qui peut être particulièrement intéressant pour la conception et l'optimisation de traitements micro-ondes.

Mots clés: Chauffage micro-ondes; Inactivation enzymatique; Propriétés diélectriques; Modélisation; Peroxydase.

RESUMO

Processamento térmico de sucos de frutas utilizando micro-ondas: modelagem multifísica e inativação enzimática

Este trabalho tem como objetivo estudar o uso do aquecimento por microondas para inativação enzimática em sucos de frutas por meio de abordagens numéricas e experimentais. Na primeira parte, é realizado um estudo sobre as propriedades dielétricas de sucos de frutas modelos, evidenciando sua alta dependência em relação à temperatura, à freqüência e à composição do produto. Em seguida, na segunda parte, a inativação da peroxidase é estudada usando aquecimento convencional e os dados são ajustados por um modelo cinético de primeira ordem. Na terceira e principal parte deste trabalho, um modelo tridimensional usando o método de elementos finitos é desenvolvido para simular o aquecimento por micro-ondas de sucos, acoplando eletromagnetismo, transferência de calor e dinâmica de fluidos, bem como a cinética de inativação de peroxidase previamente determinada. Como resultado, a distribuição espacial de temperatura, os movimentos do fluido e a inativação da peroxidase são obtidos. O modelo é validado experimentalmente e boa concordância é observada, confirmando a relevância da abordagem. Finalmente, na última parte, as potenciais reativações da peroxidase após aquecimento convencional e microondas são avaliadas e comparadas. Além disso, a possível existência de efeitos não térmicos de microondas é discutida graças a experimentos adicionais. Em conclusão, este trabalho mostra o grande interesse da simulação computacional como uma ferramenta para entender o processo multifísico de aquecimento por micro-ondas para a inativação enzimática, que pode ser particularmente interessante para futuro dimensionamento de um processo por micro-ondas otimizado.

RÉSUMÉ SUBSTANTIEL

Traitement thermique micro-onde de jus de fruits: modélisation multiphysique et inactivation enzymatique

L'un des principaux défis de l'industrie des jus de fruit est de parvenir à l'inactivation enzymatique sans nuire aux aspects sensoriels et nutritionnels du produit. Dans la recherche de procédés qui minimisent ces dommages, le chauffage par micro-ondes s'est avéré être une bonne alternative au traitement thermique conventionnel. Grâce à son caractère inhérent de chauffage volumique, la technologie micro-ondes permet de réduire le temps de traitement et donc améliore les caractéristiques nutritionnelles et sensorielles du produit. Cependant, pendant le traitement par micro-ondes, le chauffage peut se produire de manière non-uniforme, conduisant ainsi à une distribution hétérogène de la température à l'intérieur du produit, ce qui peut entraîner une inactivation insuffisante des enzymes aux niveaux des points froids.

En particulier, la présence d'une activité résiduelle de la peroxydase, une enzyme communément présente dans les produits à base de fruits et connue pour sa thermo stabilité relativement élevée, peut entraîner le développement d'arômes indésirables et d'altérations de la couleur du produit. Puisque le chauffage micro-ondes et son uniformité dépendent de l'interaction complexe entre plusieurs facteurs, la simulation numérique s'avère un outil intéressant pour prédire la distribution de la température en fonction du temps, ce qui permet d'optimiser le procédé de traitement. Par conséquent, le but de ce travail était d'étudier, de par une double approche numérique et expérimentale, le procédé de traitement thermique par micro-ondes dédié à l'inactivation de la peroxydase dans des jus de fruits modèles.

Tout d'abord, l'étude bibliographique a été présentée pour une meilleure compréhension globale des enjeux de ce travail. Les principaux concepts liés à la thématique du sujet ont été traités, y compris le principe du chauffage par micro-ondes, les différentes technologies, la mesure des propriétés diélectriques, les équations fondamentales qui régissent les phénomènes physiques impliqués, la modélisation numérique, la cinétique d'inactivation enzymatique et enfin les applications technologiques des micro-ondes et leurs effets sur les jus de fruit.

Dans la première partie de ce travail, une étude des propriétés diélectriques (constante diélectrique et facteur de pertes) des jus de fruit modèles a été menée, démontrant leur forte dépendance à la température, à la fréquence micro-ondes et à la composition du

produit. Les propriétés diélectriques sont les paramètres prépondérants qui donnent des informations sur l'interaction entre les ondes électromagnétiques et les aliments au cours du chauffage par micro-ondes. La connaissance des propriétés diélectriques est non seulement utile pour l'optimisation du processus de traitement micro-ondes des produits, mais également pour la modélisation numérique du traitement thermique par micro-ondes.

Les propriétés diélectriques des solutions modèles de jus de fruit avec différentes teneurs en sucres solubles (entre 5 et 65 °Brix) ont été mesurées sur une large gamme de fréquences (entre 200 et 3000 MHz) à différentes températures (entre 20 et 80 °C, à intervalles de 10 °C). Les mesures des propriétés diélectriques ont été effectuées en utilisant un dispositif de sonde coaxiale ouverte. Les résultats ont été interprétés et discutés, en présentant les mécanismes physiques impliqués. Des discussions ont aussi été menées concernant l'effet de la présence d'acides dans le jus de fruit modèle sur le facteur de pertes diélectriques aux fréquences de 915 MHz et 2450 MHz. Les valeurs des profondeurs de pénétration de la puissance micro-ondes ont été également exposées à ces mêmes fréquences.

Les mesures des propriétés diélectriques ont montré une sensibilité importante à la température, à la fréquence micro-ondes et à la composition du jus de fruit modèle. Les relations obtenues entre le comportement diélectrique et les trois paramètres étudiés (température, fréquence et teneur en sucre) sont non monotones et relativement complexes. Des tendances semblables ont été observées lors de l'évaluation de jus de fruits commerciaux issus de différents produits (pomme, ananas, orange). Malgré sa complexité, l'influence de la température, de la fréquence et de la composition du produit sur la constante diélectrique et le facteur de pertes des jus de fruits modèles a pu être décrite à l'aide de modèles basés sur les réseaux de neurones. Cette approche permet d'établir des relations non linéaires entre les données d'entrée (température, fréquence et teneur en sucre) et les données de sortie (propriétés diélectriques). Les prédictions obtenues sur les propriétés diélectriques montrent un bon accord avec les données expérimentales sur une large gamme de fréquences micro-ondes, démontrant que cette approche est appropriée pour modéliser le comportement fortement non linéaire des propriétés diélectriques.

Ensuite, dans la seconde partie, l'inactivation de la peroxydase a été étudiée par un chauffage conventionnel. La solution modèle de jus de fruit à une teneur en sucre constante (10 °Brix), contenant de l'eau, du saccharose, de l'acide citrique et de la peroxydase de raifort commerciale, a été traitée avec 42 combinaisons différentes de temps et de température. Le traitement thermique a été effectué en plaçant le jus de fruit modèle dans des tubes en verre de petit diamètre et de parois minces dans un bain thermostatique sous agitation. En supposant une distribution de température homogène dans l'échantillon pendant le traitement conventionnel, l'histoire thermique complète du produit traité a pu être prise en compte par le

calcul de la létalité cumulée. Ainsi, les paramètres cinétiques estimés et liés à l'inactivation de l'enzyme sont considérés comme fiables.

L'activité de la peroxydase a été déterminée par spectrophotométrie en utilisant du pyrogallol comme substrat. Les résultats ont été exprimés en activités résiduelles, c'est-à-dire le rapport entre l'activité après traitement par rapport à celle avant (initiale). Les données obtenues ont pu être décrites par un modèle de cinétique du premier ordre. Ce modèle cinétique a été validé avec succès par comparaison avec des données expérimentales non utilisées dans l'ajustement du modèle. Le développement d'un modèle cinétique précis et fiable s'est révélé d'une grande importance pour les études de chauffage sous micro-ondes pour lequel plusieurs couplages multiphysiques ont été considérés. Cette démarche permet de prédire l'inactivation de la peroxydase lors du traitement thermique micro-ondes de jus de fruits modèles, en tenant compte de la convection naturelle dans le fluide chauffé et de la non-uniformité spatiale de la température sous micro-ondes.

Dans la troisième partie de ce travail, un modèle numérique d'une géométrie en trois dimensions a été développé par la méthode des éléments finis pour simuler le chauffage par micro-ondes du jus de fruit modèle. Pour cela, le modèle multiphysique consiste en un couplage fort entre les équations de l'électromagnétisme, le transfert de chaleur et le mouvement du fluide. De plus, le modèle cinétique d'inactivation de la peroxydase décrit dans la partie précédente a été inclus dans cette simulation. Les propriétés thermophysiques et diélectriques en fonction de la température ont également été implémentées dans le modèle de simulation.

Des stratégies spécifiques ont été adoptées pour réduire le temps de calcul et seulement un quart de la géométrie a été pris en compte (utilisation de symétries). Pour estimer le coefficient de transfert de chaleur global par convection externe, une méthode basée sur un cylindre métallique de même taille que l'échantillon traité a été mise en place.

À partir de la simulation numérique, la distribution de température dans le volume de l'échantillon a été prédite. La non-uniformité de température s'est révélée clairement perceptible, avec des zones chaudes et froides au cours du traitement micro-ondes. La partie inférieure de l'échantillon présente notamment des températures plus basses. En tenant compte des courants de convection et de la distribution non-uniforme de la température dans l'échantillon pendant le chauffage micro-ondes, l'inactivation de la peroxydase a été prédite. Des mesures expérimentales incluant les activités résiduelles de la peroxydase et les températures mesurées ont été utilisés pour comparer et valider les résultats de la simulation.

Les expériences ont été réalisées dans une cavité micro-ondes monomode (TE_{10}) à une fréquence de 2450 MHz. L'appareil expérimental était composé d'un générateur micro-ondes (type magnétron), d'un guide d'ondes (WR340), d'un applicateur et d'une charge à eau.

Un bloc de support en polystyrène extrudé a été placé à l'intérieur de l'applicateur. Le bloc a été conçu pour remplir la section transverse à la direction de propagation de l'onde, et a servi de support à un petit tube de l'échantillon de jus. L'échantillon a été placé au centre du support là où l'amplitude du champ électrique est maximale (mode fondamental TE_{10}).

Des expériences de traitement par micro-ondes ont été réalisées en deux groupes. Dans le premier cas, la solution de jus de fruits modèle a été traitée à une seule température de traitement et un temps de maintien unique à la température cible. Dans un deuxième temps, les expériences ont été effectuées à sept températures de traitement et à quatre temps de maintien. Dans le deuxième groupe d'expériences, le jus de fruit a été traité différemment, avec deux ou trois étapes de maintien (c'est-à-dire deux ou trois températures finales de traitement) au lieu d'une seule.

Dans l'ensemble, un bon accord entre les températures expérimentales et simulées a été obtenu pour tous les traitements étudiés. Cependant, on peut noter que la température prédite aux traitements avec maintien en température les plus bas était légèrement supérieure à la température mesurée expérimentalement. Par contre, à des températures plus élevées de maintien, les températures prédites par le modèle étaient légèrement inférieures à la température expérimentale. Aux températures intermédiaires, les deux températures ont présenté un très bon accord.

En ce qui concerne l'inactivation enzymatique, un bon accord a été obtenu entre les valeurs prédites et expérimentales. Comme déjà mentionné précédemment, l'inactivation dépend de la distribution spatiale de la température. Ainsi, compte tenu des résultats satisfaisants obtenus pour l'inactivation, cela démontre que la distribution de la température prédite par le modèle a été aussi correctement prédite.

Le couplage du transfert de chaleur avec l'électromagnétisme était très important du fait des changements significatifs dans les propriétés diélectriques et thermophysiques du produit au cours du chauffage. De même, le couplage de ces équations avec le mouvement convectif du fluide lors du chauffage était autant essentiel pour une simulation fiable. L'étude numérique a montré l'importance de la prise en compte des équations d'écoulement du fluide en régime laminaire pour obtenir des profils de température comparables à l'expérimental. Des résultats inappropriés ont été obtenus lorsque ces équations n'ont pas été prises en compte dans le modèle, indiquant l'importance du mouvement convectif de fluides sur la distribution de la température dans le produit. Par conséquent, le couplage des équations d'écoulement de fluide était important et nécessaire pour obtenir de bons résultats lors de la simulation du chauffage par micro-ondes de liquides.

Il convient de noter que, en utilisant le modèle cinétique obtenu par chauffage conventionnel dans la simulation, les effets non thermiques sur l'inactivation enzymatique sont

supposés inexistants ou négligeables. En fait, l'existence d'effets micro-ondes non thermiques est un sujet très controversé dans la littérature. Certaines études soutiennent l'existence de tels effets. Au contraire, d'autres affirment que l'existence n'est pas prouvée et que l'inactivation n'est donc due qu'aux effets thermiques. Afin de vérifier ces hypothèses, dans la dernière partie de ce travail, des expériences à des températures sublétales ont été réalisées.

Les effets non thermiques possibles de l'application de micro-ondes sur l'inactivation de la peroxydase ont été évalués par traitement micro-ondes en mode batch et en boucle fermée à basse température. Pour ceci, des dispositifs spéciaux comprenant l'utilisation d'air froid comme agent de refroidissement ont été développés pour éliminer autant que possible la chaleur générée par micro-ondes dans le volume de l'échantillon.

La solution de jus a été exposée aux micro-ondes à la fois en mode discontinu et en boucle fermé. Les expériences ont été réalisées en deux groupes : traitement avec refroidissement et traitement sans système de refroidissement (jets d'air comprimé avec un refroidissement de type venturi connecté au guide d'ondes). Dans les deux cas, l'incidence de la puissance micro-ondes a été maintenue constante. De faibles valeurs de puissance ont été choisies de manière à ce que la température de l'échantillon ne soit pas trop élevée, de sorte que l'utilisation d'air froid soit suffisante pour éliminer la chaleur et maintenir la température basse dans des conditions sublétales.

Après tous les traitements à des températures sublétales (inférieures à environ 40 °C), l'activité enzymatique a été réduite d'environ 5%, indépendamment de la puissance micro-ondes incidente, du temps de traitement et du mode de traitement étudiés. Alors que dans le traitement par micro-ondes sans système de refroidissement, les températures atteignaient environ 70 °C et le degré d'inactivation était supérieur à 98%. En comparant les valeurs obtenues dans chaque cas, l'effet thermique est largement prépondérant. Ainsi, cela explique pourquoi l'utilisation d'un modèle cinétique d'inactivation enzymatique basé sur le chauffage conventionnel peut être utilisé dans la simulation d'une inactivation par micro-ondes sans nuire à la qualité du modèle de simulation.

Ces résultats peuvent indiquer l'existence possible d'effets non thermiques, mais en raison des faibles valeurs (faible inactivation), ce n'est pas possible de faire une conclusion solide et d'autres études complémentaires sont nécessaires. Il serait très intéressant d'étudier en profondeur l'effet des micro-ondes sur les altérations possibles au niveau moléculaire et pour différents types d'enzymes. De telles analyses pourraient être effectuées en utilisant, par exemple, des études détaillées de dichroïsme circulaire et de fluorescence.

Enfin, la réactivation potentielle de la peroxydase après chauffage conventionnel et micro-ondes a été évaluée et comparée. De nombreuses études ont révélé que la peroxydase peut récupérer son activité après un traitement thermique, ce qui peut entraîner une perte de qualité des produits traités lors du stockage. Le mécanisme de réactivation de l'enzyme est

globalement complexe et pourrait être influencé par plusieurs facteurs, notamment les conditions de chauffage et d'environnement externe, l'origine et le type d'enzyme.

Des expériences de réactivation ont été effectuées dans des systèmes conventionnels (bain-marie) en batch et dans un dispositif micro-ondes batch traitant un liquide circulant en boucle fermée. Les échantillons traités ont été stockés à 25 °C. L'activité enzymatique a été contrôlée après 0, 1, 2 et 3 jours de traitement. L'activité relative a été calculée par le rapport de l'activité à chaque période vis-à-vis de l'activité initiale de l'échantillon non traité.

Aucune récupération de l'activité de la peroxydase n'a été observée dans le jus modèle chauffé par traitement micro-ondes en boucle fermée et par traitement discontinu conventionnel. Par contre, une faible récupération d'activité a été constatée après le traitement micro-ondes en batch. Sachant que la distribution de la température dans le traitement micro-ondes par lots en batch n'est pas uniforme, il est très probable que la réactivation soit plutôt la conséquence d'une non-uniformité de température que d'une inactivation réversible due aux micro-ondes. Ce résultat est important pour aider à la compréhension des études de traitement micro-ondes.

En conclusion, ce travail montre l'intérêt de la simulation en tant qu'outil de compréhension du processus multiphysique de chauffage par micro-ondes pour l'inactivation des enzymes, ce qui peut être particulièrement intéressant pour la conception de traitements micro-ondes optimisés.

18

RESUMO EXPANDIDO

Processamento térmico de suco de frutas por micro-ondas: modelagem multifísica e inativação enzimática

Um dos maiores desafios da indústria de suco é alcançar a inativação enzimática requerida sem prejudicar os aspectos sensoriais e nutricionais do produto. Na busca por processos que minimizem tais danos, o aquecimento por micro-ondas tem provado ser uma boa alternativa ao processamento térmico convencional. Devido ao aquecimento volumétrico, a tecnologia de micro-ondas pode reduzir o tempo de processamento e, assim, melhorar a manutenção das características nutricionais e sensoriais. No entanto, durante o processamento por micro-ondas, o aquecimento pode ocorrer de maneira não uniforme, levando a uma distribuição desigual de temperatura dentro do produto, o que pode resultar em uma inativação enzimática insuficiente sobretudo nos pontos frios.

Em particular, a ocorrência de atividade residual da peroxidase, uma enzima comumente presente em produtos de frutas e conhecida por sua termoestabilidade, pode causar o desenvolvimento de aromas indesejáveis e alterações de cor no produto. Como o aquecimento por micro-ondas e sua uniformidade dependem da interação complexa entre vários fatores, a simulação computacional pode ser uma ferramenta valiosa para prever a distribuição de temperatura dependente do tempo, permitindo a avaliação da adequação do processamento e sua otimização. Portanto, o objetivo deste trabalho foi estudar, numericamente e experimentalmente, o uso de micro-ondas para inativação da peroxidase em suco de frutas modelo.

Inicialmente, a revisão da literatura foi apresentada para uma melhor compreensão global do presente trabalho. Os principais conceitos envolvidos na temática estudada foram abordados, incluindo aquecimento e tecnologia de micro-ondas, propriedades dielétricas, equações dos fenômenos implicados no processamento de liquidos por micro-ondas, simulação computacional, cinética de inativação enzimática, aplicações de micro-ondas e seus efeitos.

Na primeira parte deste trabalho, foi realizado um estudo sobre as propriedades dielétricas (constante dielétrica e fator de perda) de sucos de frutas modelo, evidenciando sua alta dependência em relação à temperatura, à freqüência e à composição do produto. Propriedades dielétricas são parâmetros importantes que fornecem informações sobre a interação entre a energia eletromagnética e alimentos durante o aquecimento por micro-ondas. O conhecimento das propriedades dielétricas não é útil apenas para projetar condições

de processo e embalagem, mas também para a modelagem matemática de processos por micro-ondas.

As propriedades dielétricas de soluções modelo de suco de frutas com diferentes teores de sacarose (entre 5 e 65 °Brix) foram medidas em uma ampla faixa de freqüências (entre 200 e 3000 MHz) em diferentes temperaturas (entre 20 e 80 °C, em intervalos de 10 °C). Medidas de propriedades dielétricas foram realizadas usando um sistema de cabo coaxial aberto. Os resultados foram interpretados e discutidos, apresentando os possíveis mecanismos envolvidos.

As propriedades dielétricas mostraram uma importante sensibilidade à temperatura, à freqüência e à composição. As relações obtidas entre o comportamento dielétrico e os três parâmetros estudados (temperatura, frequência e teor de sacarose) foram não-monotônicas e consideravelmente complexas. Tendências comparáveis foram observadas na avaliação de sucos comerciais de diferentes frutas (maçã, abacaxi, laranja). Apesar de sua complexidade, pode-se modelar a influência da temperatura, da freqüência e da composição na constante dielétrica e no fator de perda dos sucos de frutas do modelos utilizando redes neurais. Esta abordagem permite estabelecer relações não-lineares entre os dados de entrada (temperatura, frequência e teor de açúcar) e os dados de saída (propriedades dielétricas). As previsões obtidas mostraram boa concordância com os dados experimentais, indicando que a abordagem escolhida foi efetivamente adequada para modelar o comportamento dielétrico.

Em seguida, na segunda parte, a inativação da peroxidase foi estudada usando aquecimento convencional. A solução modelo de suco de fruta com teor de sólidos constante (10 °Brix), composto de água, sacarose, ácido cítrico e peroxidase de raiz forte, foi processada em 42 combinações diferentes de tempo e temperatura. O processamento térmico foi realizado colocando o suco modelo em tubos de vidro de pequeno diâmetro e paredes finas dentro de um banho termostático com agitação. Assumindo uma distribuição de temperatura homogênea na amostra durante esse processamento, a história térmica completa foi considerada através do cálculo de letalidade acumulada. Desta forma, parâmetros cinéticos confiáveis foram estimados.

A atividade da peroxidase foi determinada espectrofotometricamente usando pirogalol como substrato. Os resultados foram expressos como atividades residuais, ou seja, a razão entre a atividade pós-processamento em relação à atividade pré-processamento (inicial). Os dados obtidos foram bem descritos por um modelo cinético de primeira ordem. Esse modelo cinético estimado foi validado com sucesso por dados experimentais não utilizados na adaptação do modelo. Particularmente, o desenvolvimento de um modelo cinético preciso e confiável foi de grande importância para a próxima parte, na qual o modelo foi implementado como parte do modelo multifísico. Ao acoplar o modelo cinético ao modelo

de simulação, pode-se prever a inativação da peroxidase durante o processamento por micro-ondas do suco de fruta modelo, tendo em conta a convecção natural no fluido aquecido e a não uniformidade espacial da temperatura sob microondas.

Na terceira parte deste trabalho, um modelo tridimensional usando o método de elementos finitos para simular o aquecimento por micro-ondas dos sucos foi desenvolvido. Para isso, os módulos de electromagnetismo, de transferência de calor e de dinâmica de fluidos foram fortemente acoplados. Além disso, o modelo cinético de inativação da peroxidase descrito na parte anterior foi inserido no modelo de simulação. As propriedades termofísicas e dielétricas em função da temperatura também foram implementadas no modelo de simulação.

Estratégias específicas foram adotadas para reduzir tempo de simulação e apenas um quarto da geometria foi considerado baseando-se no uso das simetrias. Para estimar o coeficiente de transferência de calor global por convecção externa, experimentos fundamentados no método da capacitância global foi realizado utilizando um cilindro de latão com as mesmas dimensões da amostra .

A partir da simulação, a distribuição de temperatura dentro da amostra foi prevista. As distribuições de temperatura não-uniformes foram claramente perceptíveis, apresentando zonas quentes e frias no produto ao longo do processamento. A parte inferior da amostra predominantemente apresentou temperaturas mais baixas. Desta forma, levando em conta as correntes de convecção e a distribuição espacial da temperatura dentro da amostra durante o aquecimento por micro-ondas, a inativação da peroxidase foi adequadamente prevista. Os resultados experimentais, incluindo as atividades residuais de peroxidase e as temperaturas medidas no centro da amostra, foram utilizados para comparar e validar os resultados da simulação.

Os experimentos foram realizados em um dispositivo micro-ondas monomodal (TE$_{10}$), operando na frequência de 2450 MHz. O aparato experimental foi composto por um gerador de micro-ondas (tipo magnetron), um guia de ondas (WR340), um aplicador e uma carga de água. Um bloco de suporte feito de poliestireno expandido foi colocado dentro do aplicador. O bloco foi disposto de forma a ficar perpendicular à direção de transmissão da onda, preenchendo a seção e servindo como suporte para um pequeno tubo contendo a amostra. Este tubo foi posicionado no centro do bloco, onde a amplitude do campo elétrico era máxima (modo fundamental TE$_{10}$).

Os experimentos de processamento de micro-ondas foram realizados em dois grupos. No primeiro, a solução modelo de suco de frutas foi tratada visando uma única temperatura de processamento e um único tempo de espera. Então, neste caso, os experimentos foram realizados em sete temperaturas de processamento e quatro tempos de

retenção. No segundo grupo, o suco de fruta foi tratado diferentemente, com dois ou três estágios de retenção (isto é, duas ou três temperaturas de processamento e tempos de retenção) em vez de um único.

No geral, uma boa concordância entre os resultados de temperatura experimentais e os preditos foi obtida em todos os tratamentos avaliados. No entanto, pode-se notar que as temperaturas preditas nos processamentos com temperatura final mais baixa foram ligeiramente superiores às temperaturas medidas experimentalmente. Por outro lado, em temperatura final de processamento mais alta, as temperaturas preditas foram ligeiramente inferiores às temperaturas experimentais. Em temperatura intermediária, ambas as temperaturas apresentaram uma concordância muito boa.

Em relação à inativação enzimática, uma boa concordância foi obtida entre os valores preditos e experimentais. Como já mencionado antes, a inativação depende muito da distribuição espacial da temperatura. Assim, considerando que os resultados de inativação foram satisfatórios, pode-se inferir que a distribuição de temperatura predita dentro da amostra também foi corretamente simulada.

A acoplagem de transferência de calor e eletromagnetismo foi importante devido as mudanças significativas nas propriedades dielétricas e termofísicas ao longo do aquecimento dos alimentos. Da mesma forma, a acoplagem das equações relativa à dinâmica de fluidos também foi essencial para se obter uma simulação confiável. O estudo numérico demonstrou a importância de considerar as equações do movimento do fluido em regime laminar para obter perfis de temperatura comparáveis aos experimentais. Resultados não apropriados foram obtidos quando estas equações não foram consideradas no modelo, indicando a importância do movimento convectivo do fluido na distribuição da temperatura dentro do produto. Portanto, a acoplagem das equações foi importante e necessária para obter bons resultados durante a simulação do aquecimento por micro-ondas de líquidos.

Nota-se que ao utilizar o modelo cinético de inativação obtido pelo aquecimento convencional, os possíveis efeitos não térmicos foram considerados inexistentes ou insignificantes. De fato, a existência de efeitos não térmicos de micro-ondas é um assunto bastante controverso na literatura. Alguns estudos apóiam a existência. Por outro lado, outros estudos afirmam que não há evidências suficientes para comprovar a existência e, portanto, a inativação é devida apenas aos efeitos térmicos. Assim, com o intuito de verificar essas hipóteses, nesta última parte do trabalho, experimentos a temperaturas subletais foram realizados.

Os possíveis efeitos não térmicos da aplicação de micro-ondas na inativação de POD foram avaliados através do processamento de micro-ondas nos modos batch e closed-loop a baixas temperaturas. Para este propósito, configurações especiais, incluindo o uso de ar frio

como meio de resfriamento, foram construídas para remover, tanto quanto possível, o calor dissipado pelas micro-ondas no volume da amostra.

A solução de suco foi exposta às micro-ondas tanto em dois modos: batelada e circulação da amostra em circuito fechado. Os experimentos foram realizados em dois grupos: processamento com resfriamento e processamento sem sistema de resfriamento (jatos de ar comprimido com um resfriamento do tipo venturi conectado ao guia de ondas). Em ambos os casos, a incidência de potência de micro-ondas foi mantida constante. Baixos valores de potência foram escolhidos para que a temperatura da amostra não fosse muito alta, permitindo que o uso de ar frio fosse suficiente para remover o calor e manter a temperatura baixa em condições subletais.

Após todos os tratamentos a temperaturas subletais (abaixo de 40 °C), a atividade enzimática apresentou uma diminuição de cerca de 5%, independentemente da potência incidente, do tempo de processamento e do modo de processamento estudados. Enquanto que no processamento por micro-ondas sem o sistema de refrigeração, as temperaturas atingiram cerca de 70 °C e o grau de inativação foi superior a 98%. Comparando os valores obtidos em cada caso, o efeito térmico é amplamente o mais dominante. Assim, explica-se como o uso de um modelo cinético de inativação enzimática baseado em aquecimento convencional pode ser utilizado na simulação de uma inativação por micro-ondas sem prejudicar a qualidade do modelo de simulação.

Portanto, estes resultados podem indicar a possível existência de efeitos não térmicos. No entanto, devido aos pequenos valores (baixa inativação) encontrados, não é possível fazer uma conclusão sólida e estudos complementares são necessários. Seria muito interessante estudar em profundidade os efeitos das micro-ondas em relação às possíveis alterações em nível molecular e conformacional de diferentes enzimas. Tais análises podem ser realizadas usando, por exemplo, estudos detalhados de dicroísmo circular e fluorescência.

Finalmente, na última parte deste trabalho, a potencial reativação da peroxidase após aquecimento convencional e micro-ondas foi avaliada e comparada. Muitos estudos revelaram que o POD pode recuperar sua atividade após o tratamento térmico, o que pode causar a deterioração dos alimentos processados durante o armazenamento. O mecanismo de reativação enzimática é globalmente complexo e pode ser influenciado por vários fatores, incluindo condições ambientais e de aquecimento, origem e tipo de enzima.

Experimentos de reativação foram realizados em sistema convencional (banho-maria) e em sistemas de micro-ondas usando os modos de processamento em batelada e em circulação de fluido em circuito fechado. As amostras tratadas foram armazenadas a 25 °C. A atividade enzimática foi monitorada após 0, 1, 2 e 3 dias de processamento. A atividade relativa foi calculada através da razão entre a atividade em cada período e a atividade inicial da amostra não tratada.

Nenhuma recuperação da atividade da peroxidase foi observada no suco modelo aquecido por tratamento micro-ondas em circuito fechado e por tratamento convencional em batelada. Por outro lado, uma pequena recuperação de atividade foi encontrada após o processamento por micro-ondas em batelada. Sabendo que a distribuição de temperatura no processamento em batelada não é uniforme, como verificado por simulação computacional descrita anteriormente, é muito provável que a reativação seja conseqüência da não-uniformidade do que o resultado de uma inativação reversível devido às micro-ondas. Esse resultado possui importância ao auxiliar a interpretação de estudos de processamento com micro-ondas.

Em conclusão, este trabalho mostra o interesse da simulação computacional como uma ferramenta para entender o processo multifísico de aquecimento por micro-ondas para a inativação enzimática, que por sua vez pode ser particularmente interessante para a concepção de processos otimizados usando aquecimento por micro-ondas.

LIST OF FIGURES

LIST OF TABLES

NOMENCLATURE

a	length of the waveguide [m]
A	weighted neuron input for neural network [-] or enzyme activity
b	width of the waveguide [m] or bias for neural network [-]
B	magnetic flux [T = V s A^{-1} m^{-1}] or body force [kg m^{-2} s^{-2}]
c_0	speed of light in free space / vacuum [2.9979×10^8 m s^{-1}]
C_p	heat capacity / specific heat at constant pressure [J kg^{-1} K^{-1}]
d_P	power penetration depth [m]
D_P	microwave penetration depth [m]
D	electric flux density [A s m^{-2}] or kinetic parameter [s]
e	Euler's number
E	electric field [V m^{-1}]
E_0	amplitude of the electric field [V m^{-1}]
f	frequency [Hz]
$F_{T_{ref}}$	equivalent holding time at reference temperature [s]
g	gravitational acceleration [m s^{-2}]
h	heat transfer coefficient [W m^{-2} K^{-1}]
h_i	specific enthalpy [J kg^{-1}]
h_T	total enthalpy [J kg^{-1}]
H	magnetic field [A m^{-1}]
I_i	mass source density [kg m^{-3} s^{-1}]
j	imaginary unit [-]
J	electric current density [A m^{-2}]
k	thermal conductivity [W m^{-1} K^{-1}] or reaction rate constant [s^{-1}]
L	sample height [m]
L_t	lethality [-]
m	constant for wave propagation [-]
n	normal vector [-] or constant for wave propagation [-]
n_e	number of experiments
N	result of transfer function in neural network [-]
p	pressure [Pa]
P	power [W]
q	radiation power flux density [W m^{-2} s^{-1}]
Q	heat / power dissipated per unit of volume [W m^{-3}]
r	radius [m]

34

t	time [s]
T	temperature [°C]
u	neuron input for neural network [-]
U	velocity field [m s⁻¹]
x, y, z	cartesian spatial coordinates [m]
w	weight for neural network [-]
z	kinetic parameter [°C]
Z_{TE}	impedance

Greek letters

α	relative resistance of the sensible enzyme portion
β	thermal expansion coefficient [K⁻¹] or kinetic parameter [-]
ε_r'	relative dielectric constant, relative electrical permittivity [-]
ε_r''	relative dielectric loss factor [-]
ε_r^*	relative complex permittivity [-]
ε_0	permittivity of free space [$(36\pi)^{-1} \times 10^{-9}$ F m⁻¹]
k_0	propagation constant within free-space [m⁻¹]
λ	wavelength [m]
μ	magnetic permeability [H m⁻¹]
μ_0	magnetic permeability of vacuum [$4\pi \times 10^{-7}$ H m⁻¹]
η	viscosity [Pa s]
ρ	density [kg m⁻³]
ρ_e	electric charge density [C m⁻³]
σ	electrical conductivity [S m⁻¹]
σ_{NS}	viscous stress tensor [Pa]
δ	loss angle [rad]
δ_T	kinetic parameter [s]
ω	pulsation of microwave radiation or angular frequency [rad s⁻¹, Hz]

Subscripts

0	initial or vacuum
c	cut-off
$crit$	critical
d	contribution of dipole rotation
exp	experimental
gen	generated

$global$ global

in incident

$local$ specific location

P process

r relative

R resistant

ref reference

S sensitive

σ contribution of ionic conduction

∞ maximum or ambient

Abbreviations

Abs   absorbance

ANN   artificial neural networks

EM   electromagnetic

FDTD finite difference time domain

FEM finite element method

ISM   industrial, scientific, and medical

LOX   lipoxygenase

PID   proportional–integral–derivative

PME   pectinmethylesterase

POD   peroxidase

PPO   polyphenoloxidase

SSE   sum of squared errors

TE   transverse electric

TEM transverse electromagnetic

TM   transverse magnetic

TSS   total soluble solids [°Brix]

3D   tridimensional

GENERAL INTRODUCTION

Thermal processing dictates the sensory quality and safety of food products. Microwave heating has drawn great attention not only in the food industry, but also in other domains. Due to its unique characteristics, microwave technology has been considered as a promising alternative to conventional methods. Microwave heating is primarily based on electromagnetic energy conversion into heat via friction of dipoles and ionic species that try to follow the oscillating electric field. As microwaves can rapidly transfer energy throughout the volume of the material (i.e. volumetric heating), microwave technology can overcome the issue of slow rates of heat transfer, reducing the processing time and enhancing the product homogeneity. Thus, it can potentially avoid the development of cooked off-flavors, color alteration and degradation of thermosensitive compounds during food processing, better preserving the nutritional and sensory quality of sensitive foods, such as fruit juices.

A vast number of applications of the microwave technology has been reported in food processing, including pasteurization and blanching of fruit and vegetable-based products. Thermal processing of fruit juices is generally based on the inactivation of heat resistant undesirable enzymes, since the inherent acidity of juices inhibits the development of most pathogens. As peroxidase is known to have a relatively high heat resistance whose intensity varies depending on certain conditions, the inactivation of peroxidase is often used as an index of processing adequacy. Moreover, this enzyme is involved in the oxidation of a wide range of organic and inorganic substrates, resulting in off-flavors and sensory degradation. Microwave heating has been conveniently used to inactivate several enzymes relevant for juice industry, including peroxidase.

However, one of the most important concerns of microwave processing is the non-uniform heating and the consequent uneven temperature distribution. Since insufficient inactivation may occur at the cold spots, the issue of non-uniformity can have implications in terms of food safety and quality. Therefore, a study of temperature distribution and heat transfer is needed to understand and optimize the process. Microwave heating depends on interactions of several factors and involves complex multiphysics phenomena. In the case of heating of liquids, the complexity is even greater because of buoyancy-driven flow. Hence, the use of computer simulation and development of a reliable model is desirable. Among the factors that greatly affect microwave heating and its uniformity, one can highlight the dielectric properties, which in turn can also be dependent on process and product conditions.

Therefore, the aim of this study is to evaluate numerically and experimentally the application of microwave heating on a model fruit juice, focusing in the inactivation of peroxidase. Based on that, this work is composed of five chapters and it is organized as described below.

First of all, in Chapter 1, the literature review is presented for a better global understanding of this work. The main concepts involved in the scope of this work are covered, including microwave heating and technology, dielectric properties, governing equations of the phenomena involved, computer simulation, enzyme inactivation kinetics, microwave applications and effects.

In Chapter 2, a broad study on dielectric properties is presented. Dielectric properties are of critical importance in understanding the interaction of microwaves and food materials. The information on these properties, along with thermophysical properties, is strictly required during the simulation of microwave processing. In this way, the effects of product temperature, operating frequency and composition, more particularly sucrose content, on dielectric properties are evaluated and modeled by Neural Networks.

Chapter 3 presents the evaluation of peroxidase inactivation kinetics in model juice during a conventional thermal treatment. The fruit juice model solution is processed at different combinations of time and temperature and the resulting inactivation data are fitted by a first order kinetic model.

In Chapter 4, a finite-element model coupling electromagnetics, heat transfer and fluid flow is proposed to simulate the microwave heating of juices. It is in this chapter that the elementary knowledge of the previous chapters is mainly applied. The dielectric properties of the juice as a function of temperature and the peroxidase inactivation kinetics model are implemented in the simulation model. The temperature distribution within the sample and the resulting enzyme inactivation are predicted, evaluated and experimentally validated.

In Chapter 5, the potential reactivation of peroxidase is studied by evaluating the enzyme activities during storage after conventional and microwave processing. Furthermore, this chapter also presents a discussion on the existence of non-thermal effects due to microwaves, which is an interesting and delicate subject that has generated quite controversy in literature.

Finally, to complete the present work, the mains conclusions and final considerations about the whole work are covered. Moreover, the perspectives and suggestions for future studies are given.

CHAPTER 1.   LITTERATURE REVIEW

The present literature review is basically divided into 4 main sections, namely: microwave heating, numerical modeling of microwave heating, enzyme inactivation, and microwave heating in food processing and technology.

In the first main section, some fundamental aspects related to the microwave radiation and propagation and to the interactions between microwaves and material, notably mechanism of heating and dielectric properties, are covered. In the second main section, the numerical modeling of microwave processing is presented, showing the main phenomena involved and their key governing equations. Then, in the third section, the use of microwaves in the food domain as well as the advantages and drawbacks of the microwave technology are covered. Also, the specific application of microwaves for enzyme inactivation is presented, in order to cover the central scope of this work. In the last section, more information on enzyme inactivation and its kinetics is presented, focusing on the enzyme of study (peroxidase).

1.1. Microwave heating

1.1.1. Principles and microwave systems

Microwaves are non-ionizing electromagnetic waves whose frequency varies within 300 MHz to 300 GHz, corresponding to wavelength range from 1 m to 1 mm (Meda et al., 2005; Tang, 2015). An electromagnetic wave consists of two orthogonal components: the electric field and the magnetic field, oscillating in phase normally to the direction of wave propagation (Figure 1.1).
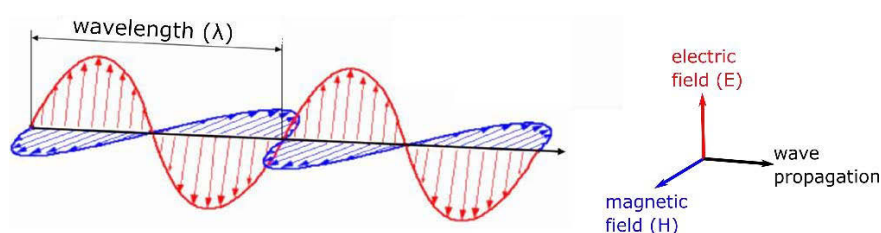
Figure 1.1. Schematic representation of an electromagnetic wave. Adapted from: Tang (2015).

On the electromagnetic spectrum (Figure 1.2), they are located between radio frequencies and infrared radiations. The use of microwaves was originally implemented for the communication systems and radar. But after, due to their potential for heat generation, the interest of using microwaves in food processing showed up and since then, it has expanded.
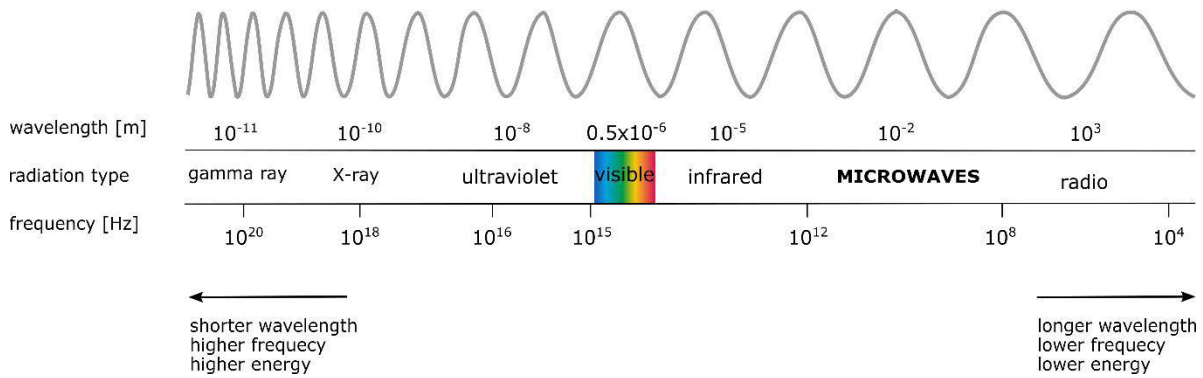
Figure 1.2. Diagram of the electromagnetic spectrum, indicating the radiation types along the range of wavelengths and frequencies.

Microwave heating systems are usually restricted to certain frequencies, within the industrial, scientific, and medical (ISM) band. This regulation is needed to avoid the risk of interference with radio communications and radars. Thus, depending on the country and application type, the frequency of microwaves used can differ. The most common frequencies are 896 MHz (in UK) and 915 MHz (in USA and China), for industrial applications; and 2450 MHz, for commercial, domestic and industrial uses in most countries (Atuonwu and Tassou, 2018; Salazar-González et al., 2012; Tang, 2015).

In general, microwave heating systems consist of a power supplier, a microwave power source (usually a magnetron), a waveguide and an applicator (or heating cavity). The magnetron is the device responsible for generation of microwave power and it is composed of a cathode, anode and static magnetic field source (permanent magnet) (Atuonwu and Tassou, 2018). These elements can be arranged in different configurations. An example of a magnetron can be observed in Figure 1.3. The microwaves generated by the magnetron are directed via the waveguide to the heating cavity, where part of microwave energy is absorbed by the product. The magnitude of this microwave interaction depends on dielectric properties of the product. The non-absorbed microwave energy can be reflected towards the magnetron or more frequently, it can be absorbed and trapped by a water load.
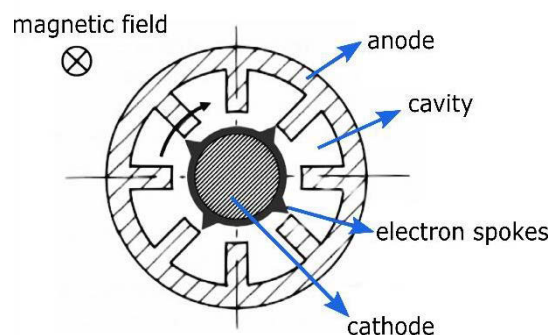
Figure 1.3. Example of a structure of magnetron shown in cross-section. Adapted from: Atuonwu and Tassou (2018); Carter (2011).

Another microwave power source also found in microwave heating systems is the solid-state generator. It is basically composed of a microwave signal generator, a high power amplifier made of transistors (which replaces the magnetron), with its heat sink, and a power supply system. Compared to magnetrons, many advantages are attributed to the solid-state technology , including more accuracy and stability for the microwave spectrum, longer lifetime and more effective power amplitude control (Atuonwu and Tassou, 2018). Nevertheless, this technology is still restricted to relatively low microwave power output (1 kW maximum). Magnetrons-based microwave generators are still largely present in domestic, commercial and industrial microwave heating applications where high microwave power is required

1.1.2. Microwave-material interactions

1.1.2.1. Mechanism of microwave heating

The mechanism of microwave heating is different from that of the conventional heating process, in which heat transfer occurs primarily by conduction and convection. The microwave heating of food materials, also called dielectric heating, is based on volumetric heating and it occurs because of two main mechanisms responsible of the conversion of electromagnetic energy into heat (Figure 1.4).

The first mechanism is the molecular dipolar rotation. This mechanism depends on the existence of polar molecules in the material. In the case of food materials, the water is generally the most dominant polar component. For the water molecule, the different electronegativity of individual atoms result in the existence of a permanent electric dipole (Meda et al., 2005). When an oscillating electromagnetic field is generated, the water molecules try to realign themselves to the direction of the electric field. Owing to the high frequency electric field, this realignment occurs at a million times per second and causes internal friction of molecules leading to the volumetric heating of the food material (Chandrasekaran et al., 2013).

The second mechanism is ionic polarization or ionic conduction. Heat is generated through the oscillatory migration of ions under the action of high frequency electric field (Datta and Davidson, 2000). These ionic movements result in collisions between them and other molecules, causing the conversion of kinetic energy of the moving ions into thermal energy (Salazar-González et al., 2012).
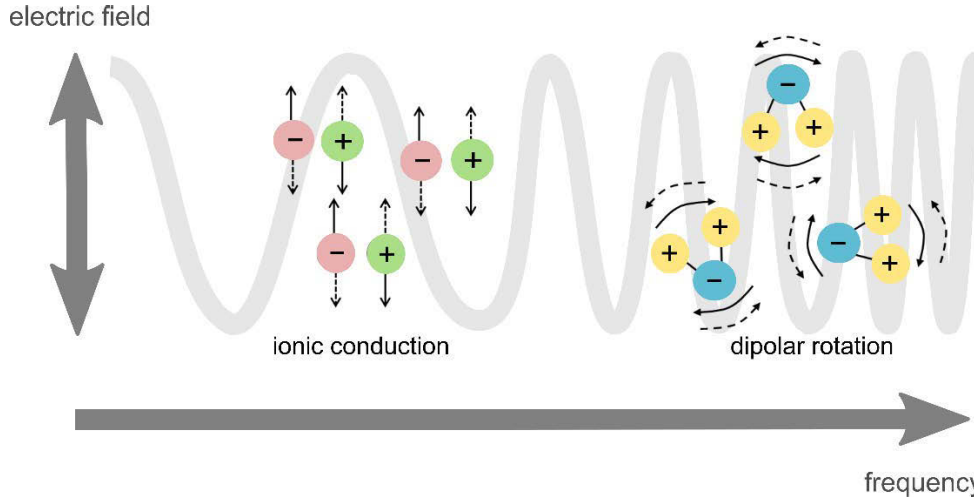
Figure 1.4. Schematic representation of the two main mechanisms related to microwave heating: dipolar rotation and ionic conduction.

1.1.2.2. Dielectric properties

1.1.2.2.1. Fundamental aspects

Dielectric properties influence the reflection of electromagnetic waves at interfaces and the attenuation of the microwave energy within materials (Birla et al., 2008; Komarov et al., 2005). Thus, these properties are closely related to the ability of food material to convert microwave energy into heat (Franco et al., 2015). Knowledge of dielectric properties is essential to evaluate the interaction between electromagnetic energy and product, to model and optimize microwave processes, to design microwave devices and ovens, to choose appropriate materials for containers or packaging, to develop new microwaveable products (İçier and Baysal, 2004a; Vadivambal and Jayas, 2010).

Dielectric properties of a material are defined by the complex permittivity, which consists of a real part, termed as dielectric constant, and an imaginary part, termed as loss factor. In practical applications, these parameters are presented as relative values to the permittivity of free space (ε_0). The relative complex permittivity is the parameter typically used (ε_r^*) and it is represented as (İçier and Baysal, 2004b):

$$\varepsilon_r^* = \varepsilon_r^{'} - j\varepsilon_r^{''} = \frac{\varepsilon^{'}}{\varepsilon_0} - j\frac{\varepsilon^{''}}{\varepsilon_0}$$

Eq. 1.1

where $j = \sqrt{-1}$, ε_0 is the permittivity of free space (ε_0 = 8.854 × 10^{-12} F m^{-1}), $\varepsilon_r^{'}$ and $\varepsilon_r^{''}$ are the relative dielectric constant and the relative loss factor, respectively. Note that both relative dielectric constant and relative loss factor are dimensionless, since they are defined in relation to the permittivity of free space.

The dielectric constant characterizes the material's ability to store energy when exposed to an electric field (İçier and Baysal, 2004a). While the loss factor is an important parameter related to the conversion of electromagnetic energy into thermal energy during microwave heating (Zhu et al., 2012). The ratio of the loss factor to the dielectric constant is given by the loss tangent, often named the dissipation factor (Chandrasekaran et al., 2013), and is expressed as:

$$\tan \delta = \frac{\varepsilon_r^{''}}{\varepsilon_r^{'}} = \frac{\dfrac{\varepsilon^{''}}{\varepsilon_0}}{\dfrac{\varepsilon^{'}}{\varepsilon_0}} \qquad \text{Eq. 1.2}$$

The mechanisms that contribute to the dielectric loss in heterogeneous mixtures include polar, electronic, atomic, and Maxwell–Wagner responses (Guo et al., 2011; Komarov et al., 2005). However, at the microwave frequency range, the loss factor of a solution is basically the combined effect of two mechanisms, dipole loss ($\varepsilon_d^{''}$) and ionic loss ($\varepsilon_\sigma^{''}$). Hence, the variation of loss factor depends on which mechanism dominates (Ryyniinen, 1995). In general, ionic conduction is more preponderant at lower frequencies when compared to dipolar rotation, as indicated in Figure 1.4. The combination of effects in dielectric loss factor is represented by Eq. 1.3. The loss factor due to ionic conduction can be calculated by the Hasted-Debye model, as shown in Eq. 1.4.

$$\varepsilon^{''} = \varepsilon_d^{''} + \varepsilon_\sigma^{''} \qquad \text{Eq. 1.3}$$

$$\varepsilon_\sigma^{''} = \frac{\sigma}{\omega \varepsilon_0} \qquad \text{Eq. 1.4}$$

where σ is the electrical conductivity and $\omega = 2\pi f$ is the angular frequency of the field. At lower frequencies, the dominant mechanism is ionic conduction, while at higher microwave frequencies, the predominant mechanism is dipolar rotation of water (Liu et al., 2009; Roebuck et al., 1972).

In general, there are three qualitative ways in which materials may be classified with respect to its microwave absorption: (i) absorbers or high dielectric loss materials which are strong absorbers of microwave; (ii) transparent or low dielectric loss materials where microwave energy passes through the material with little or no attenuation; (iii) opaque or conductors which reflect the microwaves. Hence, knowledge of dielectric properties is necessary to differentiate the materials into the above categories (Chandrasekaran et al., 2013; Yin, 2012).

The relationship between the dielectric properties and microwave power intensity within the product is characterized by penetration depth. Penetration depth of a microwave power is defined as the distance at which the incident power is reduced to 1/e (e = 2.7183) of

its value at the surface of the product, i.e. ~ 63% of the power is absorbed between the surface and this depth (Figure 1.5). Generally speaking, the penetration depth is attenuated exponentially as a function of the penetration distance within the sample.
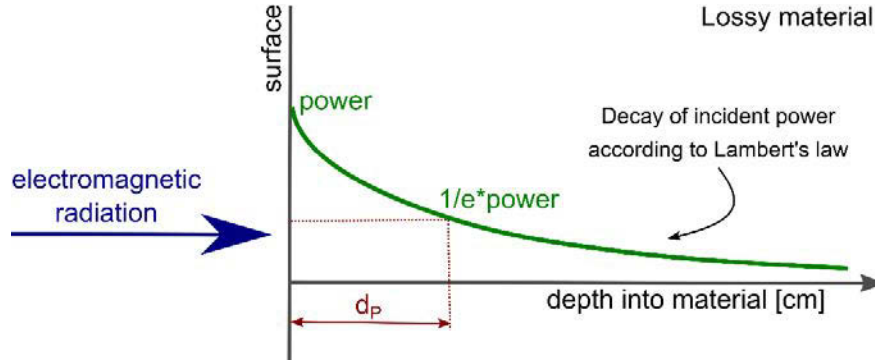
Figure 1.5. Schematic representation of a typical penetration depth inside a lossy material with dimension larger than the wavelength. Adapted from: Komarov et al. (2005).

Therefore, in a lossy food material, penetration depth can be calculated according to the following equation (Curet et al., 2008; Sosa-Morales et al., 2010):

$$d_P = \frac{c_0}{2\pi f \sqrt{2\varepsilon_r'}} \left[\sqrt{1 + \left(\frac{\varepsilon_r''}{\varepsilon_r'}\right)^2} - 1 \right]^{-\frac{1}{2}}$$

Eq. 1.5

where d_P is the penetration depth, ε_r' and ε_r'' are the values of relative dielectric constant and loss factor of solutions, c_0 is the speed of light in free space (c_0 = 2.9979 x 10^8 m s^{-1}) and f is the frequency of the electromagnetic wave. The value of microwave penetration depth can be a useful parameter when designing food package thickness for appropriate microwave heating and also when evaluating heating uniformity (Tang, 2015). For instance, Figure 1.6 illustrates representative ranges of penetration depths for some groups of foods.
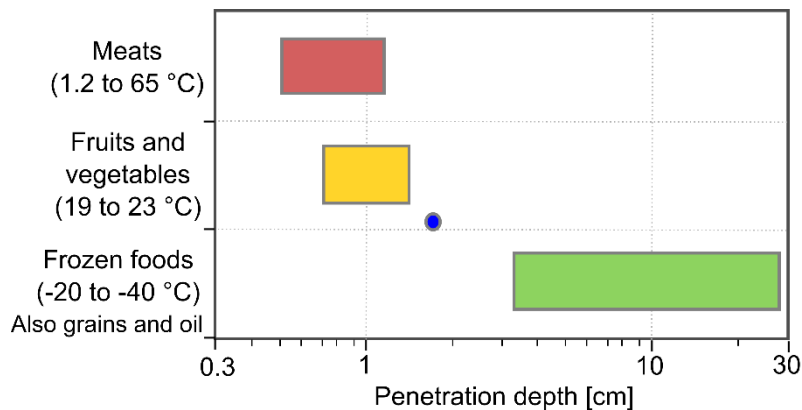
Figure 1.6. Representative ranges of power penetration depth at 2450 MHz in some groups of food materials. Adapted from: Datta (2001).

1.1.2.2.2. Factors affecting dielectric properties

The dielectric properties of food materials are mainly determined by their moisture content and chemical composition, and also by the operating temperature and the microwave frequency used (İçier and Baysal, 2004a; Komarov et al., 2005; Sosa-Morales et al., 2010).

In general, the amount of moisture or water content plays a deciding factor in determining the dielectric properties of most food materials, since water is the major food constituent and is high dielectric material (Venkatesh and Raghavan, 2004). Dielectric behavior is also influenced by other constituents, such as salts. The presence of salts particularly affects the loss factor. Salts dissolved in aqueous solutions act as conductors in an electromagnetic field, promoting ionic conduction and increasing the loss factor when compared with the behavior of pure water (Chandrasekaran et al., 2013; İçier and Baysal, 2004a).

The presence of other solutes and organic material also has an influence on dielectric properties. The intensity and variation of this influence depends on the way in which they are bound or physically restricted by other components of the material, notably water (Venkatesh and Raghavan, 2004). Chemically bound water exerts less influence than free water, in which the polar molecules can orient freely with an applied electric field (İçier and Baysal, 2004a).

Dielectric properties of most materials vary considerably with the frequency of the applied electric field, with exception of some extremely low-loss materials, i.e. materials that absorb essentially no microwave energy (Nelson and Datta, 2001). Note that the penetration depth also depends on the frequency, as can be seen in the Eq. 1.5. Increasing frequency decrease the wavelength and thus the penetration depth, depending on the dielectric properties.

The dependence of dielectric properties on frequency is due to the polarization resulting from the orientation of the dipoles with the electric field (İçier and Baysal, 2004a). As frequency increases, the polar molecules can follow the changes in the direction of the electric field up to a certain point. At high frequencies, the polar molecules have difficulty to follow the oscillation of the electric field, which results in the usual decrease of dielectric constant with increasing frequency.

The dependence of dielectric properties of pure polar liquids, such as water, on frequency can be described by the Debye model. The ideal relaxation of the Debye model for polar molecules with a single relaxation time is illustrated in the Figure 1.7. It can be observed that the loss factor reaches the maximum value at the so-called critical or relaxation frequency. The value of relaxation frequency varies as a function of the material properties. For instance,

it decreases with increasing molecular weight. The larger the molecule size, the lower its mobility and consequently the longer the relaxation time and the lower the relaxation frequency (Komarov et al., 2005). During microwave heating, relaxation is responsible for the heat generation (dielectric hysteresis).
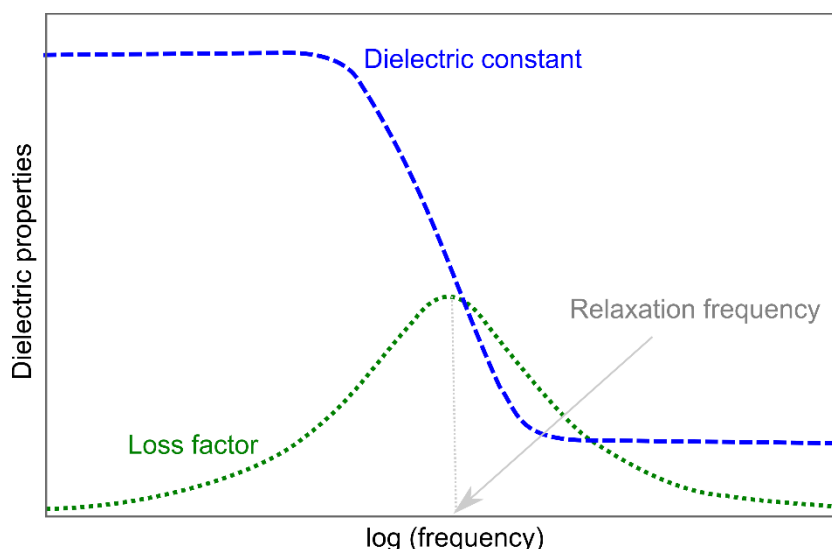
Figure 1.7. Dielectric properties for a polar material with a single relaxation time following the Debye model. Dotted line represents loss factor and dashed line represents dielectric constant. Adapted from: İçier and Baysal (2004a); Nelson and Datta (2001).

At frequencies very low and very high with respect to the polar molecule relaxation process, the dielectric constant has constant values and the losses are zero (Kuang and Nelson, 1998; Nelson and Datta, 2001). However, it is worth to note that Debye model is specifically applied for pure polar materials. Since few materials of interest consist of pure polar materials, other equations may be employed to better describe the frequency-dependent dielectric behavior of foods (Nelson and Datta, 2001).

In relation to temperature, dielectric properties also present great dependence. Dielectric constant and loss factor may either increase or decrease with temperature depending on frequency and temperature range. To illustrate this temperature dependence, general outlines of the dielectric behavior of model solutions containing water, salts and sugars are presented in Figure 1.8. These curves were proposed by Siguemoto and Gut (2016) and was based on Debye model and on the dielectric properties reported in literature. At low frequencies, in the first part of the loss factor curve, a decay with frequency related to ionic conduction mechanism (Eq. 1.4) due to the presence of salts can be observed. Further, loss factor increases with temperature. As the frequency increases until the relaxation frequency, the dominant loss mechanism is dipolar rotation and the loss factor decreases with temperature. A complex trend can also be seen for dielectric constant.
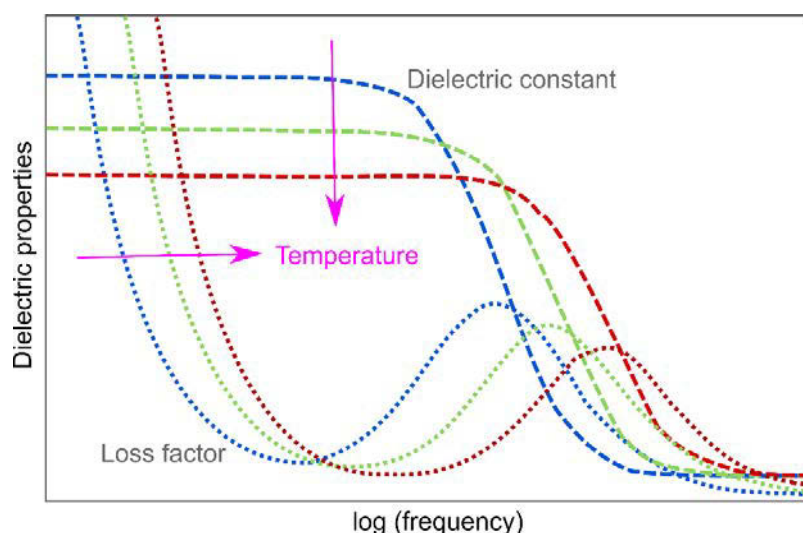
Figure 1.8. General outlines of the dielectric behavior of an aqueous solution of salts and sugars as a function of temperature and frequency. Dotted lines represent loss factor and dashed lines represent dielectric constant. Adapted from: Siguemoto and Gut (2016).

Besides the factors stated above, other ones may also influence the dielectric characteristics of food materials, such as particle size, structure, homogeneity, viscosity and density (Venkatesh and Raghavan, 2004). Particularly in granular or particulate materials, the bulk density of the air-particle mixture is an important factor that influences their dielectric properties (İçier and Baysal, 2004a). Therefore, dielectric properties are not unique for a given material, but they are specific for a given frequency and state of the material (Venkatesh and Raghavan, 2004). Hence, measurements of dielectric properties of a certain product at the desired frequency and temperature are important.

1.1.2.2.3. Measurement techniques of dielectric properties

To choose the appropriate technique for measuring of dielectric properties, some factors need to be taken into account. Among them, the following stand out: the characteristics of the dielectric materials to be measured, the frequency range, the degree of accuracy required, the availability of equipment and resources for the studies (İçier and Baysal, 2004b; Nelson and Datta, 2001). Figure 1.9 presents some techniques and their respective frequency ranges of measurement. In general, three main techniques are usually employed to measure dielectric properties of foods, namely: transmission line technique, resonant cavity technique and open-ended coaxial probe technique.
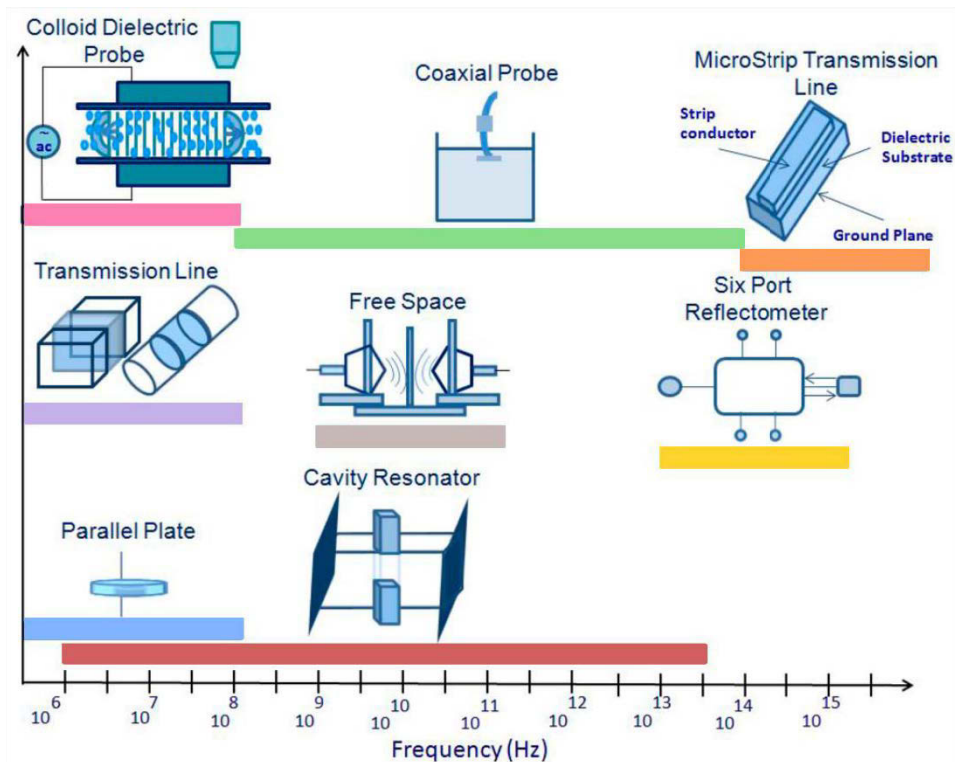
Figure 1.9. Usual techniques for measurement of dielectric properties, indicating the range of operating frequencies. Adapted from: Khaled et al. (2016).

In the transmission line technique, the dielectric properties are measured using the transmission or reflection of waves through a transmission line with the cross-section completely filled by the sample (İçier and Baysal, 2004b; Sosa-Morales et al., 2010). Usually three main types of transmission lines are employed as the measurement cell: rectangular waveguide, coaxial line, and microstrip line (Komarov et al., 2005). This method is best suited for solid or semi-solid samples. In the case of liquid samples and particulates, the system must be configured vertically, taking care in relation to the formation of meniscus on the surface of the liquids and the compaction of the particulates. Dielectric properties of gases are too low for this method (İçier and Baysal, 2004b). The accuracy of transmission line method is generally between that of the open-ended coaxial probe method and that of the resonance cavity method (Komarov et al., 2005). Because of the rigid requirements on sample shape and sizes, the sample preparation is relatively difficult and time consuming (İçier and Baysal, 2004b; Komarov et al., 2005).

The most popular resonant cavity method is based on a comparative analysis of some electromagnetic characteristics between an empty and a partially loaded cylindrical or rectangular resonance cavity (Komarov et al., 2005). In this method, sample preparation is relatively easy, and a large number of samples can be measured in a short time. The resonant cavity method is also easily adaptable to high or low temperatures and is accurate and sensitive (İçier and Baysal, 2004b). However, it does not provide broadband frequency data

and analysis may be complex (İçier and Baysal, 2004b). When the measurements are required at only one microwave frequency, the resonant cavity technique may be a reasonable choice (Nelson and Datta, 2001).

Currently, the open-ended coaxial probe method is one of the most popular techniques for measuring of dielectric properties. It is convenient and easy to use, fast, ideal for liquids and semisolids, nondestructive for many materials, broadband (radio frequency and microwave ranges), and it has no special sample preparation (İçier and Baysal, 2004b; Komarov et al., 2005). This method has been successfully employed for measurements on liquid and semisolid materials of relatively high dielectric losses, which includes most food materials (Nelson and Datta, 2001).

Open-ended coaxial probe method is not recommended for very low-loss materials and it is subject to errors in case of extensive density variations within the material. The technique requires sample thickness greater than 1 cm and flat surface in solid samples to avoid errors due to the presence of air gaps between the end of the coaxial probe and the sample (İçier and Baysal, 2004b; Nelson and Datta, 2001). In general, the surface of solid samples should present roughness of less than 0.5 µm to minimize measurement errors (Arai et al., 1995). The accuracy of this technique is generally limited (±5%), however sufficiently accurate results can be obtained for both medium-loss and high-loss materials (İçier and Baysal, 2004b; Komarov et al., 2005).

The measurement system of this method is based on an open-ended cylindrical coaxial line that is excited by transverse electromagnetic (TEM) wave. Parameters (amplitude and phase) of incident and reflected signals are detected by a network analyzer (Komarov et al., 2005). The complex permittivity (ε^*) is determined according to a reflected coefficient, which is generally calculated by a computational software attached to the system. In order to eliminate the influence of reflections caused by transmission line discontinuities, a calibration procedure is required, which typically consists of measurements of air (open circuit), short (short circuit) and water (or any material with well-known dielectric properties).

1.1.3. Fundamental aspects of electromagnetics

1.1.3.1. Maxwell's equations

Maxwell's equations describe the relation between a time-varying electric field and a corresponding time-varying magnetic field. When coupled with the appropriate boundary conditions, these equations mathematically describe the behavior of the electromagnetic fields inside a microwave applicator (Dibben, 2001; Komarov et al., 2005). Maxwell's equations in

differential form are the most used representation for solving electromagnetism studies and are presented as follows:

$$\nabla \times \overrightarrow{H} = \vec{j} + \frac{\partial \overrightarrow{D}}{\partial t}$$
Eq. 1.6

$$\nabla \times \overrightarrow{E} = -\frac{\partial \overrightarrow{B}}{\partial t}$$
Eq. 1.7

$$\nabla . \overrightarrow{D} = \rho_e$$
Eq. 1.8

$$\nabla . \overrightarrow{B} = 0$$
Eq. 1.9

where $\overrightarrow{H}$ is magnetic field, $\vec{j}$ is electric current density, $\overrightarrow{D}$ is electric flux density, $\overrightarrow{B}$ is magnetic flux, $\overrightarrow{E}$ is electric field and ρ_e is the electric charge density. The first of Maxwell's equations (Eq. 1.6) is the Maxwell-Ampere's law, which indicates that the circulation of magnetic field strength surrounded by a closed contour is equal to the net current through the surface (Chen and Tang, 2011). The second of Maxwell's equations (Eq. 1.7) is Maxwell-Faraday's law, which indicates that the circulation of electric field strength surrounded by a closed contour is determined by the rate of change of the magnetic flux (Chen and Tang, 2011). The third and fourth equations (Eq. 1.8 and Eq. 1.9) are based on Gauss electric law and Gauss magnetic law, respectively.

The interaction of microwaves with matter is expressed by the constitutive relations, where the permittivity, the conductivity, and the permeability appear to model their behavior. The constitutive relations are described as follows:

$$\overrightarrow{D} = \varepsilon_0 \varepsilon_r \cdot \overrightarrow{E}$$
Eq. 1.10

$$\overrightarrow{B} = \mu_0 \mu_r \cdot \overrightarrow{H}$$
Eq. 1.11

$$\vec{j} = \sigma . \vec{E}$$
Eq. 1.12

1.1.3.2. Wave equations and propagation

In order to deduce the wave equations for the electric or the magnetic field, the Maxwell's equations need to be mathematically rearranged. The deduction of the electric field propagation equation is presented below. Note that the same procedure can be transferred to magnetic field.

Firstly, some simplifications of no charge ($\rho_e = 0$) and no current density ($\vec{J} = 0$) were considered. From the Maxwell-Faraday's law equation (Eq. 1.7), the curl-operator ($\nabla \times$) is applied, resulting in the following equation:

$$\nabla \times \left(\nabla \times \vec{E}\right) = -\nabla \times \frac{\partial \vec{B}}{\partial t} = -\frac{\partial \left(\nabla \times \vec{B}\right)}{\partial t}$$

Eq. 1.13

Using the constitutive equation for magnetic field (Eq. 1.11), considering the permeability as constant and combining with Eq. 1.6, it yields:

$$\nabla \times \left(\nabla \times \vec{E}\right) = -\mu_0 \mu_r \frac{\partial \left(\frac{\partial \vec{D}}{\partial t}\right)}{\partial t}$$

Eq. 1.14

Then, employing the constitutive relation for electric field, combining with Eq. 1.8 and using the vector identity to simplify as $\nabla \times \left(\nabla \times \vec{M}\right) = \nabla(\nabla \cdot \vec{M}) - \Delta \vec{M}$, a so-called Alembert's equation is obtained and is expressed as:

$$\Delta \vec{E} - \mu_0 \mu_r \varepsilon_0 \varepsilon_r \frac{\partial^2 \vec{E}}{\partial t^2} = \Delta \vec{E} - \mu\varepsilon \frac{\partial^2 \vec{E}}{\partial t^2} = 0$$

Eq. 1.15

Therefore, by analogy, the propagation equation for the magnetic field is:

$$\Delta \vec{H} - \mu_0 \mu_r \varepsilon_0 \varepsilon_r \frac{\partial^2 \vec{H}}{\partial t^2} = \Delta \vec{H} - \mu\varepsilon \frac{\partial^2 \vec{H}}{\partial t^2} = 0$$

Eq. 1.16

These both last presented equations describe the propagation of an electromagnetic wave along any medium in free space.

1.1.3.3. Propagation of waves in waveguide

For guiding an electromagnetic wave, transmission lines (e.g. coaxial lines) and waveguides can be used. At higher frequencies, such as those of microwaves, waveguide present lower losses and therefore, it is mostly adopted in power applications (Regier and Schubert, 2005). The waveguide is a metal structure that is used to propagate electromagnetic waves in a confined area in order to guide the propagation. It is composed of electrically conductive walls and in most industrial applications, its cross-section is rectangular. The

waveguide is made of metal so that walls almost ideally reflect the electromagnetic waves within the guide (perfect electrical conductor).

There are different modes of wave propagation, however the most common ones are the transverse electric (TE) and transverse magnetic (TM) modes. By definition, the x- and y-axis are respectively parallel to the long and short sides of the guide, also the propagation is established to occur along the z-direction.

In the TM mode, the magnetic field has no component in the direction of propagation ($H_z = 0$), but the electric field does ($E_z \neq 0$). In the TE mode, the electric field has no component in the direction of propagation ($E_z = 0$), but the magnetic field does ($H_z \neq 0$). In order to assure a greater energy transfer, the dimensions of the waveguide are chosen so that the wave propagation occurs according to a single mode, the fundamental mode TE_{01} or TE_{10}. The subscripts numbers denote the number of semi-sinusoidal variations in the x and y directions, respectively. Thus, the TE_{10} mode has one semi-sinusoidal variation in the x direction and is constant in the y direction. TE_{10} is one of the most common propagation modes within rectangular waveguides, whose width a is equal to double the height b (Figure 1.10).
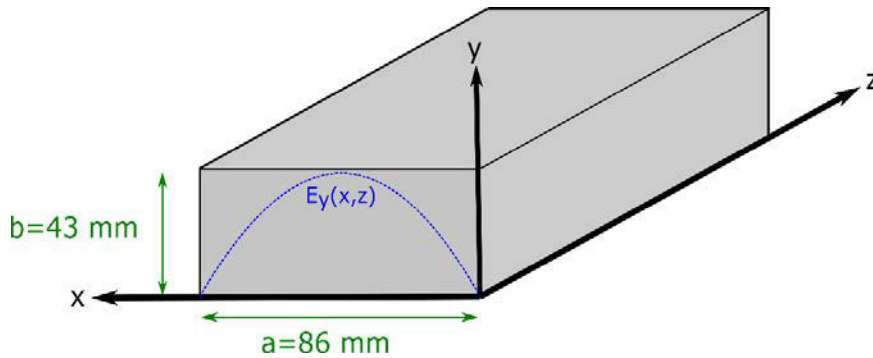
Figure 1.10. Representation of a TE_{10} mode rectangular waveguide (WR340), in which the wave propagation follows the z-direction.

The internal size of the waveguide defines a minimum frequency, the so-called cut-off frequency, below which microwaves do not propagate. Hence, the condition for wave propagation within the waveguide is defined by this value of cut-off frequency (f_c) (Regier and Schubert, 2005). The equation of cut-off frequency can be obtained by the solution of the wave equations (Eq. 1.15 and Eq. 1.16) taking into account the appropriate boundary conditions. For rectangular waveguides with cross-section dimensions a and b, the following equation can be derived:

$$f_c = \frac{\sqrt{\left(\frac{m}{a}\right)^2 + \left(\frac{n}{b}\right)^2}}{2\sqrt{\mu_r \mu_0 \varepsilon_r \varepsilon_0}} = \frac{c_0}{2}\sqrt{\left(\frac{m}{a}\right)^2 + \left(\frac{n}{b}\right)^2} \qquad \text{Eq. 1.17}$$

$$c_0 = \frac{1}{\sqrt{\mu_r \mu_0 \varepsilon_r \varepsilon_0}} = f_c \, \lambda_c$$

<div align="right">Eq. 1.18</div>

where f_c is the cut-off frequency, c_0 is the speed of light in a vacuum, λ_c is the cut-off wavelength; m and n are the numbers associated to the subscripts of different modes (e.g. for a TE mode, $m = 1$ and $n = 0$ correspond to the mode TE_{10}); a and b represent the long (x-axis) and short (y-axis) sides of the waveguide, respectively.

Considering a propagation along the z-direction within a waveguide TE_{10}, the development of the Maxwell-Ampere's law as well as the Gauss law for the electric and magnetic field gives an independence of the variables in the y-axis. Therefore, only the components E_y(x, z) of the electric field are solved. Hence, the wave propagation equation becomes:

$$\frac{\partial^2 E_y}{\partial x^2} + \frac{\partial^2 E_y}{\partial z^2} = \varepsilon\mu \frac{\partial^2 E_y}{\partial t^2} = -\varepsilon_0 \varepsilon_r \mu_0 \omega^2 E_y$$

<div align="right">Eq. 1.19</div>

1.2. Numerical modeling of microwave heating

1.2.1. Numerical approach and methods

Computer simulation of microwave processing by numerical modeling is a very interesting tool in order to evaluate, optimize and scale-up the process, since microwave heating is quite complex and measurements of process parameters in real time is still quite difficult due to the requirement of specific sensors at different locations within the material and the microwave system. Particularly, modeling of the spatial temperature distribution throughout the product is essential to predict the efficiency and lethality of the heating process along the time, therefore ensuring product safety and economical processing.

Partial differential equations are the basis of the physical models that describe the microwave heating process. Analytical solutions of these equations are not easy to derive in case of multidimensional problems, scenarios with realistic boundary conditions or complex shape of boundaries (Knoerzer et al., 2011). Hence, to deal with these difficulties and aspects, an appropriate numerical method need to be selected. There are several numerical techniques for simulating microwave heating, among them two methods have been mainly employed: finite difference time domain method (FDTD) and finite element method (FEM) (Dibben, 2001). Less frequently, the method of moments, the transmission line matrix method, and the boundary element method have also been applied (Chen and Tang, 2011; Knoerzer et al., 2011).

Briefly, FDTD method is a time-stepping procedure that simulates the continuous electromagnetic waves in a finite spatial region until the desired simulation time is attained or a stable field pattern is established (Chen and Tang, 2011). In the FDTD method, Maxwell's equations are solved alternately. The electric field at time t is used to calculate the magnetic field at time $t + \frac{1}{2}\Delta t$, which in turn is used to calculate the electric field at time $t + \Delta t$, and so on (Dibben, 2001). The main disadvantage of this method is due to the use of a regular grid. Also, the FDTD requires excessively large memory especially in the case of complex geometry; the domain should be sufficiently discretized to solve for electromagnetic wavelengths and geometrical features, which leads to long computational times (Choi et al., 2015).

In the finite element method, the studied geometry is decomposed into a union of small elements with simple geometry, usually quadrilaterals or triangles in two dimensions and tetrahedra or hexahedra in three dimensions (Dibben, 2001). Basically, the following four main steps are involved in the FEM: division of the solution region/geometry into multiple subregions or elements; obtention of the partial differential equation in each element; integration of the solutions of all elements into the solution for the entire solution geometry; solution of the obtained linear equations (Chen and Tang, 2011).

Since FEM does not require a regular grid, the decomposition of the geometry is very flexible. In fact, the method has no restrictions even in arbitrary and irregular geometries and it can deal with any types of boundary conditions (Choi et al., 2015). Thus, this method is valuable for very complex geometries (Chen and Tang, 2011). In fact, FEM has been extensively used to solve the microwave heating of foods due to its flexibility in handling irregular geometries and boundary conditions, spatial and temporal properties variations (S. Liu et al., 2013; Romano et al., 2005). Besides, FEM is suitable for solving generic partial differential equation and can be applied to simulate problems in several fields of physics and engineering (Romano et al., 2005).

1.2.2. Modeling of electromagnetism

Modeling is a valuable tool for predicting the time-dependent temperature distribution and electric field strength within the product, thus it is considered a good supportive way to evaluate microwave heating. The dielectric heating model can be based on two main approaches: applying the Lambert's law and solving the Maxwell's equations.

The Maxwell's equations govern the electromagnetic field propagation and the use of these equations depends on the knowledge of dielectric proprieties (Hamoud-Agha et al., 2013; Oliveira and Franca, 2002). The Maxwell's equations were previously presented in Eq. 1.6, Eq. 1.7, Eq. 1.8 and Eq. 1.9. The Lambert's law approach assumes an exponential decay

of microwave absorbed power as a function of penetration depth within the sample (Hamoud-Agha et al., 2013; Vadivambal and Jayas, 2010). In fact, it is an approximation for determining the microwave power intensity (Vilayannur et al., 1998). Differently of the classical Maxwell's equations method, the approach using Lambert's law does not require the calculation of the electromagnetic field within the heated material (Curet et al., 2008).

The application of the Lambert's law can provide numerical results close to experimental measurements, but only under specific conditions. According to Liu et al. (2005) and Curet et al. (2008), calculations using the Maxwell's equations are more rigorous, while the Lambert's law based approaches are less complicated and demand less computational time. The choice of the most appropriate approach varies according to the situation. There are cases in which the application of the Lambert law is possible, and in other cases the complete resolution of the Maxwell's equations is strictly required.

In general, the Lambert's law can be used to evaluate microwave heating for sufficiently thick or semi-infinite samples (Vadivambal and Jayas, 2010). When the thickness of the product in the direction of the microwave propagation is not long enough, heating must be computed from the resolution of the Maxwell's equations (Cheng et al., 1997). In the case of a sample thinner than microwave penetration depth, standing-wave configurations may appear due to reflection and transmission components inside the material, which requires the complete resolution of the electromagnetic field (Curet et al., 2008).

For agar gel cylinders, the Lambert's law approach resulted in a less accurate temperature distribution during microwave heating than the one based on the Maxwell's equations, especially around the sample edge (Yang and Gunasekaran, 2004). Generally for curved geometries, the Lambert's law approach is not appropriate for predicting focusing effect and thus, the complete set of the Maxwell's equations need to be solved (Datta, 2001). Another situation in which the solution of the Maxwell's equations is required to effectively model is the microwave thawing process. Although the Lambert's law prediction of temperature in defrosted phase has showed a good agreement comparing to experimental measurements, it does not predict accurately the power distribution in frozen phase due to the resonance phenomena (Curet et al., 2008).

Oliveira and Franca (2002) conducted a comparison of the power distribution obtained by solving the Maxwell's equation to that by using the Lambert's law. Their results indicated that a relationship between the critical radius (r_{crit}), i.e. the sample radius above which the Lambert's Law can be applied, and the microwave penetration depth (D_P) can be expressed as a linear correlation (Eq. 1.20). Then, according to the authors, as the dimensions of the sample reaches values near to the critical radius, more the difference between the Maxwell's equations and the Lambert's law approaches tends to decrease.

$$r_{crit} = 7.03 \, D_P - 0.0001$$

Eq. 1.20

1.2.3. Modeling of heat transfer

The general equation for heat transfer can be described as follows (Knoerzer et al., 2011):

$$\rho C_p \frac{\partial T}{\partial t} - \nabla \cdot (k \cdot \nabla T) = -\nabla \cdot q_R + Q_{gen}$$

Eq. 1.21

$$Q_{gen} = \frac{1}{2} \omega \varepsilon_0 \varepsilon_r^{''} |E|^2$$

Eq. 1.22

where ρ is the density, C_p is the specific heat capacity and k is the thermal conductivity of the material, q_R is the radiation power flux density, Q_{gen} is the heat generated. The left side of the Eq. 1.21 describes the heat conduction and the terms of the right side represent heat transfer by radiation and heat source by dielectric losses (Knoerzer et al., 2011).

Note that in Eq. 1.21 presented above, the term relative to mass transfer (Fick's law) was neglected. However, when the studied problem present heat transfer due to a mass source (e.g. phase change of water; diffusion or convection), an additional term need to be included and equation becomes (Knoerzer et al., 2005):

$$\rho C_p \frac{\partial T}{\partial t} - \nabla \cdot (k \cdot \nabla T) = -\nabla \cdot q_R + Q_{gen} - \sum_i h_i I_i$$

Eq. 1.23

where I_i mass sink or source density and h_i is the enthalpy of phase i. Evidently, in other specific cases, such as drying process and study of porous material, certain modifications in these equations may be required.

Considering the microwave heating of a conductive fluid material, including convection flow and assuming no mass transfer, the Eq. 1.23 can be simplified to:

$$\rho C_p \frac{\partial T}{\partial t} + \rho C_p \vec{U} \cdot \nabla T - \nabla \cdot (k \cdot \nabla T) = Q_{gen}$$

Eq. 1.24

1.2.4. Modeling of microwave heating of liquid foods

1.2.4.1. Background information

Solving simulations of microwave heating of liquid materials is complex and computational demanding, since it involves the interaction of electromagnetic field, heat transfer and fluid dynamic phenomena. In microwave heating of liquids, a non-uniform volumetric heat source causes changes in temperature which leads to differences of fluid density and hence, to fluid motion by natural convection. In turn, the movement of the fluid modifies the temperature distribution, affecting electromagnetic and heat transfer features. Therefore, due to the complex power distributions and the presence of buoyancy-driven flow, resulting in complex interactions of flow fields and local temperature distributions, the modeling of microwave heat transfer on liquids can be quite complicated (Chatterjee et al., 2007; Zhang et al., 2000).

Previously, the majority of studies concerning modeling of microwave heating have focused on simulating of the heating in a cavity and over solid materials. Now, with the computational advances and software improvements, more and more numerical investigations on microwave heating of fluids have been reported (Chatterjee et al., 2007; Chen et al., 2016; Choi et al., 2015; Curet et al., 2015; Klinbun and Rattanadecho, 2016; Ratanadecho et al., 2002; Salvi et al., 2011; Tuta and Palazoglu, 2017; Yeong et al., 2017; Zhang et al., 2000; Zhu et al., 2007).

Zhang et al. (2000) investigated the microwave heating of two containerized liquids: distilled water and corn oil. In order to study the coupled phenomena of microwave energy absorption, temperatures, and convection driven flows, finite-difference-time-domain and finite control volume methods were used. This study showed the presence of a complicated interaction between the electromagnetic fields, energy and flow fields, and it also illustrated the difference of heating a liquid and heating a solid. Thus, the authors concluded that the convection plays a significant role on the distribution of temperature during heating of liquids.

Salvi et al. (2011) studied a process of continuous flow microwave heating using carboxymethyl cellulose solution (non-Newtonian) and tap water (Newtonian). A numerical model was developed to simulate temperature profiles by iterative coupling of high frequency electromagnetism, fluid flow and heat transfer for both fluids. A similar study was conducted by Tuta and Palazoglu (2017). In their work, the heating of distilled water and carboxymethyl cellulose solutions in continuous-flow microwave unit was simulated. Numerical and experimental results showed that heating was more uniform for water in comparison to carboxymethyl cellulose solutions at all the flow rates tested.

1.2.4.2. Modeling of fluid flow

Governing equations of fluid flow are based on the conservation of mass (continuity equation, Eq. 1.25), momentum (Newton's Second Law, Eq. 1.26), and energy (first law of thermodynamics, Eq. 1.27), and can also be based on state equations (relating the physical properties of materials with process conditions, such as the Boussinesq approximation, Eq. 1.28) (Norton and Sun, 2006; Scott and Richardson, 1997).

The continuity equation is based on the principle of mass conservation. It can be expressed in a differential equation form as:

$$\frac{\partial \rho}{\partial t} + \nabla \cdot \left(\rho \vec{U} \right) = 0$$

Eq. 1.25

where $\vec{U}$ is the velocity vector.

The momentum equation is related to the rate of accumulation of momentum by convection, the rate of accumulation of momentum by molecular transfer and the sum of forces action on the system. The momentum equation is also known as Navier-Stokes equation, however, usually the term Navier-Stokes is used to include not only momentum, but also energy and continuity equations. For a Newtonian fluid, the momentum equation can be expressed as:

$$\rho \frac{\partial \vec{U}}{\partial t} = -\nabla \cdot \left(\rho \vec{U} \times \vec{U} \right) - \nabla p + \nabla \cdot \sigma_{NS} + \vec{\mathrm{B}}$$

Eq. 1.26

where σ_{NS} is the viscous stress tensor and $\vec{\mathrm{B}}$ is the body force. The body force depends on the type of flow. For Boussinesq approximation and for cases in which the only body force is the fluid weight, the body force becomes $\vec{\mathrm{B}} = \rho \vec{\mathrm{g}}$ (Scott and Richardson, 1997).

The energy equation represents the rate of accumulation by convection, the rate of accumulation by conduction and the rate of work done by surroundings on the system. It can be expressed as:

$$\frac{\partial \rho h_T}{\partial t} = -\nabla \cdot \left(\rho \vec{U} h_T \right) + \nabla \cdot (k \nabla T) + \frac{\partial p}{\partial t}$$

Eq. 1.27

where h_T is the total enthalpy, k is the thermal conductivity and p is the fluid pressure. Frequently, the pressure term on the right side of the equation is neglected. In the case of simulation model coupling microwave heating and fluid flow, the Eq. 1.24 is solved instead of the equation above.

An equation of state commonly used is based on Boussinesq buoyancy approximation, in which all fluid properties are assumed to be constant except for the density.

$$\rho = \rho_{ref}\big[1 - \beta\big(T - T_{ref}\big)\big]$$

where β is the thermal expansion coefficient, ρ_{ref} and T_{ref} are the reference density and temperature, respectively.

In computational simulation software, such as COMSOL Multiphysics®, the solution of fluid motion equations can be based on three types of flow: incompressible, compressible and weakly compressible. Liquids are much less compressible than gases. Then, for liquids under certain conditions, the flow can be considered as incompressible. It means that the density is assumed to be constant and continuity equation can be simplified. Generally, in these situations, the Boussinesq approximation is also considered. Nevertheless, in some cases, this approximation cannot be made and the coupling between velocity, pressure and temperature are needed (compressible flow). In other cases, an intermediate scenario can be assumed. The flow can be considered as weakly compressible and the density is dependent on temperature but not on pressure. In this last situation, the momentum equation is thus expressed as:

$$\rho\frac{\partial \vec{U}}{\partial t} + \rho(\vec{U}\cdot\nabla)\vec{U} = \nabla\cdot\left[-pI + \mu\left(\nabla\vec{U} + \left(\nabla\vec{U}\right)^{T}\right) - \frac{2}{3}\mu(\nabla\cdot\vec{U})I\right] - \rho\vec{g}$$

where I is the identity matrix and μ is the viscosity.

1.2.4.3. Some remarks on coupling and product properties

Considering the information presented in the previous sections, for the simulation of a microwave heat processing of liquid foods, the following main governing equations are coupled: electromagnetism (Eq. 1.6, Eq. 1.7, Eq. 1.8, Eq. 1.9), heat transfer (Eq. 1.22, Eq. 1.24), fluid flow (Eq. 1.25, Eq. 1.29).

Overall, in view of the equations presented, it is worth to note the importance of thermophysical and dielectric properties. To simulate and accurately predict the thermal effects of microwave heating processes, equations correlating thermophysical and dielectric properties of food materials to variations of temperature are needed.

As seen in the preceding sections, these properties have an important role in the governing equations. Thus, the use of approximated values by considering these properties

as temperature-independent will most likely result in less accurate results. Furthermore, it also reinforces the importance of coupling electromagnetic, heat transfer and fluid flow during the simulation, since each of these phenomena are interdependent and closely related between each other.

1.3. Microwave heating in food processing and technology

1.3.1. Applications in food processing

The use of microwave heating has been reviewed and conducted for several purposes related to food materials, such as pasteurization, sterilization, blanching, drying, concentration, thawing, tempering, cooking, roasting, extraction of compounds, assistance in freezing process (Ballard et al., 2010; Bozkir and Baysal, 2017a; Cañumir et al., 2002; Chahbani et al., 2018; Dahmoune et al., 2015; Güneş and Bayindirli, 1993; Kim et al., 2018; Luter et al., 1982; Marić et al., 2018; Monteiro et al., 2018; Pérez-Grijalva et al., 2018; Siguemoto et al., 2017; Silva et al., 2006; Simić et al., 2016; Taher and Farid, 2001; Xanthakis et al., 2014); and in other fields of application, such as torrefaction and pyrolysis in biomass and transesterification of lipids (Antunes et al., 2018; Chee Loong and Idris, 2014; Yin, 2012).

In terms of industrial applications, the microwave technology has been largely employed for tempering of meat and poultry, as a pre-processing procedure. In tempering, the hard frozen product (<0 °C) is warmed by microwave application, so that the tempered product (-5 to -2 °C) become softer, allowing to be sliced, diced, ground (Schiffmann, 2001). Conventional tempering results in high gradient of temperature and takes several days to be performed. Whereas microwaves can take only few minutes, for instance 5 – 10 min for 15 – 40 kg of frozen meat (Schiffmann, 2001). Some other industrial and commercial applications of microwave heating technology in food processing are: precooking of bacon, cooking of sausages and meat, drying of potato chips, snacks and vegetables, baking of bread, thawing of frozen products, blanching of vegetables, microwave vacuum drying of fruit juice concentrates, heating, pasteurization of fast food, pasta and cooked meals (Schiffmann, 2001; Vadivambal and Jayas, 2010).

1.3.2. Advantages of microwave compared to conventional heating

Conventional heating relies on the processes of conduction and convection to transfer heat from the heating sources (steam, hot water,…) to the product, which requires relatively longer processing times (Vadivambal and Jayas, 2010). The heat diffuses from outer surface to the core of the product. On the other hand, microwave heating has the potential to deliver

heat throughout the product due to volumetric heat generation, leading to faster heating rates. Heat is generated internally and temperature gradient is inversed compared to conventional heating process. The issue of surface damages in the product due to overheating is thus avoided.

Due to faster heating rates and shorter processing times, microwave heating can generally better preserve thermolabile compounds, maintain antioxidant activity, minimize changes in sensorial attributes including color, texture and aroma (Güneş and Bayindirli, 1993; Guo et al., 2017; Marszałek et al., 2015; Pérez-Grijalva et al., 2018). For instance, Güneş and Bayindirli (1993) reported higher retention of ascorbic acids when vegetables were treated by microwaves in comparison with conventional water blanching. Cano et al. (1997) observed that microwave treatments resulted in slight color changes and small modifications of the quantitative and qualitative composition of carotenoids in papaya and anthocyanins in strawberry.

In the particular case of drying, the use of microwaves may result in lower shrinkage, higher drying and rehydration rates and lower energy consumption than traditional drying methods (Guo et al., 2017; Schiffmann, 2001). For example, Monteiro et al. (2018) found that the recently developed innovative drying process of microwave vacuum drying produced pumpkins slices with porous structure in very short process times. The drying times were at least twelve times shorter compared to the traditional air-drying method.

In the context of the application of microwave technology for enzyme and microbial inactivation, some authors have been claimed the existence of non-thermal effects. In this way, these effects would be complementary to the thermal effects and the microwave processing would provide greater efficiency of inactivation. Nevertheless, this topic is still very contradictory in the literature. In section 1.3.4.1, the non-thermal effects are presented and discussed in more detail.

Another advantage attributed to microwave heating systems is the non-requirement of an intermediate heating fluid or additional equipment or infrastructure, such as steam boilers. Moreover, the use of microwave systems may also result in reduced cleaning times and volume of waste water. Therefore, microwave heating is a promising technology due to lower energy and water consumption, higher energy efficiency, faster heating time, cleaner work environment, reduced use of plant, potential to deliver safe foods of high nutritional and sensory quality.

1.3.3. Limitations and microwave heating uniformity

There are many factors that affect microwave heating and its heat distribution. Among them, there are dielectric properties, which in turn, may vary with food material density,

chemical composition, moisture content, microwave frequency, temperature and others (Chandrasekaran et al., 2013; Kubo et al., 2018a; Salvi et al., 2009). In an experimental and numerical study, Cheng et al. (1997) evaluated the temperature distribution during microwave heating of cylindrical samples containing various model components (agar gel, bentonite paste, mashed potato and synthetic paste) with different dielectric properties. Temperature distributions changed with dielectric properties and hot spots moved from the surroundings of the cylinder to the center as the penetration depth increased. Thus, their results confirm the influence of dielectric properties on temperature distribution during microwave heating.

Moreover, besides dielectric properties, the heat transfer and temperature distributions also depends on the microwave cavity design (size and geometry), electric field distribution, frequency and power of the incident electromagnetic wave, placement of material inside the oven, load, shape and the size of food materials, thermal conductivity, specific heat, viscosity (Anantheswaran and Liu, 1994; Salvi et al., 2009; Vadivambal and Jayas, 2010).

For example, Vilayannur et al. (1998) studied the effect of size and shape using potato samples of different shapes (brick-, cylinder-, and hexagonal prism-shaped) and sizes/volumes (75, 90, and 105 cm^3). By means of a finite element model, the authors found different patterns of temperature distribution depending on shape and size. For the cylinder, hot spot was at the center. However, in the hexagonal prism-shaped product, the center was cold and the hot spots were found along the boundary. In the brick-shaped products, hot spots were at the corners and cold spot was at the geometric center. The lowest non-uniformity of temperature was found in the case of hexagonal prism-shaped products, while the highest non-uniformity was observed in cylindrical products of low volumes (75 cm^3).

Uniform and effective heating depend on the proper integration of all these parameters at the same time. Due to the large number of factors which influence the process, it is difficult to obtain a desired uniform temperature distribution. Even though dielectric heating is generally considered as more uniform than many conventional heating methods, non-uniform temperature distribution is one of the major drawbacks associated with the microwave heating (Chandrasekaran et al., 2013; Chen et al., 2014; Vadivambal and Jayas, 2010).

Non-uniform heating is especially problematic for solid foods and frozen foods under thawing (since the transition from ice to water produces a huge increase in the loss factor). In liquid foods, the problem also occurs but it may be less severe because the differences in temperature may be attenuated by mixing and convective fluid motion. However, the extent of convective flow critically depends on thermal, physical and dielectric properties of the material. For instance, an increase in viscosity reduces the natural convection, then decreasing the associated fluid mixing and leading to more uneven temperature distribution (Prosetya and Datta, 1991).

Non-uniformity is a limiting factor that restrain the broad application of microwave technology in the industry. The non-uniform temperature distribution not only affects the energy efficiency of the microwave processing (due to overheating of hot spots) but also raises the issue of food quality and safety when the undesirable enzymes and microorganisms may not be inactivated in the cold spots within the heated product. As thermal effects remain the main lethal mechanism known in microwave processing, non-uniform heating likely results in non-uniform inactivation. For solid product experiencing microwave drying processing, uneven temperature distribution may cause non-uniformity in moisture distribution, which results in selective drying of certain portions, affecting the product texture (Vilayannur et al., 1998).

Some propositions for heating uniformity improvement have been reported. Some authors proposed: the use of mode stirrers and turntables (Cinquanta et al., 2010; Cuccurullo et al., 2017; Kurniawan et al., 2015; Ye et al., 2017), the manipulation of the heat cycle and performance of pulsed heating (Datta, 2001; Gunasekaran and Yang, 2007), the control of sample geometry (Vadivambal and Jayas, 2010; Vilayannur et al., 1998), the processing at lower frequencies (896 or 915 MHz instead of 2450 MHz) to increase penetration depth, and the combination of microwaves with infrared or hot air, in particular for drying processes (Guo et al., 2017; Ren and Chen, 1998). Operating in continuous or semi-continuous systems using conveyor belts or pipes instead of batch systems has also been suggested (Atuonwu and Tassou, 2018). However, it should be remembered that these propositions to reduce non-uniformity were based on specific conditions of each product and process, and therefore cannot be generalized for any application.

1.3.4. Microwave heating for enzyme inactivation

In order to minimize the undesirable effects (e.g., off-flavors, nutrient destruction and color changes) caused by conventional thermal methods, microwave heating has been considered as an interesting alternative technology for enzymatic and microbial control in foods with certain thermal sensibility, such as fruit and vegetable products (Kim et al., 2018; Latorre et al., 2012; Pérez-Grijalva et al., 2018; Stratakos et al., 2016).

It has been reported the application of microwave heating to inactivate various food enzymes relevant for fruit beverage industry such as peroxidase (POD), polyphenoloxidase (PPO) and pectinmethylesterase (PME) (Benlloch-Tinoco et al., 2013; Cinquanta et al., 2010; Huang et al., 2007; Matsui et al., 2008; Nikdel and Mackellar, 1992; Siguemoto et al., 2018b; Tajchakavit and Ramaswamy, 1997; Villamiel et al., 1998; Zhou et al., 2016).

In a study of processing of fresh cloudy apple juice by continuous flow microwave assisted pasteurization using a pilot scale unit, Siguemoto et al. (2018a) evaluated the POD, PPO and PME inactivation. Thermal history was integrated and inactivation kinetics was

considered to follow first order with two fractions. According to the authors, microwave heating allowed the desired process temperature to be achieved much faster than using a tubular heat exchanger, being closer to the ideal case of instantaneous heating.

Matsui et al. (2007) evaluated POD and PPO inactivation in coconut water model solutions, verifying the influence of the major chemical constituents (sugars and salts) of coconut water on enzyme activities. According to their results, sugars influenced POD more than PPO inactivation and salts significantly affected enzyme stability. At temperatures above 90 °C, the combined effect of salts and microwave heating reduced PPO and POD enzymatic activity to undetectable levels.

In another study, Matsui et al. (2008) studied the inactivation kinetics of enzymes PPO and POD for batch microwave treatment of green coconut water. Based on time-temperature profiles of the experimental runs, the kinetic parameters were determined and all data were fitted by a first order kinetic model. The authors also observed that the thermal inactivation of PPO and POD during microwave processing was significantly faster in comparison to conventional processes reported in the literature.

The results presented by Benlloch-Tinoco et al. (2013) indicated that microwave heating of kiwifruit puree was more effective for POD, PPO and PME inactivation than conventional thermal processing. Moreover, batch microwave treatment resulted in lower loss of antioxidant capacity. Tajchakavit and Ramaswamy (1997) also observed that batch microwave treatment was remarkably more effective by comparing the D-values of orange juice PME inactivation under the conventional and microwave heating modes.

In view of the reported studies that show a greater efficiency of microwave heating processing in comparison with conventional thermal processing, such as those mentioned above, the existence of non-thermal or enhanced effects of microwaves have been the subject of intense debate. Contradictory results have been reported and some theories have been proposed in the literature.

1.3.4.1. Non-thermal effects of microwaves

The possible existence of non-thermal effects is certainly a very controversial subject. This is mainly related to the complexity of the phenomenon of microwave heating, which depends on several factors, as previously described this chapter. The complication of the topic already begins with the definition of the terms used in each study. According to Anantheswaran and Ramaswamy (2001) and Ramaswamy et al. (2002), during the microwave processing four types of effects may exist: thermal, non-thermal (or athermal), enhanced and specific effects.

Thermal effects are those that can be explained by the rise of temperature. These effects are well-accepted and heat is the responsible to inactivate microorganisms and enzymes and degrade compounds in the same way as conventional thermal processes. Non-thermal effects of microwaves refer to effects that cannot be explained by macroscopic temperature increase, time-temperature histories or temperature gradients (Ramaswamy et al., 2002). The cases in which microwave heating results in a particular time-temperature profile and gradients that cannot be achieved by other methods are specific microwave effects (Shamis et al., 2012). The definition of enhanced thermal effects was based on the organic reactions in which microwave heating does not alter the reactions but simply provide faster and efficient method of carrying out the reactions (Anantheswaran and Ramaswamy, 2001; Ramaswamy et al., 2002).

In a practical point of view, these terms are quite confusing and the distinction between each one may not be possible experimentally. Therefore, in this work, as most of studies in the literature, the term non-thermal effects includes all the effects of microwaves except for thermal effects. Thus, an overview of controversial studies dealing with non-thermal effects of microwaves is presented below.

Extensive research has been conducted to determine the existence of non-thermal effects and to measure the extent of the phenomenon if it exists. Such effects are claimed to change the chemical, biochemical or physical behavior of some systems due to microwave exposure and interaction of the electric field with specific molecules in the reaction medium (Huang et al., 2009). Several studies have been carried out using different experimental procedures and designs, approaches, techniques and systems of study to assess and possibly distinguish thermal and non-thermal effects.

Shazman et al. (2007) evaluated different chemical, biological and physical systems in high microwave radiation intensity system (2.45 GHz, up to 1000 W/kg, with continuous radiation up to 48 h). The systems that were tested included: Maillard reaction, protein denaturation and polymer solubility, mutagenesis of bacteria, mutarotation equilibrium of D-glucose, and saturation solubility of sodium chloride. No significant non-thermal effects was observed in any of the evaluated systems.

With respect to microbial inactivation, some researchers found evidences that support the existence of non-thermal effects. Dreyfuss and Chipley (1980) studied the effects of microwave radiation at 2.45 GHz on metabolic cellular activity of *Staphylococcus aureus* at maximum temperature of 46 °C. The results were compared with conventional heating and considerable differences were found. The authors thus reported the possible existence of non-thermal effects. However, since the temperature was not very well controlled during heating, the accuracy of the reported results may be questionable.

Zhang et al. (2012) designed a microwave coaxial cavity in which the sample was subjected to very high electric field (in order of 10^6 V m^{-1}) at 100 W power level and 2.45GHz frequency. High inactivation rate of *Escherichia coli* was observed without much raise in temperature (8.6 °C), suggesting the existence of non-thermal effects.

In a study on the effects of microwave radiation (at 18 GHz) under sublethal temperature (<40 °C) on *Escherichia coli*, Shamis et al., (2011) observed that bacteria cells exhibited a cell morphology significantly different from that of the conventional heating. However, scanning electron microscopy also showed that this effect was temporary, since morphology appeared to revert to its initial state after some minutes from microwave exposure. The authors proposed that microwave exposure can cause an electrokinetic modification, resulting in more porosity within the cell membrane. Alterations in cell membrane at low temperatures was also observed by Rougier et al. (2014).

On the other hand, Kozempel et al. (2000) did not find evidences of non-thermal effects. The authors employed a microwave continuous system with an inner cooling tube to remove the thermal energy and to control temperature at below 45 °C. The process was carried out at turbulent flow to assure a uniform temperature. No detected nonthermal effects of microwaves were observed for yeast, *Pediococcus* sp., *Escherichia coli*, *Listeria innocua*, or *Enterobacter aerogenes* in various test fluids, such as water, liquid egg, beer, apple juice, apple cider, and tomato juice. The absence of non-thermal effects was also reported in the inactivation of spores of *Clostridium sporogenes* (Welt et al., 1994).

Regarding enzyme inactivation, as observed in microbial inactivation, there are some studies that support the existence of non-thermal effects of microwaves, while others do not. Among the studies that reported the occurrence of effects that cannot be explained by temperature increase, one can cite the work of Latorre et al. (2012). The authors evaluated the inactivation of PPO and POD in red beet by traditional and microwave heating treatments. Since faster enzyme inactivation was found at microwave-treated samples compared with conventionally processed samples subjected to similar temperature, it could be inferred the existence of an additional non-thermal effects of microwaves.

In a study reported by Lin and Ramaswamy (2011), raw milk was subjected to conventional isothermal water bath heating, continuous flow microwave heating and continuous flow thermal holding, and alkaline phosphatase residual activities were evaluated. Inactivation data were assessed and adjusted to a first order model. No significant enzyme inactivation was observed at lower temperatures (<60 °C) with short residence times during continuous flow microwave heating. Thus, there was no evidence for the existence of non-thermal effect under these conditions. However, at higher temperatures (65 – 70 °C), enzyme inactivation under continuous-flow microwave heating occurred much faster than conventional

heating, indicating the existence of additional effects associated with microwave heating. Similar results were reported for PME in orange juice (Tajchakavit and Ramaswamy, 1995).

According to Kermasha et al. (1993a, 1993b), who reported non-thermal effects due to microwave heating on soybean lipoxygenase and wheat germ lipase, the protein molecules containing polar and charged fractions can be affected by the electric field. As a result of a strong and random electromagnetic field, the disruption of non-covalent bonds such as hydrophobic, electrostatic and hydrogen bonds can occur. However, other authors state that microwaves cannot break any chemical bonds due to lack of energy, unlike ultraviolet, visible and probably infrared rays that can provide enough energy to break weak hydrogen bonds (Ramaswamy et al., 2002).

Another theory to explain the non-thermal effects of microwaves on enzymes is based on conformational alterations. Bohr and Bohr (2000) studied the conformational changes of the protein β-lactoglobulin during microwave exposure at 2.45 GHz and incident power of 800 W. It was found that microwave could induce denaturation/refolding. The same observation could not be replicated using conventional heating at similar temperature profiles, thus indicating that microwave effect was non-thermal. Similar findings were reported by De Pomerai et al. (2003). Alterations in protein conformation when exposed to microwave radiation without measurable temperature changes were observed in bovine serum albumin. Lopes et al. (2015) reported that in the case of horseradish peroxidase, the glycosylated regions of the enzyme may be a good microwave radiation absorber material. Its dipole may quickly reorient under microwave, destroying the three dimensional structure of the enzyme, more severely as compared with conventional heating.

On the other hand, some studies did not detect the occurrence of non-thermal effects of microwaves. For example, Xu et al. (2016) evaluated the inactivation kinetics of lipase and lipoxygenase from wheat germ. The samples were treated by conventional heating in a water bath and by microwave heating in a single mode focused microwave system operated at 2.45 GHz. Comparing the results of both treatments, no significant differences were observed and hence, no evidence of non-thermal effects was found. Similar findings were reported by Chen et al. (2016) for wheat germ lipase and by Galvin et al. (1981) for acetylcholinesterase and creatine phosphokinase activities at sublethal temperatures.

Siguemoto et al. (2018b) also did not reported the existence of non-thermal effects when evaluating the inactivation of PPO, POD and PME in cloudy apple juice by microwave processing. In fact, in their work, very small differences between conventional and microwave results were found. For instance, for the temperature of 70 °C, the average difference between the predicted residual enzymatic activity for both treatments was less than 2% for PME, 3% for PPO and 2% for POD. The existence of non-thermal effects was then discarded due to the low values and the prediction uncertainties.

1.4. Enzyme inactivation

Depending on the process temperature and product, some microorganisms can be inactivate more easily than certain enzymes (Dorantes-Alvarez and Parada-Dorantes, 2005). Hence, the evaluation of the processing efficiency can be carried out by monitoring the inactivation of thermoresistant enzymes. For instance, peroxidase and pectin methyl esterase activity has been used to determine the adequacy of blanching and of fruit juice pasteurization, and alkaline phosphatase inactivation has been used to verify the pasteurization of milk (Gonçalves et al., 2007; Lin and Ramaswamy, 2011).

1.4.1. Enzyme inactivation kinetics

The thermal inactivation curve for enzymes is obtained by subjecting a sample containing the enzyme to specific process condition, and then testing for residual enzyme activity. Generally, an exponential decrease with time in the inactivation curve is observed, indicating a first order reaction (Eq. 1.30).

$$\frac{A}{A_0} = e^{-kt} \text{ , at constant temperature} \qquad \text{Eq. 1.30}$$

where A/A_0 is the residual enzymatic activity, k is the reaction rate constant and t is the independent variable expressed as the treatment time. The temperature dependence of the rate constant is described by an Arrhenius equation.

In food processing, first-order reactions can be also expressed in terms of D_T and z values. Hence, the residual activity can be written as:

$$log\left(\frac{A}{A_0}\right) = -\frac{t}{D_T} \text{ , at constant temperature} \qquad \text{Eq. 1.31}$$

with:

$$e^{-kt} = 10^{-t/D_T} \qquad \text{Eq. 1.32}$$

$$k(T) = \frac{ln10}{D_T} \qquad \text{Eq. 1.33}$$

where D_T value is the time required for a 90% reduction of the enzymatic activity under isothermal conditions at a given temperature. The effect of temperature on the D_T value is

expressed as a z value, which is the temperature increase that reduces D_T by 90%. This relationship can be described by:

$$log\left(\frac{D_T}{D_{Tref}}\right) = \frac{T_{ref} - T}{z}$$

Eq. 1.34

Thus, the parameter z is considered as a reference of the heat resistance of enzymes. Its value can be obtained be plotting the logarithm of D_T versus temperature.

Several studies have reported the use of first order kinetic model to describe the denaturation of different enzymes, including peroxidase (POD), polyphenoloxidase (PPO), pectinmethylesterase (PME), lipoxygenase (LOX). For instance, this model was found suitable to describe the inactivation of: lipase and LOX from wheat germ (Xu et al., 2016), PPO and POD from coconut water (Matsui et al., 2008), POD from tomato juice (Ercan and Soysal, 2011), PME from orange juice (Nienaber and Shellhammer, 2001), polygalacturonase from carrot (Anthon et al., 2002), tyrosinase from mushroom (Labus et al., 2015), amylase from apple juice (Riahi and Ramaswamy, 2004), POD from potatoes (Yu et al., 2010), among others.

Nevertheless, deviations from first order kinetic model can be observed in certain enzymes and conditions. These deviations may be explained by the fact that plants naturally present multiple forms of the same type of enzyme (the so-called isozymes or isoenzymes) (Thongsook and Barrett, 2005). Even if these isozymes catalyze the same reaction, they may show different thermal resistance behavior. In this way, an alternative model has been proposed, although still based on first order kinetics. The first order two-fraction (biphasic) inactivation model was developed assuming the presence of two groups of isozymes with different thermostability: one group more thermoresistant (denoted as R) and another more thermolabile (denoted as S), both following first order inactivation kinetics, as shown below (Fujikawa and Itoh, 1996; Ling and Lund, 1978).

$$\frac{A_t}{A_0} = \alpha . e^{(-k_S.t)} + (1 - \alpha) . e^{(-k_R.t)}$$

Eq. 1.35

where α is the relative resistance of the sensible enzyme portion and the subscripts S and R indicate respectively the sensitive and resistant fractions.

The two-fraction model has been successfully used to describe the inactivation kinetics of different enzymes from several fruit and vegetable products. For example, the literature describes the inactivation of: POD and LOX from broccoli, green asparagus and carrots (Morales-Blancas et al., 2002), POD from blueberry (Terefe et al., 2017), POD from

cowpea leaves (Wawire et al., 2016), POD, PPO and PME from apple juice (Siguemoto et al., 2018b), POD and PPO from green coconut (Murasaki-Aliberti et al., 2009), POD from carrot (Soysal and Söylemez, 2005), PME from carrot (Ly-Nguyen et al., 2003), LOX from tomato (Anese and Sovrano, 2006).

Considering that enzymes are complex protein structures and several different phenomena may be involved during the inactivation process, first order and two-fraction kinetic models may not be always enough to properly describe the inactivation of enzymes (Rudra Shalini et al., 2008). In such cases, empirical models as the Weibull distribution model have been proposed as alternative models. Initially, the Weibull distribution was used in engineering science to predict the time of failure of electronic or mechanical system (Rojas et al., 2017). Later, it was adapted to model microbial survival curves and enzyme inactivation (Aragao et al., 2007; Peleg and Cole, 1998).

The Weibull frequency distribution function applied for enzymatic inactivation can be expressed as follows:

$$log\left(\frac{A_t}{A_0}\right) = -\left(\frac{t}{\delta_T}\right)^{\beta}$$

Eq. 1.36

where δ_T represents the time for the first decimal reduction at a given temperature T and β is the parameter that indicates the shape of the inactivation curve. In a semi-log plot, $\beta > 1$ indicates that the curve has a convex shape and $\beta < 1$ indicates that the curve has a concave shape. In the case when $\beta = 1$, the curve is log-linear and the parameter δ_T is equivalent to D_T from the first order model (Rojas et al., 2017).

According to Rudra Shalini et al. (2008), Weibull distribution is a stochastic model that is sufficiently flexible to account for enzyme inactivation at different processing conditions. Some studies have been reported the use of models based on Weibull distribution to successfully describe enzyme inactivation after different processing technologies. For example, one can cite the inactivation of: POD from coconut water (Rojas et al., 2017), commercial pectinesterase (Giner et al., 2005), POD from mint leaves (Rudra Shalini et al., 2008) and POD form orange juice (Elez-Martinez et al., 2008).

1.4.2. Peroxidase

1.4.2.1. Characteristics and importance in food processing

Peroxidase (POD, donor: hydrogen peroxide oxidoreductase, EC1.11.1.7) is a heme-containing enzyme which catalyzes oxidation reactions using either peroxides or oxygen as

hydrogen acceptor (Stanciuc et al., 2015). POD is widely distributed in plants, but it is also found in some animal tissues and in microorganisms. Depending on its source, POD can be present in different forms (isozymes), presenting different characteristics in terms of structure and stability.

The presence of POD in many fruits and vegetables is associated to enzymatic browning and reduction in sensory quality. Its catalytic action produces a deteriorative effect in non-treated fruit and vegetable products, since it contributes to browning action and other oxidative reactions. In fact, peroxidase catalysis is associated with four types of activity: peroxidatic, oxidatic, catalatic, and hydroxylation (Dorantes-Alvarez and Parada-Dorantes, 2005).

Peroxidatic activity on phenolic compounds, such as ferulic acid, can generate phenolic crosslinks that connect polymer chains; this action affects the mechanical properties of cell walls and therefore the texture of vegetables (Dorantes-Alvarez and Parada-Dorantes, 2005). Its activity can also cause chlorophyll degradation. The mechanism of POD in chlorophyll degradation is based on the oxidation of phenolic compounds in the presence of hydrogen peroxide, resulting in phenoxy radical. These phenoxy radical then oxidizes chlorophyll to colorless low molecular weight compounds through the formation of C13-hydroxy- chlorophyll-a and a bilirubin-like compound as an intermediate (Rudra Shalini et al., 2008).

Because of its relatively high thermal stability and relative simplicity of the activity assay method, the POD activity is generally used as an index of proper blanching of vegetables and of thermal processing efficiency (Anese and Sovrano, 2006; Dorantes-Alvarez and Parada-Dorantes, 2005; Stanciuc et al., 2015). Some studies reported that the presence of a heme group might provide the rigidity of the structure of the enzyme, thereby contributing to the conformational stability under denaturing conditions (Cha et al., 2017). Figure 1.11 shows an example of a horseradish POD structure, indicating the localization of the heme group.
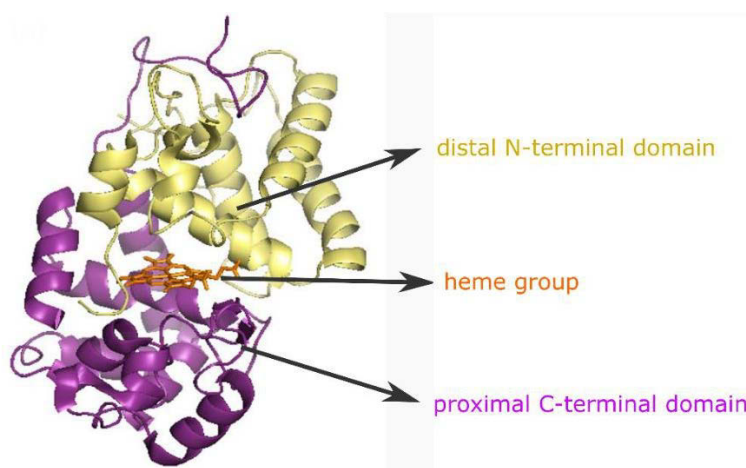
Figure 1.11. Representation of horseradish peroxidase structure. Adapted from: Cha et al. (2017).

1.4.2.2. Inactivation mechanisms and kinetics

It has been hypothesized that the inactivation of POD involves three steps, namely: dissociation of the prosthetic (heme) group from the holoenzyme (active enzyme system); conformational change in the apoenzyme (protein part of the enzyme); and modification or degradation of the prosthetic group (Anthon et al., 2002; Lemos et al., 2000; Tamura and Morita, 1975; Terefe et al., 2017).

The heme dissociation is pH dependent and the release of this group from the enzyme can occur more rapidly at low pH values (below 5). Some studies reported that the irreversible inactivation at acid pH is due to the irreversible changes in the apoenzyme. Therefore, POD may be more susceptible and sensitive to thermal inactivation at low pH. Besides it can be inferred that inactivation kinetics is a result of a relative equilibrium between these mechanisms of inactivation (Lemos et al., 2000). As pH increases, detachment of the heme group become less important and conformational changes are the main responsible for inactivating the enzyme. At neutral pH, POD show higher stability (Anthon et al., 2002; Lemos et al., 2000).

Besides pH, other factors may also affect the inactivation of POD. For example, the variation of composition, such as sugar and salt content, was found to be a factor that considerably influences the inactivation kinetics of POD (Chang et al., 1988; Lu and Whitaker, 1974; Marshall et al., 1985; Matsui et al., 2007; Tan et al., 2014). In general, the enzymatic thermostability and inactivation kinetic of enzymes can also be dependent on origin of enzymes, incidence of multiple isozymes, presence of acids and organic compounds, process conditions (Liu et al., 2013; Marszałek et al., 2016).

The inactivation kinetics of peroxidase from different sources have been described by first order, two-fraction and Weibull models. The use of first order model was reported to describe the inactivation of POD from: coconut water (Matsui et al., 2008), tomato juice (Anthon et al., 2002; Ercan and Soysal, 2011), potatoes (Yu et al., 2010), red beet (Latorre et al., 2012), broccoli (Thongsook and Barrett, 2005), horseradish (Joffe and Ball, 1962; Matsui et al., 2007; Rodrigo et al., 1997).

Generally, simple first order model is usually less suitable for POD from crude plant homogenates because most plants contain multiple isoforms of the enzyme. Then, the application of two-fraction model has been more predominant. For example, the use of first order two-fraction model was reported to describe the inactivation of POD from: broccoli, carrot and potato (Połata et al., 2009), broccoli, green asparagus and carrots (Morales-Blancas et al., 2002), blueberry (Terefe et al., 2017), cowpea leaves (Wawire et al., 2016), apple juice (Siguemoto et al., 2018b), carrot (Soysal and Söylemez, 2005), watercress (Cruz et al., 2006), horseradish (Ling and Lund, 1978; Machado and Saraiva, 2002; Stanciuc et al., 2015).

The application of Weibull model is more frequent in works dealing with thermal and non-thermal processing or emerging technologies. For example, this kinetic model was found to describe the inactivation of POD from: coconut water (Rojas et al., 2017), tomato (Elez-Martinez et al., 2008), mint (Rudra Shalini et al., 2008), horseradish (Sampedro and Fan, 2014).

1.4.2.3. Reactivation after processing

It has been reported in literature that, under certain conditions, POD can reactivate (i.e. regenerate, partly recover its enzymatic activity) after processing during storage, which may results in development of off-flavors and other sensorial damages (Lu and Whitaker, 1974; Tamura and Morita, 1975). According to Lu and Whitaker (1974), this issue occurs more frequently when the product is processed by high temperature-short time treatment.

The reactivation is a complex process and its occurrence depends on several factors, such as operational treatment conditions, origin of enzymes, type of isozymes, pH, food matrix, and enzyme molecular weight (Rodrigo et al., 1997; Siguemoto et al., 2018b; Thongsook and Barrett, 2005). Some authors suggest that the recovery of activity might be related to: the fraction of ionically bound isoperoxidases, the dissociation/reassociation of the heme group from/to the enzyme, the conformational change from a reversible denatured form to native form, the refolding capacity (Machado and Saraiva, 2002; Siguemoto et al., 2018b; Tamura and Morita, 1975).

Machado and Saraiva (2002) evaluated the reactivation of horseradish POD and used a logarithmic model to fit the experimental data. The authors observed that there was evidence that the reactivation rate was dependent on the amount of intermediate enzyme forms obtained and remained after inactivation. Rodrigo et al. (1997) also studied the reactivation of horseradish POD and they reported that as the severity of the treatment increased, the absolute value of the reactivation decreased. Also, they verified the influence of storage temperature on reactivation rate and reported that the reactivation occurred more rapidly when the storage temperature was higher.

1.5. Conclusions

The literature review presented in this chapter brings into perspective the main aspects associated to the simulation of a microwave processing aiming enzyme inactivation, which is the main purpose of this work. Firstly, the principles of microwave technology were discussed. A summarized presentation on how the microwaves interact with the material and

what are the factors that influence this interaction was shown, highlighting the importance of dielectric properties of the material on microwave heating. The principles involving electromagnetism and wave propagation were also briefly presented. In particular, the propagation within rectangular waveguides was evidenced, since such structures were used in the microwave systems employed in the experimental part of this work.

Then, after covering the theoretical basis of microwaves and electromagnetism, the topic concerning numerical simulation was introduced. Considering that the focus of this work was to simulate a processing of fruit juice by microwave heating, the physical modules described were: electromagnetism, heat transfer and fluid flow. The implementation and coupling of these three modules are necessary for the simulation. Thus, the main governing equations of these phenomena were shown.

In the next section, the use of microwave technology in food processing was addressed, presenting the main applications in both research and industry, as well as the advantages and drawbacks of microwave heating. In particular, the use of microwave heating for enzymatic inactivation was presented. Moreover, the controversial existence of possible non-thermal effects on enzymatic and microbial inactivation was discussed, reporting some results and theories of studies already performed.

Finally, in the last part of this chapter, the enzyme inactivation was further covered. The main inactivation kinetics models were presented. Then, since the purpose of this work is to study the microwave processing for peroxidase inactivation, some important features specifically of the enzyme peroxidase were presented. The kinetics of peroxidase inactivation and its potential reactivation ability were presented and exemplified based on the existing literature.

CHAPTER 2.   DEPENDENCE OF DIELECTRIC PROPERTIES ON COMPOSITION, FREQUENCY AND TEMPERATURE FOR FRUIT JUICES SOLUTIONS [1]

2.1. Introduction

Dielectric properties are the important parameters that provide information about the interaction between the electromagnetic energy and foodstuffs during microwave heating. Knowledge of the dielectric properties is not only useful for designing process and packaging conditions, but also for the mathematical modeling of microwave processes. Thus, this chapter is dedicated to the study of dielectric properties.

Firstly, the dependence of dielectric constant and loss factor on composition, temperature and frequency were evaluated. For this purpose, the dielectric properties of fruit juice model solutions with different total soluble solids (TSS) content (between 5 and 65 °Brix) were measured over a wide range of frequencies (between 200 and 3000 MHz) at different temperatures (between 20 and 80 °C, at 10 °C intervals). The results were interpreted and discussed, presenting the possible mechanisms involved.

Then, the dielectric properties of commercial fruit juices were determined under the same conditions of frequency and temperature. The results were later compared with the values obtained from the model juices and the accordance of the model juice composition were verified.

Finally, in the third part of this chapter, the experimental data obtained from model solutions were modeled. Dielectric properties of fruit juice model solutions as a function of TSS, frequency and temperature were used to develop Artificial Neural Network (ANN) models. The predictions and suitability of the ANN approach were evaluated.

2.2. Material and methods

2.2.1. Fruit juice model solution

The preparation of solutions was based on a model fruit juice, which is used to mimic real juices through a simplified composition. The use of model solutions was chosen to have

---

better control of the sample properties and to obtain results with greater reproducibility (Augusto et al., 2011; Knoerzer et al., 2004).

The base mixture of each solution was 9 g L^{-1} citric acid (Merck, Germany), 0.3 g L^{-1} ascorbic acid (Puratos, France), sucrose (Merck, Germany) and distilled water. This composition was chosen based on model juices proposed by Kaimainen et al. (2015). In order to evaluate the influence of different contents of TSS on dielectric properties, 8 different quantities of sucrose were added to obtain the following concentrations: 5, 10, 20, 30, 40, 50, 60, 65 °Brix. In general, 10 °Brix is the average content of most fruit juices and 65 °Brix is the usual content of concentrated fruit juices. Using a sodium hydroxide solution, the pH of the 8 solutions was adjusted to 3.4 – 3.8. The TSS values and pH were determined using a refractometer (Maselli Misure, Italy) and pHmeter (Bioblock Scientific, Germany), respectively. The refractometer readings were given in °Brix, which express percent total soluble solids by weight.

2.2.2. Commercial fruit juices

Apple (11.10 °Brix, pH = 3.65; Scamark, France), pineapple (11.54 °Brix, pH = 3.74; Scamark, France) and orange (10.12 °Brix, pH = 3.69; Bricfruit, France) juices were bought in a local supermarket (Nantes, France). These commercial products were composed of pure fruit juice and did not contain other ingredients or additives.

2.2.3. Determination of dielectric properties

Dielectric properties determinations were carried out using an open-ended coaxial line probe system with a Dielectric Probe Kit 85070E (high temperature configuration) connected to an Electronic Calibration Module 85092-60010 and a Network Analyzer E5062A (Agilent Technologies, Malaysia) which is interfaced with a laptop computer. Schematic diagram of the measurement system is shown in Figure 2.1.

Prior to taking the measurements, the network analyzer and the electronic calibration module were switched on for at least 90 min to warm up the electronic components. The system was then calibrated with the equipment standard protocol at 20 °C using air (open circuit), short (short circuit) and deionized water. After calibration, a dielectric measurement of distilled water at 20 °C was made to verify that proper dielectric property values were being obtained.

A volume of 50 mL of the sample was placed in cylindrical flask with cap (height x diameter: 7 x 3.5 cm) and the temperature was adjusted using a water bath with circulating

water (Bioblock Sientific, Germany). The samples were heated from 20 °C (representing the ambient temperature) to 80 °C (representing temperatures of juice thermal process and concentration under vacuum) at 10 °C intervals (Assawarachan and Noomhorm, 2011; Bozkir and Baysal, 2017b; Petruzzi et al., 2017). Right after the temperature was confirmed with a thermocouple (AOiP, France), measurement was carried out with the probe tip in the central surface of the sample. Care was taken to insure that no air bubbles were trapped in the measurement region.

The measurements were performed for frequencies between the limits of network analyzer 200 MHz and 3000 MHz. Frequency sweep of the software scanned 101 frequencies in this range with a linear scale. A procedure to refresh the calibration through the Electronic Calibration Module was carried out and the probe was washed with distilled water and wiped dry between each measurement.

An Agilent program (85070) controlled the system to perform the frequency sweep and measured the complex reflection coefficient of the material in contact with the active tip of the probe, which was converted to the complex permittivity. Relative dielectric constant (ε_r') and dielectric loss factor (ε_r'') values were then collected. Five measurements were done for each sample at each temperature evaluated. The results were presented as mean values and standard deviations.
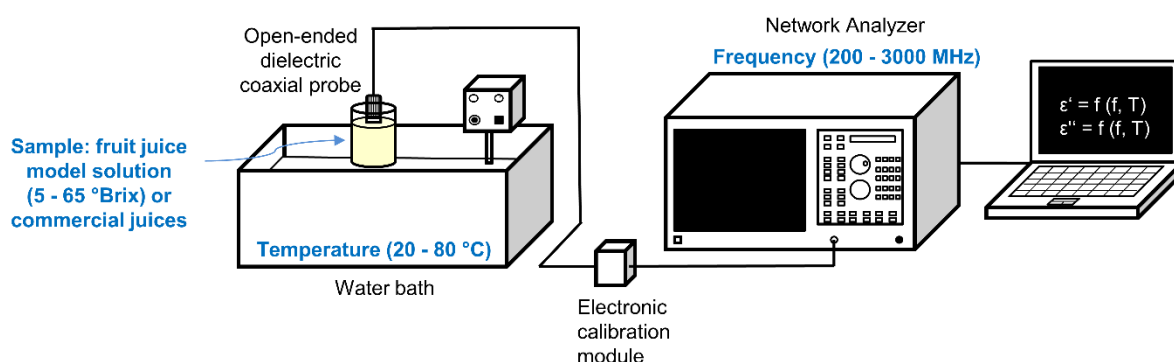
Figure 2.1. Schematic diagram of dielectric properties measurement system (not to scale).

2.2.4. Penetration depth

The microwave power intensity decays as the wave propagates into the food sample. Penetration depth of a microwave power is defined as the distance at which the incident power is reduced to 1/e (e = 2.7183) of its value at the surface of the material, i.e. ~ 63% of the power is absorbed between the surface and this depth.

The penetration depth in a lossy food material can be calculated according the following equation (Curet et al., 2008; Sosa-Morales et al., 2010):

$$d_P = \frac{c_0}{2\pi f\sqrt{2\varepsilon_r^{'}}}\left[\sqrt{1+\left(\frac{\varepsilon_r^{''}}{\varepsilon_r^{'}}\right)^2}-1\right]^{-\frac{1}{2}} \qquad \text{Eq. 2.1}$$

where d_P is the penetration depth, $\varepsilon_r^{'}$ and $\varepsilon_r^{''}$ are the values of relative dielectric constant and loss factor of solutions, c_0 is the speed of light in free space (c_0 = 2.9979 x 10^8 m s^{-1}) and f is the frequency of the electromagnetic wave.

After measuring the dielectric properties, the penetration depths of electromagnetic energy in model solutions were calculated. The penetration depths of each solution and temperature at usual microwave frequencies (915 and 2450 MHz) were calculated from mean values of dielectric constant and loss factor. Results were reported as function of temperature.

2.2.5. Modeling of dielectric properties with Artificial Neural Networks

ANNs are a relevant way to establish relationships between data, especially in the presence of nonlinearities as in the case of dielectric properties behavior (Hagan et al., 1996; Haykin, 1999). In this work, the use of multilayer perceptron models (Rumelhart et al., 1986), which have demonstrated success in a large range of applications, has been selected. Multilayer perceptron models are composed of an input layer containing a number of nodes equal to the number of different variables of the database, one or more hidden layers with a number of neurons, which is particularly difficult to adjust, and an output layer where the number of neurons is equal to the number of targets.

The number of hidden layers and the number of neurons in these hidden layers are particularly difficult to choose. An insufficient number of hidden layers do not permit to take into account all the nonlinearities, especially in presence of non-monotonic evolutions, whereas a large number of hidden layers can lead to problems of convergence during the learning phase. Similarly, a too large number of neurons would lead to an over-fit model, perfect by considering only the learning residues, but totally inappropriate for the validation phase. On the contrary, the learning ability would be limited in case of insufficient number of neurons.

Thus, to design the multilayer perceptron neural network able to predict loss factor and dielectric constant, the structure must be adequately chosen. Using 2 targets in a same neural network require either an increasing of the number of neurons or of the hidden layers, inducing potential problems of convergence. Therefore, to avoid the problem of convergence, 2 different neural networks were considered, with respectively 18 and 16 neurons on the hidden layer, as

represented in Figure 2.2. The number of neurons in the input and output layers were given by the quantity of variables in the process. The number of neurons in the hidden layer were determined by trial and error procedure.
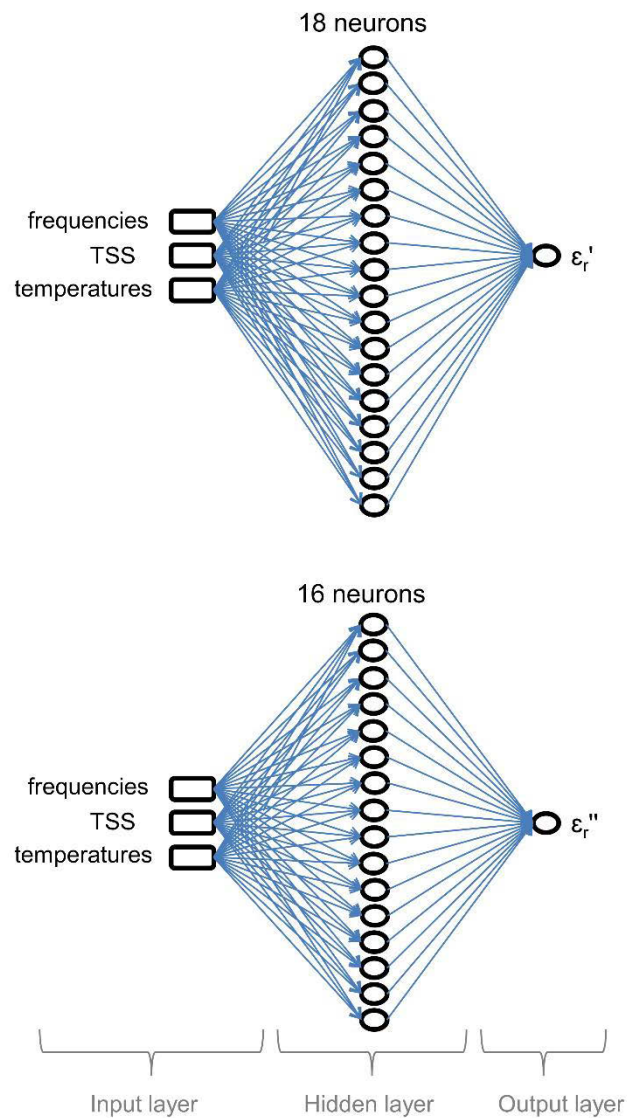
Figure 2.2. Schematic description of the Artificial Neural Networks where frequencies, total soluble solids (TSS) and temperatures are independent input variables and dielectric constant (ε_r') and loss factor (ε_r'') are the dependent output variables.

Each connection between two neurons has a weight (w) coefficient attached to it. Also, each neuron has a bias (b), which is added to the weighted inputs ($w \cdot In$), forming the neuron input (A) (Hernández-Pérez et al., 2004) as shown in the Eq. 2.2. Then, this sum is computed by a transfer function. The hidden layer of each ANN was associated to a tangent sigmoid function, as shown in the Eq. 2.3. The output layers were associated to a linear function.

$$A = (w_1 \cdot u_1) + (w_2 \cdot u_2) + (w_3 \cdot u_3) + b_n \qquad \text{Eq. 2.2}$$

$$N = \text{tansig}(A) = \frac{2}{1 + e^{-2A}} - 1 \qquad \text{Eq. 2.3}$$

The learning phase consists in adjusting the weights using a large part of experimental data. Once the learning is achieved, a validation is carried out by comparing the remaining data with predictions supplied by the ANNs. For each phase, experimental data sets concerning the dielectric properties of the model solutions were properly distributed. Learning phase was performed using Back-Propagation algorithm, thanks to the Neural Network Toolbox of Matlab® (The MathWorks, Inc., USA).

2.3. Results and discussion

2.3.1. Dielectric properties of model solutions

2.3.1.1. Dielectric constant as a function of soluble solids content, temperature and frequency

The relative dielectric constants of the solutions with different TSS content over the frequency ranging from 200 to 3000 MHz at temperatures between 20 and 80 °C are shown in Figure 2.3. Results are presented as mean values of five measurements. The vertical bars indicate the corresponding standard deviations (values between 0.0190 and 1.3412).
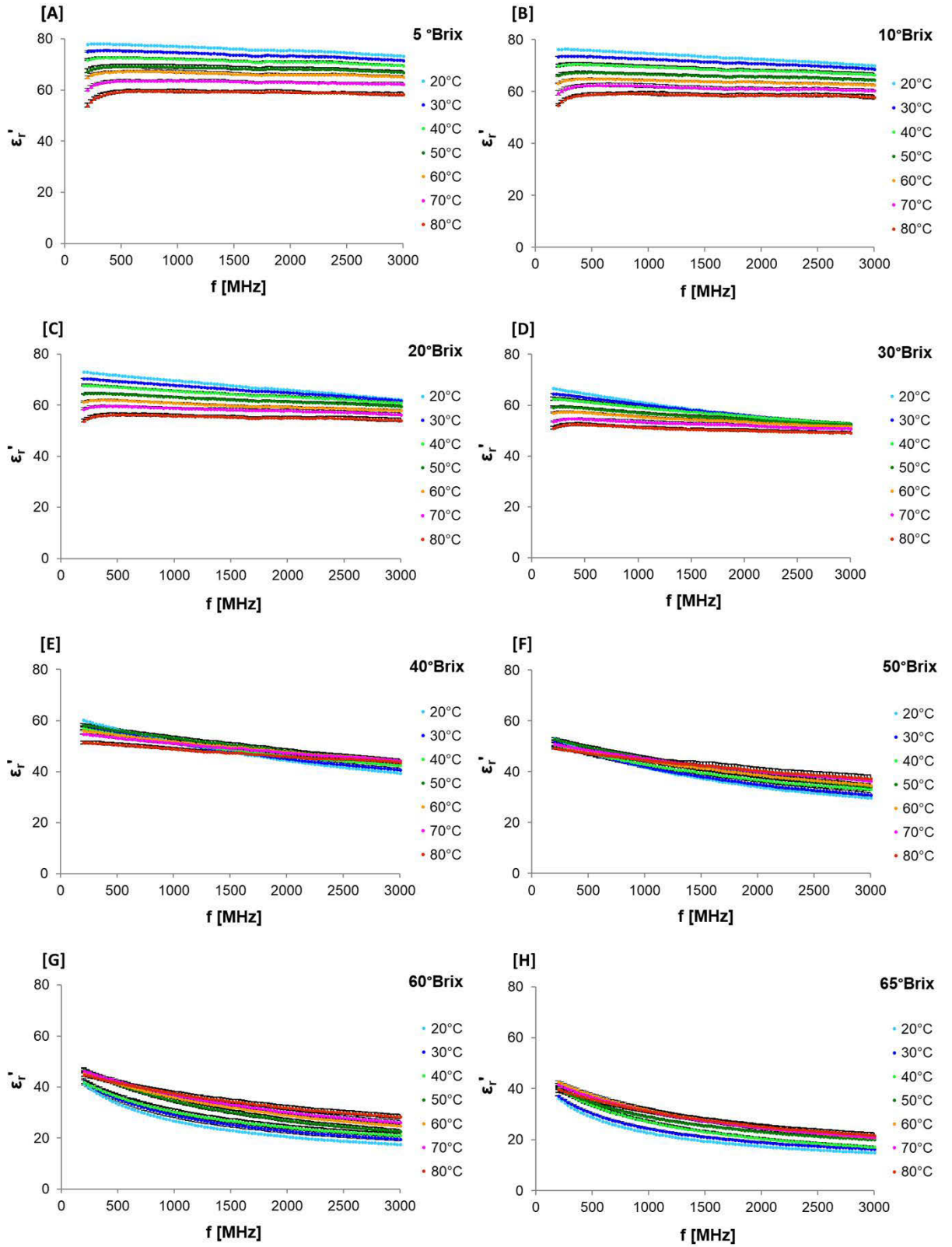
Figure 2.3. Relative dielectric constants (ε_r') of model solutions with 5 °Brix [A], 10 °Brix [B], 20 °Brix [C], 30 °Brix [D], 40 °Brix [E], 50 °Brix [F], 60 °Brix [G], 65 °Brix [H] over the frequency (f) range of 200 – 3000 MHz at different temperatures (20 – 80 °C).

Firstly, a frequency dependence of dielectric constant can be observed. The main phenomenon associated to frequency dependence is the polarization, which is resulting from the orientation and physical rotation of molecular dipoles with electric field. In most of the evaluated solutions, a decrease of dielectric constant with increasing frequency can be generally observed, which seems to be in accordance with the Debye equations for pure polar materials and with the empirical equation of Cole-Cole model for water-carbohydrates mixtures at the studied frequency range (Debye, 1929; Gabriel et al., 1998).

The drop of dielectric constant can be explained by the reduced ability of the molecule dipoles to follow the rapid electric field reversals at higher frequencies (Datta et al., 2005). When frequency increases, polarization of water molecules begins to be out of phase (lag) with the electric field oscillations, leading to a dielectric constant decay and thus, to a lesser energy storage (Gabriel et al., 1998). Dielectric constant decrease with frequency was also reported for several fruit juices, including grape juice at 20 °C and apple juice at 24 °C and at 10 – 90 °C (García et al., 2001; Guo et al., 2011; Siguemoto and Gut, 2016).

However, in the diluted solutions (up to 30 °Brix) at high temperatures (higher than 50 °C), an increase of dielectric constant with frequency is oddly observed in the beginning of the frequency range (200 – 500 MHz). Resembling trends were found by Midi, Sasaki, Ohyama, & Shinyashiki (2014) for sodium chloride aqueous solutions at frequencies around 100 MHz. Although this increase of dielectric constant with frequency was repeatedly observed during experiments, the physical explanation of this particular behavior is unknown. Therefore, the ANNs were developed excluding the values at the questionable range and considering only the data at the frequency range of 500 – 3000 MHz.

Besides the dependence on frequency, a dependence of dielectric constant on TSS is also present. Reduction of relative dielectric constant values as result of increasing TSS content can be observed. The Figure 2.4 shows examples of graphs at constant temperature (20 and 50 °C), where this decrease of dielectric constant with TSS content can be clearly noticed. It suggests that less electromagnetic energy is stored in concentrated solutions. This drop of the dielectric constant is correlated with the increase of viscosity due to high TSS content and hence with the decrease of molecule mobility and polarization.
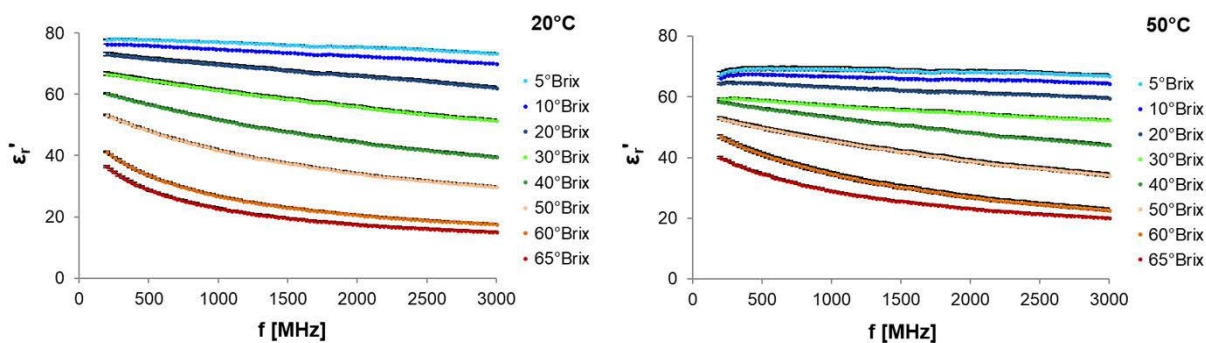
Figure 2.4. Effect of total soluble solids content (5 – 65 °Brix) on the relative dielectric constants (ε_r') of model solutions at 20 °C and 50 °C along the frequency (f) range of 200 – 3000 MHz.

Regarding the variation of dielectric constant with temperature, three groups of solutions based on TSS content can be considered: 5 – 30 °Brix (Figure 2.3A, B, C, D), 40 – 50 °Brix (Figure 2.3E, F) and 60 – 65 °Brix (Figure 2.3G, H).

In the first group (5 – 30 °Brix), the dielectric constant decreases with increasing temperature. The decline of dielectric constant with temperature is attributed to the increase of Brownian movement and thermal agitation that can disturb the alignment of the water molecule dipole with the electric field, reducing the polarization of the medium (Franco et al., 2015; Komarov et al., 2005; Zhu et al., 2012). Differences between dielectric constant values at distinct temperatures are greater at lower frequencies than at higher ones. This can be clearly observed especially in the 30 °Brix solution (Figure 2.3D), in which, for instance, the difference between dielectric constant at 20 and 80 °C is around 12 at 500 MHz, but it is around 4 at 2500 MHz.

In the second group (40 and 50 °Brix), the curves of relative dielectric constant as a function of frequency at different temperatures intersect each other. From this crossing, the behavior is reversed, i.e. dielectric constant starts to increase with increasing temperature. In the 40 °Brix solution (Figure 2.3E), the intersection of curves occurs at around 1500 MHz. In the 50 °Brix solution (Figure 2.3F), the relative dielectric constant behavior with temperature starts to invert at around 500 MHz. This difference is related to the increase of TSS and decrease of free water molecules in the solution, which may affect the polarization. Thus, this group has an intermediate behavior between the ones from the first and third groups.

In the third group (60 and 65 °Brix), the dielectric constant increases with temperature in almost all the evaluated frequency range. For frequencies greater than 700 MHz, in 65 °Brix solution (Figure 2.3H) at 60 – 80 °C, the dielectric constant values are quite close to each other. However, the curves corresponding to low temperatures (20 – 40 °C), in both solutions, can be readily distinguished and their values of dielectric constant are small. These lower values can be due to the lesser presence of free water in concentrated solutions that affects

the polarization of the system and can be correlated with higher viscosities at colder temperatures.

Therefore, these results demonstrate that the material's ability to store electric energy (indicated by dielectric constant) is dependent on its solids content. Moreover, they reveal the existence of a critical concentration that inverts the dielectric constant behavior with increasing temperature, which can be particularly important for concentration (dehydration) processes design.

2.3.1.2. Loss factor as a function of soluble solids content, temperature and frequency

The dielectric loss factor graphs of the solutions with different TSS content over the frequency range of 200 – 3000 MHz at temperatures from 20 to 80 °C are presented in Figure 2.5. Results are presented as mean values of five measurements. The vertical bars indicate the corresponding standard deviations (values between 0.0041 and 1.5783). The increasing of temperature either increases or decreases the loss factor of solutions, depending on frequency and TSS content, which leads to a complex behavior.

At the frequency range evaluated, the loss factor of a solution is basically the combined effect of two mechanisms, dipole loss and ionic loss. Thus, the variation of loss factor depends on which mechanism dominates (Ryyniinen, 1995). At lower frequencies, the dominant mechanism is ionic conduction, while at higher frequencies, the predominant mechanism is dipolar rotation of water (Liu et al., 2009; Roebuck et al., 1972).

Below 50 °Brix, the change of mechanisms contributions to loss factor from an intersection of the curves and the distinct effect of temperature on each type of mechanism can be observed. Ionic loss increases with temperature, while dipole loss decreases. For example, in the 5 °Brix solution (Figure 2.5A), the intersection of the curves occurs at around 1250 MHz; then, the increase of temperature from 20 to 80 °C at 500 MHz increases the dielectric loss factor from 13 to 23, but at 2000 MHz it decreases the loss factor from 12 to 8. This observation is in agreement with what was reported in the literature (Mudgett, 1986; Ryyniinen, 1995). Higher temperatures increases mobility of charged ions, thereby increasing the contribution of ionic conduction to dielectric loss factor at low frequencies (Liu et al., 2009). Similar temperature- and frequency-dependent behavior was reported for fruit juices at 15 up to 95 °C from 20 to 4500 MHz (Zhu et al., 2012).

Additionally, in the Figure 2.5, the effect of frequency can also be observed. The intersection of loss factor curves of 5 – 50 °Brix solutions at different temperatures moves toward lower frequency direction with increasing TSS content. Thus, the frequency in which the change of predominant loss factor mechanism occurs varies according to the content of

the solution. For instance, the interception of curves in 5 °Brix solution (Figure 2.5A) occurs at around 1250 MHz, while in 40 °Brix solution (Figure 2.5E), it occurs at around 350 MHz.

Regarding the loss factor behavior along the frequency range, in solutions up to 40 °Brix, especially in 5 – 20 °Brix solutions (Figure 2.5A, B, C), the loss factor values drop sharply at lower frequencies and then after the interception of curves, mildly change either in upward or downward direction. In 50 °Brix solution (Figure 2.5F), the interception of loss factor curves occurs at the beginning of the evaluated frequency range (200 MHz) and the loss factor values slightly increase with frequency. In concentrated solutions, 60 and 65 °Brix (Figure 2.5G, H), the changes of loss factor are even slighter. Loss factor either increases or decreases depending on frequency and temperature. This might be associated with changes in the viscosity of the solution and with the mobility of bound and free forms of water.
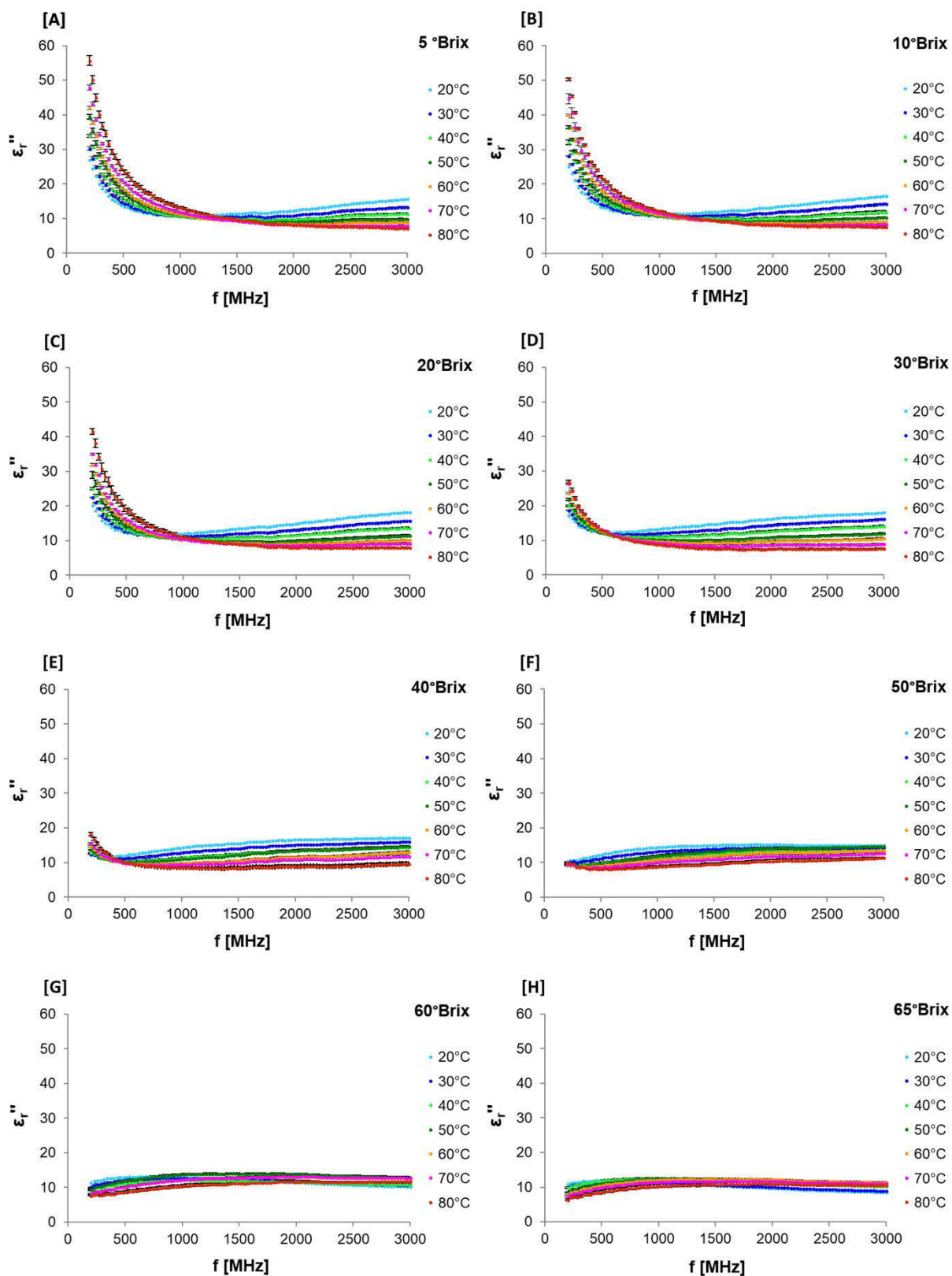
Figure 2.5. Relative dielectric loss factors (ε_r'') of model solutions with 5 °Brix [A], 10 °Brix [B], 20 °Brix [C], 30 °Brix [D], 40 °Brix [E], 50 °Brix [F], 60 °Brix [G], 65 °Brix [H] over the frequency (f) range of 200 – 3000 MHz at different temperatures (20 – 80 °C).

Ionic conduction is the main responsible for ionic loss and plays a major role at frequencies below 1000 MHz. For aqueous ionic solutions, the following general equation is available to describe the frequency dependent behavior of ionic loss (Liu et al., 2009; Mudgett, 1986):

$$\varepsilon_\sigma'' = \frac{\sigma}{2\pi f \varepsilon_0}$$

Eq. 2.4

By taking the logarithm on both sides, Eq. 2.5 indicates a log-log plot of the ionic contribution to the dielectric loss factor (ε_σ'') and frequency (f) is linear with a slope of -1:

$$\log \varepsilon_\sigma'' = \log \frac{\sigma}{2\pi\varepsilon_0} - \log f$$

Eq. 2.5

Then, to verify the appropriateness of the correlation above, log-log graphs of loss factor versus frequency considering a range between 200 and 1012 MHz were plotted. Negative linear correlations between ionic loss factor and frequency were observed only in the solutions with lesser TSS content at high temperatures, as shown in Figure 2.6A and B.
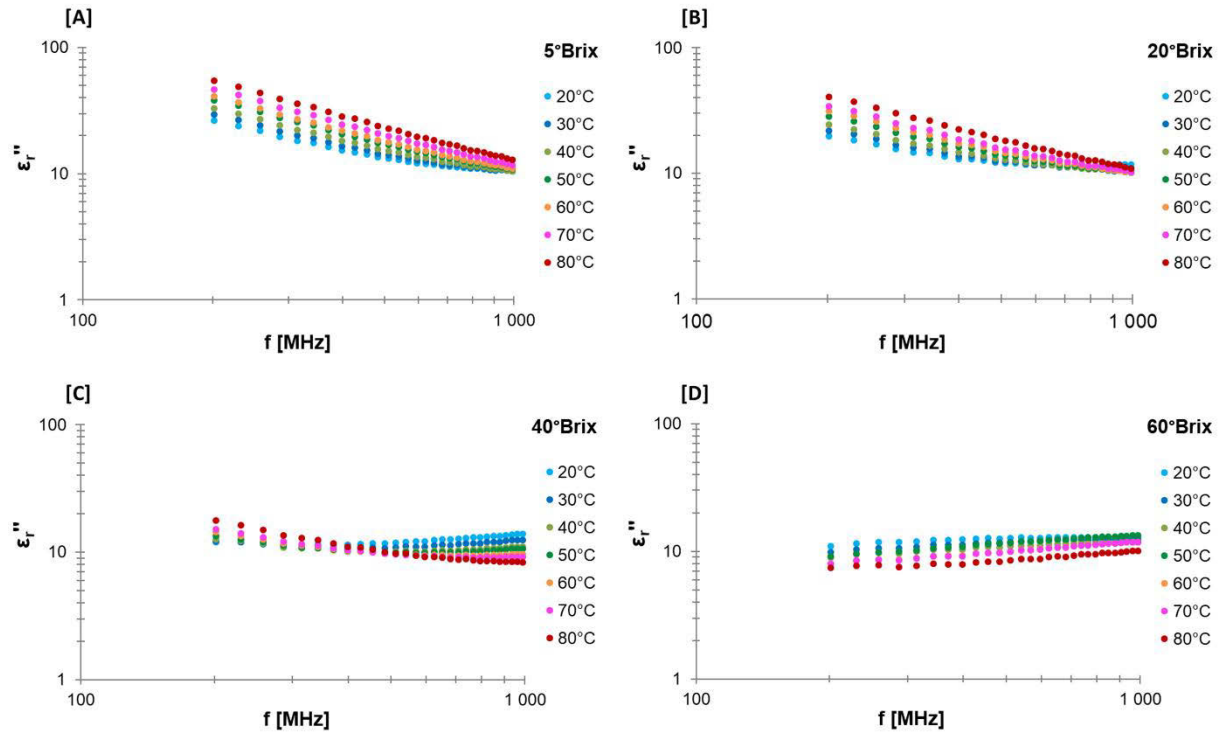
Figure 2.6. Log-log plot of relative dielectric loss factor (ε_r'') of model solutions with 5 °Brix [A], 20 °Brix [B], 40 °Brix [C] and 60 °Brix [D] over the frequency (f) range of 200 – 1012 MHz at different temperatures (20 – 80 °C).

Some researchers have also reported a negative relationship in other foods, such as: apple, grape, pear and pineapple juices (Guo et al., 2011; Zhu et al., 2012); milk (Guo et al., 2010); egg whites and whole eggs (Wang et al., 2009). According to Liu et al. (2009), for liquid or high moisture foods, in general, the slope of log-log plots regression should be close to -1. However, in the present study, the slope values closer to -1 correspond only to the 5 and 10 °Brix solutions at 70 and 80 °C. For the 5 °Brix solution at 80 °C, the slope is -0.9, the steepest slope and the closest to -1, thus confirming ionic conduction is indeed the dominant mechanism in these determined conditions of TSS content, frequency and temperature.

Low TSS content, greater free water availability, low frequencies and high temperatures contribute to the increase of ionic movement. On the other hand, high concentration of sugars weakens the mobility of charged ions; hence for more concentrated solutions and lower temperatures, the slope values are greater (further from -1) and in some cases, even positives, as shown in Figure 2.6C and D. Therefore, in these conditions, ionic conduction is not the predominant mechanism; there is a combined effect of both mechanisms (ionic conduction and dipolar rotation).

It is important to note that the ionic content of model solutions comes from the presence of acids (citric acid and ascorbic acid) used in the formulation, even if these acids are classified as weak or relatively weak acids (i.e. they do not ionize fully when dissolved in water). To verify it, some preliminary tests were performed comparing 10 °Brix model juice solutions with and without acid. Loss factors of both solutions at 20, 40, 60 and 80 °C are shown in Figure 2.7. All the curves of the solution without acids (Figure 2.7A) are nearly linear and the values of loss factor increase with frequency throughout the frequency range. On the other hand, in the solution with addition of acid (Figure 2.7B), a sharp decrease with increasing frequency until around 1000 MHz is observed, as expected since it is characteristic of ionic behavior.
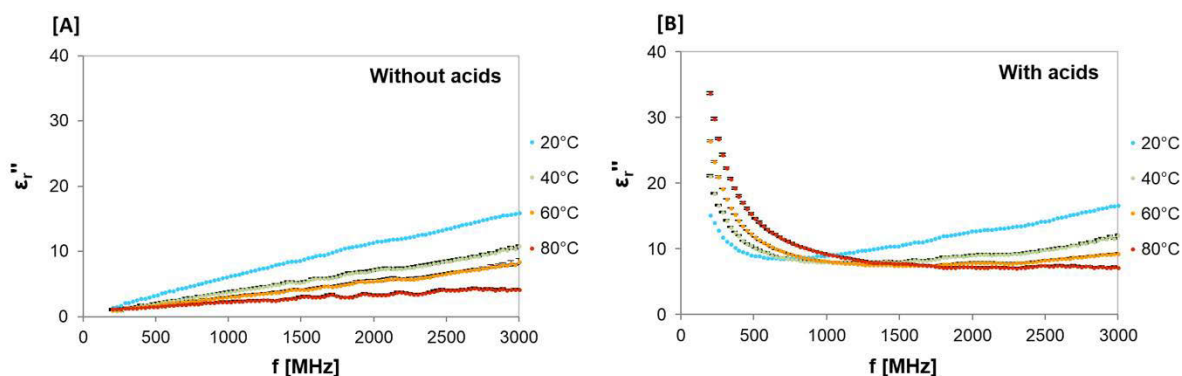
Figure 2.7. Relative dielectric loss factors (ε_r'') of 10 °Brix model solutions with [A] and without acid [B] over the frequency (f) range of 200 – 3000 MHz at 20, 40, 60 and 80 °C.

2.3.1.3. Dielectric properties and penetration depth at usual microwave frequencies

In general, domestic microwave appliances operate at 2450 MHz, while industrial microwave systems operate at frequencies of 2450 MHz and, especially, 915 MHz. Influence of temperature and TSS on the dielectric constant and loss factor of solutions at microwave frequencies (915 and 2450 MHz) are shown in Figure 2.8.
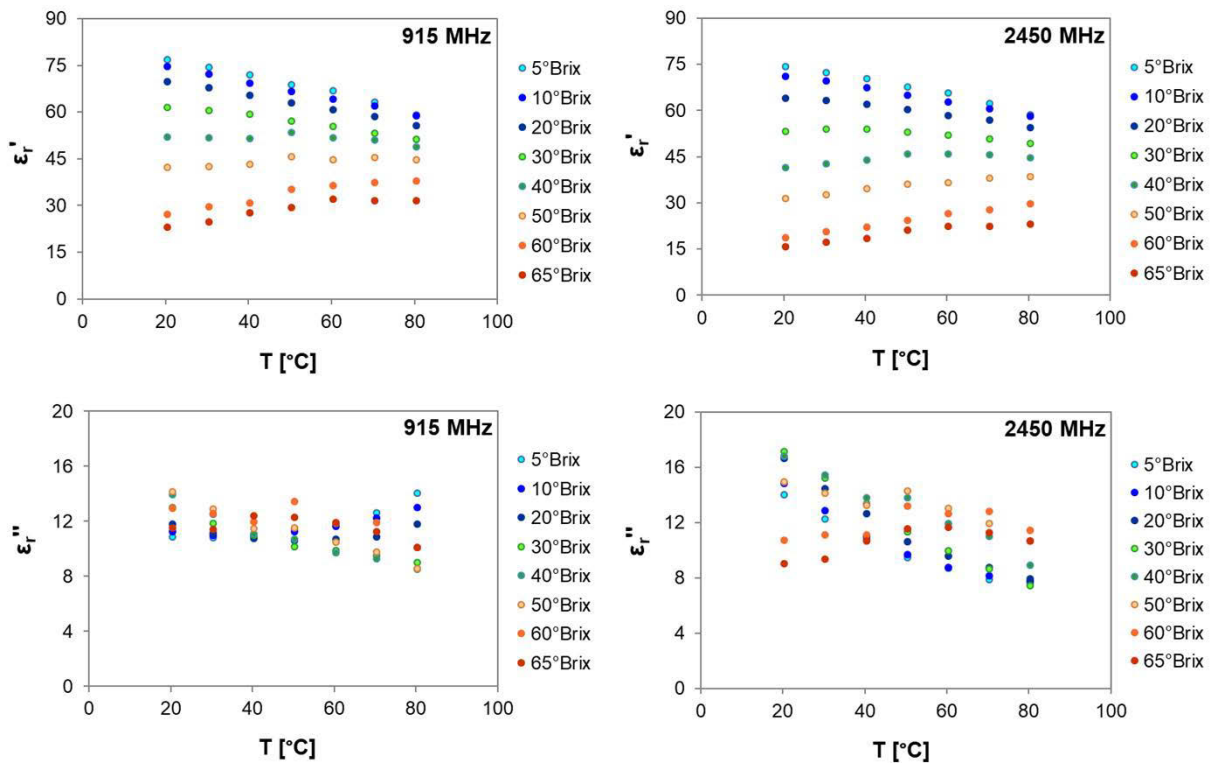
Figure 2.8. Effect of temperature (T) on the relative dielectric constant ($\varepsilon_r^{'}$) and loss factor ($\varepsilon_r^{''}$) of model solutions with different total soluble solids content (5 – 65 °Brix) at frequencies of 915 and 2450 MHz.

At both frequencies, for a given temperature, the dielectric constant decreases with increasing of TSS content. This is due to the binding of free water by sucrose, which reduces the presence of water molecules and consequently, the dielectric polarization of the system. The increase of viscosity due to high TSS content and hence the decrease of molecule mobility is also correlated with the drop of the dielectric constant. A similar behavior was reported in α-D-glucose solutions with concentrations from 10 to 60% at 2450 MHz (Liao et al., 2003) and in sugar cane solutions with concentrations from 20 to 250 % (weight of sugar to water) at 2450 MHz (Tulasidas et al., 1995).

In relation to the loss factor, there are no well-defined and constant trends for the loss factor variation with TSS content at both frequencies. The increase of TSS results in a complex behavior, either increasing or decreasing the loss factor depending on temperature. At

2450 MHz, at a given temperature, an increase of dielectric loss factors with increasing TSS seems to be more predominant, except for the most concentrated solutions (50, 60 and 65 °Brix). At 915 MHz, there seems to be no predominant tendency of loss factor with TSS content. It can be explained since this frequency is comprised within the range of frequencies where the intersection of curves (change of mechanisms predominance) occurs, as discussed in the previous section.

From these experimental data at 915 and 2450 MHz, the penetration depth values were calculated. The knowledge of penetration depth is useful as a guideline to the heating effectiveness of a food material. Hence, it is an important parameter for the development of product and design of food processes. Penetration depths of model solutions as a function of TSS and temperature are shown in Figure 2.9.
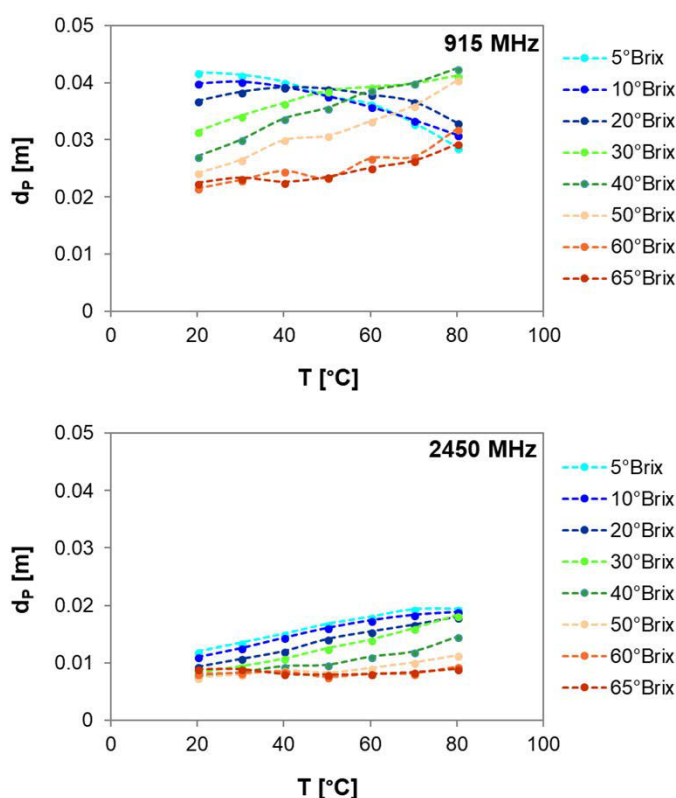
Figure 2.9. Calculated penetration depths of model solutions with various total soluble solids content (5 – 65 °Brix) as a function of temperature (T) from 20 to 80 °C at 915 MHz and 2450 MHz.

Distinct behaviors and penetration depths ranges can be observed at both microwave frequencies. All the values of penetration depth at 915 MHz are higher than at the 2450 MHz. This is expected, since the penetration depth of a material is inversely related to the frequency, as stated by Eq. 2.1.

At 2450 MHz, there is a positive correlation between penetration depth and temperature for all solutions, except for 65 °Brix solution in which penetration depth are almost

invariant with temperature. At 915 MHz, the penetration depths for solutions with TSS content between 30 and 65 °Brix also increase with increasing temperature. However, the opposite behavior is observed for the 5 – 20 °Brix solutions, and it can be a consequence of the dielectric loss factor raise with temperature in these solutions, as shown in Figure 2.8.

By evaluating the equation of penetration depth calculation (Eq. 2.1), it is clear that higher loss factors tend to reduce the penetration depth of a microwave power at a given frequency, since they are inversely proportional. A decrease in the value of penetration depth with increasing temperature was also observed in soy beverage and milk at 915 MHz (Coronel et al., 2008).

Furthermore, considering all the evaluated temperature range and comparing results of both frequencies, penetration depth in general varies in a lesser extent with temperature at 2450 MHz. Thus, it means that the microwave heating of a given and appropriate thickness of solution may be more uniform at 2450 MHz, especially in solutions with higher TSS content (50 – 65 °Brix).

In relation to the influence of sugar content, the penetration depth values decrease with increasing TSS content at 2450 MHz. At 915 MHz, similar behavior is observed, except for 5 – 20 °Brix solutions at temperatures from 40 °C. A decrease of penetration depth with solids concentration was also reported for maple syrup with moisture content between 98% and 35% at 25 °C (Favreau et al., 1997). Moreover, it can be noticed that, in general, the variation of penetration depth with TSS content is smaller at 2450 MHz than at 915 MHz.

The study of penetration depth is important in designing the processing equipment for optimal employment of the microwave power for heating. These considerable differences between penetration depth values indicate that processes that were designed at one frequency may have a different outcome when the frequency is modified, as in the case of a scaling-up from laboratory (2450 MHz) to industrial (915 MHz) (Favreau et al., 1997; Franco et al., 2015).

2.3.2. Dielectric properties of commercial fruit juices

In order to compare results and verify the accordance of the model juice composition, three real fruit juices (apple, orange and pineapple juices) were evaluated. Measurements of dielectric properties were carried out under the same conditions of temperature and frequency as described above for the model solutions. Both dielectric constants and loss factors are shown in Figure 2.10. Results are presented as mean values of five measurements. The vertical bars indicate the corresponding standard deviations (values between 0.0118 and 1.5915 for dielectric constant and between 0.0022 and 1.2733 for loss factor).
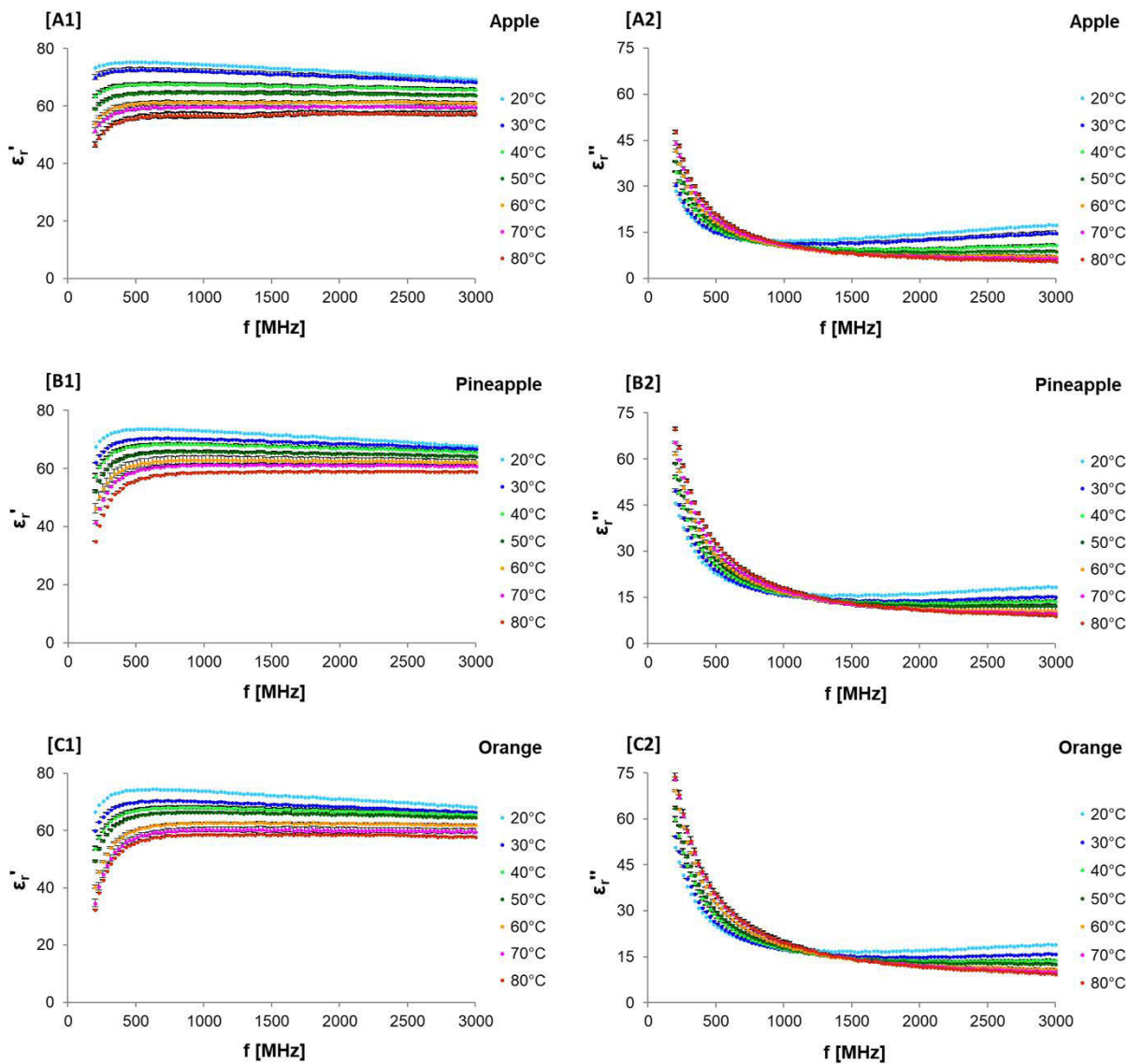
Figure 2.10. Effect of temperature (20 – 80 °C) on the relative dielectric constant (ε_r') and loss factor (ε_r'') of commercial apple [A], pineapple [B] and orange [C] juices along the frequency range of 200 – 3000 MHz.

The soluble solids contents of the apple, pineapple and orange juices are 11.10, 11.54 and 10.12 °Brix, respectively. In general, comparing the results of the real juices with those of the model solutions with low sugar content (5 – 20 °Brix), it can be observed that the dielectric trends are generally comparable. Particularly, apple juice presents dielectric properties quite similar to the obtained data for 10 °Brix model fruit juice solution. Figure 2.11 better illustrates this observation, presenting the dielectric constant and loss factor as a function of temperature at two usual microwave frequencies (915 and 2450 MHz).
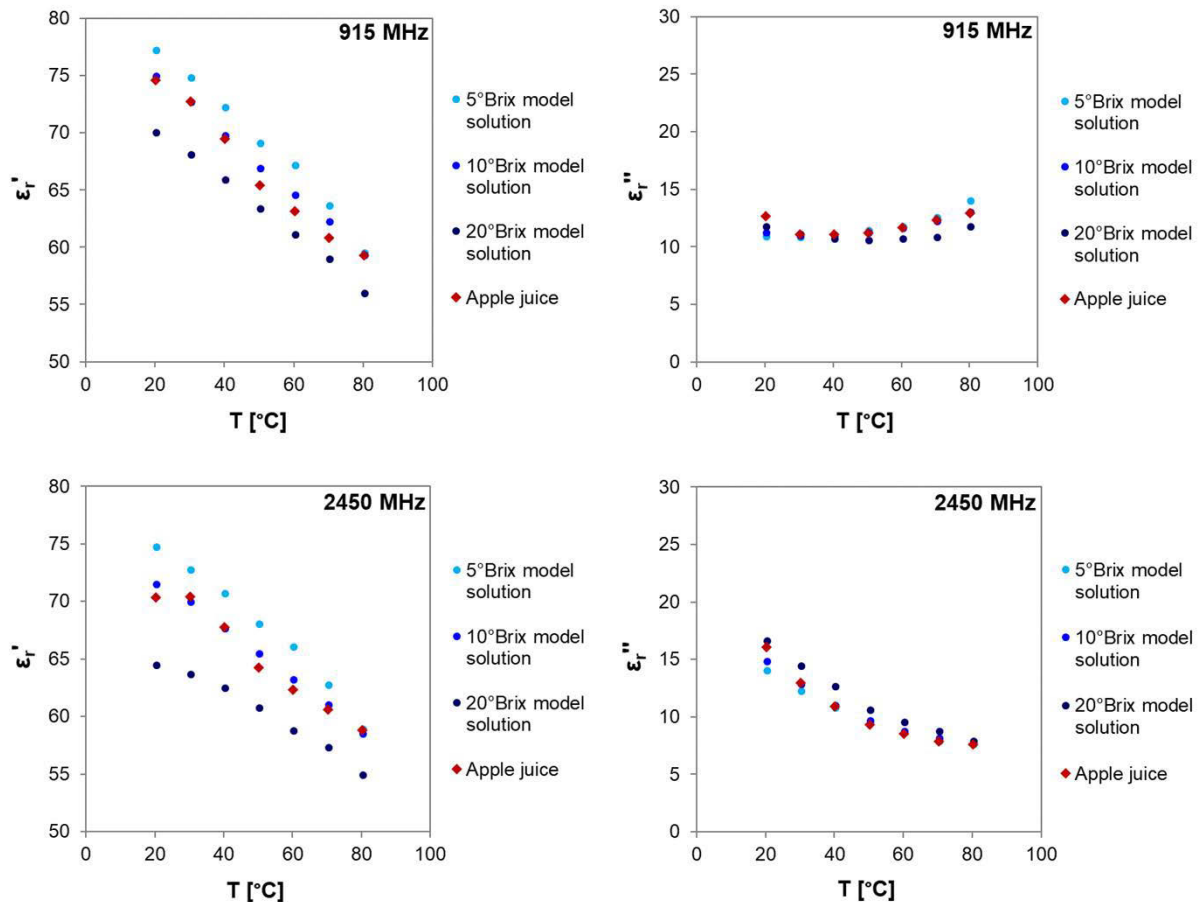
Figure 2.11. Effect of temperature (20 – 80 °C) on the relative dielectric constant (ε_r') and loss factor (ε_r'') of apple juice and model solutions with 5, 10 and 20 °Brix at usual microwave frequencies (915 and 2450 MHz).

Comparing the numerical values in Figure 2.10, some differences can be noticed between the three fruit juices and the model solutions. Also, the effect of frequency on dielectric properties in pineapple and orange juice seems to be larger than in apple juice and model solutions. These differences are closely associated with the distinct compositions of each solution.

While model solutions have a simplified composition, real fruit juices have a more complex and variable composition that includes an insoluble phase. Insoluble material (cloud particles), such as pectin and cell fragments (originated from pulp tissues), can affect the molecular and ionic mobility, thus leading to effects on dielectric properties. The quantity and size of these insoluble fragments vary in each type of juice (clear or cloudy juice) and type of fruit, which also justify the obtained differences in dielectric properties.

Clear juices obtained after clarification and filtration contain a reduced content of insoluble solids; this is the case of the evaluated apple juice. On the other hand, cloudy juices, such as the orange and pineapple juices, contain more insoluble pulpy particles. Thus, it may

explain the higher similarities between the dielectric behavior of the apple juice and the model solution.

2.3.3. Dielectric properties modeling and prediction using Artificial Neural Networks

ANNs were designed in order to model and predict the dielectric behavior of fruit juice model solutions previously presented, taking into account its dependence on temperature, frequency and TSS. As shown in Figure 2.2, both neural network were composed of 3 neurons (frequency, TSS and temperature) in the input layer, 18 neurons or 16 neurons in the hidden layer, and 1 neuron in the output layer (dielectric constant or loss factor). In total, the dielectric constant neural network was composed of 90 coefficients, being 54 weights and 18 biases in the input and 18 weights in the output. For the loss factor neural network, 80 coefficients were obtained, being 48 weights and 16 biases in the input and 16 weights in the output.

The experimental database was composed of frequencies between 500 and 3000 MHz combined with 8 TSS and 7 temperature levels. In total, 299 combinations were used for the learning phase and 152 combinations were used for the validation.

The distribution of data sets used for the learning phase and the validation is presented in Table 2.1. The 299 learning triplets are composed with the 13 non underlined frequencies (600, 800, 915, 1200, 1400, 1600, 1800, 2000, 2200, 2450, 2600, 2800, and 3000 MHz) combined with the 23 couples of temperature/TSS represented by the grayed-out and blacked-out cases.

Table 2.1. Learning and validation data sets used for Artificial Neural Networks (ANN) modeling. Non underlined frequencies combined with grayed-out and blacked-out cases correspond to data for learning phase. Bolded frequencies combined with blacked-out cases correspond to both learning and validation phases. Bolded and underlined frequencies combined with ticked and circle-marked cases correspond to validation phase.

Frequency [MHz]	TSS [°Brix]	Temperatures [°C]						
		20	30	40	50	60	70	80
_500_ – 600 – 800 – **915** – 1200 – 1400 – _1500_ – 1600 – 1800 – **2000** – 2200 – **_2450_** – 2600 – 2800 – **3000**	5	▓			▓			▓
	10	■	O	■	O	■	O	■
	20	▓		▓		▓		
	30	X	X	X	X	X	X	X
	40	▓	▓	▓		▓		▓
	50	X	X	X	X	X	X	X
	65	■	O	O	■	O	■	■

The 152 validation triplets are distributed as follows:

- 32 triplets (8 blacked-out boxes combined with the 4 bolded frequencies) are used to validate the learning phase because these triplets were a part of the 299 learning triplets;

- 84 triplets (the 14 ticked boxes combined with the 6 bolded and underlined frequencies) were specifically used for the validation;

- 36 triplets (the 6 circle-marked boxes combined with the 6 bolded and underlined frequencies) were specifically used for the validation.

Plots of the validation phase, comparing the dielectric properties predicted by the neural networks and the ones measured experimentally, are presented in Figure 2.12 and Figure 2.13. Overall, the results were in good agreement, especially in the 10 °Brix solution.

With increasing TSS, the experimental values become closer to each other, varying less with the temperature, which complicate the discrimination and hinder the learning phase at higher TSS. Thus, discrepancies are increasingly visible with TSS rise. In addition, some deviations observed are also related to the choice of data set taken for each phase of ANN development (learning or validation phase). For instance, in the 50 °Brix solution, greater discrepancies are observed since its data was exclusively used for the validation phase.
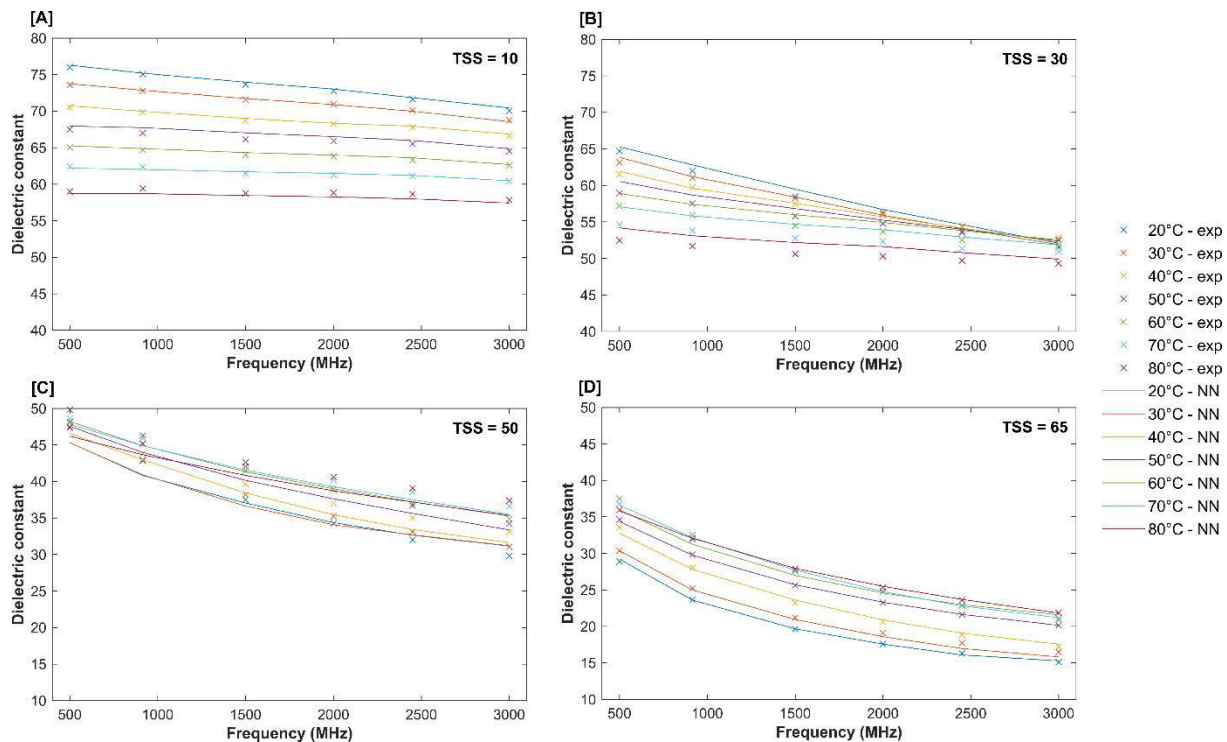
Figure 2.12. Experimental (exp) and predicted (NN) dielectric constants of model solutions with the following total soluble solids (TSS): 10 °Brix [A], 30 °Brix [B], 50 °Brix [C] and 65 °Brix [D], over the frequency range of 200 – 3000 MHz at different temperatures (20 – 80 °C), used in the validation phase of the neural networks.
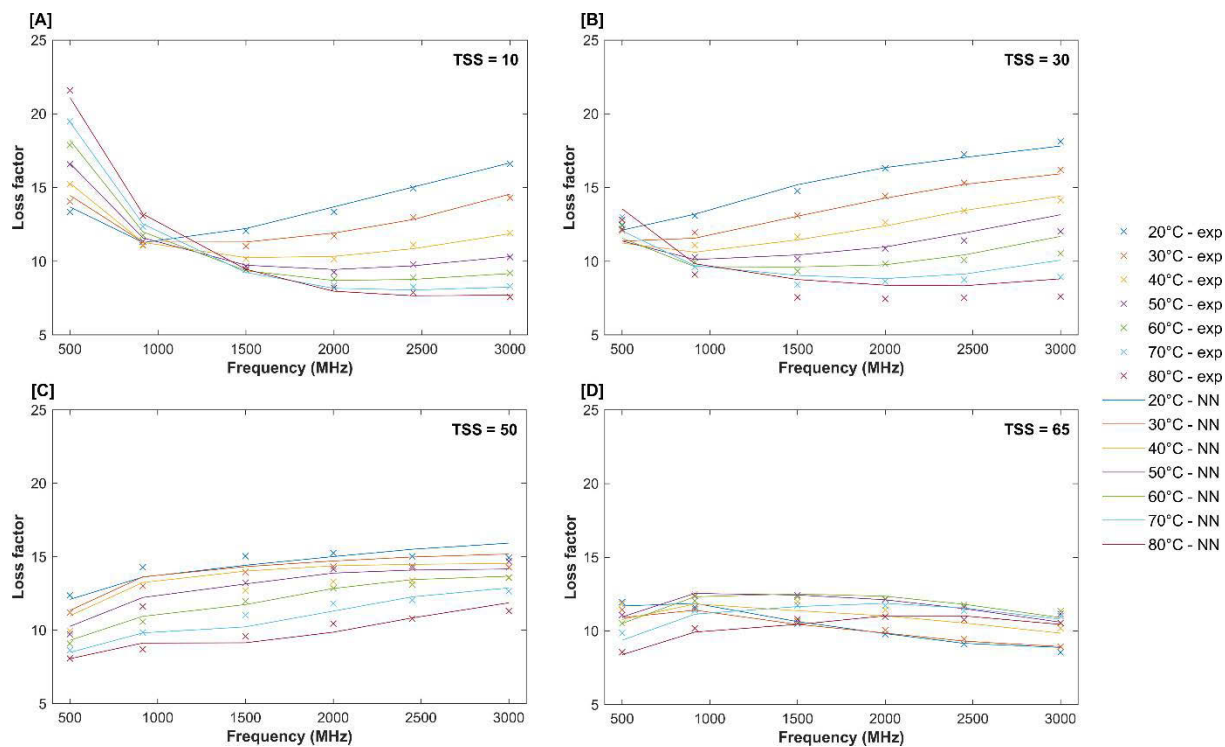
Figure 2.13. Experimental (exp) and predicted (NN) loss factors of model solutions with the following total soluble solids (TSS): 10 °Brix [A], 30 °Brix [B], 50 °Brix [C] and 65 °Brix [D], over the frequency range of 200 – 3000 MHz at different temperatures (20 – 80 °C), used in the validation phase of the neural networks.

The relative errors of both dielectric constant and loss factor are presented in Figure 2.14 and Figure 2.15, respectively. For dielectric constant, the maximum error was around 5 % and for loss factor, around 10 %. Therefore, despite the relative errors in large TSS solutions, the developed neural networks can be considered as satisfactory tool for dielectric behavior prediction.
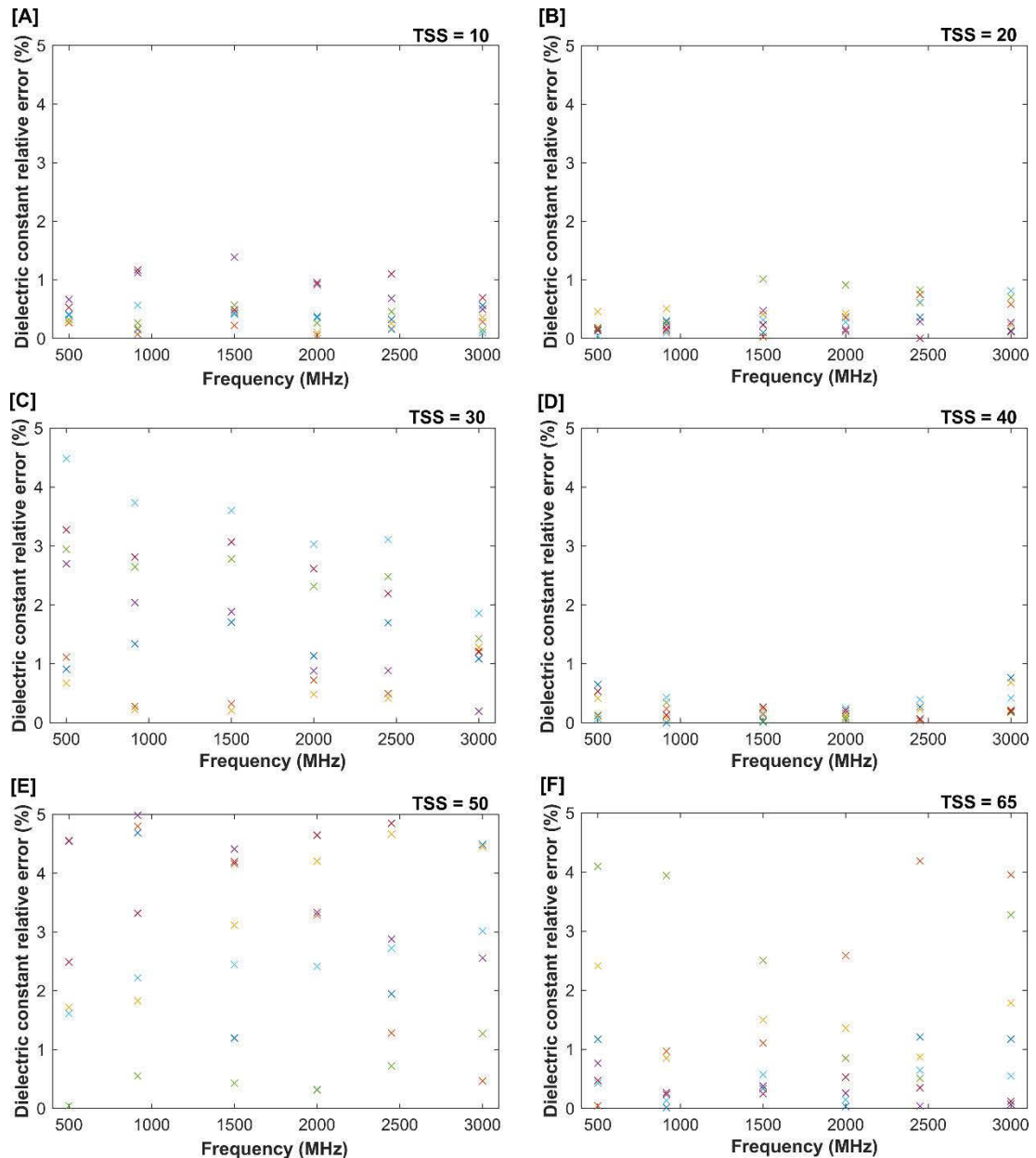
Figure 2.14. Relative errors between ANN modeled dielectric constant and experimental dielectric constant of models juices with 10 °Brix [A], 20 °Brix [B], 30 °Brix [C], 40 °Brix [D], 50 °Brix [E], 65 °Brix [F] at frequencies of 500 – 3000 MHz at different temperatures (20 – 80 °C).
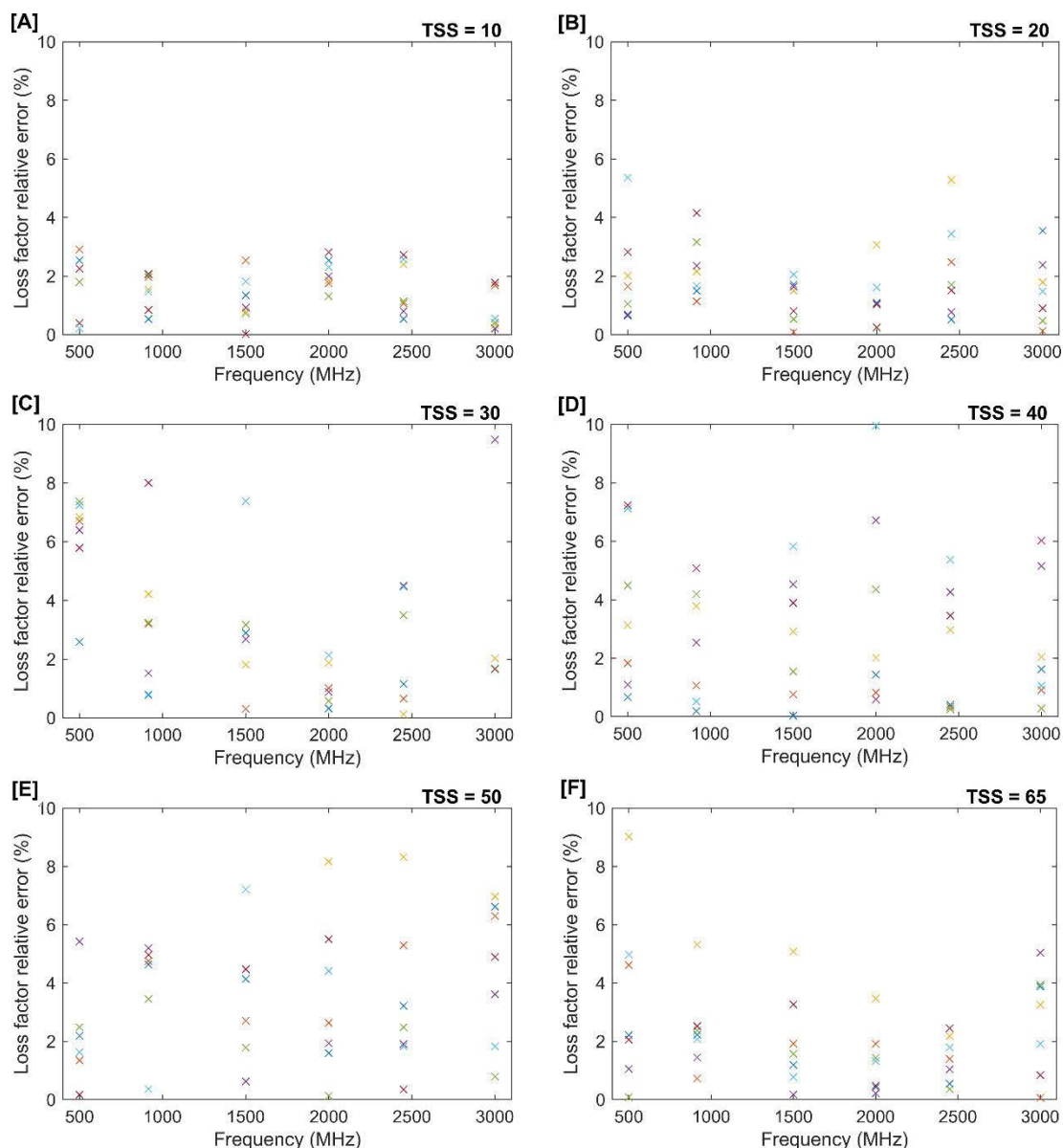
Figure 2.15. Relative errors between ANN modeled loss factor and experimental loss factor of models juices with 10 °Brix [A], 20 °Brix [B], 30 °Brix [C], 40 °Brix [D], 50 °Brix [E], 65 °Brix [F] at frequencies of 500 – 3000 MHz at different temperatures (20 – 80 °C).

Thus, having validated the ANN models, one can make predictions in conditions beyond the ones studied experimentally. For example, it is possible to predict values of solutions with intermediate TSS contents. Figure 2.16 and Figure 2.17 illustrate the predictions of dielectric properties for TSS values between 10 and 20 °Brix, which is the range of most fruit juices. Thick lines represent the experimental results for TSS = 10 °Brix and TSS = 20 °Brix, whereas the fine lines represent the predictions for TSS at intermediate values (equals to 11, 12, 13, 14, 15, 16, 17 and 18 °Brix). The predicted values seem to be consistent. Therefore, the ANNs may be useful for future models of fruit juice thermal processing using microwaves.
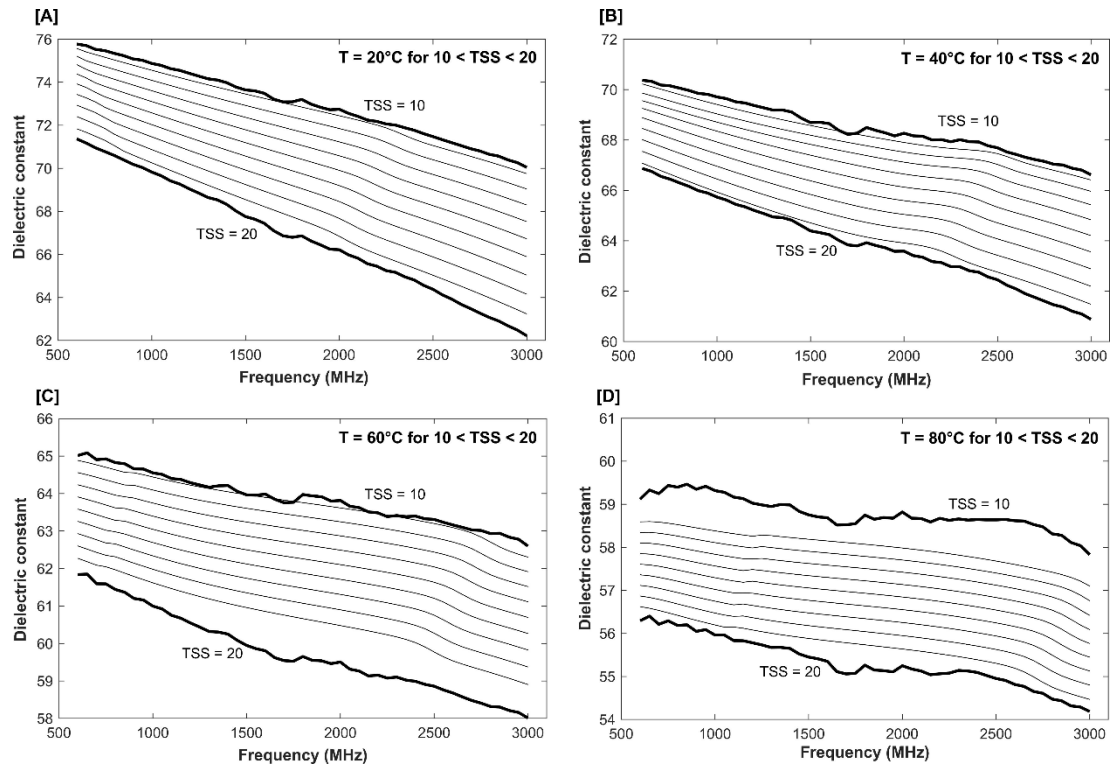
Figure 2.16. Predicted dielectric constants for solutions containing total soluble solids (TSS) between 10 and 20 °Brix at 20 °C [A], 40 °C [B], 60 °C [C] and 80 °C [D] over the frequency range of 200 – 3000 MHz. Thicker continuous lines represent the experimental data for 10 and 20 °Brix solutions.
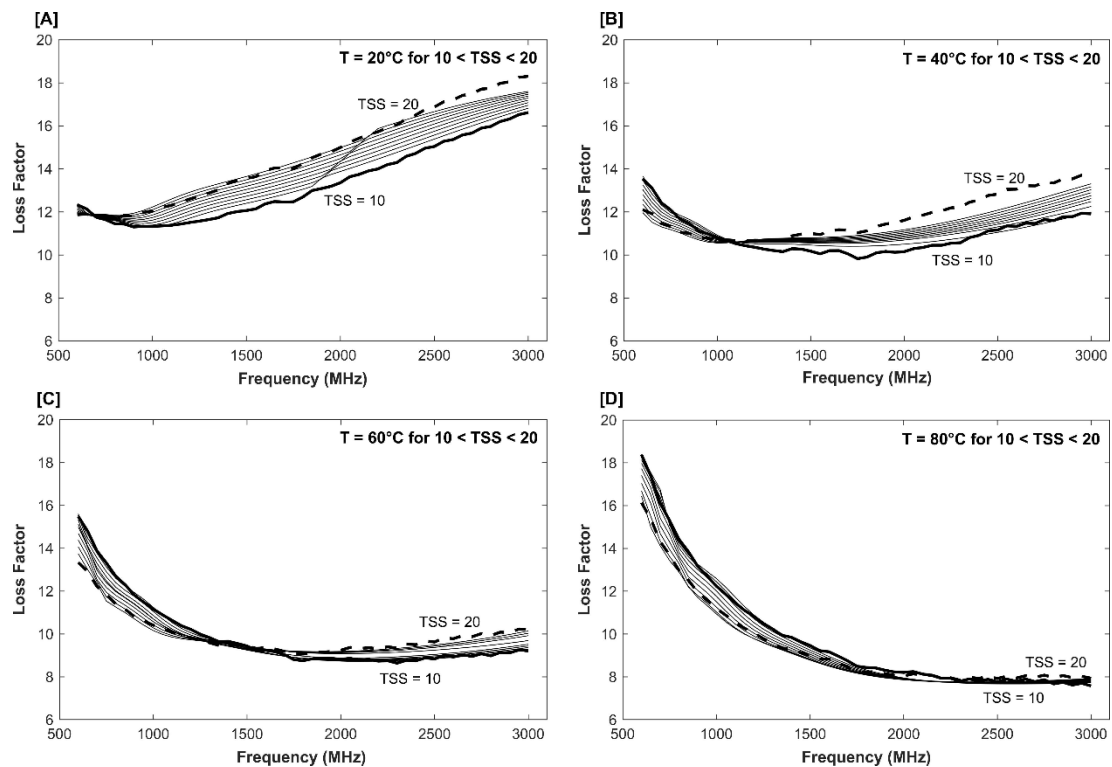
Figure 2.17. Predicted loss factors for solutions containing total soluble solids between 10 and 20 °Brix at 20 °C [A], 40 °C [B], 60 °C [C] and 80 °C [D] over the frequency range of 200 – 3000 MHz. Thicker continuous and dotted lines represents the experimental data for 10 and 20 °Brix solutions, respectively.

2.4. Conclusions

Measurements of the dielectric properties of model fruit juice solutions with different sugar content (5 – 65 °Brix), over a large frequency range (200 – 3000 MHz) at different temperatures (20 – 80 °C) showed the important effect of temperature, frequency and composition on dielectric constant and loss factor. For example, the rise of temperature either increased or decreased the dielectric properties, depending on frequency and TSS content. The contributions of two different mechanisms to loss factor were observed and the different ways in which the temperature affects these mechanisms (ionic conduction and dipolar rotation) were identified. In all the evaluated solutions, dielectric constants decreased with increasing TSS content, however the same remark cannot be made for loss factors. Thus, the obtained relationships between the dielectric behavior and the three studied parameters (temperature, frequency and sugar content) were non-monotonic and quite complex. Comparable trends were observed when evaluating commercial juices made of different fruits (apple, pineapple, orange).

Despite its complexity, the temperature, frequency and composition-dependence of dielectric constant and loss factor was modeled. For that, ANN models were developed. The obtained predictions showed good agreement with experimental data, indicating that ANN was a suitable approach to model the dielectric behavior. The results presented in the present chapter are important since knowledge of the dielectric properties is required to the design and mathematical modeling of microwave processes. Further, the results demonstrate and highlight the importance of implementing dielectric properties as a function of temperature, product composition and microwave frequency in the simulation models. Particularly, the consideration of dielectric properties as constants with temperature can be found in some studies. However, in view of the presented results, this simplification can be a source of considerable errors. Therefore, in Chapter 4, where a numerical study of the microwave processing of juice is presented, the temperature-dependence of dielectric properties was necessarily taken into account.

CHAPTER 3. THERMAL INACTIVATION KINETICS OF PEROXIDASE IN MODEL FRUIT JUICE UNDER CONVENTIONAL HEATING[2]

3.1. Introduction

Peroxidase (POD) is an enzyme naturally present in fruits and can cause deterioration in terms of sensory quality of the product. POD is known as a relatively resistant enzyme, being an interesting target enzyme for the study of thermal processes. The present chapter presents the evaluation of POD inactivation kinetics in model juice during a conventional thermal treatment. The fruit juice model solution containing horseradish peroxidase was processed at 42 different combinations of time and temperature. The resulting inactivation data were fitted by a kinetic model

Since the temperature distribution could be considered as homogeneous within the sample during the processing, the actual thermal history could be taken into account. Thus, reliable kinetic parameters were estimated. The obtained kinetic model will be key information to be implemented in the 3D-model for the simulation of POD inactivation by microwave heating, later described in next chapter.

3.2. Material and methods

3.2.1. Fruit juice model solution

The present work was carried out using the fruit juice model solution proposed by Kubo et al. (2018). Its composition was based on the model juices proposed by Shah et al. (2010) and on the solutions of the previous chapter, with some modifications. The fruit juice model solution was made using sucrose (Synth, Brazil), citric acid (Synth, Brazil), horseradish peroxidase (POD, type X commercialized under crystalline suspension in 3.2 mol L^{-1} ammonium sulfate; EC: 1.11.1.7; P6140 - 25 KU; Sigma-Aldrich Co., USA) and distilled water.

For the preparation of 100 mL of model solution, 11.2 g of sucrose, 8 mL of 0.5 g L^{-1} citric acid solution, 1.6 mL of 250 U mL^{-1} peroxidase stock solution and distilled water were mixed. The final soluble solids content and pH of the solution were 10 °Brix and 3.8, respectively. The enzymatic activity in the model solution was 4 U mL^{-1}.

---

[2] **The content of the present chapter is based on Kubo, M.T.K., Rojas, M.L., Curet, S., Boillereaux, L., Augusto, P.E.D., 2018. Peroxidase inactivation kinetics is affected by the addition of calcium chloride in fruit beverages. LWT - Food Sci. Technol. 89, 610–616.**

The peroxidase stock solution was prepared by combining the commercial peroxidase solution with distilled water and stored at -20 °C until use. Fresh fruit juice model solution was prepared daily, just before the thermal processing.

3.2.2. Thermal processing

The thermal processing was conducted by placing 4 mL aliquots of the model juice in glass tubes with small diameter (10 mm) and thin walls (0.6 mm). The tubes were positioned in a holder inside a thermostatic water bath (Dubnoff MA 095/CFRE, Marconi, Brazil) with orbital shaking at 150 rpm, as illustrated in Figure 3.1.
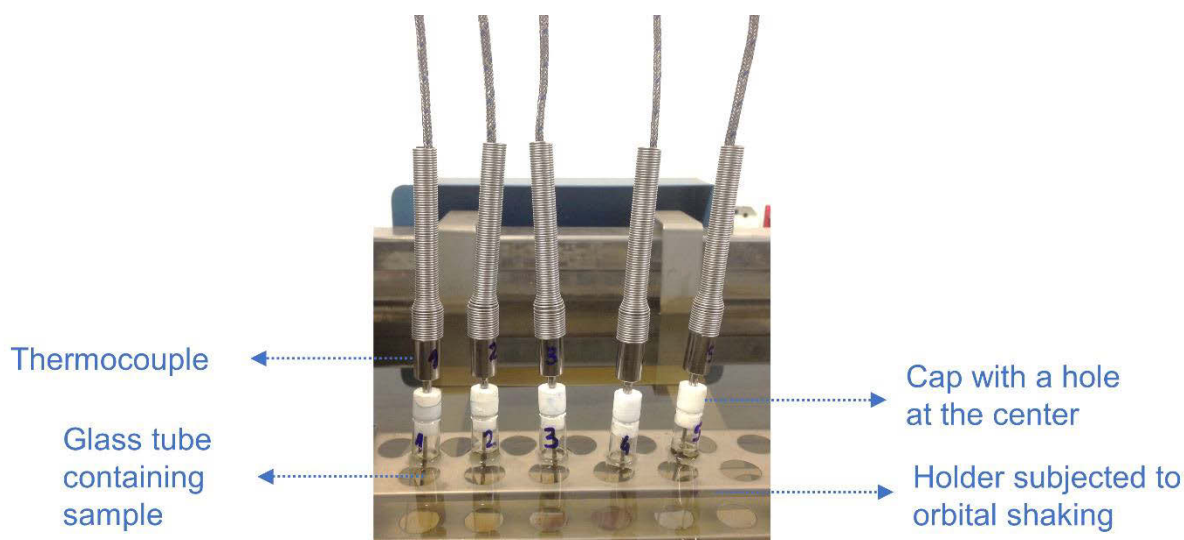
Figure 3.1. Experimental set up for the conventional thermal processing of fruit juice model solution in a water bath.

The thermal process was carried out at seven process temperatures (T_P = 60, 62, 64, 66, 68, 70, 72 °C) and six process times (heating + holding times) for each T_P. The combinations of temperature and time employed are shown in Table 3.1. For a better understanding of the notation above, the definition of process temperature, heating and holding times is illustrated further below, in Figure 3.3A.

After the desirable holding time, the samples were quickly cooled in an ice-water bath until the temperature reached 5 °C. The temperature history of each sample was monitored using T-thermocouples fixed in the center of the tube through a cap and connected to a data logger (Almemo 2890-9, Ahlborn, Germany), with sampling rate of 1 per second. All experiments were performed in triplicate.

Table 3.1. Process time (heating + holding times) and final temperature combinations performed during the conventional heating of fruit juice model solution.

Process time [min]	\ Temperature [°C]						
	60	62	64	66	68	70	72
1.0			x	x	x	x	
2.0	x	x		x	x	x	x
3.0			x		x	x	x
3.5							x
4.0		x		x		x	x
4.5							x
5.0	x		x		x		x
6.0		x		x		x	
7.0			x		x		
8.0	x	x		x		x	
9.0			x		x		
10.0	x	x		x			
11.0			x				
12.0		x					
13.0	x						
15.0	x						

3.2.3. Enzyme activity assay

The POD activity was determined according to the method described by Augusto et al. (2015). The enzyme activity assays were performed at room temperature and pH 6.0. The desired pH was obtained using a McIlvaine's buffer solution, which was prepared by combining determined volumes of 0.1 mol L^{-1} citric acid (Synth, Brazil) solution and 0.2 mol L^{-1} sodium phosphate dibasic (Synth, Brazil) solution (McIlvaine, 1921). The POD activity was evaluated using pyrogallol as the substrate.

In each assay, 160 µL of sample, 2.25 mL of McIlvaine's buffer solution at pH 6.0 and 320 µL of 5% (m/v) pyrogallol solution (Sigma-Aldrich Co., UK) were mixed in a quartz cuvette with a 1-cm light path. The mixture of all reactants was used as a reference solution (0.000 absorbance). Then, 160 µL of 0.147 mol L^{-1} hydrogen peroxide solution (Synth, Brazil) was added to start the reaction: the oxidation of pyrogallol to purpurogallin, as illustrated in Figure 3.2. The increase in the solution absorbance at 420 nm was measured every 1 s for 2 min using a UV-Vis spectrophotometer (UV-1240, Shimadzu, Japan).
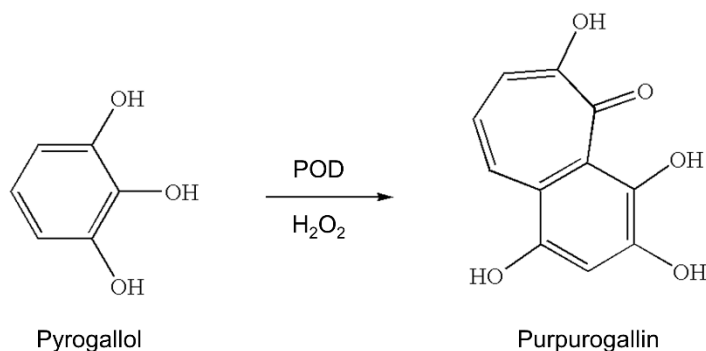
Figure 3.2. Illustration of the oxidation of pyrogallol to purpurogallin catalyzed by the enzyme peroxidase.

The variation of absorbance at 420 nm in relation to the reaction time shows an increasing curve with concave shape, which can be described by a composite exponential function (Augusto et al., 2015):

$$Abs_{(tAbs)} = Abs_\infty - (Abs_\infty - Abs_0) \cdot e^{(-k_{Abs} \cdot t_{Abs})}$$ Eq. 3.1

where $Abs_{(tAbs)}$ is the sample absorbance at any time t_{Abs}, Abs_0 is its initial absorbance, Abs_∞ is the maximum absorbance and k_{Abs} is the kinetic parameter. The enzyme activity (A) was then defined as the maximum reaction rate, which is observed when $t_{Abs} = 0$ (Augusto et al., 2015):

$$A = \left(\frac{dAbs_{t_{Abs}}}{dt_{Abs}}\right)_{t_{Abs}=0} = (Abs_\infty - Abs_0) \cdot k_{Abs}$$ Eq. 3.2

The parameters of the equations above were obtained by regression using a generalized reduced gradient algorithm implemented in the 'Solver' tool of software Excel 2016 (Microsoft, USA). The enzyme activity and the relative activity of each thermally processed tube were evaluated in duplicate. The relative activity (A/A_0) was calculated by the ratio of the enzyme activity after the process (A) to the original or initial activity (A_0) before thermal processing for each solution.

3.2.4. Enzyme inactivation kinetics

Three possibilities of inactivation kinetics were firstly evaluated: first order kinetic, two-fraction kinetic and Weibull distribution models. These three approaches cover most of the literature regarding POD inactivation by different technologies (Augusto et al., 2015;

Gonçalves et al., 2007; John et al., 2017; Murasaki-Aliberti et al., 2009; Rojas et al., 2017; Sampedro and Fan, 2014; Siguemoto et al., 2018b; Terefe et al., 2017).

Preliminary results showed that first order kinetic, two-fraction kinetic and Weibull distribution models were adequate to describe the inactivation of peroxidase. The obtained values of fit criteria and model parameters were quite comparable. To select the most appropriate model, following the principle of parsimony, it is advisable the choice of models that are as simple as possible; then, models with the smallest possible number of parameters for adequate representation of the data should be preferred (Van Boekel, 2002). Therefore, since the first order model presents fewer parameters and the three kinetic models provided good fit to the experimental data, the first order kinetic model was selected to describe the peroxidase inactivation kinetic in the juice model solution.

3.2.4.1. First order kinetic

The simplest behavior for the enzyme inactivation mechanism describes the passage of the native form of the enzyme to a single inactive state due to denaturation (Augusto et al., 2015). It considers only one enzymatic portion to be inactivated, and it can be described by the first order kinetics:

$$\frac{A}{A_0} = e^{-kt}$$
<div align="right">Eq. 3.3</div>

In order to have more practical parameters for food processing, the residual activity can also be written as:

$$log\left(\frac{A}{A_0}\right) = -\frac{t}{D_T}$$
<div align="right">Eq. 3.4</div>

with:

$$e^{-kt} = 10^{-t/D_T}$$
<div align="right">Eq. 3.5</div>

$$k(T) = \frac{ln10}{D_T}$$
<div align="right">Eq. 3.6</div>

where D_T value is the time required for a 90% reduction of the enzymatic activity under isothermal conditions.

The effect of temperature on the D_T value is expressed as a z value, which is the temperature increase that reduces D_T by 90%. This relationship can be described as follows:

$$log\left(\frac{D_T}{D_{Tref}}\right) = \frac{T_{ref} - T}{z}$$
<div align="right">Eq. 3.7</div>

3.2.4.2. Enzyme inactivation under non-isothermal processing

During the performed thermal processing, the samples were processed in a non-isothermal way, i.e. the heating and cooling of the samples were not instantaneous. Thus, the temperature profile has 3 steps: heating (come-up), holding and cooling, as shown in Figure 3.3A. Figure 3.3B illustrates the difference between a temperature profile found in the present work (non-isothermal heating) and its respective ideal profile (instantaneous or isothermal heating).
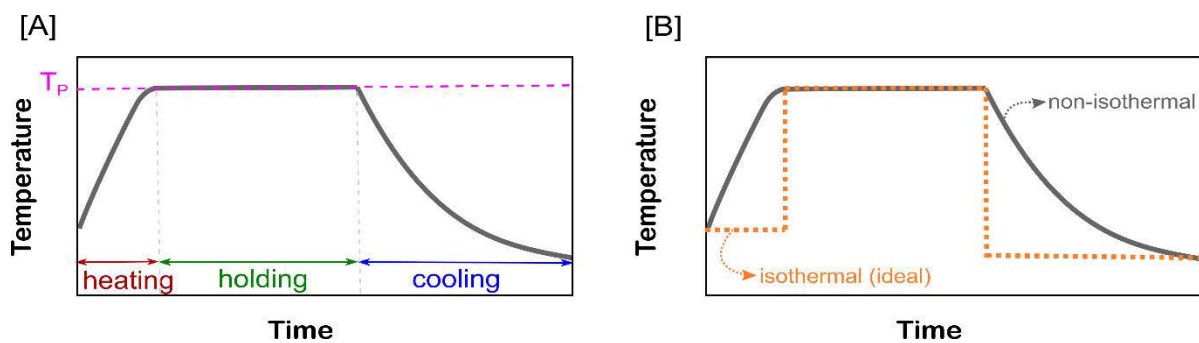
Figure 3.3. Representation of the time-temperature profile: (A) during a non-isothermal processing, including the periods of heating, holding at the desired process temperature - T_P, and cooling; (B) during a non-isothermal and an isothermal processing with instantaneous heating and cooling.

Therefore, in order to take into account the contribution of the whole temperature history to the inactivation, the concept of lethality L_t, defined in Eq. 3.8, was applied. The accumulated lethality at any location in the sample is generally obtained by integrating the temperature profile effects on inactivation during the heating, holding and cooling periods (Lin and Ramaswamy, 2011; Tajchakavit and Ramaswamy, 1997).

The accumulated lethality is expressed as the equivalent holding time ($F_{T_{ref}}$), which is the equivalent processing time at reference temperature (T_{ref}) if instantaneous heating and cooling were possible, yielding the same inactivation as the actual process (Rojas et al., 2017). The $F_{T_{ref}}$ was obtained through the Eq. 3.9, which was evaluated numerically using the trapezoidal method (Murasaki-Aliberti et al., 2009). Due to small tube diameter, thin walls, vigorous agitation and low fluid viscosity, the temperature inside the sample was assumed as homogeneous.

$$L_t = 10^{\left(\frac{T_t - T_{ref}}{z}\right)} \hspace{3cm} \text{Eq. 3.8}$$

$$F_{T_{ref}} = \int_0^t L_t \, dt = \int_0^t 10^{\left(\frac{T_t - T_{ref}}{z}\right)} dt \hspace{2cm} \text{Eq. 3.9}$$

Therefore, considering the non-isothermal temperature profile, the predicted residual activities by the first order kinetic were calculated from the numerical evaluation of the following equation (combination of Eq. 3.4 and Eq. 3.9):

$$\frac{A_t}{A_0} = 10^{\left(-\frac{F_{T_{ref}}}{D_{Tref}}\right)} \hspace{3cm} \text{Eq. 3.10}$$

The parameters of the kinetic model were iteratively adjusted by a non-linear estimation procedure, minimizing the sum of squared errors (SSE) between experimental and predicted residual enzymatic activities. For that, a generalized reduced gradient algorithm was implemented in the 'Solver' tool of software Excel 2016 (Microsoft, USA). Uncertainty estimates were calculated by the macro 'SolverAid' (De Levie, 2004).

The SSE is defined by Eq. 3.11, where n_e is the number of experiments (i.e., including all the process temperature, time and replicates), subscript 'exp' indicates experimental data and subscript 'model' indicates values predicted from the model (Matsui et al., 2008). To report the fit criteria of the model, it was considered the minimized SSE and the coefficient of determination R^2.

$$SSE = \sum_{j=t_{initial}}^{t_{final}} \sum_{i=1}^{n_e} \left[\left(\frac{A_t}{A_0}\right)_{i,exp}(j) - \left(\frac{A_t}{A_0}\right)_{i,model}(j) \right]^2 \hspace{2cm} \text{Eq. 3.11}$$

In order to validate the adjusted kinetic model, independent experimental data that were not used in the model fitting were evaluated. The data were obtained from the experiments performed to evaluate the POD reactivation, presented later in Chapter 5. The thermal processes were carried out following the same procedures mentioned above, but in different laboratories. The combinations of process temperature and holding time were: 60 °C/2 min, 66 °C/3 min, 72 °C/6 min.

3.3. Results and discussion

3.3.1. Enzyme inactivation kinetics by conventional heating process

3.3.1.1. Modeling

Fruit juice model solution was processed using conventional heating in a water bath. The profiles of thermal history represent the changes on product temperature along the process, as shown in Figure 3.4. The three stages of a non-isothermal processing (heating, holding and cooling) can be observed. It can also be noted that although the heating rate was fast (around 60 – 70 °C/min), the product did not reach the process temperature instantaneously. Thus, even using tubes with small diameter and wall thickness and working with a small volume of sample solution under stirring, the process was still not ideally isothermal. Further, the shorter the process time, the higher the importance of the heating and cooling stages, with regard to the thermal lethality during the whole processing. Therefore, it clearly justifies the adopted approach of accumulated lethality and equivalent holding time for the kinetic modeling.
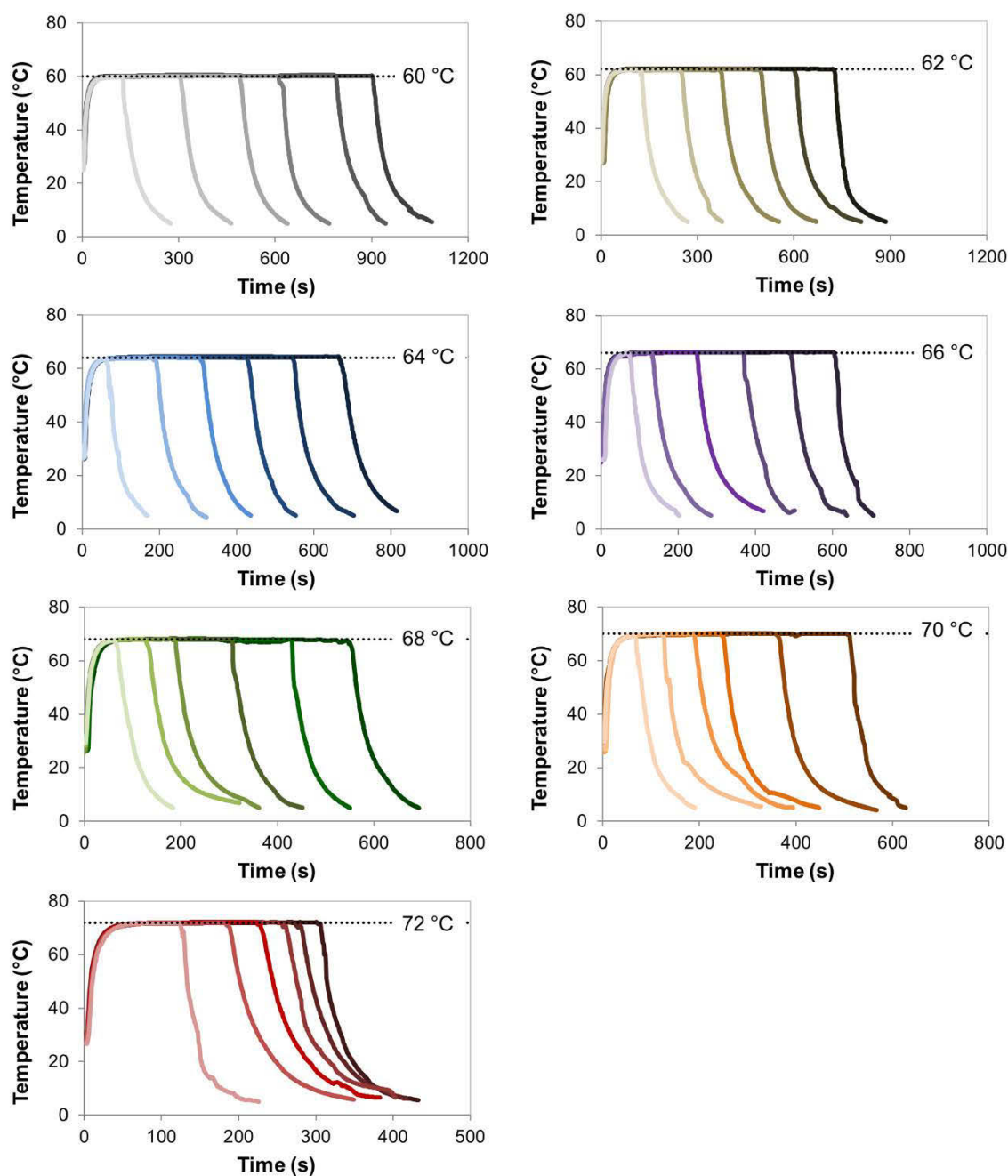
Figure 3.4. Examples of thermal history of fruit juice model solution along the conventional processing at the following process temperatures and process times (heating + holding): 60 °C for 2, 5, 8, 10, 13 and 15 min; 62 °C for 2, 4, 6, 8, 10 and 12 min; 64 °C for 1, 3, 5, 7, 9 and 11 min; 66 °C for 1, 2, 4, 6, 8 and 10 min; 68 °C for 1, 2, 3, 5, 7 and 9 min; 70 °C for 1, 2, 3, 4, 6 and 8 min; 72 °C for 2, 3, 3.5, 4, 4.5 and 5 min.

For each process time-temperature combination, the treatment was performed in triplicate. After each treatment, the residual POD activity was measured in duplicate. In the previous figure, examples from just one repetition were presented. Although being quite similar, thermal histories were not exactly the same ones in each processing repetition. Thus, this fact, along with possible experimental errors, resulted in some differences of residual activity at the same time-temperature combination, as shown in Figure 3.5. This figure presents

the residual enzymatic activities obtained from all the thermal treatments as a function of the process time. As expected, the inactivation rates increased with increasing process temperatures.
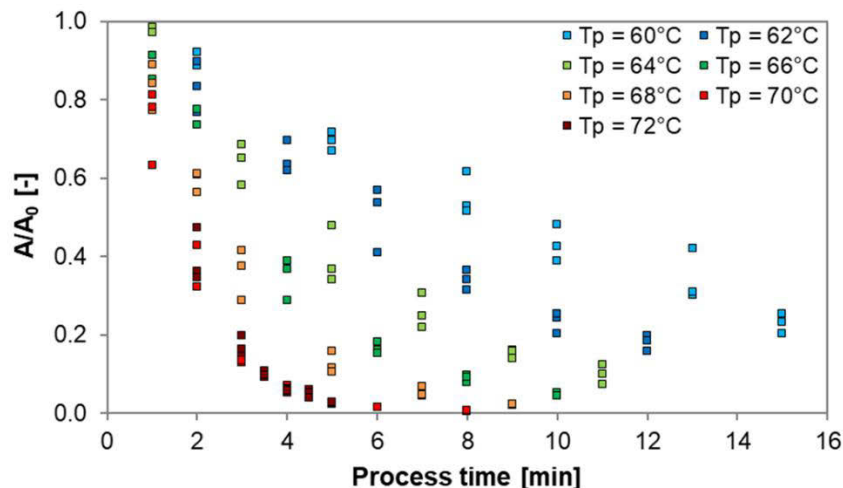
Figure 3.5. Residual POD activities in fruit juice model solution as a function of process time after conventional processing at seven different process temperatures (T_P).

For the inactivation kinetics modeling, all the residual enzymatic activities as well as their corresponding thermal histories from all the processing repetitions were employed. Since there is no specific isothermal holding time, any temperature within the range of study (60 – 72 °C) could be used as a reference temperature (Tajchakavit and Ramaswamy, 1997). The reference temperature T_{ref} was then set to 70 °C.

Thus, considering the non-isothermal profile of the processing, the accumulated lethality at 70 °C was calculated and inactivation data were fitted to a first order kinetic model. Adjusted kinetic parameters and fit criteria obtained from an iterative non-linear estimation procedure are shown in Table 3.2. The predicted inactivation curve and experimental residual activities as a function of $F_{T_{ref}}$ for 70 °C are presented in Figure 3.6A. A parity chart comparing the predicted data and the experimental values obtained after thermal processing at different T_P is shown in Figure 3.6B.

Table 3.2. Kinetic parameters and fit criteria of the adjusted first-order kinetic model for peroxidase inactivation in fruit juice model solution by conventional heating.

Parameters		Fit criteria	
$D_{70°C}$ [s]	234.377 ± 7.068	SQE	0,223
z [°C]	12.072 ± 0.295	R^2	0,97
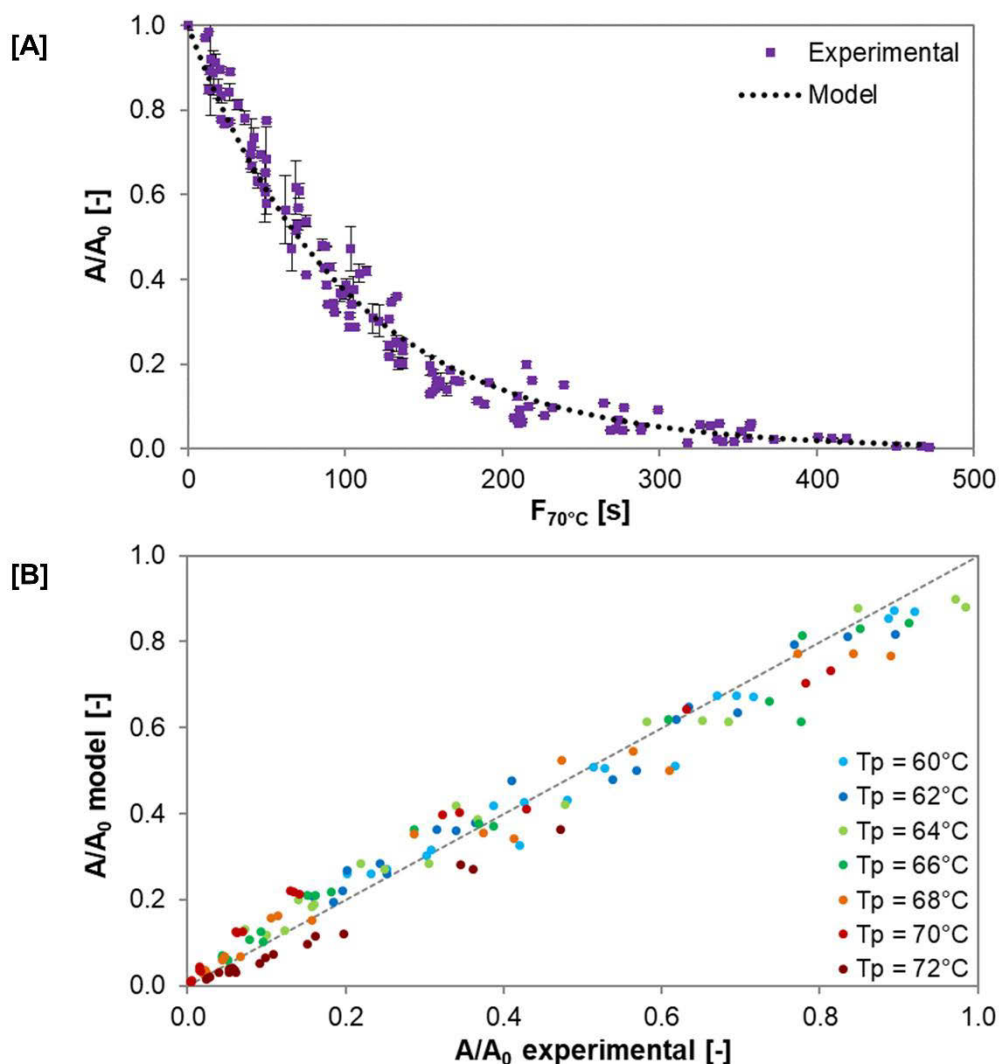
Figure 3.6. (A) Residual peroxidase activity (A/A_0) as a function of the equivalent time ($F_{70°C}$, considering 70 °C as the reference temperature), where purple square dots are the experimental values, the vertical bars are the standard deviation and the black dotted curve is the adjusted first-order model. (B) Parity chart between the values predicted by the model and the experimental data obtained after thermal treatment at different process temperatures (T$_P$).

By observing the fit criteria and the figures, the first order kinetic model showed good suitability to fit POD inactivation data under the evaluated conditions. Aiming to compare the obtained results with literature, the values of D_T at different temperatures were calculated based on Eq. 3.7, using the estimated kinetic parameters from Table 3.2. Then, the temperature sensitivity curve, also known as thermal destruction time (TDT) curve, was extrapolated and plotted beyond the experimental temperature range, as shown in Figure 3.7. In this way, the results obtained in the present work could be compared with data from literature at different temperatures.
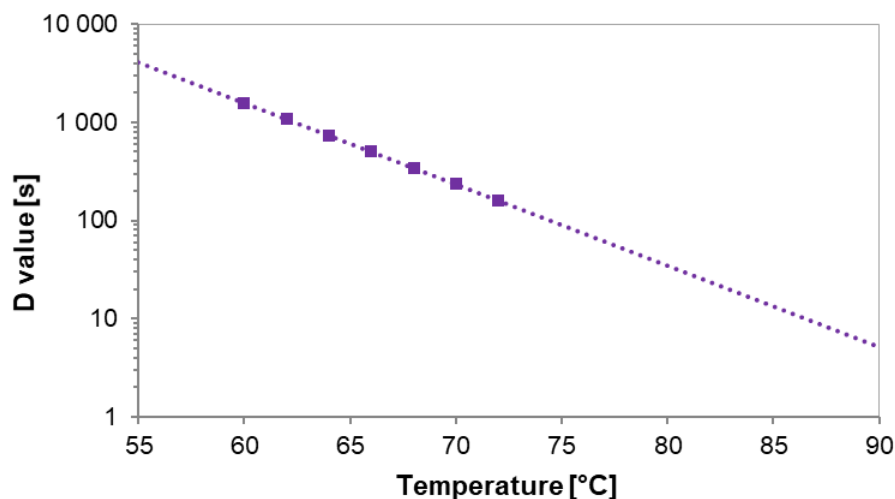
Figure 3.7. Temperature sensitivity curve of peroxidase inactivation in model fruit juice during conventional thermal treatment. Square-dots indicate D values at the experimental process temperatures.

In a study of green coconut water model solutions, Matsui et al. (2007) evaluated the POD inactivation kinetics in different aqueous solutions by microwave heating. In a solution composed of horseradish POD and water, the $D_{91.5°C}$ and z values of the first-order model were 44 s and 24 °C. However, when sugars (sucrose, glucose, fructose) were added to produce another solution (4.5 °Brix), the $D_{92°C}$ and z values were reported to be 20.5 s and 19.5 °C. Thus, the addition of sugars decreased both kinetic values. Chang et al. (1988) also reported a decrease of horseradish POD thermal stability in the presence of small amounts (up to 20% w/w) of sucrose. According to the previous figure, the D value at 92 °C was around 5 s. Thus, the values of the estimated kinetic model of the present work were considerably lower than the ones reported by Matsui et al. (2007), which may be explained by the higher TSS content (10 °Brix) in the model juice.

In addition, another factor that justifies the difference between these solutions is the pH. While in the solutions from literature the pH was around 6.5, in the fruit juice model solution the pH was 3.8. It is known that the closer to neutrality is the pH, the greater the thermal stability of horseradish POD (Lemos et al., 2000). For example, Joffe and Ball (1962) studied the horseradish POD inactivation kinetics in phosphate buffer solution (pH 7.0) during conventional thermal treatment and reported a first-order model with $D_{85°C}$ and z values equal to 143 min (8580 s) and 9.9 °C, respectively. As it can be noted, the D value was much higher than the one found in the present work ($D_{85°C}$ = 13 s).

Lemos et al. (2000) evaluated the thermal inactivation of horseradish peroxidase in aqueous solutions containing sodium hydroxide or hydrochloric acid at different pH (3.0 – 12.5). The inactivation data were fitted by a two-fraction kinetic model, in which a heat-labile and a heat-resistant fractions were considered. In the more acid solutions, at pH between 3

and 4 (pH range of the model fruit juice), the resistant fraction presented $D_{70°C}$ and z values of around 85 min and 30 °C, respectively. While the labile fraction, which was reported as the major fraction (80%), showed $D_{70°C}$ value of around 2 – 9 min and z value close to 10 °C. In the present work, the data did not show the presence of two enzymatic fractions, thus the first-order model was chosen. When comparing the estimated and reported results, it can be noted that the obtained kinetic values ($D_{70°C}$ = 3.9 min and z = 12 °C) were quite consistent to those reported for the labile fraction.

3.3.1.2. Validation

The accuracy of the kinetic model was validated using different experimental data, which were not used for the kinetic parameters estimation. Three thermal treatments using conventional heating were evaluated: 60 °C/2 min, 66 °C/3 min, 72 °C/6 min. Examples of their temperature profiles are shown in Figure 3.8A. A parity chart comparing predicted values and experimental residual activities is presented in Figure 3.8B. It can be observed that the model showed good ability to predict enzymatic inactivation in the assessed treatments. Therefore, the adjusted model and its kinetic parameters can be considered as appropriate to describe the kinetics of inactivation of peroxidase in model fruit juices.
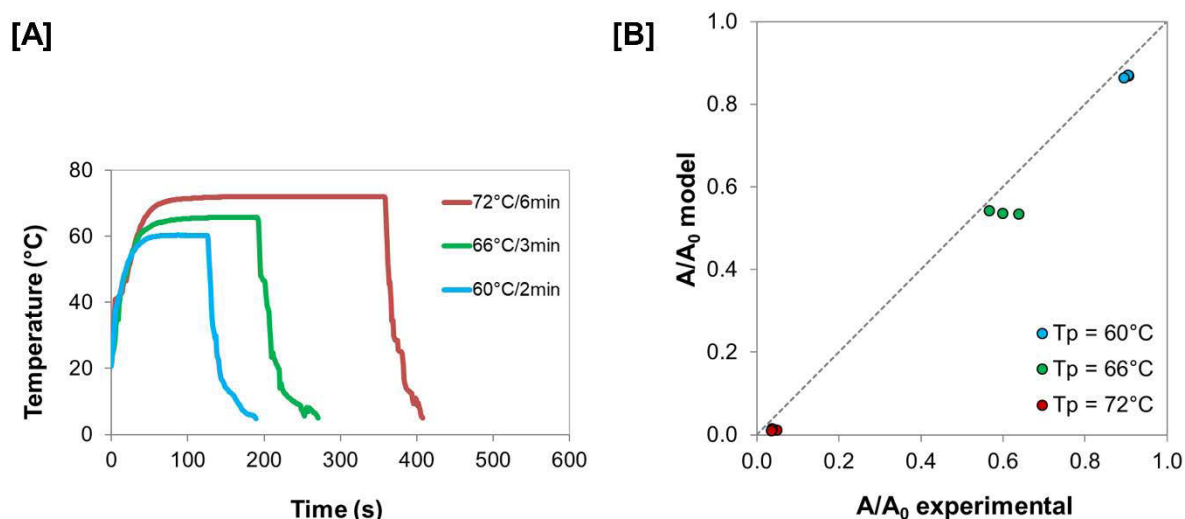
Figure 3.8. (A) Examples of thermal history of fruit juice model solution along the conventional processing. (B) Parity chart between the values of residual peroxidase activity (A/A_0) predicted by the adjusted model and the experimental data.

3.4. Conclusion

Peroxidase (POD) is an enzyme responsible for undesirable effects on fruit and vegetable products. The thermal inactivation of POD by conventional heating was evaluated

in the fruit juice model solution. The evaluation was conducted over the temperature range from 60 to 72 °C, considering the non-isothermal profile of processing. The accumulated lethality of each treatment was calculated from the recorded thermal history. The obtained data were well described by the adjusted first-order kinetic model. By comparing the obtained results with literature, some discrepancies due to environmental differences (e.g., pH, sugar content, processing conditions) were found. However, the kinetic parameters were consistent with the expected trends. The estimated first-order kinetic model was successfully validated by experimental data not used in the model fitting.

Particularly, the development of an accurate and reliable kinetic model is of great importance for the next chapter, in which the model is implemented as part of the 3D-multiphysics model. It will allow to predict the peroxidase inactivation during the microwave processing of the model fruit juice, considering the fluid flow and the non-uniformity of the spatial temperature distribution.

CHAPTER 4.   MULTIPHYSICS MODELING OF A BATCH MICROWAVE PROCESSING FOR ENZYME INACTIVATION

4.1. Introduction

This chapter deals with the batch microwave processing of the fruit juice model solution, considering two parts: experimental and numerical. First, the processing of juice samples by microwaves was described and the resulting enzymatic inactivation was evaluated. Then, a numerical study by finite element method was performed. In order to simulate the processing, a multiphysics model was developed coupling electromagnetic energy, heat transfer and fluid flow. In addition, the kinetic model of peroxidase inactivation described in the previous chapter was also included in the simulation model. In this way, the peroxidase inactivation could be predicted, taking into account the convection currents and the spatial distribution of temperature within the sample during the microwave heating. The experimental results, including peroxidase residual activities and measured temperatures, obtained in the first part of the present chapter, were used to compare and validate the results from simulation. Besides, a discussion concerning the importance of fluid flow in the modeling of microwave heating of liquids was presented.

4.2. Material and methods

4.2.1. Fruit juice model solution

Fruit juice model solution was prepared following the same procedure described in the Chapter 3, using sucrose (Merck, Germany), citric acid (Merck, Germany) and horseradish peroxidase (POD, type X commercialized under crystalline suspension in 3.2 mol L^{-1} ammonium sulfate; EC: 1.11.1.7; P6140-5KU; Sigma-Aldrich Co., USA). The final soluble solids content, enzymatic activity and pH of the model solution were 10 °Brix, 4 U mL^{-1} and 3.8, respectively.

4.2.2. Enzyme activity assay

The POD activity was determined according to the same method described in the Chapter 3. In a quartz cuvette with a 1-cm light path, 160 µL of sample was added to 2.25 mL of McIlvaine's buffer solution at pH 6.0 and 320 µL of 5% (w/v) pyrogallol solution (Sigma, UK).

This mixture was used as a reference solution (0.000 absorbance). Then, 160 µL of 0.147 mol L^{-1} hydrogen peroxide solution (Sigma-Aldrich, Italy) was added to start the reaction.

The increase in the solution absorbance at 420 nm was recorded every 5 s for 2 min using a UV-Vis spectrophotometer (UviLine 8100, Secomam, France). From the curve of absorbance as a function of time, the enzyme activity was then calculated by regression using a generalized reduced gradient algorithm implemented in the 'Solver' tool of software Excel 2016 (Microsoft, USA). The enzyme activity was evaluated in duplicate. The residual activity (A/A_0) was calculated by the ratio of the enzyme activity after processing to the initial activity before microwave processing.

4.2.3. Microwave processing

4.2.3.1. Microwave system

Microwave processing was performed in a microwave apparatus, which supplied monochromatic waves in the fundamental mode, denoted TE$_{10}$, operating at a frequency of 2.45 GHz. The experimental apparatus was composed of: a microwave generator (magnetron type), a waveguide, an applicator and a water load. A schematic diagram of the microwave system, indicating its main components, is shown in Figure 4.1.

The generator (GMP03KSM, Sairem, France) was connected to the waveguide through a coaxial cable connected to a WR340 waveguide transition. Microwave energy was transmitted along the z-direction of the rectangular waveguide (cross-section 86 mm X 43 mm) made of brass. To ensure that a minimal amount of microwave was reflected back to the sample and magnetron, a water load was fixed at the bottom end of the guide, located about 40 cm distance from the applicator. This water load consisted of a quartz tube through which water at 15 °C from a thermostatic bath circulated at a flow rate of around 820 mL min^{-1}.

The applicator was positioned in the middle of the waveguide. Since both of them had the same rectangular transversal section, the applicator can be considered as a continuation of the waveguide. It is in the applicator that the sample to be processed is placed. The small holes on the right side of the applicator enable the insertion of temperature sensors, such as fiber optic sensors and thermocouples. By the way, the use of optical fibers for temperatures measurement during microwave processing is more recommended. While the metal constituents of the thermocouples may disturb the electromagnetic field, the fiber optic sensors do not interact with the field due to its nonmetallic nature. Thus, the experimental temperature of the sample was measured and recorded by a fiber optic sensor connected to a data logger (Reflex-4, Neoptix, Canada).
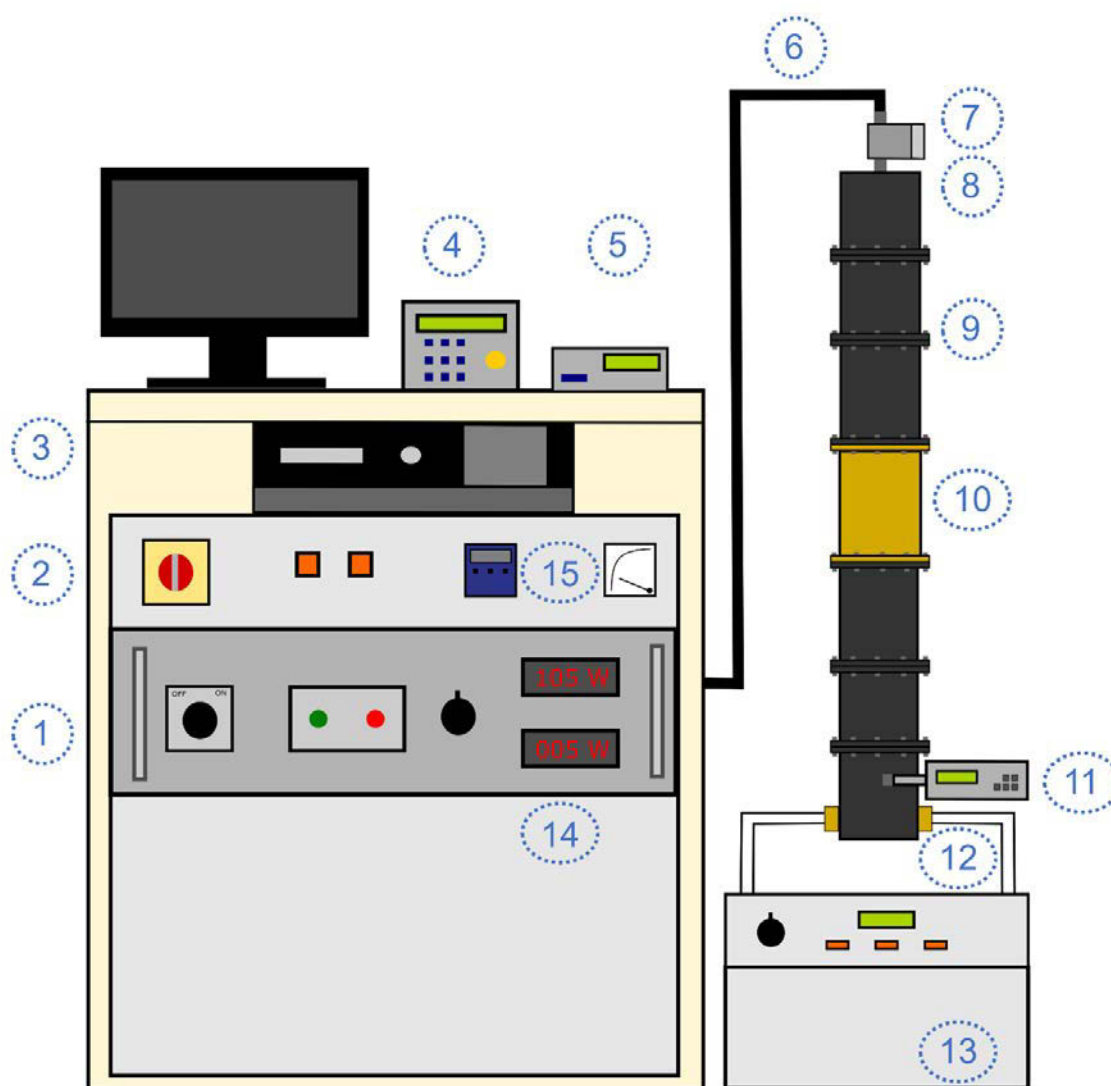
Figure 4.1. Schematic representation of the microwave system and its main components: 1) microwave generator, 2) energy control panel, 3) computer, 4) data logger for power and temperature records, 5) data logger for fiber optic sensors, 6) coaxial cable, 7) coaxial isolator, 8) WR340 waveguide transition, 9) rectangular waveguide, 10) applicator, 11) power meter, 12) water load, 13) water bath, 14) power control, 15) temperature controller.

In order to monitor the microwave processing along the time, the generator and the waveguide were instrumented by incident and reflected power sensors that were connected to a data logger (Datalog 20, AOIP, France). Knowledge of power values is important not only for control and monitoring of the process but also as an input data in the models for microwave heating simulations. However, for numerical simulations, an accurate incident power (transmitted power) through the waveguide is necessary. During the transmission of the microwave energy from the generator to the waveguide, some losses in the transmission lines can occur along the path, such as losses in the coaxial cable and waveguide transition. Therefore, using a coupler terminated in a 50 Ω load connected to a power meter (Techniwave,

France), the maximum actual incident power was measured and found to be equal to 105 W. This value was then implemented in the simulation model as the maximum input power.

4.2.3.2. Experimental setup

A support block made of extruded polystyrene with 60 mm in height was placed inside the applicator. The block was arranged to be perpendicular to the wave transmission direction, filling the section and serving as a support for a small tube of 10.13 mm external diameter, 7.93 mm internal diameter and 35.80 mm height. This tube containing an aliquot of 1.2 mL of sample was placed in the center of the block, where the amplitude of electric field was maximum (TE_{10} mode). A cylindrical polystyrene cap was used to close the tube, to limit possible sample evaporation and to ensure the position of the fiber optic sensor. A schematic diagram of the applicator is shown in Figure 4.2.

Preliminary tests were performed to compare the transmitted power through the empty applicator and through the applicator containing the polystyrene block and plastic tube (without sample). The same values of power were obtained in both cases, indicating these materials do not absorb microwave energy.

Two groups of microwave processing experiments were performed. In the first, the fruit juice model solution was treated aiming a single processing temperature and a single holding time. Then, in this case, the experiments were performed at seven process temperatures (T_P = 60, 62, 64, 66, 68, 70, 72 °C) and four holding times for each T_P. The combinations of temperature and time employed are shown in Table 4.1.

Table 4.1. Holding time and process temperature combinations performed during the microwave heating of fruit juice model solution.

		Temperature [°C]						
		60	62	64	66	68	70	72
	No holding	x	x	x	x	x	x	x
Holding time [min]	1.0	x			x		x	x
	2.0		x	x		x	x	x
	3.0				x		x	x
	4.0	x	x	x		x		
	5.0				x			
	6.0		x			x		
	7.0			x				
	8.0	x						

In the second group, the fruit juice was treated differently, with two holding stages (i.e. two process temperatures and holding times) instead of one. In this case, two different treatments were performed: 62 °C/3 min + 70 °C/3.5 min, and 50 °C/3 min + 65 °C/3 min (holding temperature/holding time).

A PID temperature controller was used to maintain T_P at its expected setpoint during the appropriate residence time by acting on the incident power. The temperature was measured at the geometrical center of the sample using a fiber optic sensor connected to a data logger (Reflex-4, Neoptix, Canada).

The incident and reflected powers as well as the inlet and outlet temperatures of the water load were recorded using a data logger (Datalog 20, AOIP, France). After each treatment, the samples were removed from the applicator and rapidly cooled in an ice bath until 5 °C. All experiments were performed in triplicate. Enzyme activity of the samples was determined shortly after the processing and the residual activity was calculated.
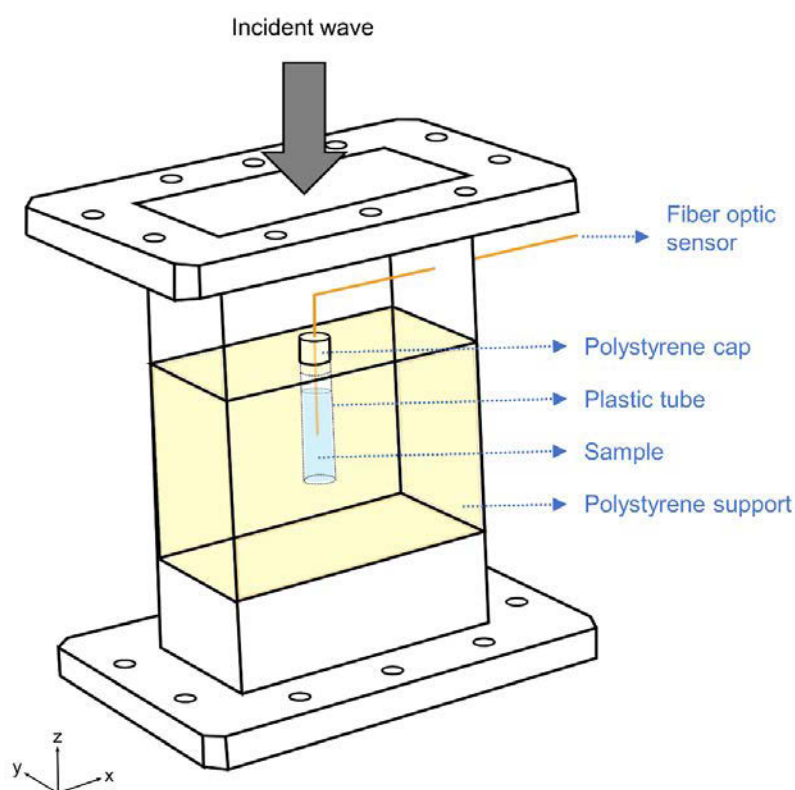
Figure 4.2. Schematic diagram of the applicator and experimental setup for the microwave processing of fruit juice model solution.

4.2.4. Model development

4.2.4.1. Geometry and assumptions

The model geometry was based on the real apparatus used for microwave processing of the juice. However, some modifications and considerations were needed. Since 3D-models require considerable computational effort, it is highly recommendable to simplify the geometry of the problem whenever possible. In the present case, the fact of using a TE_{10} mode waveguide allowed an interesting simplification. For an empty rectangular waveguide filled with air, in the plane xy, the electric field has only one component (E_y), whose maximum amplitude is located in the center of the waveguide and in turn, in the center of the sample, as shown in Figure 4.3. Also, the distribution of the electric field is uniform along b (y-axis), varying only along a (x-axis) and direction of wave propagation (z-axis). Thus, instead of considering all the initial geometry, it is possible to model only ¼ of the waveguide. Therefore, the geometry was defined as ¼ of the waveguide and sample, which allowed a substantial reduction of computational resources and time required for simulations.
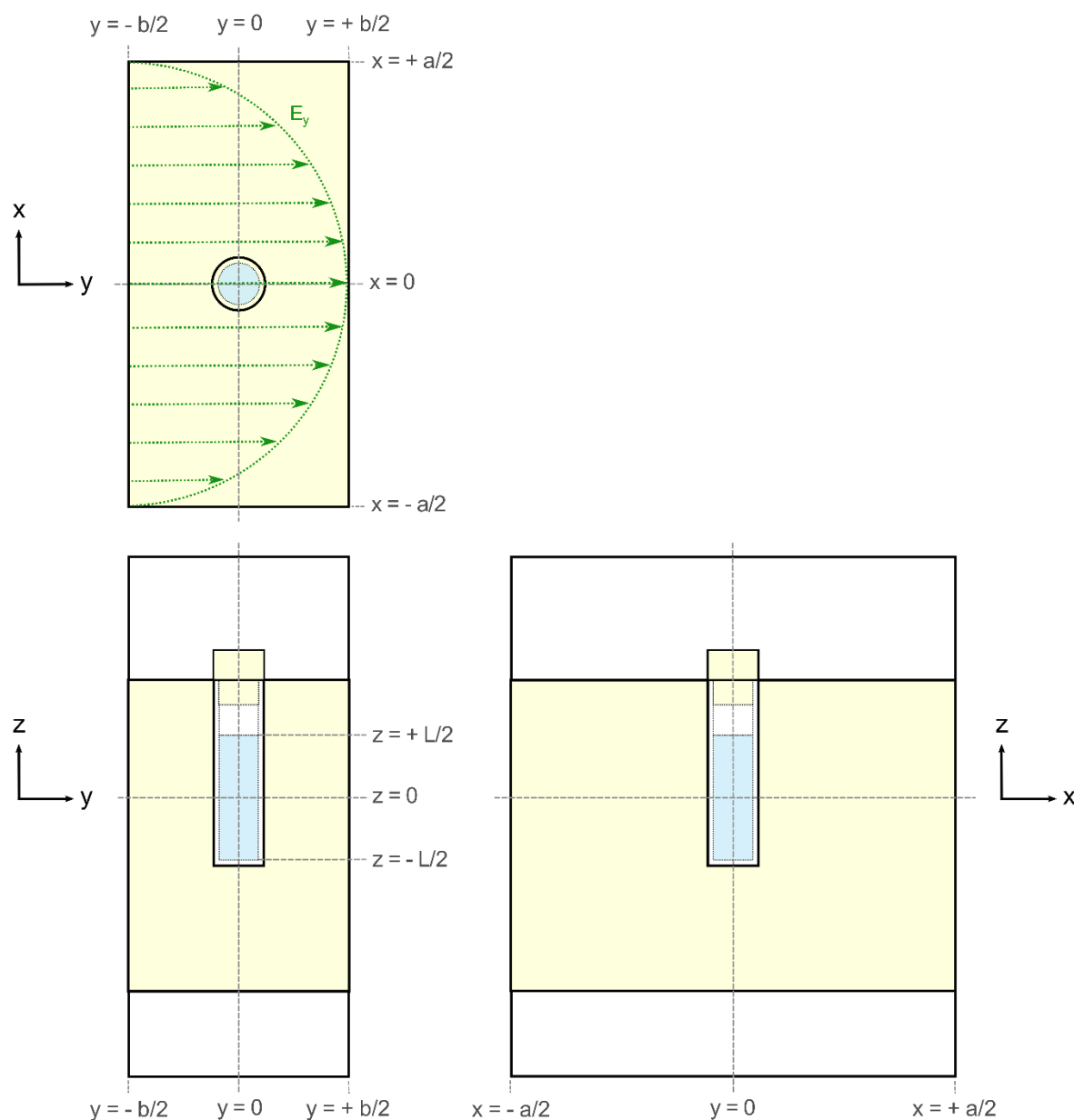
Figure 4.3. Arrangement of the sample, plastic tube, polystyrene cap and support inside the TE_{10} mode rectangular waveguide, where a = 86 mm, b = 43 mm, L = 24.3 mm. Electric field distribution within an empty TE_{10} waveguide in the plane xy is illustrated by dotted lines in green.

Another important simplification was made in the model. It consisted of not consider neither the plastic tube, nor the support block, nor the cap in the computational domain. In this way, the sample was assumed to be surrounded by air. Preliminary tests showed that none of these neglected items absorb microwave energy, indicating that this modification does not affect the electromagnetic field modeling. However, it affects the modeling of heat transfer, since the sample surface loses heat to the tube, the support, the cap and the surrounding air during processing. Therefore, the knowledge of heat transfer around the sample was needed and it was obtained through the determination of a global heat transfer coefficient. This coefficient was estimated experimentally according to the procedure described later (section

Global heat transfer coefficient). Figure 4.4 illustrates the final simplified geometry considered in the computational domain.
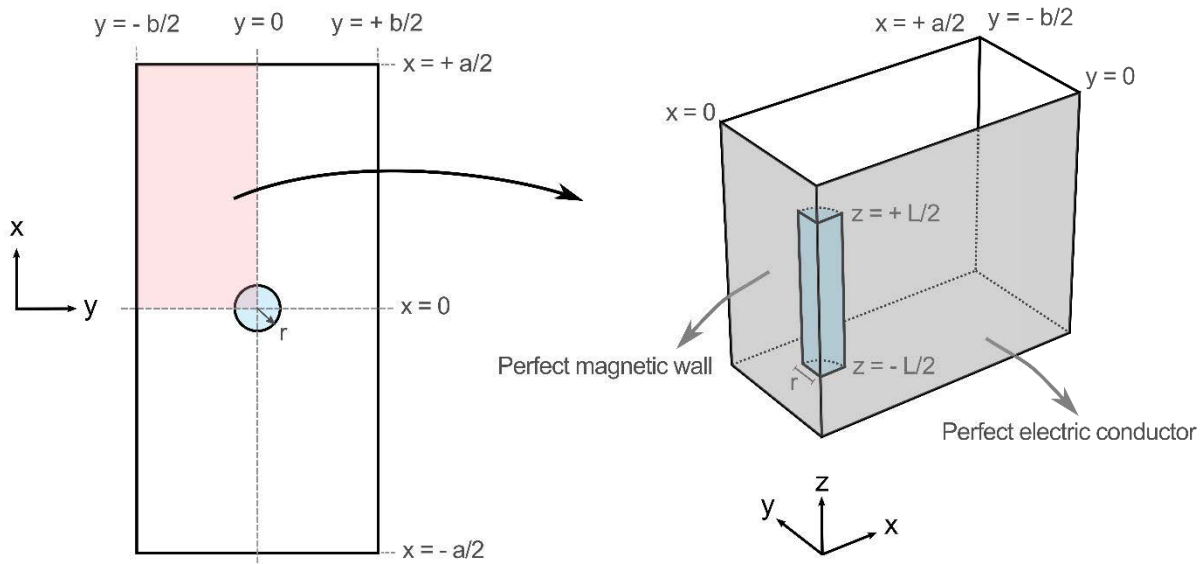
Figure 4.4. Model design and computational domain, where a = 86 mm, b = 43 mm, L = 24.3 mm and r = 3.965 mm.

In order to model the microwave heating of the fruit juice model solution, the following assumptions were also made:

- The product was considered as homogeneous and isotropic (i.e. it had the same physical properties independently of direction);
- The initial temperature of the solution was uniform;
- There was no mass transfer and evaporation;
- The external environment temperature was constant and fixed to 20 °C;
- The sample was initially at rest (i.e., $U_x = U_y = U_z = 0$);
- Sample flow was considered as a weakly compressible flow, in which the density variation with temperature was evaluated at a reference atmospheric pressure;
- The walls of the rectangular waveguide were considered as perfect electric conductors;
- Sample was considered as non-magnetic;
- The product was surrounded by a medium with zero dielectric losses (air), thus, heat transfer was not spatially solved within the surrounding medium (air). However, natural convection to the air was considered as a boundary condition with the global heat transfer coefficient;
- Polystyrene support and plastic tube did not interact with the electromagnetic field;
- At the end of the waveguide, there was no wave reflection (perfectly matched water load).

4.2.4.2. Modeling of electromagnetic field and microwave propagation

The modeling of microwave interactions with dielectric materials is governed by the classical Maxwell's equations, which were computed within both air and sample. The microwave heating generation was deduced from the electromagnetic field distribution.

The following governing equation for electric field propagation was solved:

$$\nabla \times \mu_r^{-1}\left(\nabla \times \vec{E}\right) - \kappa_0^2 \left(\varepsilon_r' - \frac{j\sigma}{\omega\varepsilon_0}\right)\vec{E} = 0 \qquad \text{Eq. 4.1}$$

With the propagation constant within free-space, the electrical conductivity of a dielectric sample, the pulsation of microwave radiation and the complex permittivity defined as follows, respectively:

$$\kappa_0 = \omega\sqrt{\varepsilon_0\mu_0} \qquad \text{Eq. 4.2}$$

$$\sigma = \omega\varepsilon_0\varepsilon_r'' \qquad \text{Eq. 4.3}$$

$$\omega = 2\pi f \qquad \text{Eq. 4.4}$$

$$\varepsilon^* = \varepsilon' - j\varepsilon'' = \varepsilon_0(\varepsilon_r' - j\varepsilon_r'') \qquad \text{Eq. 4.5}$$

The main associated initial and boundary conditions were:

- $\vec{E} = \vec{0}$ at $t = 0, \forall xyz$ \hfill Eq. 4.6

- $E_{in} = E_0 \cos\left(\frac{\pi x}{a}\right) = \sqrt{4\, Z_{TE}\frac{P_{in}}{ab}}\cos\left(\frac{\pi x}{a}\right)$ at $z = +\infty, \forall xy$ \hfill Eq. 4.7

- $\vec{n} \times \left(\vec{H}_{air} - \vec{H}_{sample}\right) = \vec{0}$ at $z = -\frac{L}{2}, z = \frac{L}{2}, \forall xy \in [0, r]$ \hfill Eq. 4.8

- $\vec{n} \times \left(\vec{H}_{air} - \vec{H}_{sample}\right) = \vec{0}$ at $x, y = r, \forall z \in [-\frac{L}{2}, \frac{L}{2}]$ \hfill Eq. 4.9

- $\vec{n} \times \vec{H} = \vec{0}$ at $x = 0, \forall zy, \forall t > 0$ \hfill Eq. 4.10

- $\vec{n} \times \vec{E} = \vec{0}$ at $x = \frac{a}{2}, \forall zy, \forall t > 0$ \hfill Eq. 4.11

- $\vec{n} \times \vec{E} = \vec{0}$ at $y = 0, \forall zx, \forall t > 0$ \hfill Eq. 4.12

- $\vec{n} \times \vec{E} = \vec{0}$ at $y = -\frac{b}{2}, \forall zx, \forall t > 0$ \hfill Eq. 4.13

Due to the simplification of the computational domain, some conditions were particularly needed for the modeling of electromagnetism. The conditions of perfect electric conductor (Eq. 4.12) and of perfect magnetic wall (Eq. 4.10) were considered in the walls where the geometry was cut, as indicated in gray in the Figure 4.4. These boundary conditions were implemented to consider the symmetry at the center of the waveguide.

4.2.4.3. Modeling of heat transfer

Heat transfer was solved within the liquid sample and was based on the general heat equation with source term:

$$\rho C_p \frac{\partial T}{\partial t} + \rho C_p \vec{U} \cdot \nabla T - \nabla \cdot \vec{q} = Q_{gen}$$

Eq. 4.14

where $\vec{q} = k \cdot \nabla T$

Eq. 4.15

It is worth to note that the heat equation is closely dependent on thermophysical properties of the sample, which in turn are temperature-dependent. Thus, the appropriate properties were required to correctly model the heat transfer. The sample properties as a function of temperature were inserted in the model as described later (section Thermophysical properties of fruit juice model solution).

The heat generation due to microwave was computed from the local electric field strength at any point of the cylindrical sample:

$$Q_{gen} = \frac{1}{2} \omega \varepsilon_0 \varepsilon_r^{''} |E_{local}|^2$$

Eq. 4.16

The term Q_{gen} is defined as the amount of heat dissipated per unit of volume within a dielectric material. In other words, it represents the heat source responsible for the temperature rise in the product. During the experiments of microwave processing, a PID temperature controller was used to modulate the incident power in order to maintain the temperature at specific values of T_P. The incident power of each experiment along the processing time were measured and directly supplied by the sensors of the microwave generator. Then, the measured values were normalized in relation to the maximum value to be between 0 and 1. For modeling, these normalized values were applied to modulate the heat source considering the incident power during the processing time.

The heat losses due to convection/conduction phenomena around the sample were also calculated, taking into consideration the global heat transfer coefficient (h_{global}):

$$q_{global} = h_{global}(T_\infty - T)$$

Eq. 4.17

The main associated initial and boundary conditions for heat transfer modeling were:

- $T = T_{initial}$ at $t = 0, \forall x \, \forall y \, \forall z$ Eq. 4.18

- $T_\infty = 20\,°C, \forall t \geq 0$ Eq. 4.19

- $-n \cdot \vec{q} = q_{global}$ at $x, y = r, \forall z \in \left[-\frac{L}{2}, \frac{L}{2}\right], \forall t \geq 0$ Eq. 4.20

- $-n \cdot \vec{q} = q_{global}$ at $z = -\frac{L}{2}, z = \frac{L}{2}, \forall xy \in [0, r], \forall t \geq 0$ Eq. 4.21

4.2.4.4. Modeling of fluid flow

Motion of fluid is the result of a natural convection of the fluid when heated by microwaves. The convection currents are due to the differences of fluid density at different temperatures. Thus, in the present study, fluid flow was modeled considering a laminar flow of a weakly compressible fluid, in which density is temperature-dependent.

The Navier-Stokes equation governs the fluid flow and in this case is represented as follows:

$$\rho \frac{\partial \vec{U}}{\partial t} + \rho(\vec{U} \cdot \nabla)\vec{U} = \nabla \cdot \left[-pI + \mu\left(\nabla \vec{U} + (\nabla \vec{U})^T\right) - \frac{2}{3}\mu(\nabla \cdot \vec{U})I\right] - \rho \vec{g} \qquad \text{Eq. 4.22}$$

From left to right, the different terms in the equation above correspond to the inertial forces, pressure forces, viscous forces and gravitational force applied to the fluid. Besides the Navier-Stokes equation, the continuity equation was also solved:

$$\frac{\partial \rho}{\partial t} + \nabla \cdot \left(\rho \vec{U}\right) = 0 \qquad \text{Eq. 4.23}$$

While the Navier-Stokes equation represents the conservation of momentum, the continuity equation represents the conservation of mass.

The main associated initial and boundary conditions for fluid flow modeling were:

- $\vec{U} = \vec{0}$ at the sample side and bottom walls (no slip condition), $\forall t \geq 0$ Eq. 4.24

- $U_x = 0; \; U_y = 0; \; U_z = 0$ at $t = 0$ Eq. 4.25

- $p = p_{atm} + \rho g \left(z - \frac{L}{2}\right), \forall z$ with $-\frac{L}{2} \leq z \leq +\frac{L}{2}$ Eq. 4.26

4.2.4.5. Modeling of enzyme inactivation

The enzyme inactivation during microwave processing was calculated by integrating the equation of lethality (L) from the peroxidase inactivation kinetic model developed in Chapter 3 (first order model with kinetic parameters: $D_{70°C}$ = 234.377 s and z = 12.072 °C). However, for the development of this kinetic model in a conventional water bath treatment, the sample temperature was homogeneous, which is not the case of the microwave heating process. Thus, since the temperature distribution within the sample was non-uniform during the microwave processing, the accumulated lethality (or equivalent holding time, $F_{T_{ref}}$) was computed taking into account not only the time but also the space, as shown below:

$$F_{T_{ref}} = \int^t \iiint^{xyz} L(t,x,y,z) dt\, dxdydz = \int^t \iiint^{xyz} 10^{\left(\frac{T(t,x,y,z)-T_{ref}(t,x,y,z)}{z}\right)} dt\, dxdydz$$
$$= \int^t \iiint^{xyz} 10^{\left(\frac{T(t,x,y,z)-70}{12.072}\right)} dt\, dxdydz$$

Eq. 4.27

From the equation above, the temperature effect within the whole 3D geometry of the sample throughout the treatment time was considered. The integration was performed during the post-processing stage. Using the obtained value of accumulated lethality, the global enzyme inactivation was calculated as follows:

$$\frac{A}{A_0} = 10^{\left(-\frac{F_{T_{ref}}}{D}\right)} = 10^{\left(-\frac{F_{T_{ref}}}{234.377}\right)}$$

Eq. 4.28

In this way, the predicted value of residual enzyme activity could be compared with the value obtained experimentally.

4.2.4.6. Thermophysical properties of fruit juice model solution

All the thermophysical properties of the sample were implemented in the model in the form of equations as a function of temperature. For thermal conductivity (k), heat capacity (C_p) and viscosity (η), data were obtained from the properties of 10% (w/w) sucrose solution found in literature. Density (ρ) and dielectric properties (ε_r', ε_r'') were obtained experimentally using the fruit juice model solution.

Density was measured by weighing the volume of model juice contained in standard volumetric pycnometers previously calibrated with distilled water at each temperature (20 – 80 °C) (Figura and Teixeira, 2007). Water density data obtained from Haynes (2014) were used as reference. Measurements were carried out in triplicate.

Dielectric properties determinations of the model fruit juice were carried out using an open-ended coaxial line probe system with a Dielectric Probe Kit 85070E (high temperature configuration) connected to an Electronic Calibration Module 85092-60010 and a Network Analyzer E5062A (Agilent Technologies, Malaysia). Dielectric constant ($\varepsilon_r^{'}$) and loss factor ($\varepsilon_r^{''}$) were measured at 2.45 GHz in the temperature range of 20 – 80 °C according to the procedure described in the Chapter 2. The experiments were performed in triplicate. Ten measurements were done for each repetition and temperature evaluated.

Note that the results presented in Chapter 2, including the ANN model for dielectric properties at 2450 MHz, could have been used in the present chapter. However, in order to limit the uncertainties since the ANN was developed for a large range of variation (temperature, sucrose concentration and frequency), it was preferred to measure the dielectric properties of the selected model solution at the fixed operational frequency of the processing studied in this chapter. In this way, instead of the three variables, the measurements were performed by only varying the temperature. Moreover, the composition of the model solutions evaluated in Chapter 2 was different in relation to the solutions of the others chapters (Chapter 3, 4 and 5). The difference is due to the presence of the enzyme POD and the consequent adaptation of composition that was needed to not alter the enzyme activity.

To model the relationship between each property and temperature, data from literature and mean experimental values were fitted by polynomial functions using Excel 2016 (Microsoft, USA). The goodness-of-fit for the regression models was reported by the coefficient of determination (R^2). These obtained functions were directly implemented in the software and associated to the sample material.

4.2.4.7. Global heat transfer coefficient

During processing, there are some heat losses from the sample surface to its surrounding via convection and conduction, due to the presence of air in the microwave cavity. Thus, in order to model this heat flux taking into account all the involved materials and geometries, an experimental approach was performed and the global heat transfer coefficient (h_{global}) was estimated via Lumped Capacitance Method (Incropera et al., 2007).

In the experiment, a solid cylinder made of a high thermal conductive material (in this case, yellow brass) with the same dimensions of the plastic tube was heated until around 70 °C or cooled until around 5 °C. For that, the cylinder was immersed in a hot water bath or an ice bath, respectively. Then, the cylinder was removed and rapidly placed inside the polystyrene support block, which in turn was placed in the applicator. Both support and applicator were the same used in the experiments of microwave processing. A similar polystyrene cap was placed

in the top of the cylinder. The placement of each component was also kept the same, with the brass cylinder replacing the plastic tube and the sample.

The increase or decrease of the temperature until the equilibrium (close to room temperature) was measured using a thermocouple and registered every second with a data logger (OM-CP-Quadtemp2000, Omega, USA). The thermocouple was embedded at the geometric center of the cylinder through a hole of about the same diameter as the thermocouple. The temperature of the surrounding air (T_∞) was also measured and recorded. Figure 4.5 presents the main components of this experiment.
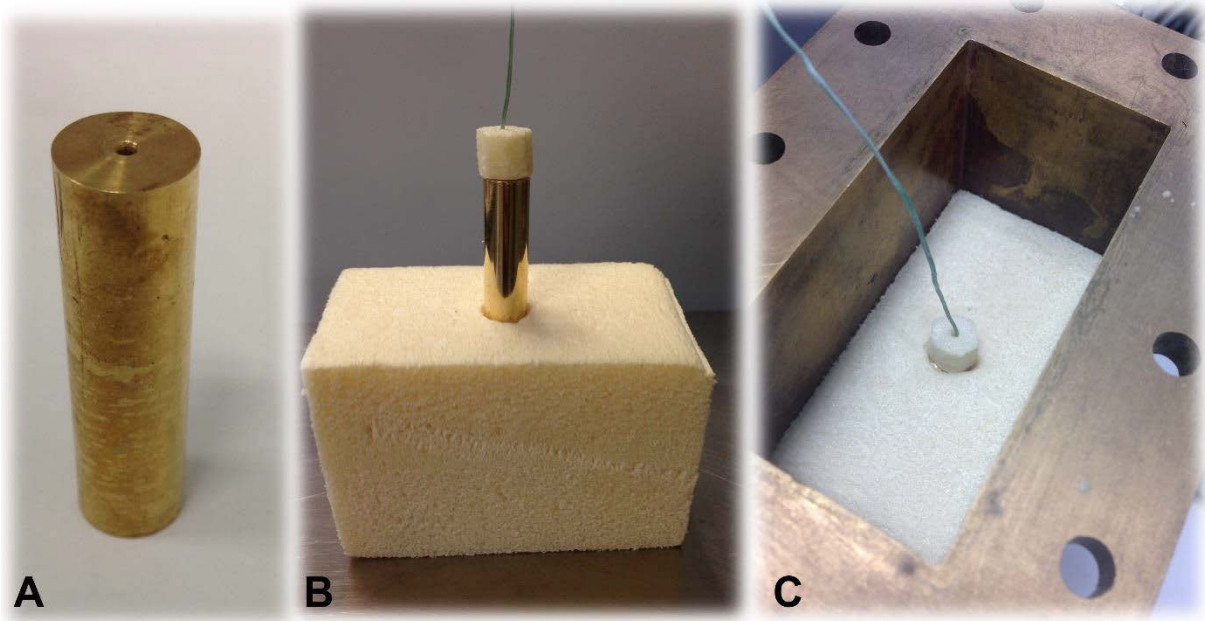
Figure 4.5. Experimental setup for the estimation of global heat transfer coefficient: A) brass cylinder, B) thermocouple placed at the geometric center of the brass cylinder and polystyrene cap and support, C) cylinder and support placed inside the applicator.

The principle of h_{global} calculation from this experiment was based on a thermal energy balance, equaling the input and output energy and neglecting the temperature gradient within the metallic sample:

$$-hA(T - T_\infty) = mC_p \frac{dT}{dt}$$

Eq. 4.29

By integrating this equation, it yields to:

$$ln\left(\frac{T_0 - T_\infty}{T - T_\infty}\right) = \frac{hA}{mC_p}t$$

Eq. 4.30

Therefore, the data of $ln\left(\frac{T_0 - T_\infty}{T - T_\infty}\right)$ along the time were plotted and the slopes of the graphs were used to calculate h_{global}:

$$h_{global} = \frac{(slope)\ mC_p}{A}$$

Eq. 4.31

Experiments of cooling and heating were carried out in triplicate. The mean of the 6 repetitions was defined as the final value of h_{global}.

With the purpose of verifying that the final value of h_{global} was calculated and obtained correctly, a numerical study was performed. For that, a simple simulation of this experiment, taking into account the calculated h_{global} and the consequent heat flux, was carried out. The simulation was run using COMSOL Multiphysics® 5.3a, considering only the ¼ of the cylinder as a computational domain (mesh with 34827 tetrahedral elements). The adequacy of the model was verified by the temperature profile in the center of the cylinder, through the comparison of predicted and experimental values.

Both for the simulation and for the calculation of h_{global}, some thermophysical properties of the brass were necessary. All of them were considered as constant with temperature. Thermal conductivity was obtained from literature. Density was calculated by weighing a known volume of brass. Heat capacity was determined using a differential scanning calorimeter (µDSC7, Setaram, France). For that, around 100 mg of brass was sealed in an aluminum pan and subjected to a programmed thermal scan. The heating rate was set to 1 °C min^{-1} over a range of 10 to 30 °C. An empty aluminum pan was used as a reference. Heat capacity data were obtained from the equipment's software and evaluated in the temperature range of 20 to 27 °C.

4.2.4.8. Computational details and numerical procedures

Based on a Finite Element Method, the numerical study was performed using the software COMSOL Multiphysics® 5.3a in a Dell Precision T7910 workstation (2x processors Intel Xeon at 2.5GHz, 256 GB of RAM, Windows 8.1 Professional, 64 bits). The time required for the simulations coupling electromagnetism, heat transfer and fluid flow was around 2 – 4 days.

The user-defined mesh consisted of 113679 tetrahedral elements in the total domain and of 76468 elements in the sample domain. The maximum element sizes were 0.0004 m for the sample and 0.00432 m for the rest of the domain. This very fine mesh within the sample was necessary in order to capture efficiently the fluid flow coupled with the heat generation due to microwaves. For the fluid flow resolution, a boundary layer mesh was applied to the sample walls, as shown in Figure 4.6.
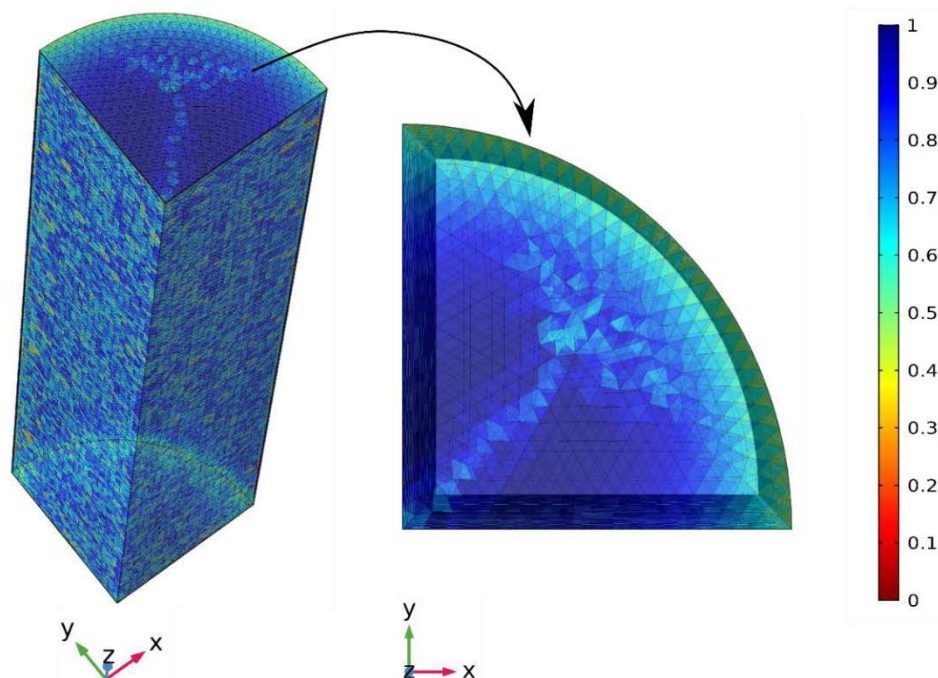
Figure 4.6. Sample mesh established for the simulation of microwave heating of fruit juice.

The simulation of microwave processing was run in two steps. Firstly, a stationary study solving only the fluid flow was performed. This stationary study was performed in order to initialize the velocity field within the fluid by considering a constant initial temperature of 20°C. Then, in the second step, a complete time-dependent study was performed. Electromagnetism, heat transfer and fluid flow equations were considered and coupled together.

The simulated time interval varied according to each microwave treatment (i.e. each time-temperature combination) and was implemented in the model based on the experimental values. The same was done for the values of input power and initial temperature of the sample. Thus, for the model validation, a simulation had to be calculated for each repetition of each treatment. However, due to the large number of experimental treatments and knowing that each microwave processing experiment was performed in triplicate, only one repetition of each treatment was simulated. The simulated temperature profile in the center of the sample and the predicted residual enzyme activity were compared with the experimental data.

4.3. Results and discussion

4.3.1. Experimental results and enzyme inactivation by microwave processing

The first group of microwave processing experiments was performed at seven T_P (60, 62, 64, 66, 68, 70, 72 °C) and four holding times for each T_P, totaling 28 treatments. Examples

of the temperature profile at the center of the sample along the time of each treatment are shown in Figure 4.7. The temperature profiles include three steps: heating, holding (or retention) and cooling.
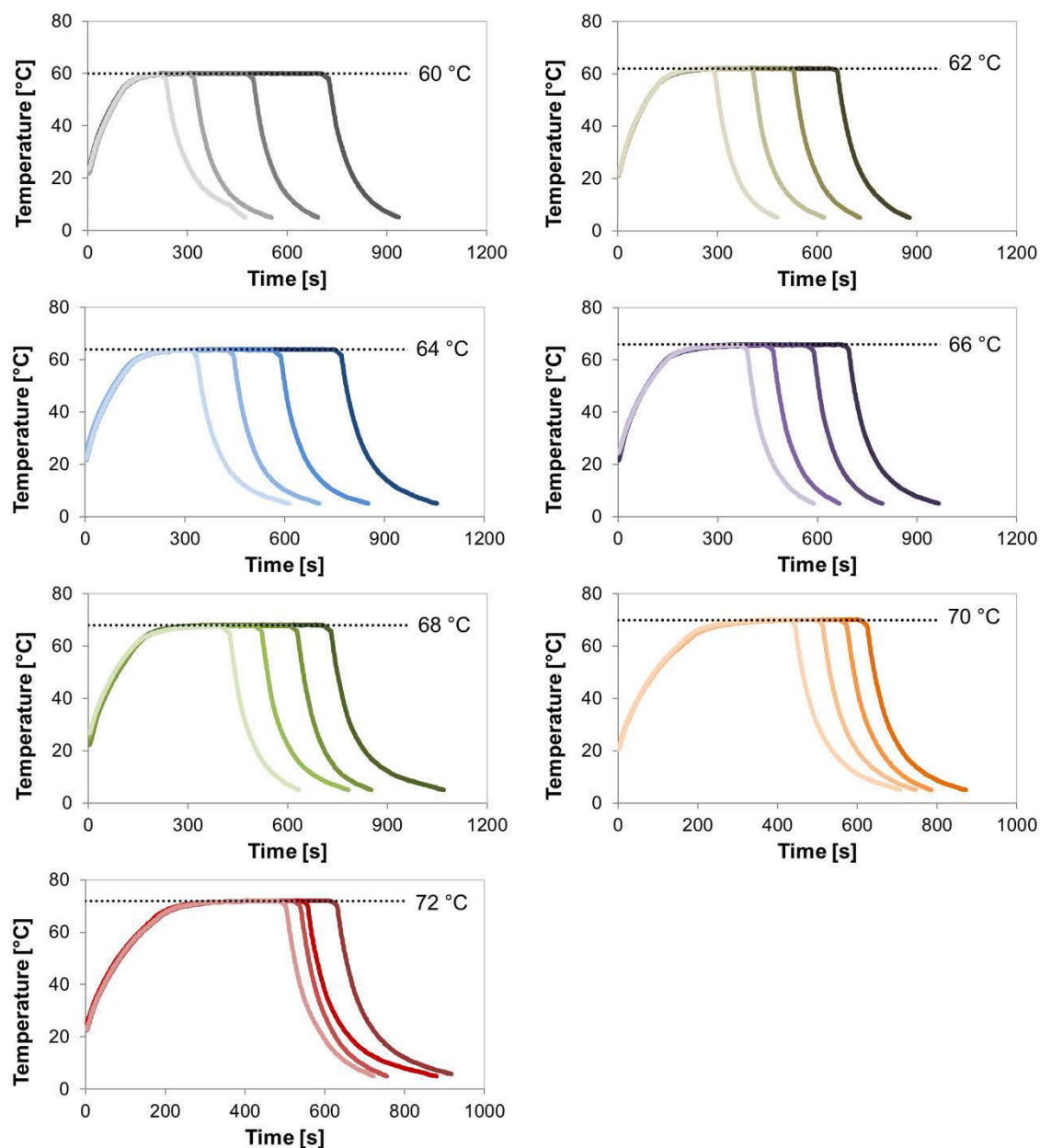
Figure 4.7. Temperature profiles at the center of the fruit juice model solution along the microwave processing at the following holding temperatures and times: 60 °C for 1, 4, 8 min and no holding time; 62 °C for 2, 4, 6 min and no holding time; 64 °C for 2, 4, 7 min and no holding time; 66 °C for 1, 3, 5 min and no holding time; 68 °C for 2, 4, 6 min and no holding time; 70 °C for 1, 2, 3 min and no holding time; 72 °C for 1, 2, 3 min and no holding time.

The second group of experiments was performed following a different procedure. As it can be observed in Figure 4.8, the temperature profiles of these treatments include two stages of holding.
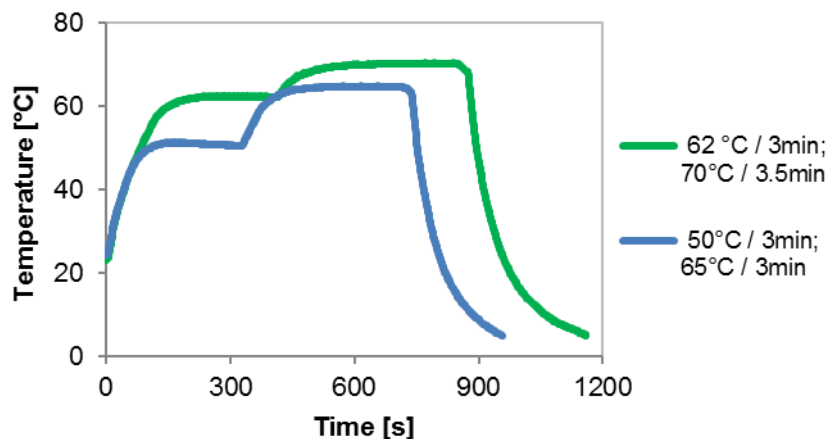
Figure 4.8. Temperature profiles at the center of the fruit juice model solution along the microwave processing with two stages of holding.

During each processing, a temperature controller was used to modulate the incident microwave power in order to maintain the temperature in the center of the sample at the desired T_P. Figure 4.9 presents examples of the variation of the incident power supplied within the waveguide along the time, during the three repetitions of four different treatments. The presented values were normalized based on the power measured within the empty waveguide using a power meter (105 W). It can be observed that the power varied differently not only in each treatment but also in each repetition. To evaluate this difference numerically, the integral of the power versus time curves was calculated using the software MATLAB® 7.10 (The MathWorks, Inc., USA), thus obtaining the incident energy values within the waveguide. The results of energy as well as the residual peroxidase activities assessed after microwave processing are presented in the Table 4.2. As expected, at a determined T_P, as expected, the longer the processes, the greater the inactivation degree and the larger the amount of energy required.
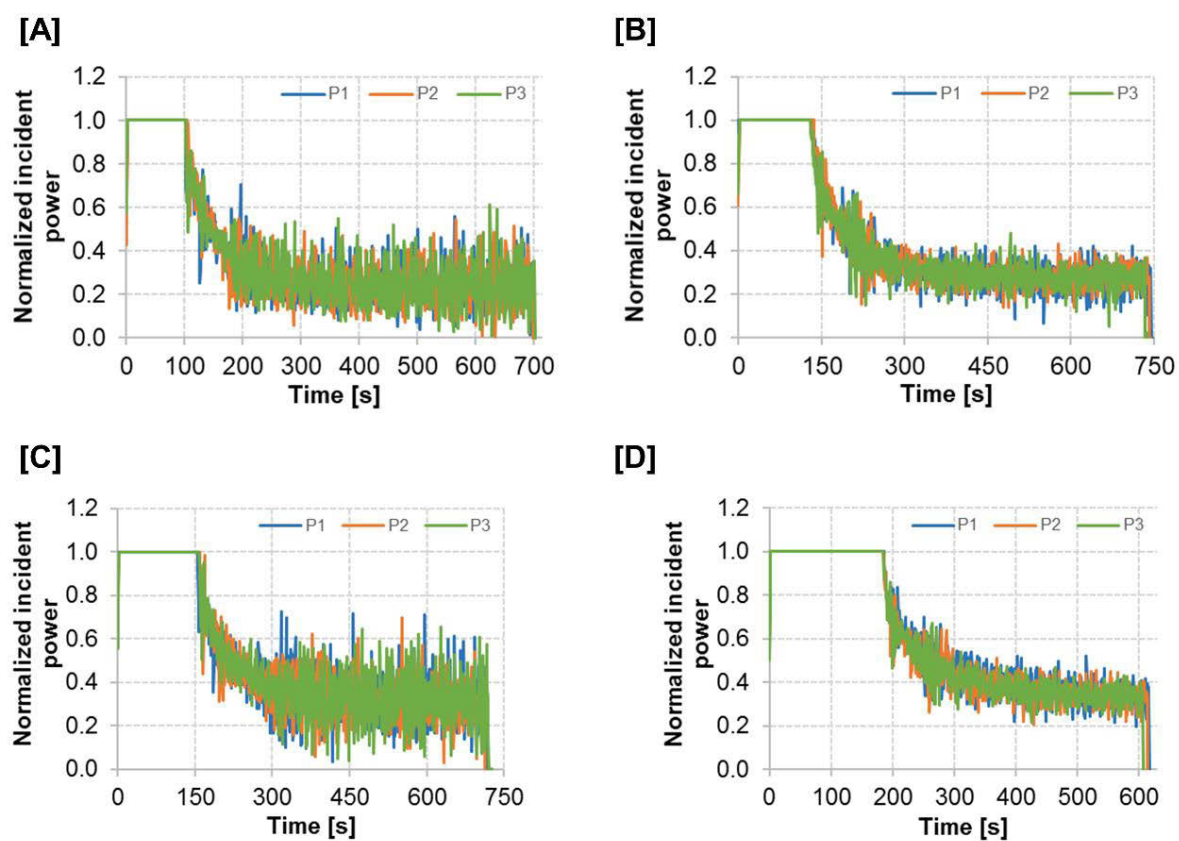
Figure 4.9. Incident power measured by the microwave generator sensor during the repetitions of processes (P1, P2, P3) at the following conditions of processing temperature and holding time: 60 °C/8 min (A), 64 °C/7 min (B), 68 °C/6 min (C) and 72 °C/3 min (D).

Table 4.2. Residual peroxidase activities after microwave processing at different temperatures, holding times and incident energy. Mean value ± standard deviation of the process triplicate.

T [°C]	Holding time [min]	Residual peroxidase activity [%]	Incident microwave energy [kJ]
60	-	84.50 ± 2.90	16.937 ± 0.123
	1	77.65 ± 1.10	19.040 ± 0.340
	4	60.92 ± 0.91	23.680 ± 0.239
	8	38.64 ± 1.25	28.816 ± 0.095
62	-	76.65 ± 1.65	19.600 ± 0.251
	2	61.80 ± 1.62	23.785 ± 0.245
	4	46.60 ± 1.45	26.768 ± 0.228
	6	34.72 ± 1.46	29.699 ± 0.262
64	-	58.90 ± 1.68	23.521 ± 0.801
	2	42.15 ± 1.01	26.001 ± 0.347
	4	25.69 ± 0.94	30.393 ± 0.246
	7	13.60 ± 1.56	35.306 ± 0.256
66	-	52.69 ± 0.60	25.139 ± 0.290
	1	39.76 ± 0.67	26.886 ± 0.341
	3	24.04 ± 0.78	31.297 ± 0.879
	5	13.97 ± 0.55	34.624 ± 0.383
68	-	24.85 ± 2.21	26.547 ± 0.089
	2	10.15 ± 0.72	30.828 ± 0.441
	4	4.89 ± 0.06	34.994 ± 0.274
	6	3.12 ± 0.36	38.181 ± 0.414
70	-	21.82 ± 3.42	31.300 ± 0.162
	1	11.39 ± 0.65	33.676 ± 0.162
	2	7.81 ± 0.75	35.968 ± 0.395
	3	5.35 ± 0.24	37.318 ± 0.059
72	-	2.05 ± 0.04	33.888 ± 0.156
	1	1.19 ± 0.26	34.738 ± 0.273
	2	1.03 ± 0.08	35.735 ± 0.694
	3	0.52 ± 0.11	38.236 ± 0.520
62 70	3 3.5	1.27 ± 0.10	41.413 ± 0.513
50 65	3 3	28.57 ± 0.43	30.958 ± 0.266

As previously mentioned, the temperature profiles were obtained from temperature measurements in the center of the sample during the microwave processing. However, it is known that the temperature distribution during microwave processing is generally not homogeneous. Thus, the temperature profile does not reflect the thermal history of the product as a whole, but only of the specific location of measurement.

Since the values of residual enzyme activity refer to the whole sample, an inactivation kinetic model cannot be correctly obtained without the thermal history data. However, an approximate kinetic model can be obtained assuming a hypothetical uniform distribution of temperature in the sample during microwave heating. Thus, using the same procedure performed in the Chapter 3, the residual activities from the first group of experiments and temperature data were fitted to a first-order model.

The obtained values for the parameters D at 70°C and z are shown in Table 4.3. It can be observed that both parameters were higher than the values found for conventional heating with homogeneous temperature ($D_{70°C}$ = 234.377 s and z = 12.072 °C) . The hypothetic model was then super estimated. Hence, it corroborates the presumption that the temperature distribution was not uniform within the sample, indicating the existence of cold and hot regions, which was later confirmed in the numerical study (section Simulation of the microwave processing).

Table 4.3. Kinetic parameters and fit criteria of a hypothetic kinetic model for peroxidase inactivation by microwave heating.

Parameters		Fit criteria	
$D_{70°C}$ [s]	298.94 ± 11,66	SQE	0.113
z [°C]	13.65 ± 0,43	R^2	0.98

4.3.2. Thermophysical properties of fruit juice model solution

4.3.2.1. Thermal properties and viscosity

The main components of the fruit juice model solution are water and sucrose. Thus, it is reasonable to consider that the thermal properties and viscosity of the 10 °Brix juice are close to that of a 10% (w/w) sucrose solution. In this way, data on thermal conductivity (Figure 4.10), heat capacity (Figure 4.11) and viscosity (Figure 4.12) at different temperatures were obtained from literature and fitted by equations, which are presented in Table 4.4.
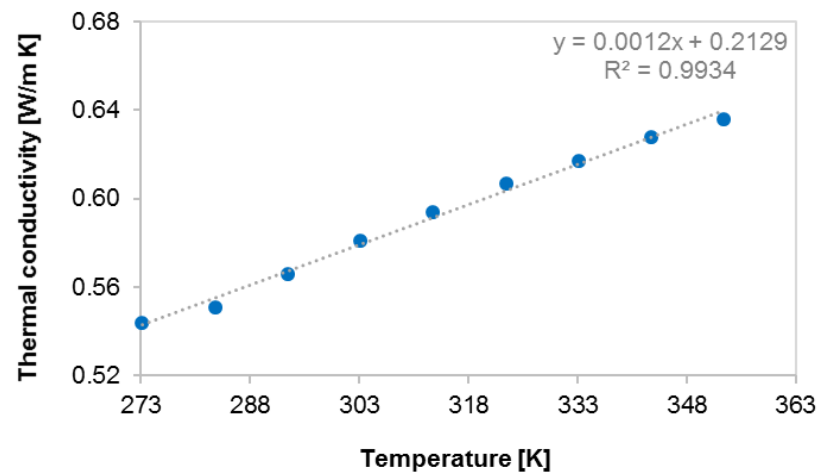
Figure 4.10. Thermal conductivity of 10% (w/w) aqueous sucrose solution as a function of temperature. Data from Honig (1953).
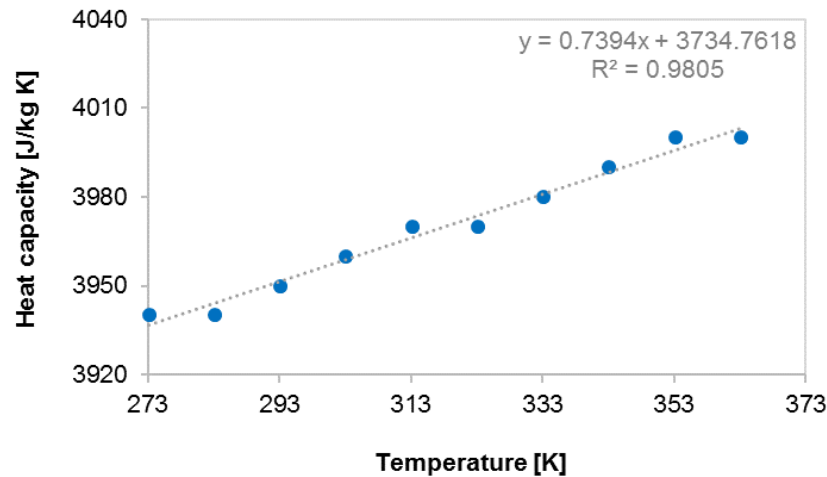
Figure 4.11. Heat capacity of 10% (w/w) pure sucrose solution as a function of temperature. Data from Asadi (2006).
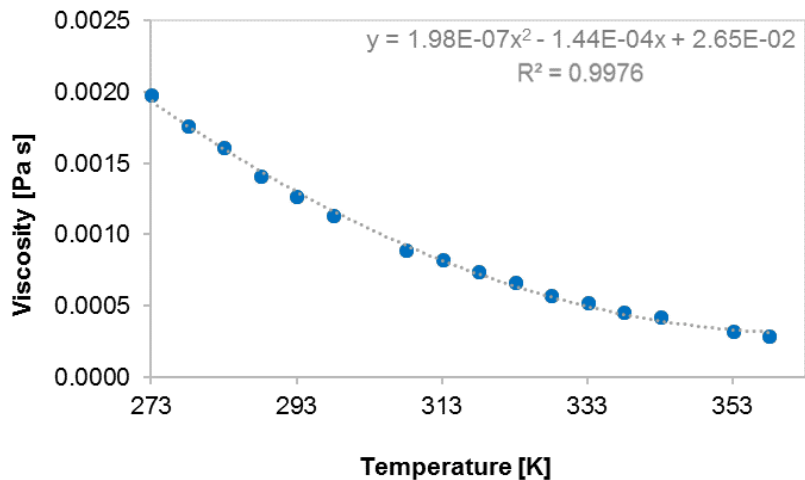
Figure 4.12. Viscosity of 10% (w/w) sucrose solution as a function of temperature. Data from Telis *et al.* (2007).

4.3.2.2. Density

Since many materials undergo thermal expansion, i.e. increase in volume when heated, the density of a liquid usually decreases with temperature. As expected, the density of the fruit juice model solution decreased with increasing temperature (Figure 4.13). Data was fitted to a quadratic equation, which is presented in Table 4.4.
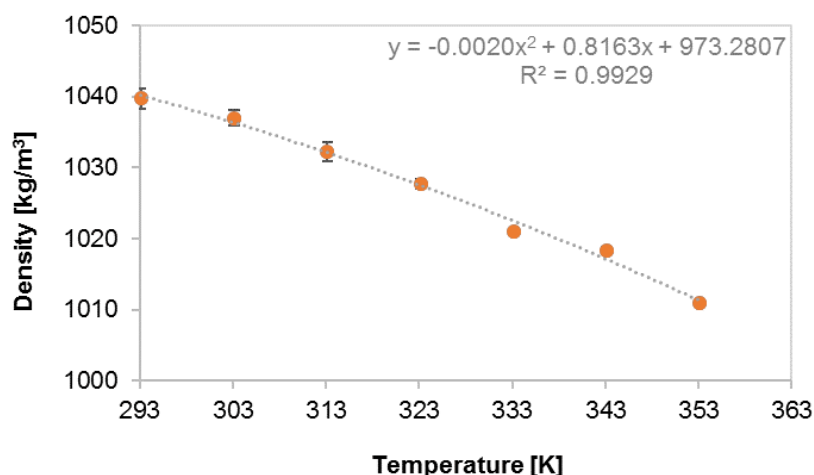
Figure 4.13. Experimental density of the fruit juice model solution as a function of temperature. Vertical bars indicate the standard deviation.

By performing a comparison with the literature, as shown in Figure 4.14, it can be seen that the experimental values were close to the values found for 10 °Brix sucrose solution by Honig (1953) and Mathlouthi and Reiser (1995). This suggests that data for sucrose solution could also be used in the simulation model, as it was done for the other properties mentioned above.
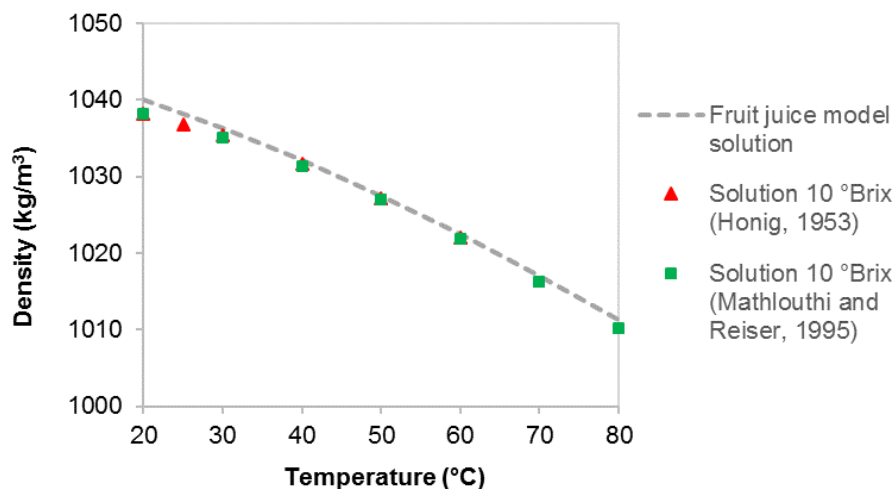
Figure 4.14. The equation of density of the fruit juice model solution obtained experimentally compared with the values of density for 10 °Brix sucrose solution reported by Honig (1953) and Mathlouthi and Reiser (1995).

4.3.2.3. Dielectric properties

The dielectric properties of the model juice solution at 2.45 GHz are presented in Figure 4.15. As the other properties above, both dielectric constant and loss factor data were adjusted to polynomial equations. In this case, the use of ANN models, as presented in Chapter 2, was not necessarily required since the dielectric properties were only function of temperature.
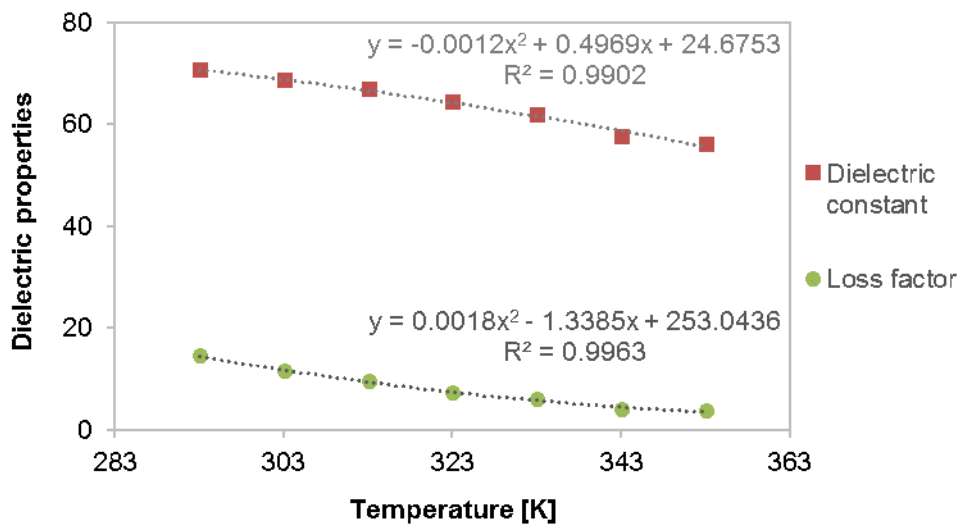
Figure 4.15. Dielectric constant and loss factor of the fruit juice model solution at 2.45 GHz as a function of temperature.

All the equations relative to thermophysical properties mentioned above, including all the digits considered in the simulation model, are presented in Table 4.4.

Table 4.4. Equations implemented in the simulation model to describe the variation of thermophysical properties of the fruit juice model solution as a function of temperature (T in K).

Property	Equation
Thermal conductivity [W m^{-1} K^{-1}]	$k = (1.208711 \cdot 10^{-3} \cdot T) + (2.129341 \cdot 10^{-1})$
Heat capacity [J kg^{-1} K^{-1}]	$C_p = (7.393939 \cdot 10^{-1} \cdot T) + (3.734762 \cdot 10^{3})$
Viscosity [Pa s]	$\eta = (1.977074 \cdot 10^{-7} \cdot T^{2}) - (1.438718 \cdot 10^{-4} \cdot T) + (2.648232 \cdot 10^{-2})$
Density [kg m^{-3}]	$\rho = (-2.007069 \cdot 10^{-3} \cdot T^{2}) + (8.163102 \cdot 10^{-1} \cdot T) + (9.732807 \cdot 10^{2})$
Dielectric constant [-]	$\varepsilon_r^{'} = (-1.1591163420 \cdot 10^{-3} \cdot T^{2}) + (4.9685629334 \cdot 10^{-1} \cdot T) + (2.4675349765 \cdot 10^{1})$
Loss factor [-]	$\varepsilon_r^{''} = (1.7900147908 \cdot 10^{-3} \cdot T^{2}) - (1.3385095961 \cdot T) + (2.5304357446 \cdot 10^{2})$

4.3.3. Global heat transfer coefficient

In order to correctly model the heat flux within the experimental microwave processing system, an appropriate global heat transfer coefficient need to be determined. For that, different methodologies can be employed. In the present work, it was preferred to perform the determination of h_{global} by experimental means.

However, initially, during the development phase of the simulation model, the coefficient has been pre-estimated by an inverse heat transfer problem (Augusto and Cristianini, 2011). In this approach, an initial value for h_{global} was chosen and implemented in the simulation. Then, data of temperature profile obtained numerically and experimentally were compared. The value of h_{global} was changed (increased or decreased) until the difference between both experimental and predicted values was small enough. In fact, this procedure was based on trial and error. From this numerical method, it was observed that h_{global} was around 6 W m^{-2} K^{-1}. Also, it could be verified how h_{global} affects the temperature profile in the center of the sample, as shown in Figure 4.16.
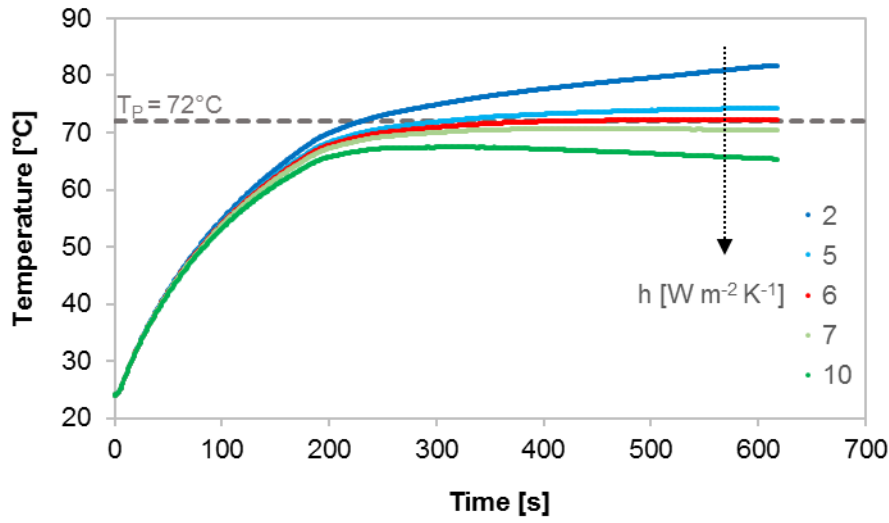
Figure 4.16. Effect of the global heat transfer coefficient on the predicted temperature profile in the center of the fruit juice model solution during microwave processing.

As expected, the value of h_{global} plays an important role in the temperature profile. Higher values of h_{global} resulted in lower values of temperature, which was consistent due to greater heat losses to the surroundings. Hence, the choice of a value for h_{global} as accurately as possible is of great interest. In the experimental method, the geometries and conditions of microwave processing experiments were reproduced. Both heating and cooling of the brass cylinder were evaluated. Data of temperatures were properly calculated and plotted, as exemplified by Figure 4.17. The slopes of the graphs were used to calculate h_{global}.

[A]

[B]
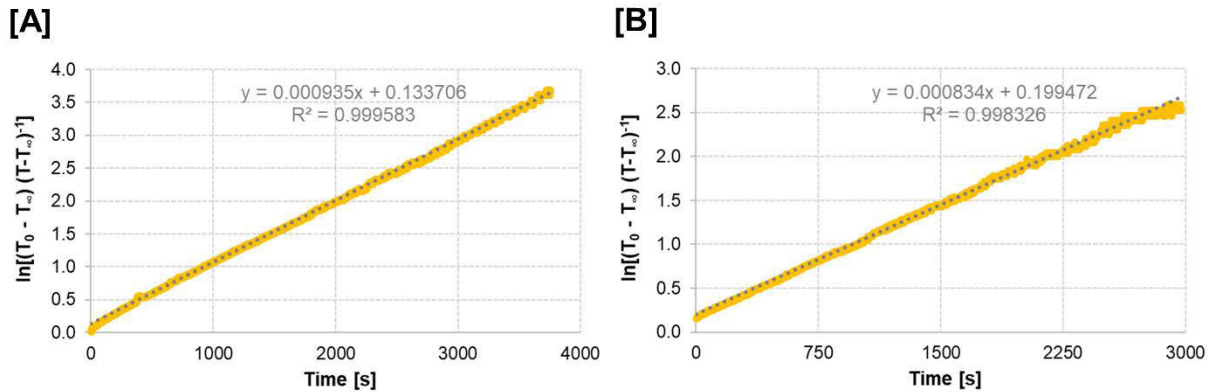
Figure 4.17. Data of experimental temperatures along time obtained from cooling (A) and heating (B) of a brass cylinder for the calculation of the global coefficient heat transfer.

To calculate h_{global} according to Eq. 4.31, the slopes, heat capacity of brass, mass and area of the cylinder were used. Heat capacity (C_p) was experimentally determined at the range between 20 and 27 °C and its mean value was 404.3 J kg^{-1} K^{-1}. The area of cylinder was 0.0013005 m² and the mass was 0.0235051 kg. Then, after calculating the values of h_{global}

for the six experiment repetitions, the mean and final value of h_{global} was 6.48 W m^{-2} K^{-1}. It is worth to note that this value is close to the one pre-estimated by the numerical method.

Aiming to verify if the final value of h_{global} was correct, a numerical study was performed to evaluate the heat flux and temperature profile. In the simulation, the following properties of brass were inserted:

- Heat capacity: C_p = 404.3 J kg^{-1} K^{-1} (experimental);

- Density: ρ = 8182 kg m^{-3} (experimental);

- Thermal conductivity: k = 116 W m^{-1} K^{-1} (from Davis (2001), for C26800 yellow brass).

Predicted and experimental temperature profiles are presented in Figure 4.18. Good agreement between them can be observed, especially for data from the experiment of heating (Figure 4.18B). Therefore, the estimated value of h_{global} was considered as appropriate for implementation in the simulation of microwave processing of fruit juice model solution.
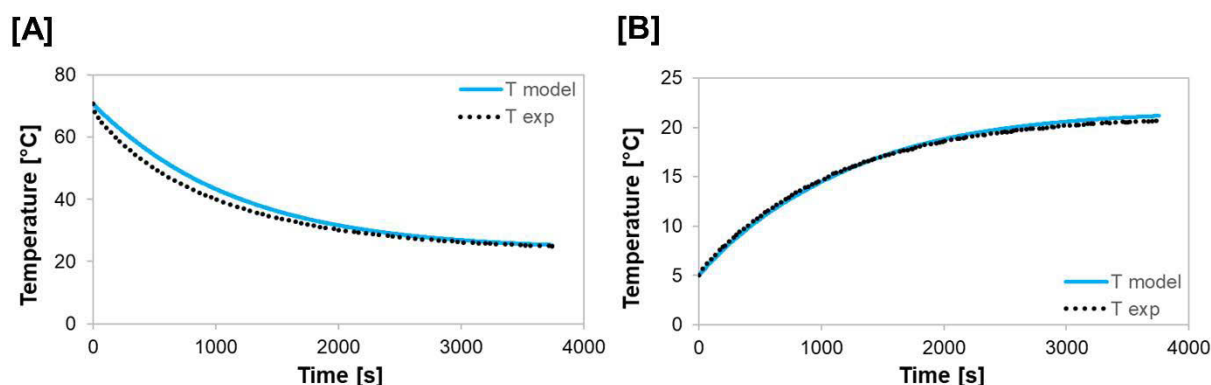
Figure 4.18. Experimental and predicted temperature profiles in the center of the cylinder during cooling (A) and heating (B) process.

4.3.4. Simulation of the microwave processing

A finite element model coupling electromagnetism, heat transfer and fluid flow was developed to simulate the microwave processing of fruit juice model solution. The thermophysical properties of the sample (juice) and the global heat transfer coefficient, previously described, were inserted in the simulation model.

From the simulation, 3D temperature distribution within the sample was predicted. Figure 4.19 illustrates some examples of temperature distributions during two microwave treatments: 60 °C/1 min and 72 °C/3 min, at the middle and the final processing times. Uneven temperature patterns are clearly distinguished. The bottom side of the sample presented lower temperatures, which is probably result of the combination of resonance, thermal and flow phenomena within the small sample. It can be observed that the differences of temperature at

hot and cold zones were about 8 – 12 °C. However, over the time, these differences tend to slightly decrease and the temperature distribution has tendency to present less heterogeneity.

Therefore, as already suspected from the enzyme inactivation data and kinetic model, previously discussed, the temperature distribution was not uniform. Hence, the higher values of the kinetic parameters D and z can be explained by the presence of a cold region below the geometric center of the sample, i.e. below the location where the experimental temperatures were measured.
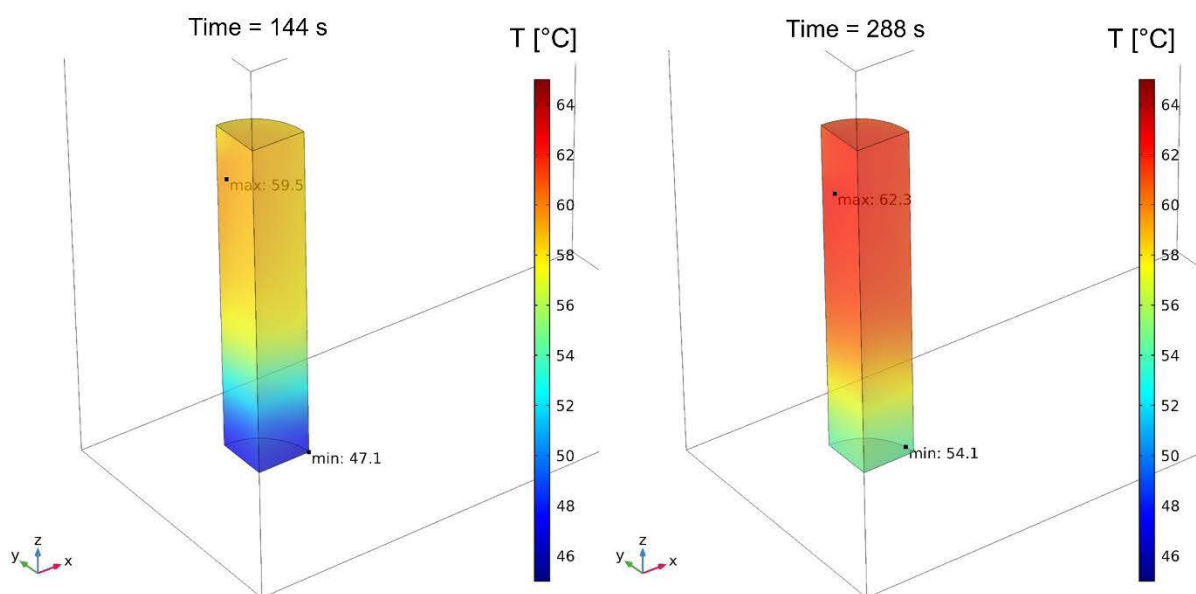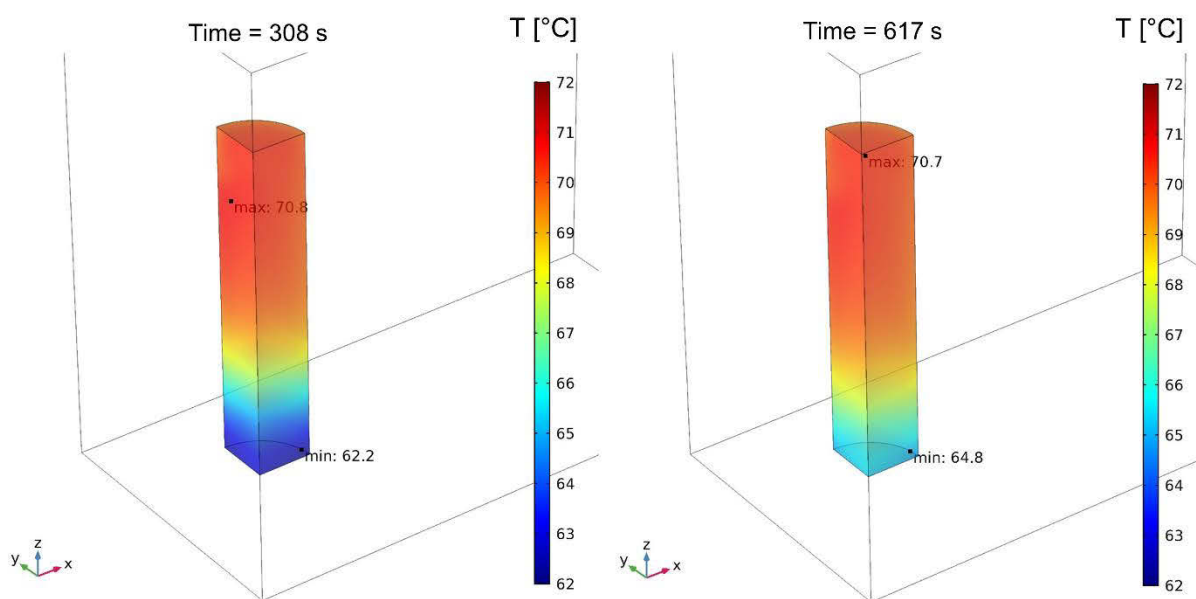
Figure 4.19. Temperature distribution within the sample at the middle and the final processing times of two microwave treatments: 60 °C/1 min and 72 °C/3 min.

In addition to the temperature, the simulation also provided information about the fluid flow and velocity field within the sample. The modeling of the fluid motion was mainly the result of the coupling between fluid flow and heat transfer equations. The temperature rise during the process promotes natural convection currents due to the differences of fluid density at different temperatures. Figure 4.20 present an example from the treatment at 66 °C/5 min, in which temperature and velocity of fluid flow are shown. It can be noticed that velocity values are higher at the upper region of the sample, where the temperatures are also higher. Magnitudes of the predicted velocities are quite significant, considering the size of the sample. In this example, the maximum velocity was around 1.8 mm s^{-1}.
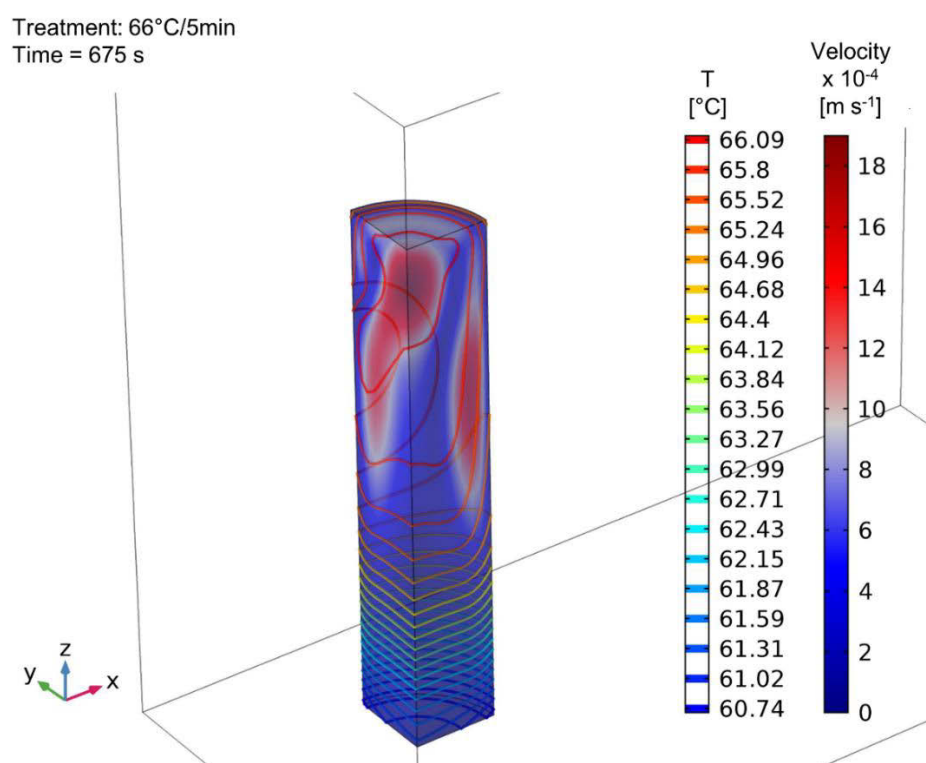
Figure 4.20. Distribution of temperature (contour plots) and velocity of fluid flow (volume plots).

4.3.5. Model validation

4.3.5.1. Analysis of temperature profile

Predicted values of the temperature profile at the geometric center of the sample were compared with the experimental values. The results for the treatments at T_P equal to 60, 62, 64, 66, 68, 70 and 72 °C are presented in Figure 4.21, Figure 4.22, Figure 4.23, Figure 4.24, Figure 4.25, Figure 4.26, Figure 4.27, respectively. The results for the second group of experiments, in which the processing were performed using two stages of holding: 62 °C/3 min + 70 °C/3.5 min, and 50 °C/3 min + 65 °C/3 min, are presented in Figure 4.28.

[A]

[B]

[C]

[D]
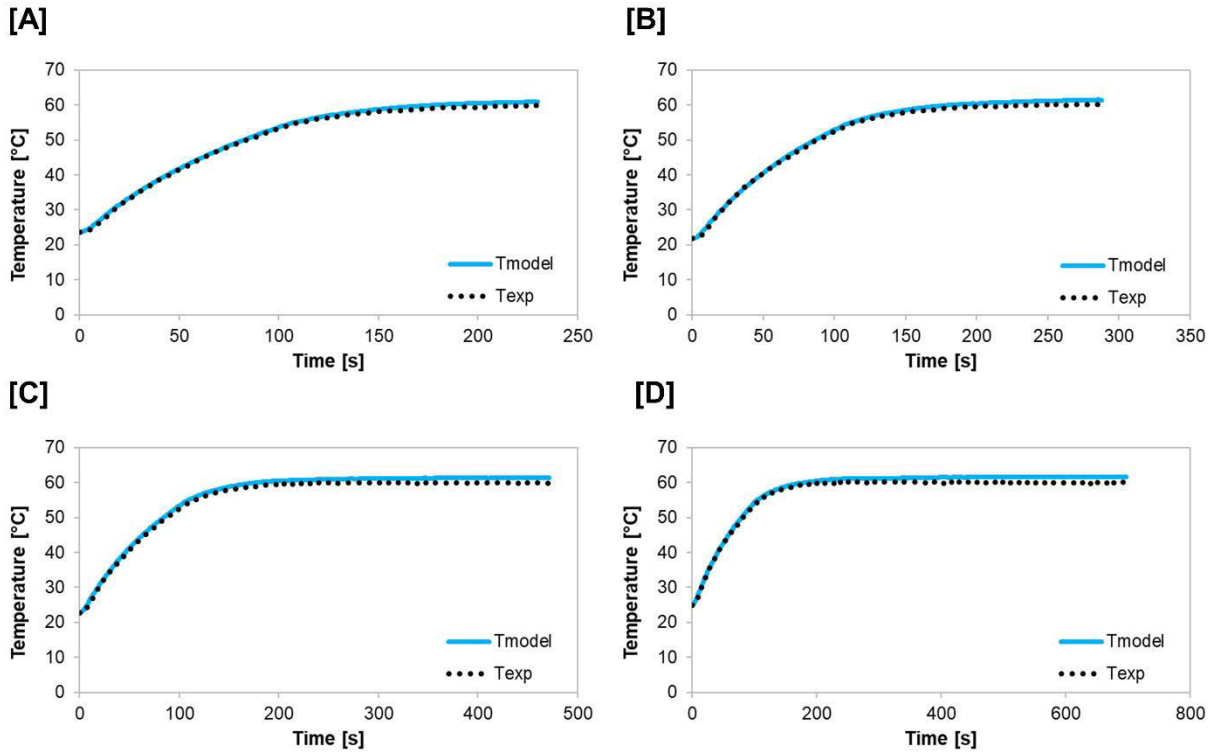
Figure 4.21. Predicted and experimental temperature profile at the center of the sample during the following microwave treatments: 60 °C without holding time (A), 60 °C for 1 min (B), 60 °C for 4 min (C), 60 °C for 8 min (D).

[A]

[B]

[C]

[D]
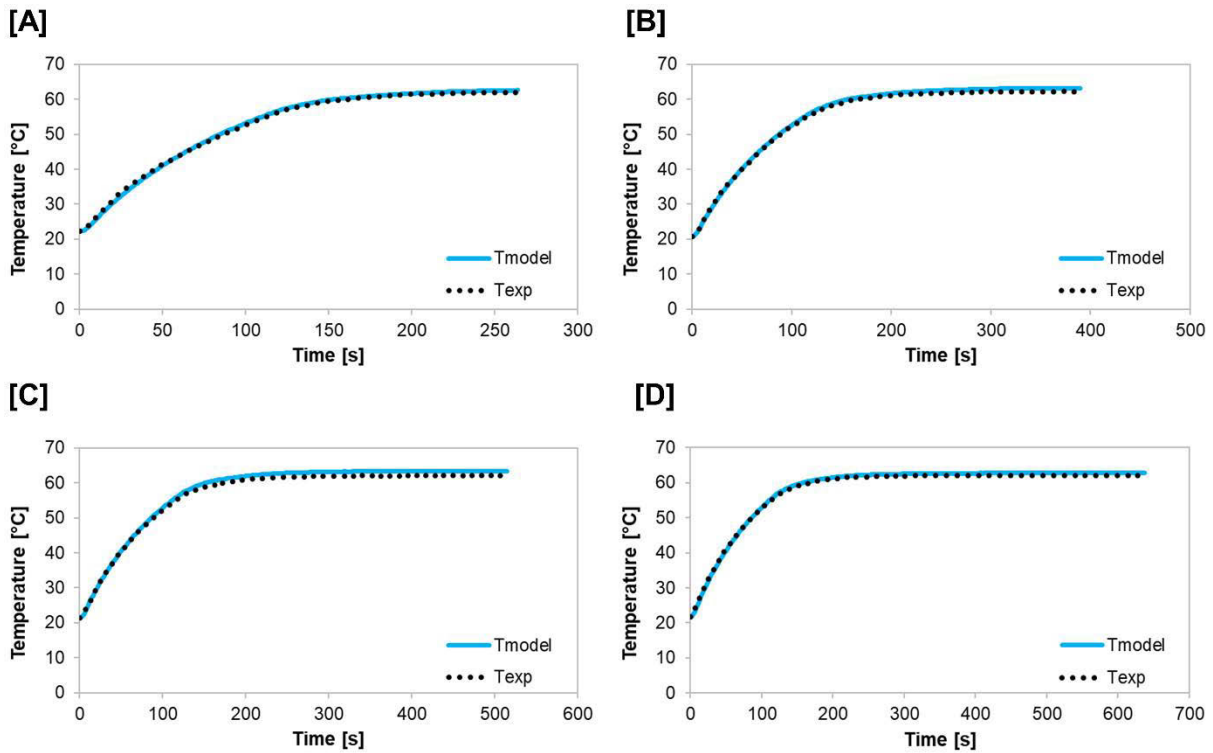
Figure 4.22. Predicted and experimental temperature profile at the center of the sample during the following microwave treatments: 62 °C without holding time (A), 62 °C for 2 min (B), 62 °C for 4 min (C), 62 °C for 6 min (D).
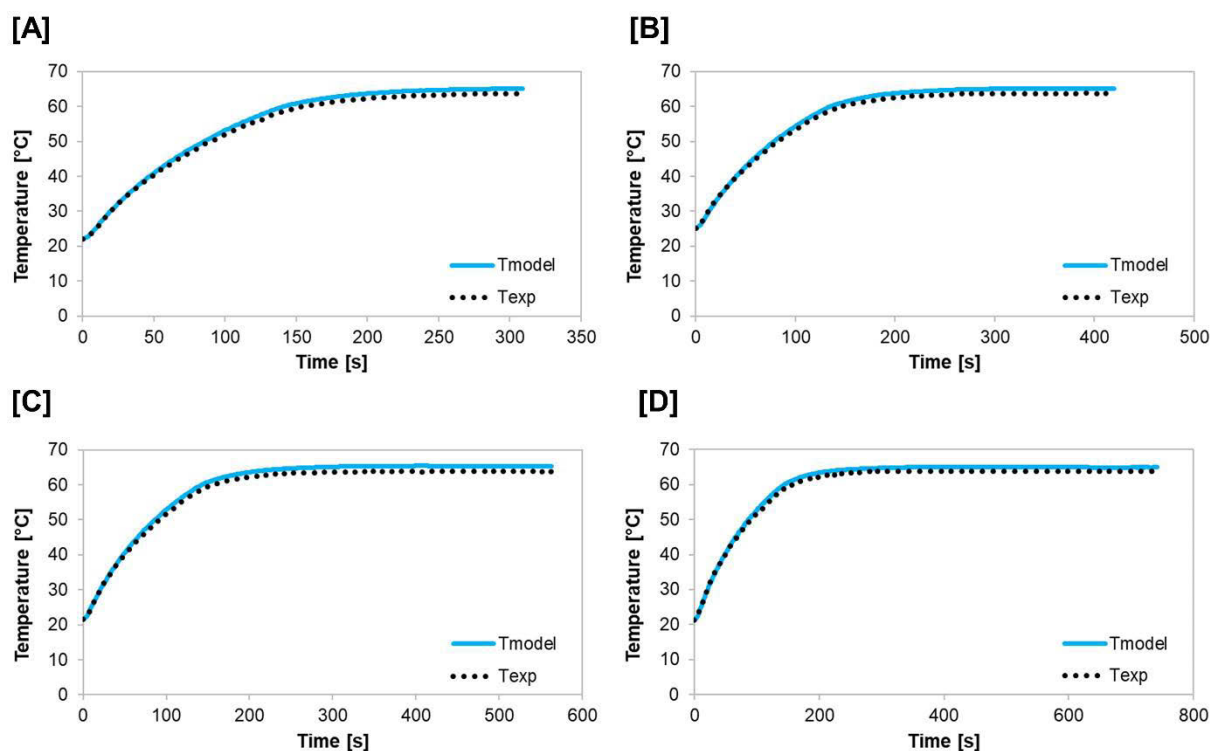
Figure 4.23. Predicted and experimental temperature profile at the center of the sample during the following microwave treatments: 64 °C without holding time (A), 64 °C for 2 min (B), 64 °C for 4 min (C), 64 °C for 7 min (D).
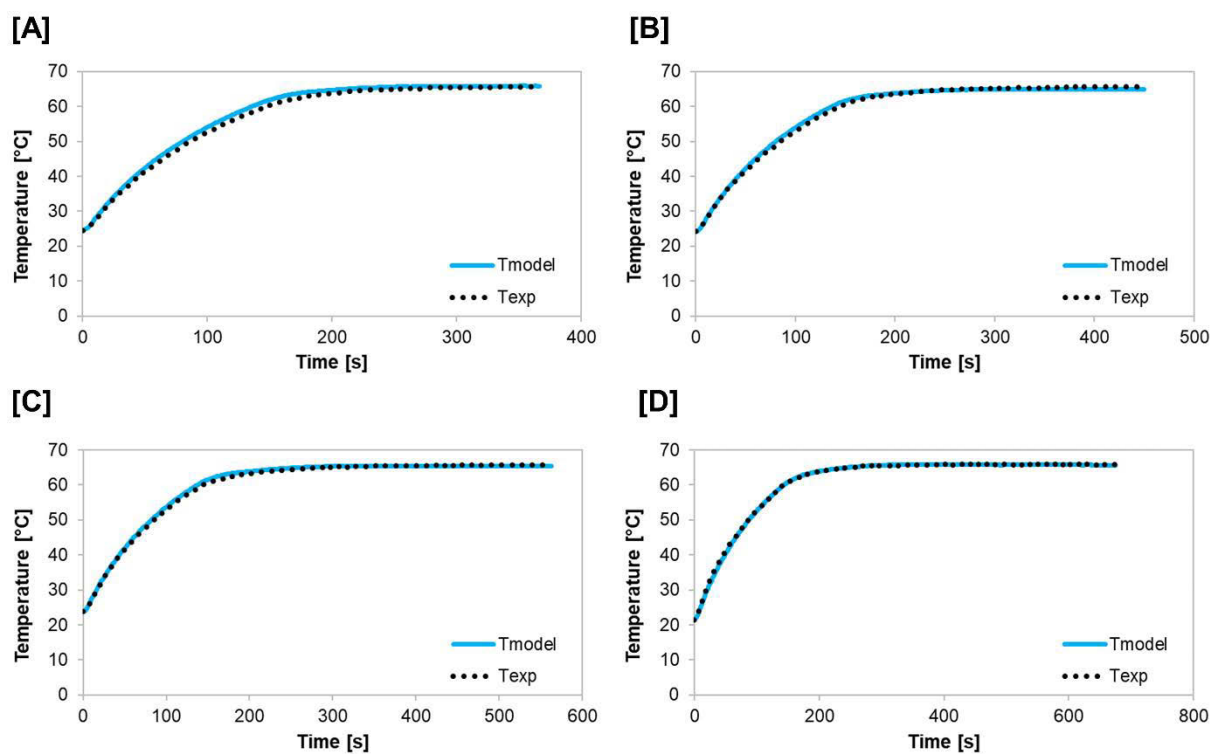
Figure 4.24. Predicted and experimental temperature profile at the center of the sample during the following microwave treatments: 66 °C without holding time (A), 66 °C for 1 min (B), 66 °C for 3 min (C), 66 °C for 5 min (D).
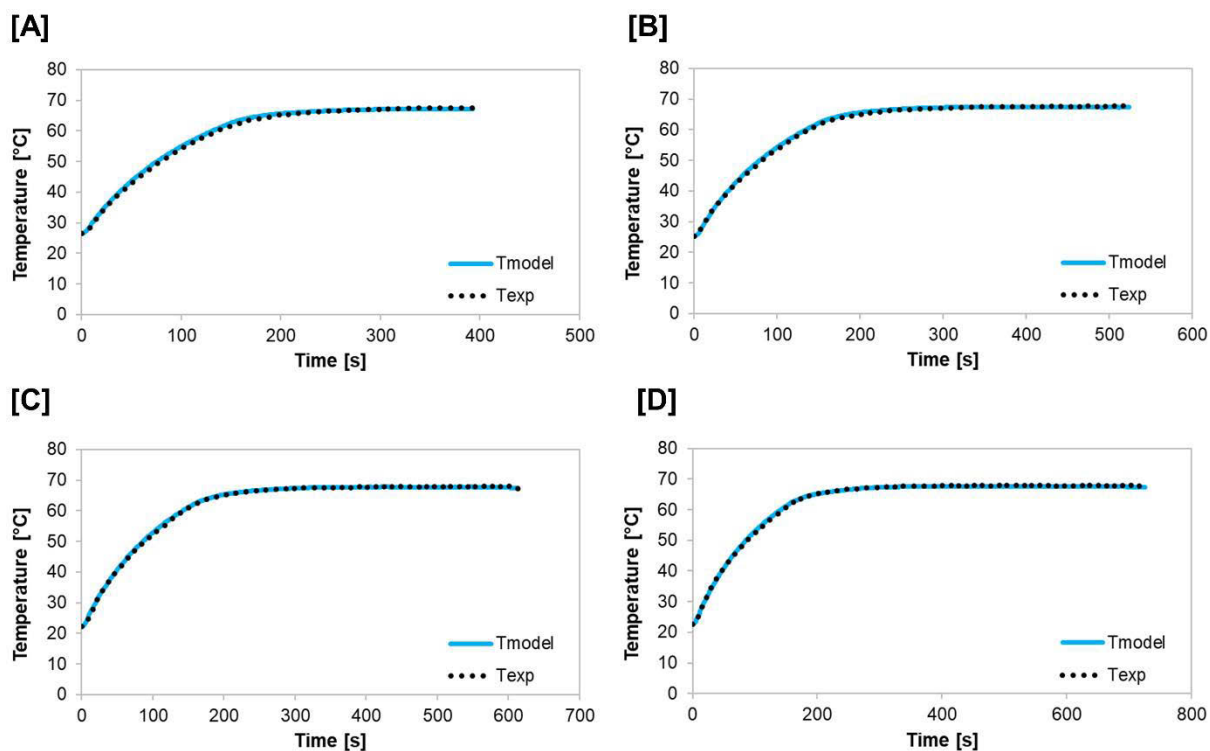
Figure 4.25. Predicted and experimental temperature profile at the center of the sample during the following microwave treatments: 68 °C without holding time (A), 68 °C for 2 min (B), 68 °C for 4 min (C), 68 °C for 6 min (D).
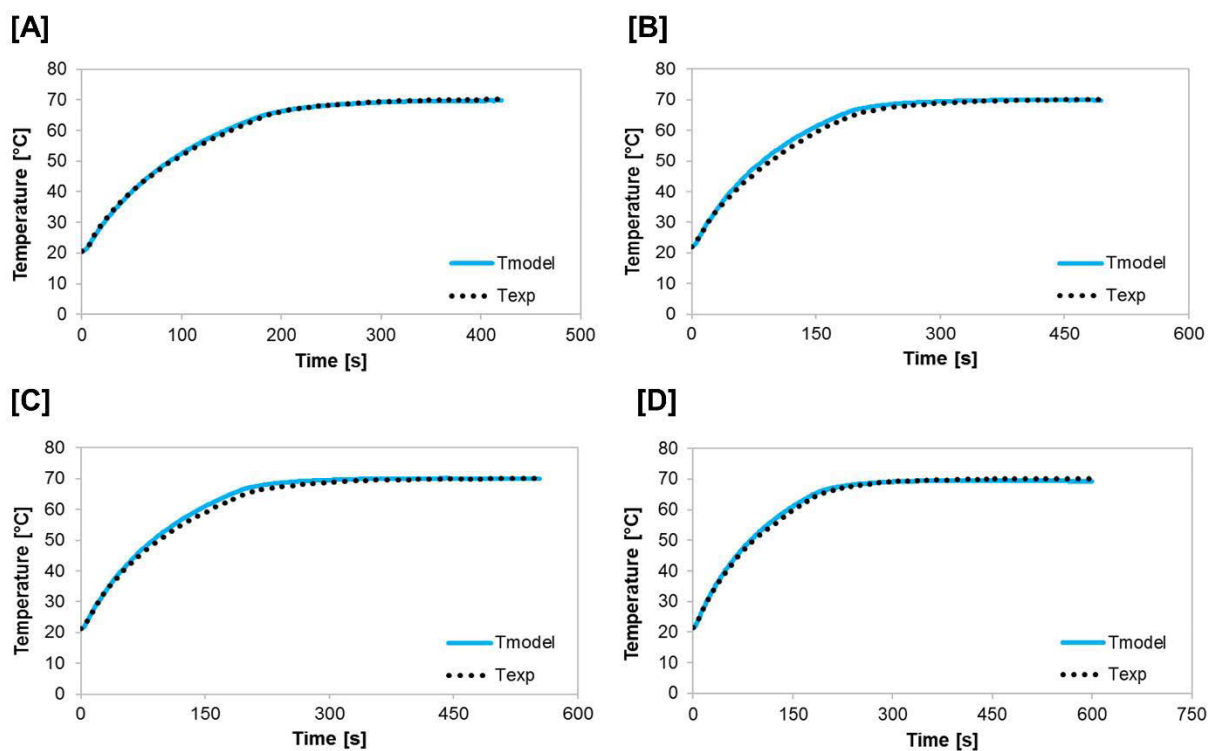
Figure 4.26. Predicted and experimental temperature profile at the center of the sample during the following microwave treatments: 70 °C without holding time (A), 70 °C for 1 min (B), 70 °C for 2 min (C), 70 °C for 3 min (D).
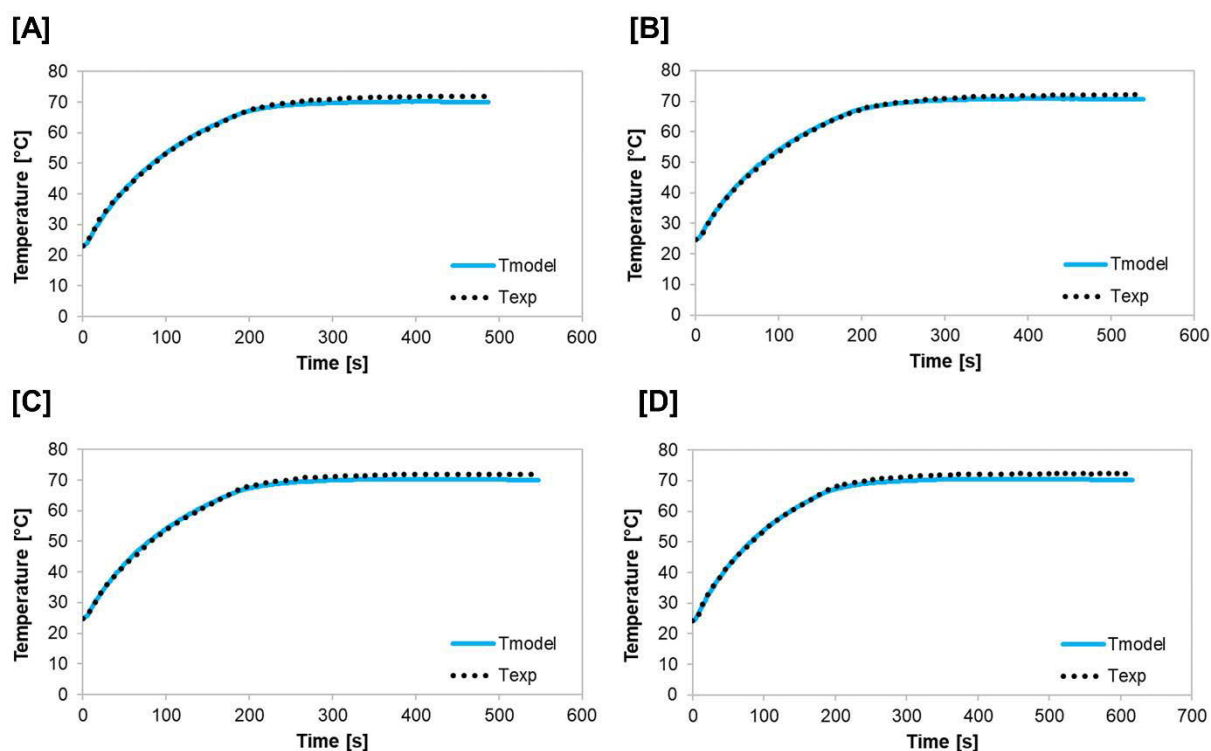
Figure 4.27. Predicted and experimental temperature profile at the center of the sample during the following microwave treatments: 72 °C without holding time (A), 72 °C for 1 min (B), 72 °C for 2 min (C), 72 °C for 3 min (D).
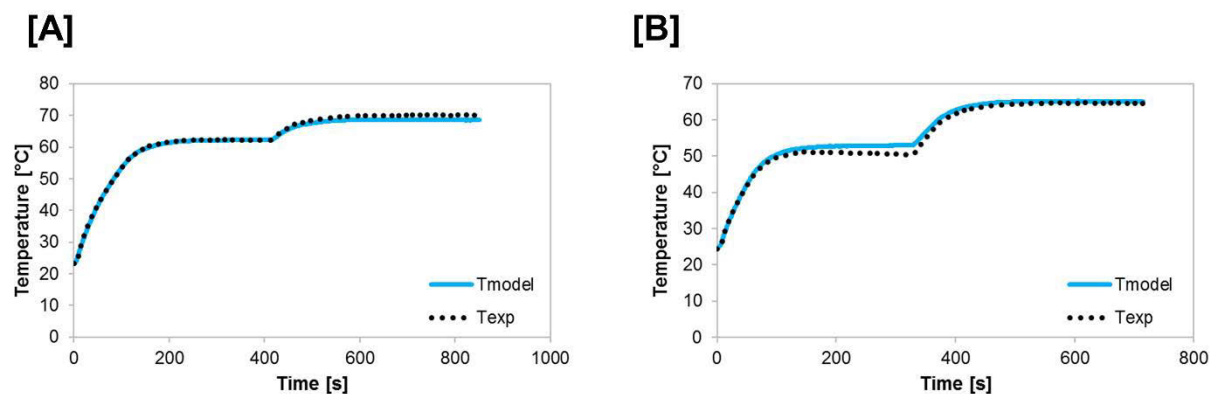
Figure 4.28. Predicted and experimental temperature profile at the center of the sample during the following microwave treatments: 62 °C for 3 min + 70 °C for 3.5 min (A), and 50 °C for 3 min + 65 °C for 3 min (B).

Overall, a good agreement was obtained in all the simulated treatments. However, it can be noticed that the predicted temperature at lower T_P (60 – 64 °C) was slightly above the temperature measured experimentally. On the other hand, at higher T_P (70 – 72 °C), the predicted temperatures were slightly below the experimental temperature. At intermediate T_P (66 – 68 °C), both temperatures presented a very good agreement. These results may be due

to the consideration of a single and constant coefficient of heat transfer between sample and surrounding, which might actually be variable along the process. Small differences in temperature can also be related to the precision of the temperature measurements, since the maintenance and assurance of the exact position of the fiber optic sensor is complicated. In addition, the accuracy of the sensor itself is 0.5 – 0.8 °C.

4.3.5.2. Analysis of enzyme inactivation

Predicted values of the residual peroxidase activity after microwave processing were compared with the experimental values. As shown in Figure 4.29, a quite good agreement was obtained between both predicted and experimental values. As already mentioned before, the inactivation is closely dependent on spatial temperature distribution. Thus, considering the satisfactory results, the values of inactivation may indirectly indicate that the temperature and velocity distribution within the sample were also correctly predicted. Besides, these results demonstrated the successful employment of the inactivation kinetic model from conventional (water bath) to microwave heating.
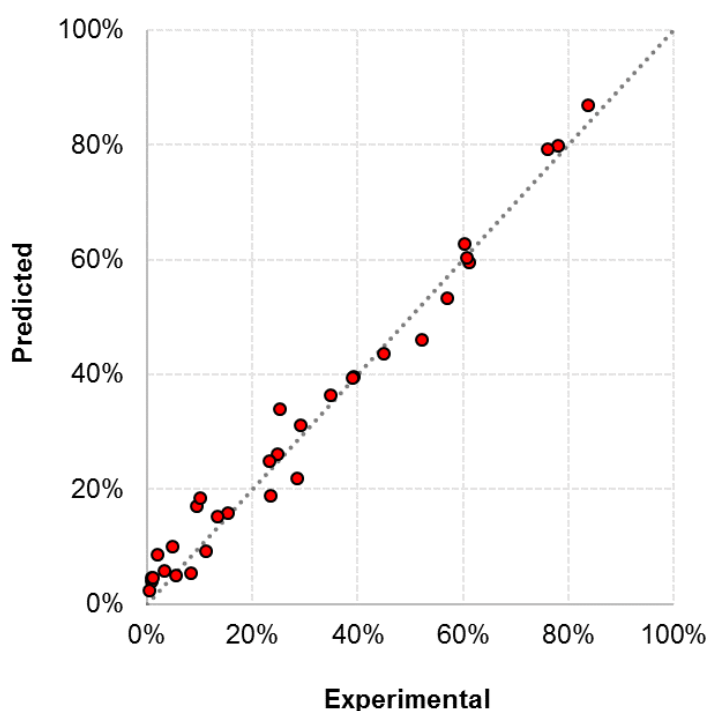
Figure 4.29. Parity plots comparing the predicted and experimental residual peroxidase activity after different microwave treatments.

4.3.6. Effect of fluid flow

Modeling of microwave processing of liquids is considerably more demanding in relation to computational effort than in the case of solids. The presence of fluid motion leads to complex interactions of velocity fields and temperature distributions within the liquid. In order to verify the importance of the fluid flow coupling, two simulations of the treatment 66 °C/5min were compared: one solving and coupling the fluid flow equations, and another neglecting the fluid flow.

A great difference is already observed in relation to the simulation time. While the complete model took 87 h, the model without fluid flow needed only around 20 h to be solved. Comparing the temperature profile at the center of the sample (Figure 4.30), the shape of the profile curve was different and the temperature from the simulation without fluid flow was lower than the experimental temperature and the temperature from the complete model.
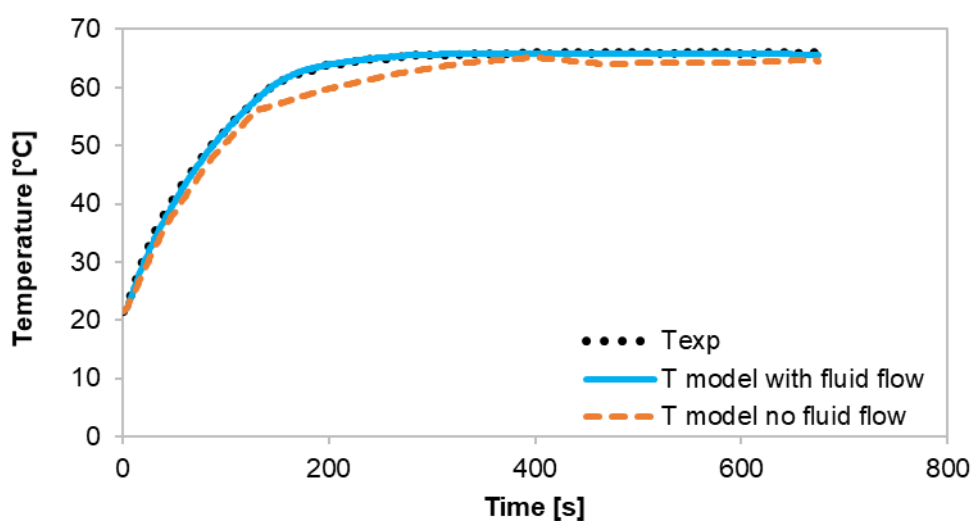
Figure 4.30. Temperature profile from experiments and from simulations considering or not the fluid flow equations.
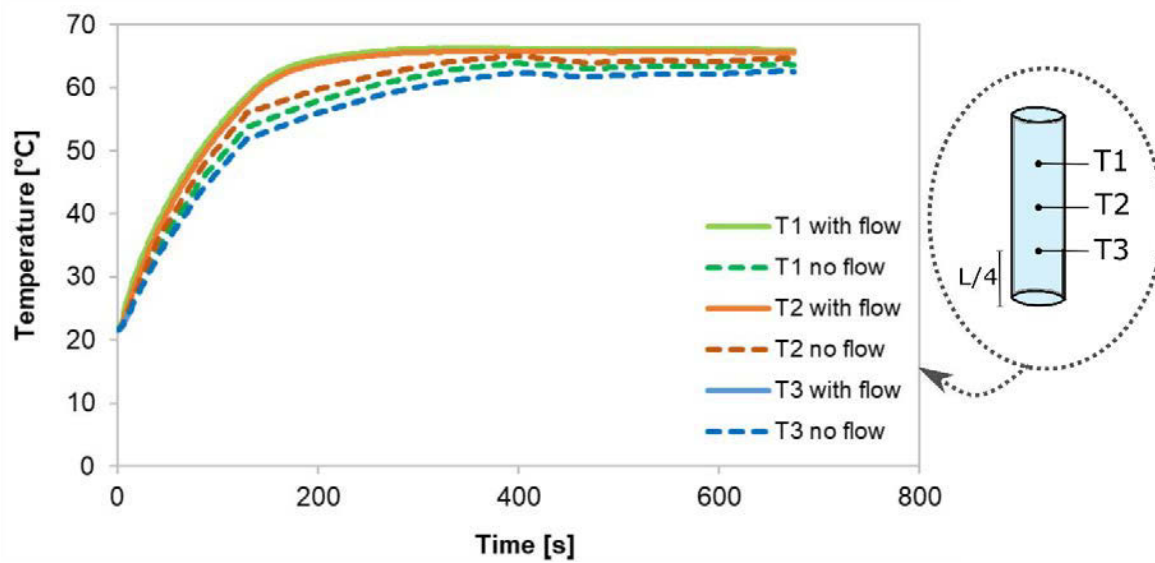
Figure 4.31. Temperature profile at three different points within the sample obtained from the simulations considering or not the fluid flow equations.

In fact, during microwave heating, fluid flow plays a significant role on the spatial temperature distribution. Fluid motion induces more natural convection and influences the temperature distribution. The difference of temperature distribution can be observed by comparing Figure 4.32 and Figure 4.33. In the simulated processing without considering fluid flow, the temperature distribution is clearly more uneven, with hot zones around the center of the sample and two cold zones located in the top and bottom side.
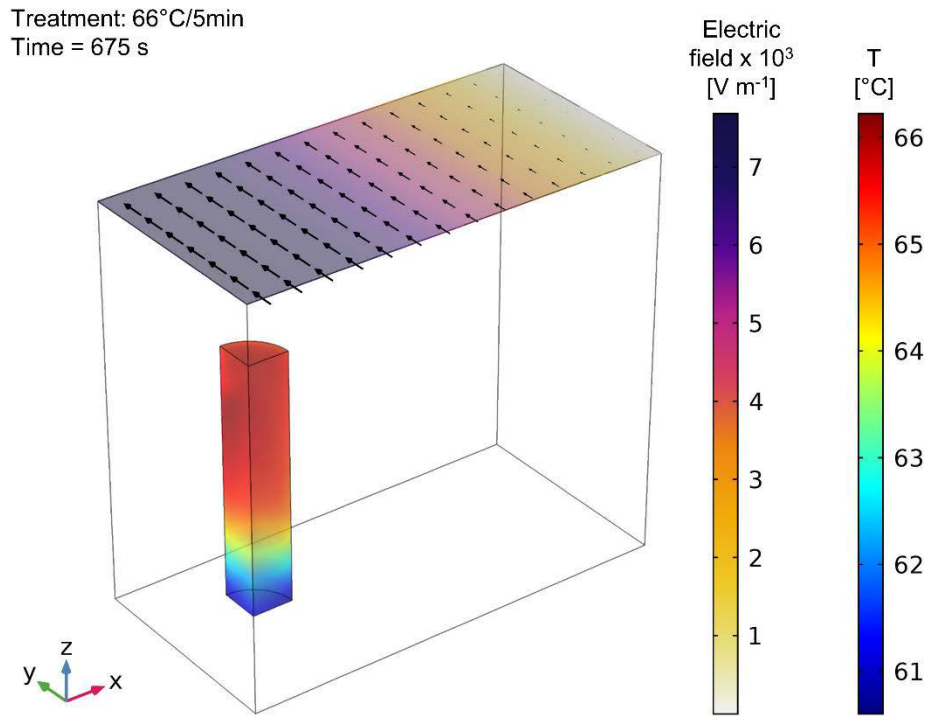
Figure 4.32. Temperature distribution within the sample from simulation considering fluid flow.
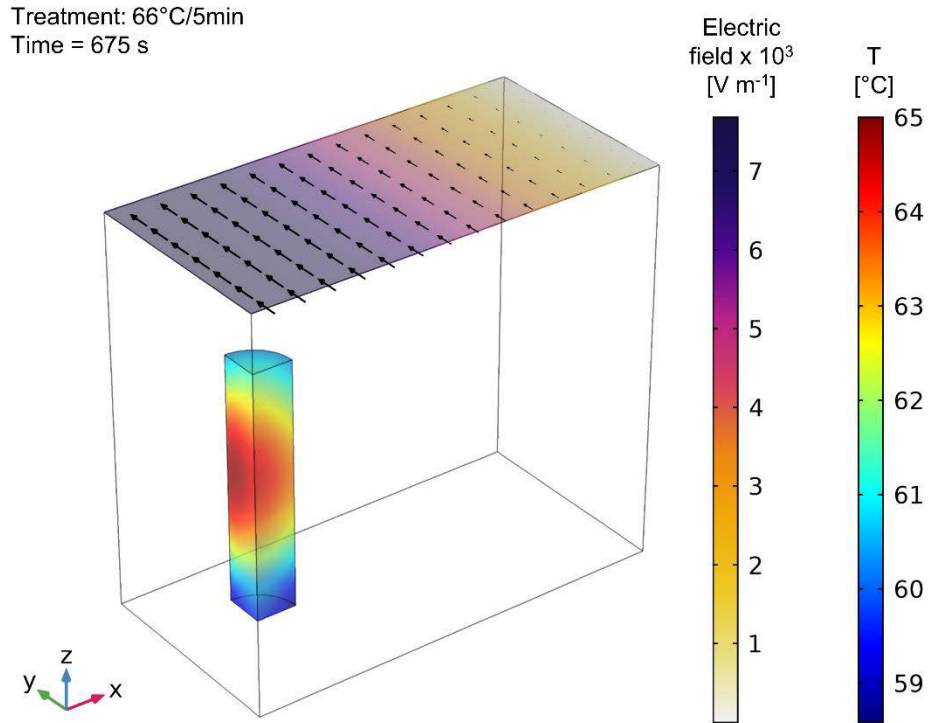
Figure 4.33. Temperature distribution within the sample from simulation without fluid flow.

Due to the different temperature distribution, the global enzyme inactivation was also different, as it can be observed in Figure 4.34. When fluid flow was not solved, less inactivation occurred since more cold zones were found within the sample. Thus, it is worth to note that the difference of enzyme inactivation efficiency between conventional (water bath) and microwave processing would be even more consequential if there was no fluid flow modelling.

Thus, in view of all the presented results, one can conclude that fluid flow generates a great impact. Therefore, to obtain a reliable model of microwave heating of liquid, the resolution of the fluid flow equations is strictly necessary, even if the required computational effort is greater.
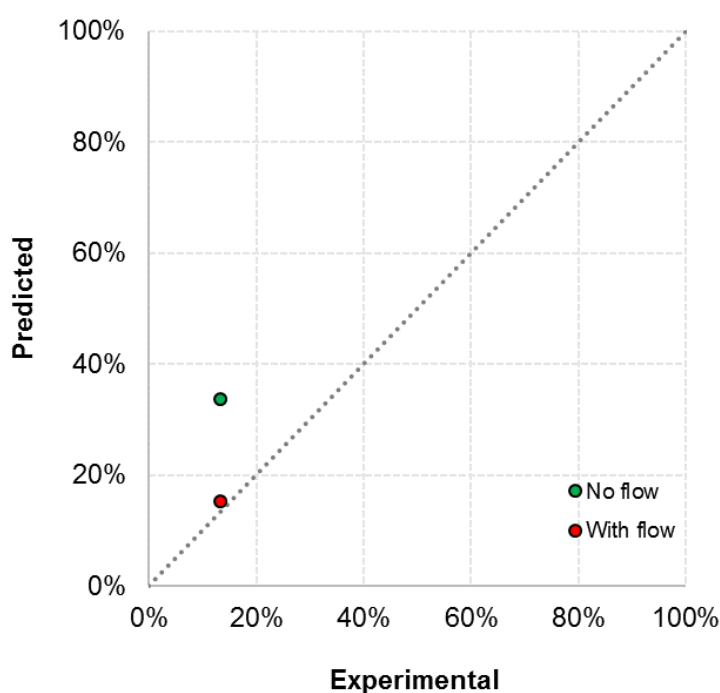
Figure 4.34. Parity plots comparing the predicted, considering or not fluid flow, and experimental residual peroxidase activity after the microwave treatment at 66 °C/5 min.

4.4. Conclusions

In the first part of the present chapter, the experimental study was presented. Microwave treatments of the model fruit juice solution at different temperature and time conditions were performed. Information on temperature profile at the geometric center of the sample as well as peroxidase inactivation data were obtained. Experimental results were later used to validate the simulation model.

In the second part of the chapter, the numerical study was described. By using a Finite Element method, a multiphysics model to simulate the experimental microwave processing and predict peroxidase inactivation was proposed. Dielectric and thermophysical properties as

a function of temperature were considered in the model. Governing equations of electromagnetic propagation, heat transfer and fluid flow were coupled and solved. The kinetic model of peroxidase inactivation, resulting from experiments with conventional heating (Chapter 3), was also implemented in the model.

Since results showed the presence of convection currents and uneven temperature distribution within the sample, the lethal effect of temperature evolution over the whole geometrical volume was numerically integrated and taken into account to estimate the enzyme inactivation. Then, the developed model was successfully validated, showing good agreement between experimental and predicted data of temperature profile at the center of the sample and peroxidase inactivation.

Moreover, in a comparison between simulations considering or not considering the fluid flow equations, the results clearly demonstrated the effect of fluid motion on the temperature distribution. Considering the validation of the model was well accomplished, it is reasonable to consider that the model also correctly predicted the spatial distribution of temperature. Therefore, coupling the fluid flow equations was important and necessary to obtain good results during the simulation of microwave heating of liquids.

It is important to note that by considering the kinetic model of peroxidase inactivation obtained from conventional heating in the microwave heating simulation, the non-thermal effects of microwaves on enzyme was neglected. By the way, this topic is covered in the following chapter, in which the possible existence of non-thermal effects was evaluated experimentally.

CHAPTER 5.   EVALUATION OF ENZYME REACTIVATION AND POSSIBLE NON-THERMAL EFFECTS OF MICROWAVES

5.1. Introduction

This chapter brings into perspective two topics related to the POD inactivation.

The first deals with the existence of non-thermal microwave effects, which is a very controversial subject in the literature. Some studies support the existence. On the other hand, others studies claim that the existence is not evidenced and thus inactivation is only due to thermal effects. Therefore, possible non-thermal effects of microwave application on POD inactivation were evaluated through microwave processing in batch and closed-loop modes at low temperatures. For this purpose, special set-ups including the use of cold air as a cooling medium were built to remove, as much as possible, the dissipated heat.

The second issue deals with the POD reactivation. POD from several sources have shown an ability to recover its activity while being stored after heat treatment, which can cause deterioration in flavor, color, and nutritional quality of processed foods. Reactivation of the enzyme is suggested to be a complex process and is influenced by several factors. In this work, the recovery of POD activity in model fruit juice after conventional and microwave heating was evaluated and compared.

5.2. Material and methods

5.2.1. Fruit juice model solution

Fruit juice model solution was prepared following the same procedure described in Chapter 3, using sucrose (Merck, Germany), citric acid (Merck, Germany), horseradish peroxidase (POD, type X commercialized under crystalline suspension in 3.2 mol L^{-1} ammonium sulfate; EC: 1.11.1.7; P6140-5KU; Sigma-Aldrich Co., USA) and distilled water. The final soluble solids content and pH of the solution were 10 °Brix and 3.8, respectively. The enzymatic activity in the model solution was 4 U mL^{-1}. Fresh fruit juice model solution was prepared just before each processing.

5.2.2. Enzyme activity measurement

The POD activity was determined according to the same method described in the Chapter 3. In a quartz cuvette with a 1-cm light path, 160 μL of sample was added to 2.25 mL of McIlvaine's buffer solution at pH 6.0 and 320 μL of 5% (w/v) pyrogallol solution (Sigma, UK).

This mixture was used as a reference solution (0.000 absorbance). Then, 160 µL of 0.147 mol L^{-1} hydrogen peroxide solution (Sigma-Aldrich, Italy) was added to start the reaction.

The increase in the solution absorbance at 420 nm was recorded every 5 s for 2 min using a UV-Vis spectrophotometer (UviLine 8100, Secomam, France). From the curve of absorbance as a function of time, the enzyme activity was then calculated by regression using a generalized reduced gradient algorithm implemented in the 'Solver' tool of software Excel 2016 (Microsoft, USA). Measurements were carried out in at least duplicate.

5.2.3. Assessment of non-thermal microwave effects

To evaluate the existence of non-thermal effects due to microwaves on POD inactivation, microwave treatments in batch mode and in closed-loop flow were performed. The experiments were carried out in two groups: processing with external cooling of the inner quartz tube and processing without cooling. In both cases, the incidence of microwave power was maintained constant. While in the cooled processing cold air was employed to limit the increase in sample temperature, in the non-cooled processing the microwave heating took place without the cold air injection. More details are given below. The enzyme activity of the sample was measured just after each processing. The residual activity was calculated by the ratio of the activity of the sample after treatment to the initial activity of the untreated sample.

5.2.3.1. Microwave processing in a closed-loop flow system with and without cooling

The microwave processing in a closed-loop flow was carried out in a system composed of: a solid-state microwave generator at 2.45 GHz (MKS SG524E.2, Alter Power Systems Products, Italy), an aluminum WR340 waveguide, two neoprene tubes, two concentric quartz tubes and a peristaltic pump with a container. Reflected power was minimized by regulating three stubs near to the top of the waveguide and a sliding short in the waveguide bottom. An overview of the experimental apparatus is shown in Figure 5.1. The set of quartz tubes was positioned within the waveguide, so that it was parallel to the smaller side of the rectangular waveguide (Figure 5.1C). The neoprene tubes were used to link the inlet and outlet of the pump reservoir and the waveguide/quartz tube.
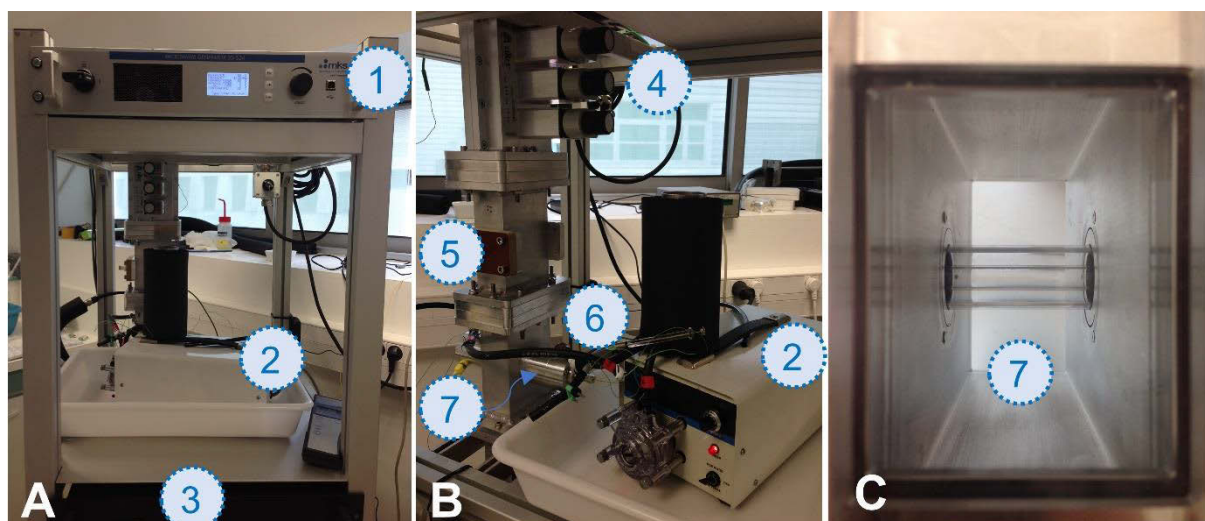
Figure 5.1. Different views of the closed-loop flow microwave system: front (A), lateral (B) and waveguide inside view (C); and its main components: 1) solid state microwave generator, 2) peristaltic pump, 3) temperature controller, 4) stubs, 5) waveguide, 6) neoprene tubes, 7) quartz tubes.

The incident power was maintained constant at 90 W. The processing time was fixed to 30 min. During this time, 50 mL of model fruit juice were continuously circulated in the system at a flow rate of 4.12 L h^{-1} in a closed-loop, passing through the neoprene tubes and the inner quartz tube, and returning to the container (Figure 2). Temperature were gathered at four locations in the system using K-type thin-wire thermocouples centrally inserted into the neoprene tubing. The temperatures in the outlet of the container (T1), in the outlet of the pump (T2), in the inlet of the quartz tube (T3) and in the outlet of the quartz tube (T4) were recorded using thermocouples connected to a data logger (OM-CP-Quadtemp2000, Omega, USA). The measurement points are illustrated in Figure 5.2.

A compressed air pipe with a venturi-type cooler was connected to the waveguide applicator. For the cooled microwave processing, air was injected within the waveguide at the same time that the microwaves were applied to the sample, removing dissipated heat and keeping the temperature at sublethal values. Also, to assist in the maintenance of low temperatures, the container was surrounded by a layer of crushed ice. In the case of processing without cooling, the container was wrapped with insulating foam and cold air was only employed after the processing time to decrease the temperature of the processed sample.

To get the untreated sample for later calculation of the residual activity, before each processing, the sample was placed in the container and pumped for around 2 min without microwave application. Then, an aliquot of sample was withdrawn and the microwave treatment at 90 W for 30 min was started. After each experiment, distilled water was run through the system at high flow for around 2 min to clean the pipe.
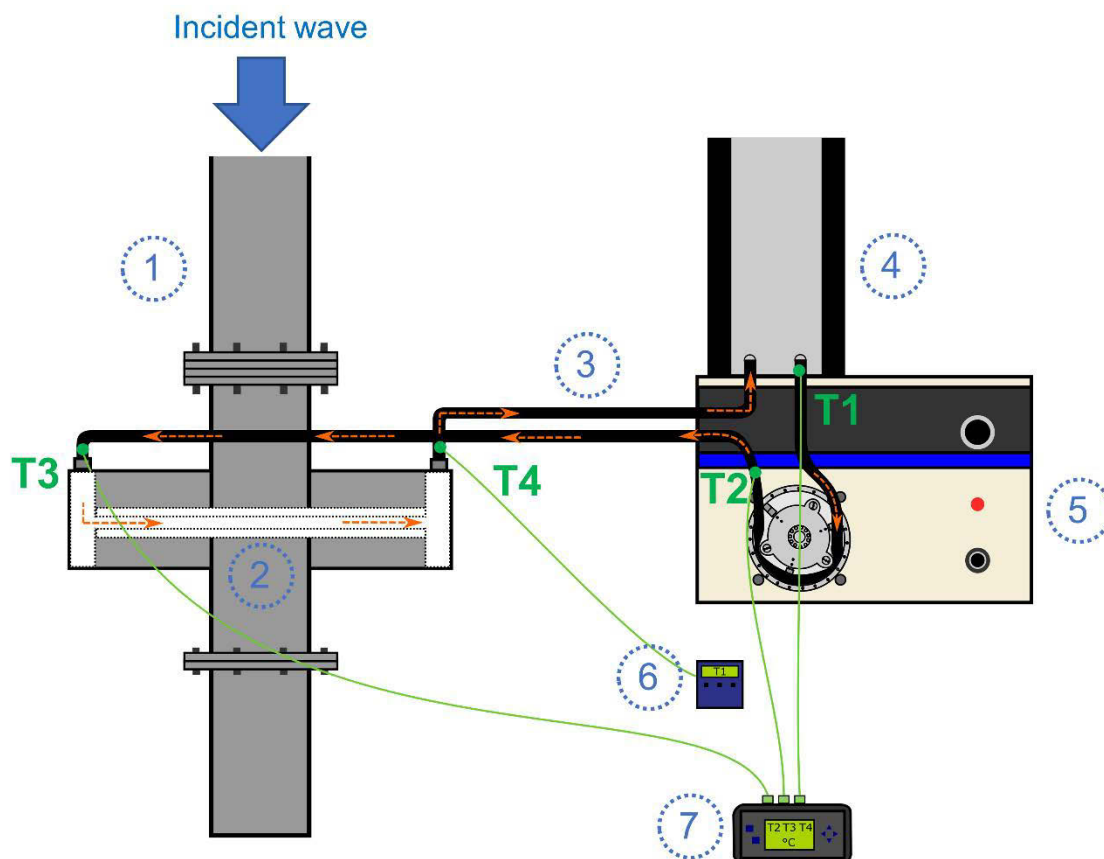
Figure 5.2. Schematic diagram of the closed-loop flow microwave system, showing the locations of temperature measurement (denoted as T1, T2, T3, T4 in green), the direction of sample flow (indicated by orange arrows), and some main components of the system: 1) waveguide, 2) quartz tubes, 3) neoprene tubes, 4) container, 5) peristaltic pump, 6) PID temperature controller, 7) data logger.

5.2.3.2. Microwave processing in a batch system with and without cooling

Microwave batch processing was performed in the microwave apparatus described in section 5.2.3.1, but with some modifications. The same solid state microwave generator at 2.45 GHz (MKS SG524E.2, Alter Power Systems Products, Italy), aluminum WR340 waveguide and two concentric quartz tubes were employed. However, instead of circulating the sample through the tubes, water at 15 °C from a thermostatic bath was used. Due to the high microwave power available to treat a small sample (1.2 mL) in batch configuration, it was necessary to add the water circulation within the quartz tube in order to insure a proper monitoring of the temperature increase within the sample. The circulating water also served as a matched water load for absorption of remaining microwave power within the cavity.

An aliquot of 1.2 mL of fruit juice model solution was placed in small plastic tube (10.13 mm external diameter, 7.93 mm internal diameter, 35.80 mm height), identical to the one used in Chapter 4. A plastic cap with a hole in the center, through which an optical fiber sensor was positioned, was used to close the tube. A perforated rectangular plate with 11 mm

in height made of polytetrafluoroethylene was used as a support for the tube, being placed within the waveguide applicator next the cold air inlet, filling the section. The tube containing the sample was positioned in the center of the plate. To expose the entire lateral surface of the tube and to maximize eventual contact with cold air, a plastic ring was used to keep the tube slightly above the plate height, as shown in Figure 5.3.
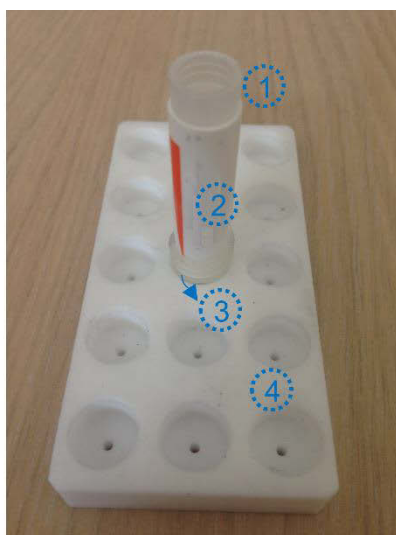
Figure 5.3. Some materials used in the microwave batch processing: 1) plastic cap, 2) plastic tube, 3) plastic ring, 4) polytetrafluoroethylene support plate.

A compressed air pipe with a venturi-type cooler was connected to the waveguide applicator. A general illustration of the experimental set up is presented in Figure 5.4. For the cooled microwave processing, air was injected within the waveguide at the same time that the microwaves were applied to the sample, removing dissipated heat and maintaining low temperatures. The temperature of the inlet air was monitored using a K-type thermocouple and a data logger (OM-CP-Quadtemp2000, Omega, USA). In the non-cooled processing, cold air was only employed after the desired process time to decrease the temperature of the treated sample until around 5 °C. In both processes, the incident power was maintained constant for a determined time. Three combinations of power and time were carried out: 90 W/15 min, 45 W/15 min and 45 W/60 min. The temperature at the geometrical center of the sample was recorded by a fiber optic sensor and a data logger (Reflex-4, Neoptix, Canada).
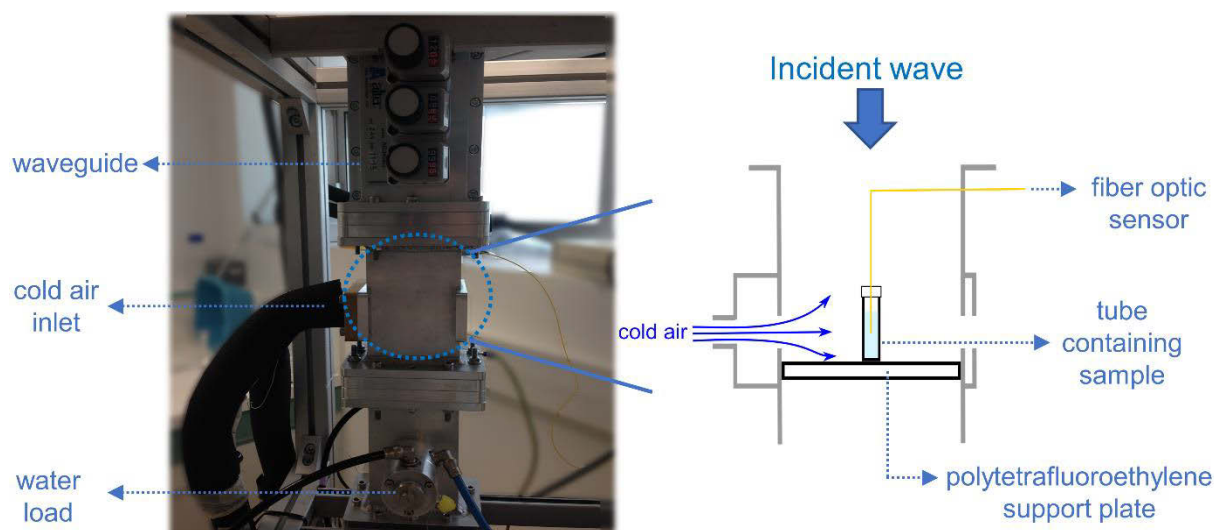
Figure 5.4. Schematic diagram of the microwave system for the batch processing of model fruit juice with use of cold air.

5.2.4. Assessment of POD reactivation

The recovery of POD activity was evaluated in the model fruit juices treated by three different systems: conventional heating (water bath), microwave heating in batch mode and microwave heating in closed-loop flow. Treated samples were stored in closed polypropylene cryotubes and kept in the dark at 25 °C. The enzyme activity was monitored after 0, 1, 2 and 3 days of processing. The relative activity was calculated by the ratio of the activity in each period to the initial activity of the untreated sample.

Conventional and microwave batch processing were performed at three time-temperature combinations in order to obtain relative activities of around 90%, 60% and 4%. Microwave processing in closed-loop flow was carried out at one time-temperature condition to attain initial relative activities of 60%.

All experiments were performed in triplicate. Statistical analysis was carried out at the 95% confidence interval using Minitab version 18 statistical software (Minitab Inc., USA).

5.2.4.1. Treatment by conventional heating

The thermal processing was conducted as previously described in Chapter 3, using the same glass tubes with small diameter (10 mm) and thin walls (0.6 mm). Aliquots of 4 mL of the fruit juice model solution were placed in these tubes, which in turn were positioned inside a thermostatic water bath (Bioblock Scientific, Germany) with orbital shaking. The treatments were performed at three combinations of final temperature and process time: 60 °C for 2 min, 66 °C for 3 min and 72 °C for 6 min. After the desirable holding time, the samples were quickly

cooled in an ice-water bath until the temperature reached 5 °C. The temperature history of each sample was gathered using thermocouples (K-type), fixed in the center of the tube through a cap and connected to a data logger (Datalog 20, AOIP, France).

5.2.4.2. Treatment by microwave heating in a batch system

Microwave batch processing was performed as described in Chapter 4, using the same microwave apparatus (TE_{10} mode, frequency of 2.45 GHz) and experimental procedures. A small plastic tube (10.13 mm external diameter, 7.93 mm internal diameter, 35.80 mm height) containing an aliquot of 1.2 mL of model fruit juice was placed in the center of a support block (60 mm height) made of extruded polystyrene. The block was placed inside the applicator and arranged to be perpendicular to the wave transmission direction. The treatments were performed at three final temperatures: 60 °C and 66 °C without holding times and 72 °C for 1.5 min of holding time. In the treatment at 66 °C, in order to obtain around 60% of inactivation, the incident power was limited to half of maximum power, increasing the come-up time. For the other treatments, no power limitations were needed. After heating, the samples were removed from the applicator and rapidly cooled in an ice bath until 5 °C. The temperature was measured at the geometrical center of the sample using a fiber optic sensor attached to a data logger (Reflex-4, Neoptix, Canada).

5.2.4.3. Treatment by microwave heating in a closed-loop flow system

The microwave processing in a closed-loop flow was carried out in the same system previously described in section 5.2.3.1. However, the experimental procedures were a little different. A PID temperature controller was used and the incident power was modulated instead of being constant.

Temperature at four different locations in the system were monitored using K-type thin-wire thermocouples centrally inserted into the neoprene tubing, as illustrated in Figure 5.2. The temperatures at the outlet of the container (T1), at the outlet of the pump (T2) and at the inlet of the quartz tube (T3) were recorded using thermocouples connected to a data logger (OM-CP-Quadtemp2000, Omega, USA). The temperature at the outlet of the quartz tube (T4) was recorded and used as reference by a PID temperature controller. The incident power was modulated by the controller in order to achieve and maintain the set-point temperature (process temperature). The maximum incident power was fixed to be 35% of the generator nominal power, i.e. 35% of 450 W.

In each treatment, 50 mL of model fruit juice were placed in the pump container, which was wrapped by an insulating foam layer to minimize heat loss. The sample was pumped continuously at a flow rate of 4.12 L h^{-1} in a closed circuit. After establishing apparent steady flow (around 2 min of pumping), an aliquot of sample was withdrawn (untreated sample) and then, the microwave treatment was started. The process temperature was set to be 60 °C and the process time was 30 min. After this time, the treated sample was collected and cooled in an ice-water bath until 5 °C. After each experiment, distilled water was run through the system at high flow for around 2 min to clean the tubing.

5.3. Results and discussion

5.3.1. Evaluation of possible non-thermal microwave effects on POD inactivation

The study of non-thermal effects during microwave processing is still a very controversial subject in the literature. Different experimental systems and strategies have been evaluated. Most of the works evaluated the differences between conventional and microwave processing, considering quasi-similar or equivalent thermal histories. However, this approach may not be ideal to assess the non-thermal microwave effects, mainly when sample temperature is not well controlled.

Furthermore, each heating mode can supposedly cause different structural changes in the enzyme, which in turn may be related to non-thermal effects and/or other factors, such as specific effects of microwaves on protein conformation (Ramaswamy et al., 2002). According to Lopes et al. (2015), the inactivation of horseradish POD under conventional heating is governed by changes in secondary and tertiary structure of the enzyme, while under microwave heating the inactivation is governed mainly by changes in tertiary structure. Thus, to specifically focus on microwave effects, another approach was performed by exposing the model fruit juice to microwaves at sublethal temperatures. Similar approach was reported by other studies, such as Ramaswamy et al. (2002) and Tajchakavit (1997).

In this work, only microwave treatments were evaluated. The experiments were carried out in two groups: processing with cooling and processing without cooling. The effect of exposition to a continuous and fixed microwave power during a certain time was studied. Low power values were chosen so that the temperature of the sample was not too high, allowing the use of cold air was enough to remove the generated heat and keep the temperature low (sublethal) during the processing with cooling. In this way, thermal effects were prevented with the purpose of evaluating possible non-thermal effects. The study was performed by microwave treatments in closed-loop flow and in batch mode.

5.3.1.1. Microwave processing in a closed-loop flow system

In the microwave processing in a closed-loop flow, the incident power was set at 90 W. The sample was circulated through the system for 30 min at flow rate of 4.12 L h^{-1}. Examples of temperature profiles measured at four different locations during the processing without cooling (A) and the processing with cooling by air injection at around -8 °C (B) is presented in Figure 5.5. It can be observed that in the processing without cooling the maximum temperature reached 60.7 °C, while in the processing with cooling the temperatures remained below 39.4 °C.

[A]

[B]
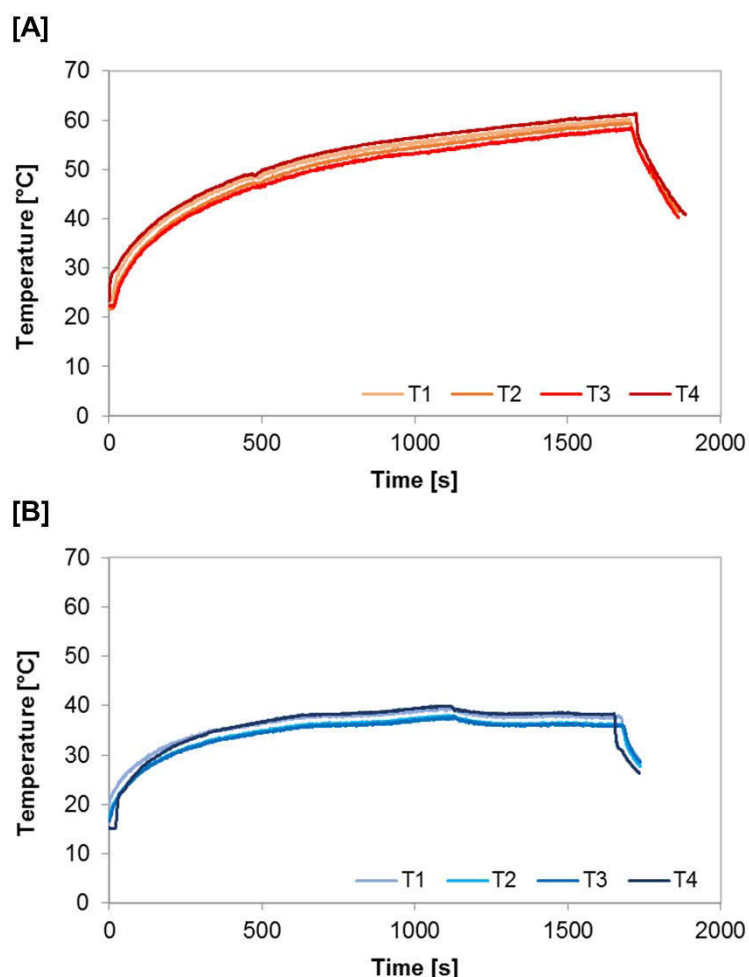
Figure 5.5. Example of time-temperature profiles at outlet of the container (T1), outlet of the pump (T2), inlet of the quartz tube (T3) and outlet of the quartz tube (T4) in the microwave processing at 90 W for 30 min in closed-loop flow system without cooling (A) and with cooling (B).

Results of the POD residual activity after processing without cooling and processing with cooling are presented in Figure 5.6. A decrease of around 23% in POD activity was

observed after the processing without cooling. In the processing with the use of cold air, the activity had a much smaller decrease (about 5%).
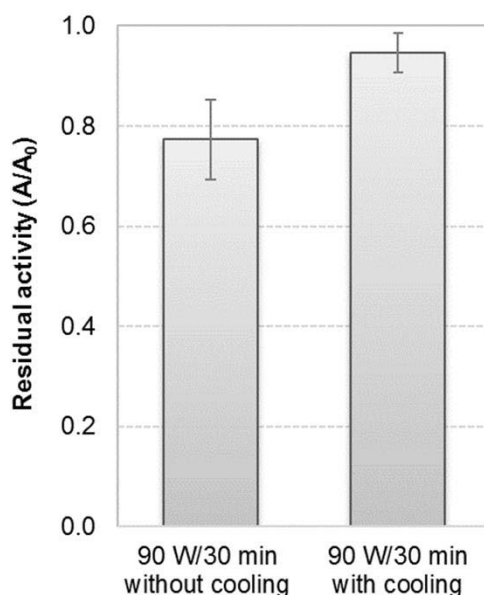
Figure 5.6. Residual activity of peroxidase in model fruit juice after microwave processing in closed-loop flow system without cooling and with cooling. Values are presented as mean values ± standard deviation (n = 3).

In general, the loss of POD activity by conventional heating occurs at temperatures above 45 °C. Thus, it was expected that no inactivation would be found after the processing with cooling, since the maximum measured temperature was around 39.4 °C. However, the POD activity showed a small decrease in relation to the initial activity (A_0). It is worth to note that the initial activity was obtained from the sample that was previously circulated through the system, thus eliminating eventual (but unlikely) pumping effects. Therefore, this result may indicate the existence of non-thermal effects of microwave. Even so, it also demonstrates that the eventual non-thermal microwave effects are quite small, being much smaller than the thermal effects. Another set of experiments were then assessed to verify it.

5.3.1.2. Microwave processing in a batch system

In the microwave processing in batch mode, the incident power was firstly set at 90 W and the process time was 15 min. An example of the thermal history during the processing of model fruit juice without and with cooling at this time-power combination is shown in Figure 5.7. Note that the maximum temperature at the center of the sample was 70.6 °C in the processing without cooling and 32.1 °C in the processing with cooling. Results of the POD residual activity after processing are presented in Figure 5.8. As expected, a huge POD

inactivation occurred after the processing without cooling and the residual activity was around 0.11%. In the processing with cooling, the activity decreased about 5.2%, which is a value very close to the one found in the closed-loop processing.
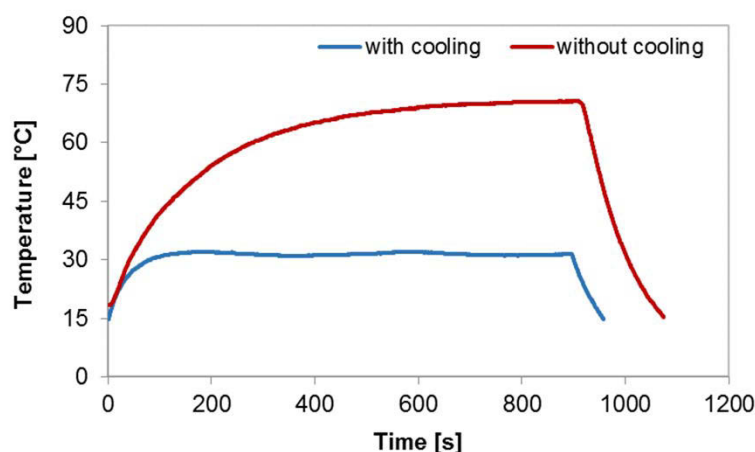
Figure 5.7. Example of thermal history at the center of the fruit juice model solution during microwave processing at 90 W for 15 min in a batch system without and with cooling.
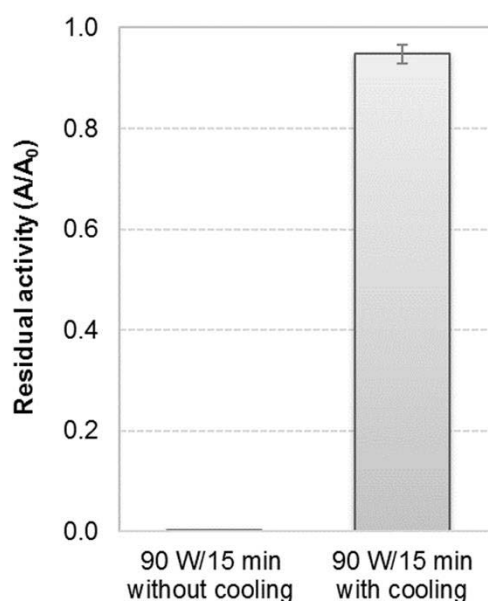
Figure 5.8. Residual activity of peroxidase in model fruit juice after microwave processing at 90 W for 15 min in batch system without and with cooling. Values are presented as mean values ± standard deviation (n = 3).

To verify the enzymatic behavior at even lower temperatures, other experiments at reduced incident power were performed. Microwave processing of model fruit juice in batch mode at 45 W for 15 min was carried out. An example of the thermal history during the processing of model fruit juice without and with cooling at this time-power combination is shown in Figure 5.9. The maximum temperature at the center of the sample was 52.1 °C in the processing without cooling and only 18.5 °C in the processing with cooling. POD residual

activities are presented in Figure 5.10. After the processing without cooling, residual activity was around 72%, while after the processing with cooling it was around 95.1%. Thus, even at very low temperatures, once again the POD activity decreased about 5%.
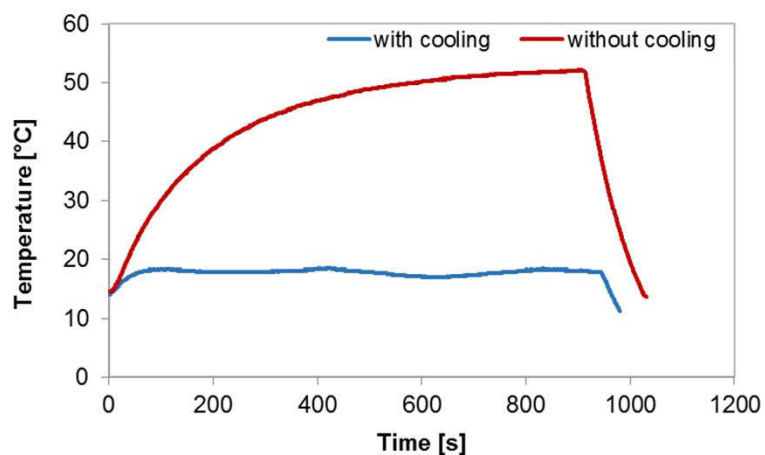
Figure 5.9. Example of thermal history at the center of the fruit juice model solution during microwave processing at 45 W for 15 min in a batch system without and with cooling.
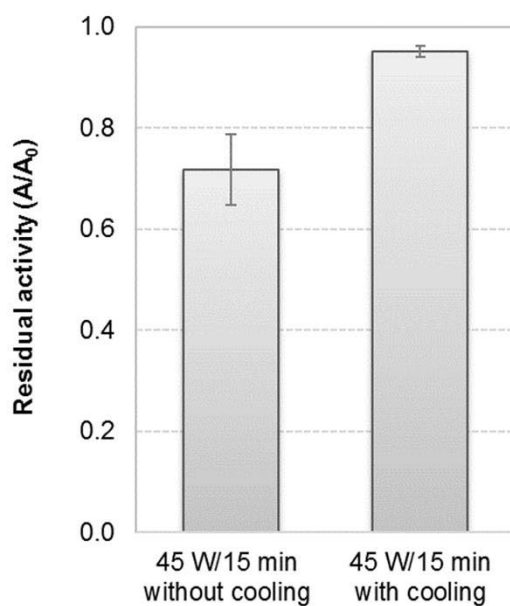
Figure 5.10. Residual activity of peroxidase in model fruit juice after microwave processing at 45 W for 15 min in batch system without and with cooling. Values are presented as mean values ± standard deviation (n = 3).

Microwave processing of model fruit juice in batch mode with cooling at 45 W for 60 min was carried out to verify the influence of the microwave exposure time on enzymatic activity at low temperatures. Figure 5.11 presents an example of thermal history during this processing. The sample temperature remained throughout the process time below 18.3 °C and varied according to the temperature variation of the cold inlet air, which is also shown in the

figure. POD residual activity after the processing was 96.1 ± 1%. Thus, the process time did not influence the extent of non-thermal inactivation.
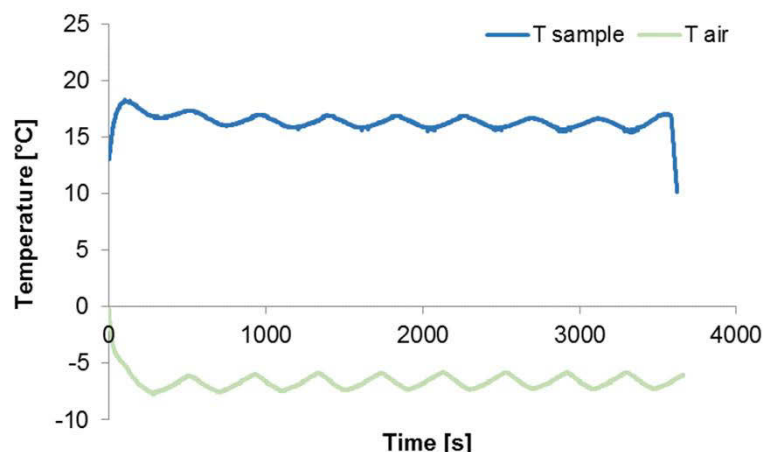
Figure 5.11. Example of thermal history at the center of the fruit juice model solution during microwave processing at 45 W for 60 min in a batch system with cooling and the temperature profile of the inlet cold air.

Therefore, in view of the presented results, it is possible that non-thermal effects due to microwaves may contribute along with thermal effects to the POD inactivation. However, thermal inactivation continues to be much more dominant compared to non-thermal inactivation, as it can be observed in Figure 5.6, Figure 5.8 and Figure 5.10. De Pomerai et al. (2003) reported a small but consistent effect of microwaves on protein conformation, even though this effect seemed less striking when temperature was increased. Tajchakavit (1997) and Ramaswamy et al. (2002) reported pectin methyl esterase inactivation when orange juice was exposed to high microwave power (700 W) for 90 min at the sublethal temperature (<40 °C). However, the extent of this inactivation was also relatively small as compared with that at higher temperatures. According to the authors, the non-thermal effect at sublethal temperature was then not considered to be significant.

5.3.2. POD reactivation in model fruit juice after different thermal treatments

Reactivation of horseradish POD in model fruit juice during dark storage at 25 °C after 0, 1, 2 and 3 days of the thermal treatment was assessed. In order to verify the influence of the type of heating on POD reactivation, thermal treatments using conventional and microwave heating were performed. The process time-temperature combinations were chosen so that different extents of inactivation (and reactivation) could be studied.

5.3.2.1. Reactivation of POD after conventional heating

In the conventional heating processing, the three combinations of time and final temperature were: 60 °C/2 min, 66 °C/3 min and 72 °C/6 min. An example of the thermal history of each combination is shown in Figure 5.12. Results of the POD relative activity at each time of storage are presented in Figure 5.13. Activities remained almost unchanged and no significant differences along the storage time were observed in any of the three time-temperature conditions.

Figure 5.12. Example of thermal history during processing by conventional heating at three combinations of process temperature and time.

Figure 5.13. Relative activity of peroxidase during storage at 25 °C for 0, 1, 2 and 3 days after heat treatment at 60 °C/2 min, 66 °C/3 min and 72 °C/6 min. Values are presented as mean values ± standard deviation (n = 3). Means in the same treatment identified by the same letter do not significantly differ by Tukey's test (p > 0.05).

Rodrigo et al. (1997) studied the reactivation of horseradish POD in citrate-phosphate buffer solution (pH 5.5). POD solution was heated in capillary tubes at the temperature range of 110 – 135 °C with exposure times ranging from 2 to 100 s, being stored for 32 h at 25 °C and for 21 days at 4 °C. The authors reported that the storage temperature did not greatly affect the percentage of reactivation, but so its velocity: the reactivation at 25°C occurred faster than at 4 °C. The maximum POD activity recovery was found during storage at 25 °C, in which the percentage of POD reactivation was 54.5%. In addition, they observed that the higher the severity of the treatment, the lower percentage of activity recovered.

Analogous observation was reported for POD from green peas in potassium phosphate solution (pH 6.0), which showed more than 80% of reactivation after heat treatment at 50 °C and incubation at 25 °C, but less than 35% of reactivation after heat treatment at 70 °C (Halpin et al., 1989). For neutral POD from broccoli, the extent of reactivation after heat treatment at 60 – 90 °C varied from almost 10 to 50%, depending on the heating conditions. For all temperatures studied, the extent of reactivation decreased as the inactivation increased. Samples with higher POD inactivation degree reactivated to a lesser extent (Thongsook and Barrett, 2005).

According to Machado and Saraiva (2002), the rate of reactivation may be dependent on the amount of intermediate forms produced resulting from thermal treatment. Therefore, reactivation can be closely related to temperature and heating time. In fact, the authors proposed an empirical model to fit the data of activity recovered in horseradish POD solution (pH 7.0) after different temperature and heating times.

However, in the present case, the POD did not recover its activity after thermal treatment, independently of the time-temperature combination used. These differences in relation to literature can be due to the complexity of a reactivation process. The ability of POD to regain activity after being denatured by heat varies with several factors, such as type and source of enzyme, characteristics of the enzyme solution, operating conditions of thermal processing, among others (Tamura and Morita, 1975; Thongsook and Barrett, 2005).

In fact, the medium properties seems to be the important factor for the observed behavior. A factor that may explain these different outcomes is the pH of the solution in which the enzyme is present, since enzyme reactivation is pH dependent (Carvalho et al., 2007; Tamura and Morita, 1975). Lu and Whitaker (1974) found that horseradish POD in solutions at low pH was inactivated very rapidly at 76 °C and there was no measurable recovery in activity. On the other hand, by increasing the pH from 4.0 to 9.0, the rate of reactivation increased from none to a maximum extent of activity recovery. While the POD reactivations previously cited were performed using solutions at pH values within a neutral range (pH around

6 – 7), this work was performed at much lower pH. The model fruit juice had a pH of 3.8, which may explain why the potential POD reactivation was not observed.

5.3.2.2. Reactivation of POD after microwave heating

The batch processing using microwave heating was performed at three final temperatures: 60 °C and 66 °C without holding times and 72 °C for 2 min of holding time. An example of the thermal history of each combination is shown in Figure 5.14. Note that the heating rate of the treatment at 66 °C was purposely lower since the incident power was limited to half of maximum power, while it was almost the same for the other two processes. In this way, the desired degree of inactivation (around 60%) could be obtained, just as the conventional heating at 66 °C. Results of the POD relative activity at each time of storage are presented in Figure 5.15.
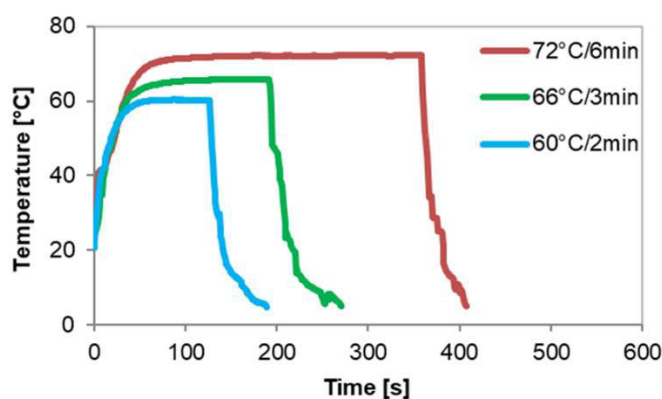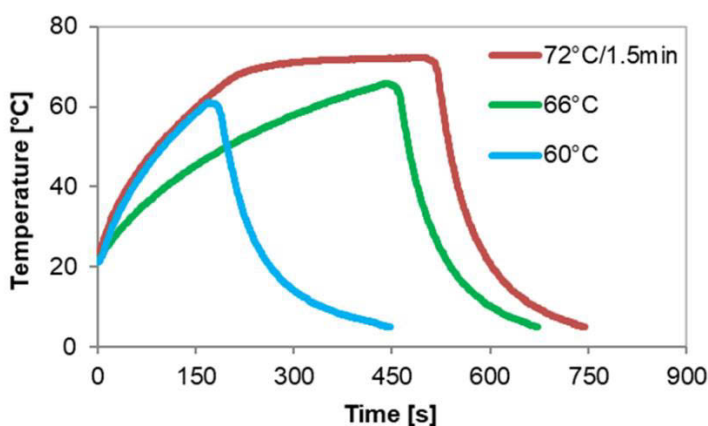

Figure 5.14. Example of thermal history during processing by microwave heating in batch mode at three combinations of process temperature and time.
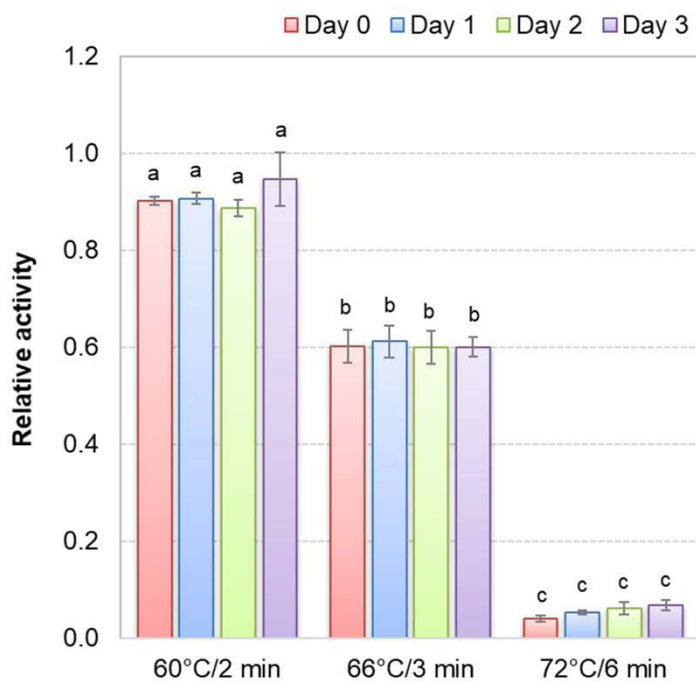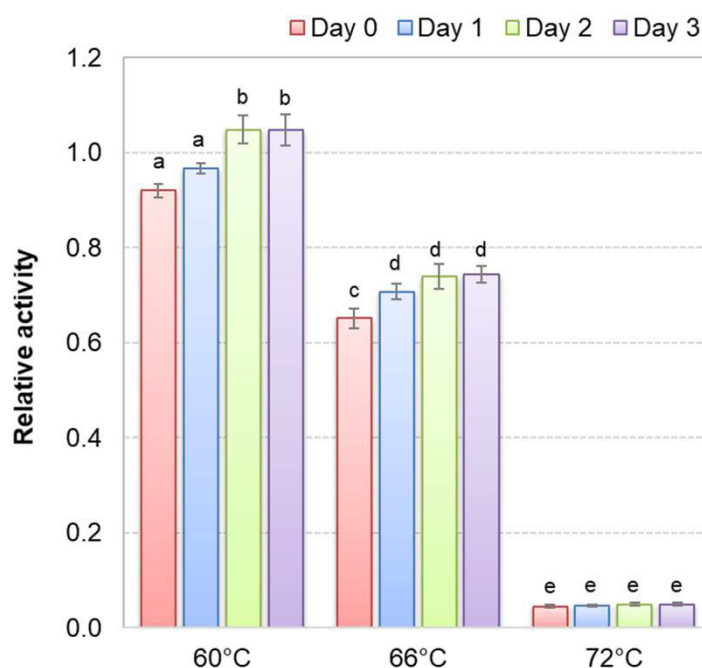
Figure 5.15. Relative activity of peroxidase during storage at 25 °C for 0, 1, 2 and 3 days after processing by microwave heating in batch mode at 60 °C and 66 °C without holding times and 72 °C/1.5 min. Values are presented as mean values ± standard deviation (n = 3). Means in the same treatment identified by the same letter do not significantly differ by Tukey's test (p > 0.05).

After the processing at 72 °C/1.5 min, relative activities did not show significant changes along the storage time. As already mentioned, some authors reported that the higher the degree of inactivation, the lower the activity reactivation (Rodrigo et al., 1997; Thongsook and Barrett, 2005). Hence, it may explain why the treatment at this combination did not result in significant reactivation, whereas at the other two time-temperature conditions (60 °C/no holding and 66 °C/no holding) a small increase of relative activities with storage time was observed.

Unlike the conventional heating, the microwave heating resulted in reactivation of POD in model fruit juice. Two possibilities can be pointed out, comparing the differences with this treatment and the conventional heating. Firstly, this difference could be justified by the possible distinct mechanisms of inactivation and conformational changes supposedly attributed to microwave heating – the so called non-thermal effects. Secondly, another possible explanation may be related to non-homogeneous temperature distribution within the sample during the microwave processing in batch mode. In fact, this temperature gradient also occurs in conventional heating, however in this work, the conventional heating was considered to provide uniform heating because of small sample volume, thin tube walls and heating under shaking.

With the purpose of verifying this second possibility, another processing using microwave heating was carried out. However, in this processing the sample was pumped into

a closed-loop, mixing the model juice (and the enzymes). In this way, the temperature distribution was much more homogeneous. The process temperature was set to be 60 °C and the process time was 30 min, aiming an intermediate degree of inactivation of around 60%.

An example of temperature profiles at four different locations in the microwave closed-loop system during processing is presented in Figure 5.16. The temperatures were denoted as T1, T2, T3 and T4, as indicated in Figure 5.2. Relatively small temperature differences were observed. Note that the temperature at the inlet of the quartz tube (T3) was the lowest one, which is coherent since it is the farthest location from the heating site considering the sample path in the system. Also, as expected, the temperature at the outlet of the quartz tube (T4) was higher than the other temperatures. The mean difference between both temperatures, T3 and T4, was around 3.5 °C.
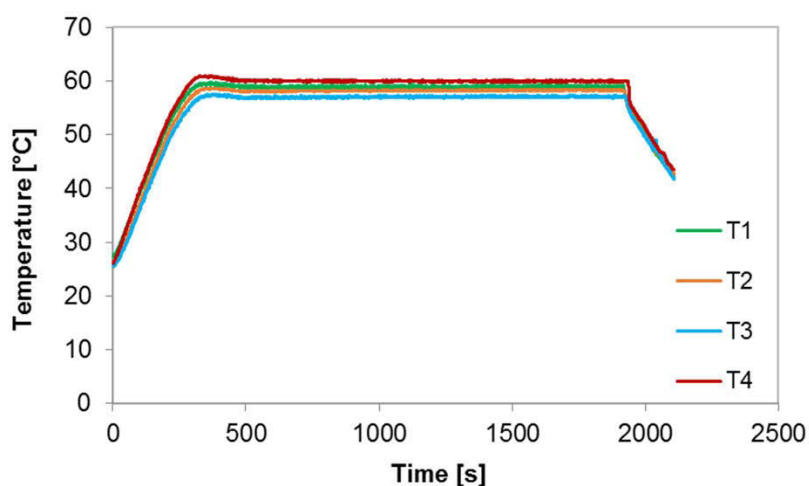
Figure 5.16. Example of time-temperature profiles at outlet of the container (T1), outlet of the pump (T2), inlet of the quartz tube (T3) and outlet of the quartz tube (T4) in the closed-loop flow microwave heating system at flow rate of 4.12 L h^{-1}.

Results of the POD relative activity at each time of storage are presented in Figure 5.17. No significant differences along the storage time were observed. It is worth to note that the processing in closed-loop resulted in degrees of inactivation quite different by comparing the three process repetitions. Knowing that the presented results are means of values from these repetitions, high standard deviations were obtained. However, within each repetition, the same trends were observed and no reactivation was found.
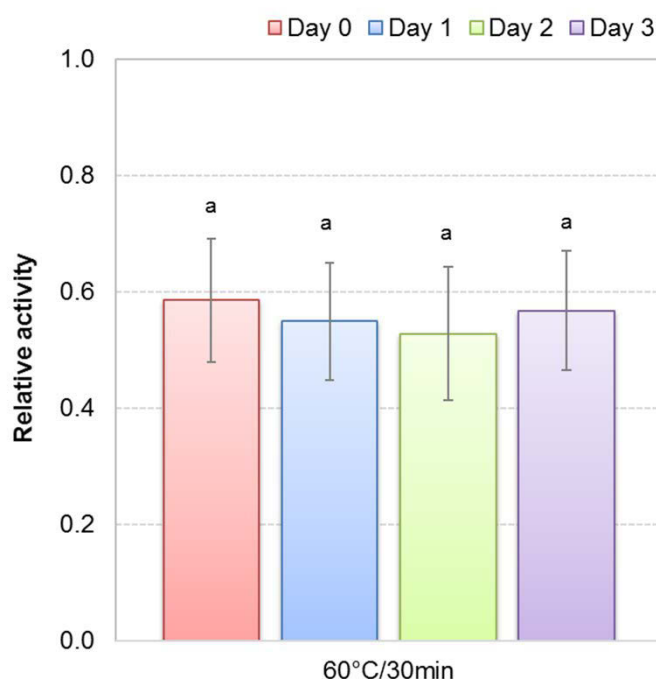
Figure 5.17. Relative activity of peroxidase during storage at 25 °C for 0, 1, 2 and 3 days after processing by microwave heating in closed-loop flow at 60 °C/30 min. Values are presented as mean values ± standard deviation (n = 3). Means identified by the same letter do not significantly differ by Tukey's test (p > 0.05).

Therefore, in view of the presented results, it is not possible to state that the occurrence of the reactivation in the model juice treated in batch by microwaves was due to the type of heating or non-thermal effects. In fact, it is more likely that the recovery of POD activity has occurred due to the heterogeneity of the spatial temperature distribution within the sample during batch processing. Non-uniformity of temperatures is a very important factor, but it is often neglected in the literature on thermal processing of foods, which can cause hasty conclusions about the occurrence of reactivation.

As presented and discussed in the previous chapter, cold regions are observed during the microwave batch processing. In these regions, the treatment is less effective, which can result in the presence of non-inactivated or partially inactivated enzymes that are more prone to reactivate even in acidic pH, as the one of the model juice. It may explain why the recovery of activity was observed in the samples treated at time-temperature conditions (60 °C and 66 °C) with lower inactivation degree. The same trend was not observed neither in the treatment by conventional heating nor the microwave processing in closed-loop since the temperature distribution within the sample was more uniform due to fluid motion.

5.4. Conclusions

The existence of non-thermal microwave effects was assessed by exposing the POD in the model fruit juice to microwaves under batch or closed-loop mode at low temperatures. To remove the effect of heat dissipated due to microwaves, maintaining temperatures lower than thermally lethal values, a cooling system using cold air was attached to the microwave system. Thus, experiments were performed to evaluate if the enzyme inactivation was due to microwave radiation itself or heat generated by dielectric losses. After all the treatments at sublethal temperatures, the POD activity decreased around 5%, independently of the studied incident power (45 and 90 W), process time (15, 30 and 60 min) and processing mode (batch and closed-loop flow). Hence, it indicates that non-thermal effects on POD inactivation are possibly existent, under the studied conditions. Since thermal effects were much more predominant than non-thermal effects, the decrease of POD activity due to non-thermal effects of microwave may be little significant, mainly when the treatment yields high inactivation degree.

Reactivation of horseradish POD in model fruit juice during dark storage at 25 °C after 0, 1, 2 and 3 days of the thermal treatment was assessed. Conventional (in batch mode) and microwave (in batch and closed-loop modes) heating were performed at different time-temperature combinations. No recovery of POD activity was observed in the model juice heated by microwave closed-loop treatment and conventional batch treatment, both under quite uniform temperature conditions. On the other hand, little recovery was found after microwave batch treatment. However, it is very likely that the reactivation is rather consequence of non-uniform temperature distribution within the sample during heating than a result of a reversible inactivation due to microwave. As already reported in previous chapter, non-uniform heating of the sample occurs during microwave batch treatment, which explain the occurrence of POD reactivation after this processing method.

In fact, in order to better understand the POD reactivation and confirm the existence of non-thermal microwave effects, further studies on conformational changes and other assessments at molecular level in the enzyme after processing are needed.

GENERAL CONCLUSIONS AND PERSPECTIVES

The objective of the present work was to study numerically and experimentally the application of microwave heating on a model fruit juice, focusing in the inactivation of enzymes.

In the literature review, the complexity of the phenomena involved during the microwave heating was pointed out. Also, the review drew attention to one of the major drawbacks of processing: the non-uniform heating. This non-uniformity has various implications related to quality and safety of the final treated product. For instance, it may result in insufficient enzyme inactivation at the cold spots. In particular, the occurrence of residual activity of peroxidase, an enzyme commonly present in fruit products and known for its relatively high thermostability, may cause the development of undesirable off-flavors and color alterations in the product. Therefore, a better understanding of interactions between microwaves, fruit juices and peroxidase was aimed.

By evaluating the dielectric properties of model fruit juice solutions with different sugar content at different temperatures and frequencies, it was verified that the dependence of dielectric properties on these factors was quite complex. For example, the rise of temperature either increased or decreased the dielectric properties, depending on frequency and TSS content. Thus, to model these dielectric non-monotonic behaviors, Artificial Neural Network models were proposed. The obtained predictions showed good agreement with experimental data, indicating that use of Neural Networks was a suitable approach to model the complex dielectric behavior.

The thermal inactivation of peroxidase by conventional heating was evaluated in the fruit juice model solution. As most thermal processing methods, the treatments were performed under non-isothermal conditions. In order to take into consideration the lethality during heating, holding and cooling times, the approach accumulated lethality was calculated by integration of temperatures. The obtained residual enzyme activities were well described by the adjusted first-order kinetic model, thus not evidencing the presence of isoenzymes with different heat resistances in the commercial enzyme solution employed in the model juice composition. The estimated first-order kinetic model was successfully validated by experimental data not used in the model fitting. This first order kinetic model was important to further implementation in the simulation model.

In order to understand the microwave heating and evaluate non-uniformity of temperature during microwave heating, a numerical study by finite element method was performed. To simulate the processing, a multiphysics model was developed coupling electromagnetic energy, heat transfer and fluid flow. In addition, the kinetic model mentioned above was also included in the simulation model. In this way, the peroxidase inactivation was predicted, taking into account the convection currents and the spatial distribution of

temperature within the sample during the microwave heating. To evaluate the validity of the model, the results were compared with experimental data of temperature profile at the center of the product and enzyme inactivation. Good agreement was obtained, thus the model was successfully validated.

Coupling of heat transfer and electromagnetics was important while considering significant changes in dielectric and thermophysical properties during heating of foods. Coupling of fluid flow was also essential for a reliable simulation. It was demonstrated by numerical evaluation the influence of fluid flow equations. Non appropriate results were obtained when these equations were not considered in the model, indicating the importance of fluid motion on the temperature distribution. Even if it demands higher computational effort and long simulation times, coupling the fluid flow equations was important and necessary to obtain good results during the simulation of microwave heating of liquids.

Note that when using the kinetic model obtained by conventional heating, the non-thermal effects were assumed to be nonexistent or negligible. In an attempt to verify this hypothesis, experiments at sublethal temperatures were carried out. The juice solution was exposed to microwaves both in batch and closed-loop flow modes. After all the treatments at sublethal temperatures, the enzyme activity had a fixed decreased of around 5%, independently of the studied incident power, process time and processing mode. These results may indicate the possible existence of non-thermal effects. However due to the small values (low inactivation) it is not possible to make a solid statement and further studies are encouraged. Even so, it reinforces the validity of assuming the non-thermal effects as nonexistent or negligible during the simulations.

Also, based on the reported potential capacity of peroxidase in recover its activities after heating, the evaluation of reactivation was performed in conventional system and in microwave systems under batch and closed-loop flow modes. Only little recovery of activity was found after microwave batch treatment. On the other hand, no recovery of peroxidase activity was observed in the model juice heated by microwave closed-loop treatment and conventional batch treatment. Knowing that the temperature distribution in the batch processing is non-uniform, as verified by computer simulation, it is very likely that the reactivation is rather consequence of non-uniformity than a result of a reversible inactivation due to microwave.

It is suggested for future research works, to study the enzyme inactivation by microwaves in real fruit and vegetable-based beverages, following similar procedures as this work. In this way, not only other enzymes can be evaluated, but also other compositions and structures. As seen in this work, dielectric properties are sensitive to various factors. Thus, for example, if fibers and pectin (compounds generally found in fruits) are present, it will might

considerably change dielectric properties and hence, microwave heating. Also the presence of these compounds can affect the thermophysical properties. In the case of products with higher viscosities, such as mango juices or concentrate juices, the interaction between microwave and the product can be very different from that described in this work. In addition, in this cited example, the fluid flow would certainly have a different pattern during microwave processing in comparison with the model juices, resulting in different temperature distributions.

Besides the suggestion of studying other products, another possibility would be the use of the proposed simulation model as a base to simulate other microwave processing conditions, such as different geometries (size and shape), operating frequencies, containers (packaging materials), among others.

Additionally, as already mentioned before, it would be very interesting to study in depth the effects of microwaves in relation to the possible alterations in molecular and conformational level of different enzymes. Such analyzes could be performed using, for example, detailed circular dichroism and fluorescence studies. Moreover, it is suggested the evaluation and comparison between enzymes that went through the same thermal history under similar conditions, evaluating both microwave and conventional heating as well. However, special attention to temperature and microwave power control would be very advisable in order to obtain reliable results.

REFERENCES

Anantheswaran, R.C., Liu, L., 1994. Effect of viscosity and salt concentration on microwave heating of model non-Newtonian liquid foods in a cylindrical container. Int. Microw. Power Inst.

Anantheswaran, R.C., Ramaswamy, H.S., 2001. Bacterial destruction and enzyme inactivation during microwave heating, in: Datta, A.K., Anantheswaran, R.C. (Eds.), Handbook of Microwave Technology for Food Applications. Marcel Dekker, New York, NY, pp. 191–215.

Anese, M., Sovrano, S., 2006. Kinetics of thermal inactivation of tomato lipoxygenase. Food Chem. 95, 131–137.

Anthon, G.E., Sekine, Y., Watanabe, N., Barrett, D.M., 2002. Thermal inactivation of pectin methylesterase, polygalacturonase, and peroxidase in tomato juice. J. Agric. Food Chem. 50, 6153–6159.

Antunes, E., Jacob, M. V., Brodie, G., Schneider, P.A., 2018. Microwave pyrolysis of sewage biosolids: Dielectric properties, microwave susceptor role and its impact on biochar properties. J. Anal. Appl. Pyrolysis 129, 93–100.

Aragao, G.M.F., Corradini, M.G., Normand, M.D., Peleg, M., 2007. Evaluation of the Weibull and log normal distribution functions as survival models of Escherichia coli under isothermal and non isothermal conditions. Int. J. Food Microbiol. 119, 243–257.

Arai, M., Binner, J.G.P., Cross, T.E., 1995. Estimating errors due to sample surface roughness in microwave complex permittivity measurements obtained using a coaxial probe. Electron. Lett. 31, 115.

Asadi, M., 2006. Beet-sugar handbook. John Wiley & Sons, New Jersey.

Assawarachan, R., Noomhorm, A., 2011. Mathematical models for vacuum-microwave concentration behavior of pineapple juice. J. Food Process Eng. 34, 1485–1505.

Atuonwu, J.C., Tassou, S.A., 2018. Quality assurance in microwave food processing and the enabling potentials of solid-state power generators: A review. J. Food Eng. 234, 1–15.

Augusto, P.E.D., Cristianini, M., 2011. Determining the convective heat transfer coefficient (h) in thermal process of foods. Int. J. Food Eng.

Augusto, P.E.D., Ibarz, R., Garvín, A., Ibarz, A., 2015. Peroxidase (POD) and Polyphenol Oxidase (PPO) Photo-Inactivation in a Coconut Water Model Solution Using Ultraviolet (UV). Food Res. Int. 74, 151–159.

Augusto, P.E.D., Tribst, A. a. L., Cristianini, M., 2011. Thermal Inactivation of Lactobacillus Plantarum in a Model Liquid Food. J. Food Process Eng. 34, 1013–1027.

Ballard, T.S., Mallikarjunan, P., Zhou, K., O'Keefe, S., 2010. Microwave-assisted extraction of phenolic antioxidant compounds from peanut skins. Food Chem. 120, 1185–1192.

Benlloch-Tinoco, M., Igual, M., Rodrigo, D., Martínez-Navarrete, N., 2013. Comparison of microwaves and conventional thermal treatment on enzymes activity and antioxidant capacity of kiwifruit puree. Innov. Food Sci. Emerg. Technol. 19, 166–172.

Birla, S.L., Wang, S., Tang, J., Tiwari, G., 2008. Characterization of radio frequency heating of fresh fruits influenced by dielectric properties. J. Food Eng. 89, 390–398.

Bohr, H., Bohr, J., 2000. Microwave-enhanced folding and denaturation of globular proteins. Phys. Rev. E - Stat. Physics, Plasmas, Fluids, Relat. Interdiscip. Top. 61, 4310–4314.

Bozkir, H., Baysal, T., 2017a. Concentration of apple juice using a vacuum microwave evaporator as a novel technique: Determination of quality characteristics. J. Food Process Eng. 40, e12535.

Bozkir, H., Baysal, T., 2017b. Concentration of apple juice using a vacuum microwave evaporator as a novel technique: Determination of quality characteristics. J. Food Process Eng. e12535.

Cano, M.P., Hernandez, a., Ancos, B., 1997. High pressure and temperature effects on enzyme inactivation in strawberry and orange products. J. Food Sci. 62, 85–88.

Cañumir, J. a, Celis, J.E., de Bruijn, J., Vidal, L. V, 2002. Pasteurisation of Apple Juice by Using Microwaves. Leb. und-Technologie 35, 389–392.

Carter, R.G., 2011. Radio-frequency power generation, in: CAS - CERN Accelerator School:Course on High Power Hadron Machines. Bilbao, Spain.

Carvalho, A.S.L., Ferreira, B.S., Neves-Petersen, M.T., Petersen, S.B., Aires-Barros, M.R., Melo, E.P., 2007. Thermal denaturation of HRPA2: pH-dependent conformational changes. Enzyme Microb. Technol. 40, 696–703.

Cha, H.J., Jang, D.S., Jin, K.S., Choi, K.Y., 2017. Structural analyses combined with small-angle X-ray scattering reveals that the retention of heme is critical for maintaining the structure of horseradish peroxidase under denaturing conditions. Amino Acids 49, 715–723.

Chahbani, A., Fakhfakh, N., Balti, M.A., Mabrouk, M., Elhatmi, H., Zouari, N., Kechaou, N., 2018. Microwave drying effects on drying kinetics, bioactive compounds and antioxidant activity of green peas (Pisum sativum L.). Food Biosci. 25, 32–38.

Chandrasekaran, S., Ramanathan, S., Basak, T., 2013. Microwave Food Processing — A review. Food Res. Int. 52, 243–261.

Chang, B.S., Park, K.H., Lund, D.B., 1988. Thermal Inactivation Kinetics of Horseradish Peroxidase. J. Food Sci. 53, 920–923.

Chatterjee, S., Basak, T., Das, S.K., 2007. Microwave driven convection in a rotating cylindrical cavity: A numerical study. J. Food Eng. 79, 1269–1279.

Chee Loong, T., Idris, A., 2014. Rapid alkali catalyzed transesterification of microalgae lipids to biodiesel using simultaneous cooling and microwave heating and its optimization. Bioresour. Technol. 174, 311–315.

Chen, H., Tang, J., 2011. Computer Simulation for Microwave Heating 101–130.

Chen, J., Pitchai, K., Birla, S., Negahban, M., Jones, D., Subbiah, J., 2014. Heat and mass transport during microwave heating of mashed potato in domestic oven--model development, validation, and sensitivity analysis. J. Food Sci. 79, E1991-2004.

Chen, Z., Li, Y., Wang, L., Liu, S., Wang, K., Sun, J., Xu, B., 2016. Evaluation of the possible non-thermal effect of microwave radiation on the inactivation of wheat germ lipase. J. Food Process Eng. 1–11.

Cheng, Y., Sakai, N., Hanzawa, T., 1997. Effects of Dielectric Properties on Temperature Distributions in Food Model during Microwave Heating. Food Sci. Technol. Int. Tokyo 3, 324–328.

Choi, W., Lee, S.H., Kim, C.T., Jun, S., 2015. A finite element method based flow and heat transfer model of continuous flow microwave and ohmic combination heating for particulate foods. J. Food Eng. 149, 159–170.

Cinquanta, L., Albanese, D., Cuccurullo, G., Di Matteo, M., 2010. Effect on orange juice of batch pasteurization in an improved pilot-scale microwave oven. J. Food Sci. 75, 46–50.

Coronel, P., Simunovic, J., Sandeep, K.P., Kumar, P., 2008. Dielectric Properties of Pumpable Food Materials at 915 MHz. Int. J. Food Prop. 11, 508–518.

Cruz, R.M.S., Vieira, M.C., Silva, C.L.M., 2006. Effect of heat and thermosonication treatments on watercress (Nasturtium officinale) vitamin C degradation kinetics. J. Food Eng. 72, 8–15.

Cuccurullo, G., Giordano, L., Metallo, A., Cinquanta, L., 2017. Influence of mode stirrer and air renewal on controlled microwave drying of sliced zucchini. Biosyst. Eng. 158, 95–101.

Curet, S., Begnini, F.B., Rouaud, O., Boillereaux, L., 2015. Modeling Microwave Heating During Batch Processing of Liquid Sample in a Single Mode Cavity. 2015 COMSOL Conf.

Curet, S., Rouaud, O., Boillereaux, L., 2008. Microwave tempering and heating in a single-mode cavity: Numerical and experimental investigations. Chem. Eng. Process. Process Intensif. 47, 1656–1665.

Dahmoune, F., Nayak, B., Moussi, K., Remini, H., Madani, K., 2015. Optimization of microwave-assisted extraction of polyphenols from Myrtus communis L. leaves. Food Chem. 166, 585–595.

Datta, a. K., Davidson, P.M., 2000. Special Supplement Kinetics of Microbial Inactivation for Alternative Food Processing Technologies (Microwave and Radio Frequency Processing).pdf. J. Food Sci.

Datta, A.K., 2001. Fundamentals of heat and moisture transport for microwaveable food

180

product and process development, in: Datta, A.K., Anantheswaran, R.C. (Eds.), Handbook of Microwave Technology for Food Applications. Marcel Dekker, New York, NY, pp. 115–172.

Datta, A.K., Sumnu, G., Raghavan, G.S. V., 2005. Dielectric Properties of Foods, in: Rao, M.A., Rizvi, S.S.H., Datta, A.K. (Eds.), Engineering Properties of Foods. CRC Press, Boca Raton, FL, pp. 501–565.

Davis, J.R. (Ed.), 2001. ASM specialty handbook: copper and copper alloys. ASM International, Materials Park, Ohio.

De Levie, R., 2004. Advanced Excel for scientific data analysis. Oxford University Press, New York.

De Pomerai, D.I., Smith, B., Dawe, A., North, K., Smith, T., Archer, D.B., Duce, I.R., Jones, D., Candido, E.P.M., 2003. Microwave radiation can alter protein conformation without bulk heating. FEBS Lett. 543, 93–97.

Debye, P., 1929. Polar Molecules. The Chemical Catalog Co., New York.

Dibben, D., 2001. Electromagnetics: fundamental aspects and numerical modeling, in: Datta, A.K., Anantheswaran, R.C. (Eds.), Handbook of Microwave Technology for Food Applications. Marcel Dekker, New York, NY, pp. 1–28.

Dorantes-Alvarez, L., Parada-Dorantes, L., 2005. Blanching using microwave processing, in: Schubert, H., Regier, M. (Eds.), The Microwave Processing of Foods. CRC Press, Boca Raton, FL, pp. 153–173.

Dreyfuss, M.S., Chipley, J.R., 1980. Comparison of effects of sublethal microwave radiation and conventional heating on the metabolic activity of Staphylococcus aureus. Appl. Environ. Microbiol. 39, 13–16.

Elez-Martinez, P., Aguiló-Aguayo, I., Martín-Belloso, O., 2008. Inactivation of tomato juice peroxidase by high-intensity pulsed electric fields as affected by process conditions. Food Chem. 107, 949–955.

Ercan, S.Ş., Soysal, Ç., 2011. Effect of ultrasound and temperature on tomato peroxidase. Ultrason. Sonochem. 18, 689–695.

Favreau, D., Sosle, V., Raghavan, G.S.V., 1997. Dielectric properties of maple sap and syrup at 2.45 GHz. J. Microw. Power Electromagn. Energy 32, 96–100.

Figura, L.O., Teixeira, A.A., 2007. Food physics: physical properties – measurement and applications, 1st ed. Springer-Verlag Berlin Heidelberg, Berlin.

Franco, A.P., Yamamoto, L.Y., Tadini, C.C., Gut, J. a. W., 2015. Dielectric properties of green coconut water relevant to microwave processing: Effect of temperature and field frequency. J. Food Eng. 155, 69–78.

Fujikawa, H., Itoh, T., 1996. Characteristics of a multicomponent first-order model for thermal inactivation of microorganisms and enzymes. Int. J. Food Microbiol. 31, 263–271.

Gabriel, C., Gabriel, S., H. Grant, E., H. Grant, E., S. J. Halstead, B., Michael P. Mingos, D., 1998. Dielectric parameters relevant to microwave dielectric heating. Chem. Soc. Rev. 27, 213.

Galvin, M.J., Parks, D.L., McRee, D.I., 1981. Influence of 2.45 GHz microwave radiation on enzyme activity. Radiat. Environ. Biophys. 19, 149–156.

García, a., Torres, J.L., Prieto, E., De Blas, M., 2001. Dielectric properties of grape juice at 0.2 and 3 GHz. J. Food Eng. 48, 203–211.

Giner, J., Grouberman, P., Gimeno, V., Martín, O., 2005. Reduction of pectinesterase activity in a commercial enzyme preparation by pulsed electric fields: Comparison of inactivation kinetic models. J. Sci. Food Agric. 85, 1613–1621.

Gonçalves, E.M., Pinheiro, J., Abreu, M., Brandão, T.R.S., Silva, C.L.M., 2007. Modelling the kinetics of peroxidase inactivation, colour and texture changes of pumpkin (Cucurbita maxima L.) during blanching. J. Food Eng. 81, 693–701.

Gunasekaran, S., Yang, H.W., 2007. Effect of experimental parameters on temperature distribution during continuous and pulsed microwave heating. J. Food Eng. 78, 1452–1456.

Güneş, B., Bayindirli, A., 1993. Peroxidase and lipoxygenase inactivation during blanching of green beans, green peas and carrots. LWT - Food Sci. Technol.

Guo, Q., Sun, D.W., Cheng, J.H., Han, Z., 2017. Microwave processing techniques and their recent applications in the food industry. Trends Food Sci. Technol. 67, 236–247.

Guo, W., Zhu, X., Liu, H., Yue, R., Wang, S., 2010. Effects of milk concentration and freshness on microwave dielectric properties. J. Food Eng. 99, 344–350.

Guo, W., Zhu, X., Nelson, S.O., Yue, R., Liu, H., Liu, Y., 2011. Maturity effects on dielectric properties of apples from 10 to 4500 MHz. LWT - Food Sci. Technol. 44, 224–230.

Hagan, M.T., Demuth, H.B., Beale, M.H., 1996. Neural network design. PWS Publishing Co., Boston.

Halpin, B., Pressey, R., Jen, J., Mondy, N., 1989. Purification and Characterization of Peroxidase Isoenzymes from Green Peas (Pisum sativum). J. Food Sci. 54, 644–649.

Hamoud-Agha, M.M., Curet, S., Simonin, H., Boillereaux, L., 2013. Microwave inactivation of Escherichia coli K12 CIP 54.117 in a gel medium: Experimental and numerical study. J. Food Eng. 116, 315–323.

Haykin, S., 1999. Neural Networks: a Comprehensive Foundation, 2nd ed. Prentice Hall, New Jersey.

Haynes, W.M. (Ed.), 2014. CRC Handbook of chemistry and physics, 95th ed. CRC Press, Boca Raton.

Hernández-Pérez, J.A., García-Alvarado, M.A., Trystram, G., Heyd, B., 2004. Neural networks for the heat and mass transfer prediction during drying of cassava and mango. Innov. Food Sci. Emerg. Technol. 5, 57–64.

Honig, P., 1953. Principles of sugar technology. Elsevier, Amsterdam.

Huang, K., Yang, X., Hua, W., Jia, G., Yang, L., 2009. Experimental evidence of a microwave non-thermal effect in electrolyte aqueous solutions. New J. Chem. 33, 1486–1489.

Huang, Y., Sheng, J., Yang, F., Hu, Q., 2007. Effect of enzyme inactivation by microwave and oven heating on preservation quality of green tea. J. Food Eng. 78, 687–692.

İçier, F., Baysal, T., 2004a. Dielectrical Properties of Food Materials—1: Factors Affecting and Industrial Uses. Crit. Rev. Food Sci. Nutr. 44, 465–471.

İçier, F., Baysal, T., 2004b. Dielectrical Properties of Food Materials—2: Measurement Techniques. Crit. Rev. Food Sci. Nutr. 44, 473–478.

Incropera, F.P., DeWitt, D.P., Bergman, T.L., Lavine, A.S., 2007. Fundamentals of heat and mass transfer, 6th ed. John Wiley & Sons, New York.

Joffe, F.M., Ball, C.O., 1962. Kinetics and Energetics of Thermal Inactivation and the Regeneration Rates of a Peroxidase System. J. Food Sci. 27, 587–592.

John, P., Califano, A., Santos, V., 2017. Kinetic Parameters for the Thermal Inactivation of Peroxidase and Lipoxygenase in Precooked Frozen Brassica Species. J. Food Sci. 00, 1–9.

Kaimainen, M., Laaksonen, O., Järvenpää, E., Sandell, M., Huopalahti, R., 2015. Consumer acceptance and stability of spray dried betanin in model juices. Food Chem. 187, 398–406.

Kermasha, S., Bisakowski, B., Ramaswamy, H., van de Voort, F., 1993a. Comparison of microwave, conventional and combination heat treatments on wheat germ lipase activity. Int. J. Food Sci. Technol. 28, 617–623.

Kermasha, S., Bisakowski, B., Ramaswamy, H., Van de Voort, F.R., 1993b. Thermal and microwave inactivation of soybean lipoxygenase. LWT - Food Sci. Technol.

Khaled, D. El, Castellano, N.N., Gázquez, J.A., Perea-Moreno, A.J., Manzano-Agugliaro, F., 2016. Dielectric spectroscopy in biomaterials: Agrophysics. Materials (Basel). 9, 1–26.

Kim, W.J., Park, S.H., Kang, D.H., 2018. Inactivation of foodborne pathogens influenced by dielectric properties, relevant to sugar contents, in chili sauce by 915 MHz microwaves. Lwt 96, 111–118.

Klinbun, W., Rattanadecho, P., 2016. Investigation into heat transfer and fluid flow characteristics of liquid two-layer and emulsion in microwave processing. Int. Commun. Heat Mass Transf. 70, 115–126.

Knoerzer, K., Regier, M., Erle, U., Pardey, K.K., Schubert, H., 2004. Development of a model food for microwave processing and the prediction of its physical properties. J. Microw. Power Electromagn. Energy 39, 167–177.

Knoerzer, K., Regier, M., Schubert, H., 2011. Simulating and Measuring Transient Three - Dimensional Temperature Distributions in Microwave Processing, in: Knoerzer, K., Juliano, P., Roupas, P., Versteeg, C. (Eds.), Innovative Food Processing Technologies: Advances in Multiphysics Simulation. John Wiley & Sons, Ltd. and Institute of Food Technologists, West Sussex, UK, pp. 131–153.

Knoerzer, K., Regier, M., Schubert, H., 2005. Simulation of microwave heating processes, in: Schubert, H., Regier, M. (Eds.), The Microwave Processing of Foods. CRC Press, Boca Raton, FL, pp. 317–333.

Komarov, V., Wang, S., Tang, J., 2005. Permittivity and Measurements. Encycl. RF Microw. Eng. 3693–3711.

Kozempel, M., Cook, R.D., Scullen, O.J., Annous, B.A., 2000. Nonthermal Effects of Microwave Energy on Microorganisms At Low Temperature '. J. Food Process. Preserv. 287–301.

Kuang, W., Nelson, S., 1998. Low-frequency Dielectric Properties of Biological Tissues: A Review with Some New Insights. Trans. ASAE 41, 173–184.

Kubo, M.T.K., Curet, S., Augusto, P.E.D., Boillereaux, L., 2018a. Artificial Neural Network for prediction of dielectric properties relevant to microwave processing of fruit juice. J. Food Process Eng. In press.

Kubo, M.T.K., Rojas, M.L., Curet, S., Boillereaux, L., Augusto, P.E.D., 2018b. Peroxidase inactivation kinetics is affected by the addition of calcium chloride in fruit beverages. LWT - Food Sci. Technol. 89, 610–616.

Kurniawan, H., Alapati, S., Che, W.S., 2015. Effect of mode stirrers in a multimode microwave-heating applicator with the conveyor belt. Int. J. Precis. Eng. Manuf. - Green Technol. 2, 31–36.

Labus, K., Bryjak, J., Polakovič, M., 2015. Kinetics of thermal inactivation of immobilized Agaricus bisporus tyrosinase. J. Mol. Catal. Enzym. B Enzym. 120, 136–140.

Latorre, M.E., Bonelli, P.R., Rojas, A.M., Gerschenson, L.N., 2012. Microwave inactivation of red beet (Beta vulgaris L. var. conditiva) peroxidase and polyphenoloxidase and the effect of radiation on vegetable tissue quality. J. Food Eng. 109, 676–684.

Lemos, M.A., Oliveira, J.C., Saraiva, J.A., 2000. Influence of pH on the thermal inactivation kinetics of horseradish peroxidase in aqueous solution. LWT - Food Sci. Technol. 33, 362–368.

Liao, X., Raghavan, G.S. V, Dai, J., Yaylayan, V.A., 2003. Dielectric properties of a - d -glucose aqueous solutions at 2450 MHz. Food Res. Int. 36, 485–490.

Lin, M., Ramaswamy, H.S., 2011. Evaluation of phosphatase inactivation kinetics in milk under continuous flow microwave and conventional heating conditions. Int. J. Food Prop. 14, 110–123.

Ling, A.., Lund, D.., 1978. Determining kinetic parameters for thermal inactivation of heat-resistant and heat- labile isozymes from thermal destruction curves. J. Food Sci. 43, 1307–1310.

Liu, C.M., Wang, Q.Z., Sakai, N., 2005. Power and temperature distribution during microwave thawing, simulated by using Maxwell's equations and Lambert's law. Int. J. Food Sci. Technol. 40, 9–21.

Liu, S., Fukuoka, M., Sakai, N., 2013. A finite element model for simulating temperature distributions in rotating food during microwave heating. J. Food Eng. 115, 49–62.

Liu, W., Zou, L.Q., Liu, J.P., Zhang, Z.Q., Liu, C.M., Liang, R.H., 2013. The effect of citric acid on the activity, thermodynamics and conformation of mushroom polyphenoloxidase. Food Chem. 140, 289–295.

Liu, Y., Tang, J., Mao, Z., 2009. Analysis of bread loss factor using modified Debye equations. J. Food Eng. 93, 453–459.

Lopes, L.C., Barreto, M.T.M., Gonçalves, K.M., Alvarez, H.M., Heredia, M.F., de Souza, R.O.M. a, Cordeiro, Y., Dariva, C., Fricks, A.T., 2015. Stability and structural changes of horseradish peroxidase: microwave versus conventional heating treatment. Enzyme Microb. Technol. 69, 10–8.

Lu, A.T., Whitaker, J.R., 1974. Some Factors Affecting Rates of Heat Inactivation and

Reactivation of Horseradish Peroxidase. J. Food Sci. 39, 1173–1178.

Luter, L., Wyslouzil, W., Kashyap, S.C., 1982. The Destruction of Aflatoxins in Peanuts by Microwave Roasting. Can. Inst. Food Sci. Technol. J. 15, 236–238.

Ly-Nguyen, B., Van Loey, a M., Smout, C., ErenÖzcan, S., Fachin, D., Verlent, I., Truong, S.V., Duvetter, T., Hendrickx, M.E., 2003. Mild-Heat and High-Pressure Inactivation of Carrot Pectin Methylesterase: A Kinetic Study. J. Food Sci. 68, 1377–1383.

Machado, M.F., Saraiva, J., 2002. Inactivation and reactivation kinetics of horseradish peroxidase in phosphate buffer and buffer-dimethylformamide solutions. J. Mol. Catal. B Enzym. 19–20, 451–457.

Marić, M., Grassino, A.N., Zhu, Z., Barba, F.J., Brnčić, M., Rimac Brnčić, S., 2018. An overview of the traditional and innovative approaches for pectin extraction from plant food wastes and by-products: Ultrasound-, microwaves-, and enzyme-assisted extraction. Trends Food Sci. Technol. 76, 28–37.

Marshall, M.R., Marcy, J.E., Braddock, R.J., 1985. Effect of Total Solids Level on Heat Inactivation of Pectinesterase in Orange Juice. J. Food Sci. 50, 220–222.

Marszałek, K., Krzyżanowska, J., Woźniak, Skąpska, S., 2016. Kinetic modelling of tissue enzymes inactivation and degradation of pigments and polyphenols in cloudy carrot and celery juices under supercritical carbon dioxide. J. Supercrit. Fluids 117, 26–32.

Marszałek, K., Mitek, M., Skąpska, S., 2015. Effect of Continuous Flow Microwave and Conventional Heating on the Bioactive Compounds, Colour, Enzymes Activity, Microbial and Sensory Quality of Strawberry Purée. Food Bioprocess Technol. 8, 1864–1876.

Mathlouthi, M., Reiser, P. (Eds.), 1995. Sucrose: properties and applications. Springer US.

Matsui, K.N., Granado, L.M., de Oliveira, P.V., Tadini, C.C., 2007. Peroxidase and polyphenol oxidase thermal inactivation by microwaves in green coconut water simulated solutions. LWT - Food Sci. Technol. 40, 852–859.

Matsui, K.N., Gut, J.A.W., de Oliveira, P.V., Tadini, C.C., 2008. Inactivation kinetics of polyphenol oxidase and peroxidase in green coconut water by microwave processing. J. Food Eng. 88, 169–176.

McIlvaine, T.C., 1921. A buffer solution for colorimetric comparison. J. Biol. Chem. 183–186.

Meda, V., Orsat, V., Raghavan, V., 2005. Microwave heating and the dielectric properties of foods, The Microwave Processing of Foods. Woodhead Publishing Limited.

Midi, N.S., Sasaki, K., Ohyama, R., Shinyashiki, N., 2014. Broadband complex dielectric constants of water and sodium chloride aqueous solutions with different DC conductivities. IEEJ Trans. Electr. Electron. Eng. 9, S8–S12.

Monteiro, R.L., Link, J. V., Tribuzi, G., Carciofi, B.A.M., Laurindo, J.B., 2018. Microwave vacuum drying and multi-flash drying of pumpkin slices. J. Food Eng. 232, 1–10.

Morales-Blancas, E., Chandia, V., Cisneros-Zevallos, L., 2002. Thermal inactivation kinetics of peroxidase and lipoxygenase from broccoli, green asparagus and carrots. J. Food Sci. 67, 146–154.

Mudgett, R.E., 1986. Electrical properties of foods, in: Rao, M.A., Rizvi, S.S.H. (Eds.), Engineering Properties of Foods. Marcel Dekker, New York, p. 398.

Murasaki-Aliberti, N.D.C., Da Silva, R.M.S., Gut, J. a W., Tadini, C.C., 2009. Thermal inactivation of polyphenoloxidase and peroxidase in green coconut (Cocos nucifera) water. Int. J. Food Sci. Technol. 44, 2662–2668.

Nelson, S.O., Datta, A.K., 2001. Dielectric properties of food materials and electric field interactions, in: Datta, A.K., Anantheswaran, R.C. (Eds.), Handbook of Microwave Technology for Food Applications. Marcel Dekker, New York, NY, pp. 69–114.

Nienaber, U., Shellhammer, T.H., 2001. High-pressure processing of orange Juice : kinetics of pectinmethylesterase inactivation. J. Food Sci. 66, 332–336.

Nikdel, S., Mackellar, D.G., 1992. A microwave system for continuous pasteurization of orange juice. Proc. Florida State Hortic. Soc. 105, 108–110.

Norton, T., Sun, D.-W., 2006. Computational fluid dynamics (CFD) – an effective and efficient design and analysis tool for the food industry: A review. Trends Food Sci. Technol. 17, 600–620.

Oliveira, M.E.C., Franca, a. S., 2002. Microwave heating of foodstuffs. J. Food Eng. 53, 347–

359.

Peleg, M., Cole, M.B., 1998. Reinterpretation of microbial survival curves reinterpretation of microbial survival curves. Crit. Rev. Food Sci. Nutr. 38, 353–380.

Pérez-Grijalva, B., Herrera-Sotero, M., Mora-Escobedo, R., Zebadúa-García, J.C., Silva-Hernández, E., Oliart-Ros, R., Pérez-Cruz, C., Guzmán-Gerónimo, R., 2018. Effect of microwaves and ultrasound on bioactive compounds and microbiological quality of blackberry juice. LWT - Food Sci. Technol. 87, 47–53.

Petruzzi, L., Campaniello, D., Speranza, B., Corbo, M.R., Sinigaglia, M., Bevilacqua, A., 2017. Thermal Treatments for Fruit and Vegetable Juices and Beverages: A Literature Overview. Compr. Rev. Food Sci. Food Saf. 16, 668–691.

Połata, H., Wilińska, A., Bryjak, J., Polakovič, M., 2009. Thermal inactivation kinetics of vegetable peroxidases. J. Food Eng. 91, 387–391.

Prosetya, H., Datta, A., 1991. Batch microwave heating of liquids. An experimental study. J. Microw. Power Electromagn. Energy 26, 215–226.

Ramaswamy, H.S., Koutchma, T., Tajchakavit, S., 2002. Enhanced thermal effects under microwave heating conditions, in: Welti-Chanes, J., Barbosa-Cánovas, G.V., Aguilera, J.M. (Eds.), Engineering and Food for the 21st Century. CRC Press, Boca Raton, FL.

Ratanadecho, P., Aoki, K., Akahori, M., 2002. A numerical and experimental investigation of the modeling of microwave heating for liquid layers using a rectangular wave guide (effects of natural convection and dielectric properties). Appl. Math. Model. 26, 449–472.

Regier, M., Schubert, H., 2005. Introducing microwave processing of food: principles and technologies, in: Schubert, H., Regier, M. (Eds.), The Microwave Processing of Foods. CRC Press, Boca Raton, FL, pp. 3–21.

Ren, G., Chen, F., 1998. Drying of American ginseng (Panax quinquefolium) roots by microwave-hot air combination. J. Food Eng. 35, 433–443.

Riahi, E., Ramaswamy, H.S., 2004. High pressure inactivation kinetics of amylase in apple juice. J. Food Eng. 64, 151–160.

Rodrigo, C., Rodrigo, M., Alvarruiz, A., Frigola, A., 1997. Inactivation and Regeneration Kinetics of Horseradish Peroxidase Heated at High Temperatures. J. Food Prot. 60, 961–966.

Roebuck, B.D., Goldblith, S. a, Westphal, W.B., 1972. Dielectric Properties of Carbohydrate-Water Mixtures At Microwave Frequencies. J. Food Sci. 37, 199–204.

Rojas, M.L., Trevilin, J.H., Funcia, E. dos S., Gut, J.A.W., Augusto, P.E.D., 2017. Using ultrasound technology for the inactivation and thermal sensitization of peroxidase in green coconut water. Ultrason. Sonochem. 36, 173–181.

Romano, V.R., Marra, F., Tammaro, U., 2005. Modelling of microwave heating of foodstuff: study on the influence of sample dimensions with a FEM approach. J. Food Eng. 71, 233–241.

Rougier, C., Prorot, A., Chazal, P., Leveque, P., Leprat, P., 2014. Thermal and nonthermal effects of discontinuous microwave exposure (2.45 Gigahertz) on the cell membrane of Escherichia coli. Appl. Environ. Microbiol. 80, 4832–4841.

Rudra Shalini, G., Shivhare, U.S., Basu, S., 2008. Thermal inactivation kinetics of peroxidase in mint leaves. J. Food Eng. 85, 147–153.

Rumelhart, D.E., Hinton, G.E., Williams, R.J., 1986. Learning internal representations by error propagation, in: Rumelhart, D.E., McClelland, J.L. (Eds.), Parallel Distributed Processing: Explorations in the Microstructure of Cognition. Cambridge, pp. 318–362.

Ryyniinen, S., 1995. The Electromagnetic Properties of Food Materials : A Review of the Basic Principles. J. Food Eng.

Salazar-González, C., Martín-González, M.F.S., López-Malo, A., Sosa-Morales, M.E., 2012. Recent Studies Related to Microwave Processing of Fluid Foods. Food Bioprocess Technol. 5, 31–46.

Salvi, D., Boldor, D., Aita, G.M., Sabliov, C.M., 2011. COMSOL Multiphysics model for continuous flow microwave heating of liquids. J. Food Eng. 104, 422–429.

Salvi, D., Ortego, J., Arauz, C., Sabliov, C.M., Boldor, D., 2009. Experimental study of the effect of dielectric and physical properties on temperature distribution in fluids during

continuous flow microwave heating. J. Food Eng. 93, 149–157.

Sampedro, F., Fan, X., 2014. Inactivation kinetics and photoreactivation of vegetable oxidative enzymes after combined UV-C and thermal processing. Innov. Food Sci. Emerg. Technol. 23, 107–113.

Schiffmann, R.F., 2001. Microwave processes for the food industry, in: Datta, A.K., Anantheswaran, R.C. (Eds.), Handbook of Microwave Technology for Food Applications. Marcel Dekker, New York, NY, pp. 299–353.

Scott, G., Richardson, P., 1997. The application of computational fluid dynamics in the food industry. Trends Food Sci. Technol. 8, 119–124.

Shah, N.P., Ding, W.K., Fallourd, M.J., Leyer, G., 2010. Improving the stability of probiotic bacteria in model fruit juices using vitamins and antioxidants. J. Food Sci. 75, 278–282.

Shamis, Y., Croft, R., Taube, A., Crawford, R.J., Ivanova, E.P., 2012. Review of the specific effects of microwave radiation on bacterial cells. Appl. Microbiol. Biotechnol. 96, 319–325.

Shamis, Y., Taube, A., Mitik-Dineva, N., Croft, R., Crawford, R.J., Ivanova, E.P., 2011. Specific electromagnetic effects of microwave radiation on Escherichia coli. Appl. Environ. Microbiol. 77, 3017–3022.

Shazman, A., Mizrahi, S., Cogan, U., Shimoni, E., 2007. Examining for possible non-thermal effects during heating in a microwave oven. Food Chem. 103, 444–453.

Siguemoto, É.S., Funcia, E. dos S., Pires, M.N., Gut, J.A.W., 2018a. Modeling of time-temperature history and enzymatic inactivation of cloudy apple juice in continuous flow microwave assisted pasteurization. Food Bioprod. Process. 111, 45–53.

Siguemoto, É.S., Gut, J.A.W., 2016. Dielectric Properties of Cloudy Apple Juices Relevant to Microwave Pasteurization. Food Bioprocess Technol. 9, 1345–1357.

Siguemoto, É.S., Gut, J.A.W., Martinez, A., Rodrigo, D., 2017. Inactivation kinetics of Escherichia coli O157:H7 and Listeria monocytogenes in apple juice by microwave and conventional thermal processing. Innov. Food Sci. Emerg. Technol.

Siguemoto, É.S., Pereira, L.J., Gut, J.A.W., 2018b. Inactivation Kinetics of Pectin Methylesterase, Polyphenol Oxidase, and Peroxidase in Cloudy Apple Juice under Microwave and Conventional Heating to Evaluate Non-Thermal Microwave Effects. Food Bioprocess Technol. 1–11.

Silva, F.A., Marsaioli, A., Maximo, G.J., Silva, M.A.A.P., Gonçalves, L.A.G., 2006. Microwave assisted drying of macadamia nuts. J. Food Eng. 77, 550–558.

Simić, V.M., Rajković, K.M., Stojičević, S.S., Veličković, D.T., Nikolić, N.Č., Lazić, M.L., Karabegović, I.T., 2016. Optimization of microwave-assisted extraction of total polyphenolic compounds from chokeberries by response surface methodology and artificial neural network. Sep. Purif. Technol. 160, 89–97.

Sosa-Morales, M.E., Valerio-Junco, L., López-Malo, a., García, H.S., 2010. Dielectric properties of foods: Reported data in the 21st Century and their potential applications. LWT - Food Sci. Technol. 43, 1169–1179.

Soysal, Ç., Söylemez, Z., 2005. Kinetics and inactivation of carrot peroxidase by heat treatment. J. Food Eng. 68, 349–356.

Stanciuc, N., Aprodu, I., Ioniţa, E., Bahrim, G., Râpeanu, G., 2015. Exploring the process-structure-function relationship of horseradish peroxidase through investigation of pH- and heat induced conformational changes. Spectrochim. Acta - Part A Mol. Biomol. Spectrosc. 147, 43–50.

Stratakos, A.C., Delgado-Pando, G., Linton, M., Patterson, M.F., Koidis, A., 2016. Industrial scale microwave processing of tomato juice using a novel continuous microwave system. Food Chem. 190, 622–628.

Taher, B.J., Farid, M.M., 2001. Cyclic microwave thawing of frozen meat: Experimental and theoretical investigation. Chem. Eng. Process. 40, 379–389.

Tajchakavit, S., 1997. Continuous-flow microwave hating of orange juice: evidence of non-thermal effects. McGill University.

Tajchakavit, S., Ramaswamy, H.S., 1997. Continuous-Flow Microwave Inactivation Kinetics of Pectin Methyl Esterase in Orange Juice. J. Food Process. Preserv. 21, 365–378.

Tajchakavit, S., Ramaswamy, H.S., 1995. Continuous-flow microwave heating of orange juice:

evidence of nonthermal effects. J. Miicrowave Power Electromagn. Energy.

Tamura, Y., Morita, Y., 1975. Thermal denaturation and regeneration of Japanese-radish peroxidase. J. Biochem. 78, 561–571.

Tan, T.C., Cheng, L.H., Bhat, R., Rusul, G., Easa, A.M., 2014. Composition, physicochemical properties and thermal inactivation kinetics of polyphenol oxidase and peroxidase from coconut (Cocos nucifera) water obtained from immature, mature and overly-mature coconut. Food Chem. 142, 121–128.

Tang, J., 2015. Unlocking Potentials of Microwaves for Food Safety and Quality. J. Food Sci. 80, E1776–E1793.

Telis, V.R.N., Telis-Romero, J., Mazzotti, H.B., Gabas, A.L., 2007. Viscosity of aqueous carbohydrate solutions at different temperatures and concentrations. Int. J. Food Prop. 10, 185–195.

Terefe, N.S., Delon, A., Versteeg, C., 2017. Thermal and high pressure inactivation kinetics of blueberry peroxidase. Food Chem. 232, 820–826.

Thongsook, T., Barrett, D.M., 2005. Heat inactivation and reactivation of broccoli peroxidase. J. Agric. Food Chem. 53, 3215–3222.

Tulasidas, T.N., Raghavan, G.S., van de Voort, F., Girard, R., 1995. Dielectric properties of grapes and sugar solutions at 2.45 GHz. J. Microw. Power Electromagn. Energy 30, 117–123.

Tuta, S., Palazoglu, T.K., 2017. Finite element modeling of continuous-flow microwave heating of fluid foods and experimental validation. J. Food Eng. 192, 79–92.

Vadivambal, R., Jayas, D.S., 2010. Non-uniform Temperature Distribution During Microwave Heating of Food Materials—A Review. Food Bioprocess Technol. 3, 161–171.

Van Boekel, M.A.J.S., 2002. On the use of the Weibull model to describe thermal inactivation of microbial vegetative cells. Int. J. Food Microbiol. 74, 139–159.

Venkatesh, M.S., Raghavan, G.S.V., 2004. An Overview of Microwave Processing and Dielectric Properties of Agri-food Materials. Biosyst. Eng. 88, 1–18.

Vilayannur, R.S., Puri, V.M., Anantheswaran, R.C., 1998. Size and shape effect on nonuniformity of temperature and moisture distributions in microwave heated food materials: Part II experimental validation. J. Food Process Eng. 21, 235–248.

Villamiel, M., del Castillo, M.D., Martín, C.S., Corzo, N., 1998. Assessment of the thermal treatment of orange juice during continuous microwave and conventional heating. J. Sci. Food Agric. 196–200.

Wang, J., Tang, J., Wang, Y., Swanson, B., 2009. Dielectric properties of egg whites and whole eggs as influenced by thermal treatments. LWT - Food Sci. Technol. 42, 1204–1212.

Wawire, M., Oey, I., Mathooko, F.M., Njoroge, C.K., Shitanda, D., Hendrickx, M., 2016. Kinetics of thermal inactivation of peroxidase and color degradation of African Cowpea (Vigna unguiculata) leaves. J. Food Sci. 81, E56–E64.

Welt, B.A., Tong, C.H., Rossen, J.L., Lund, D.B., 1994. Effect of microwave radiation on inactivation of Clostridium sporogenes (PA 3679) spores. Appl. Environ. Microbiol. 60, 482–488.

Xanthakis, E., Le-Bail, a., Ramaswamy, H., 2014. Development of an innovative microwave assisted food freezing process. Innov. Food Sci. Emerg. Technol. 26, 176–181.

Xu, B., Wang, L.K., Miao, W.J., Wu, Q.F., Liu, Y.X., Sun, Y., Gao, C., 2016. Thermal versus microwave inactivation kinetics of lipase and lipoxygenase from wheat germ. J. Food Process Eng. 39, 247–255.

Yang, H.W., Gunasekaran, S., 2004. Comparison of temperature distribution in model food cylinders based on Maxwell's equations and Lambert's law during pulsed microwave heating. J. Food Eng. 64, 445–453.

Ye, J., Hong, T., Wu, Y., Wu, L., Liao, Y., Zhu, H., Yang, Y., Huang, K., 2017. Model stirrer based on a multi-material turntable for microwave processing materials. Materials (Basel). 10, 1–13

Yeong, S.P., Law, M.C., Vincent Lee, C.C., Chan, Y.S., 2017. Modelling batch microwave heating of water. IOP Conf. Ser. Mater. Sci. Eng. 217.

Yin, C., 2012. Microwave-assisted pyrolysis of biomass for liquid biofuels production. Bioresour

Technol 120, 273–284.

Yu, B., Jin, Z., Deng, L., Xu, X., He, L., Wang, J., Tian, Y., Chen, H., 2010. Kinetic study of thermal inactivation of potato peroxidase during high-temperature short-time processing. J. Food Sci. Technol. 47, 67–72.

Zhang, Q., Jackson, T.H., Ungan, A., 2000. Numerical modeling of microwave induced natural convection. Int. J. Heat Mass Transf. 43, 2141–2154.

Zhang, Y.L., Zeng, B.Q., Zhang, H., 2012. A 2.45GHz reentarnt coaxial cavity for liquid sterilization based on non-thermal microwave effect. Prog. Electromagn. Res. C 33, 145–156.

Zhou, L., Tey, C.Y., Bingol, G., Bi, J., 2016. Effect of microwave treatment on enzyme inactivation and quality change of defatted avocado puree during storage. Innov. Food Sci. Emerg. Technol. 37, 61–67. h

Zhu, J., Kuznetsov, a. V., Sandeep, K.P., 2007. Mathematical modeling of continuous flow microwave heating of liquids (effects of dielectric properties and design parameters). Int. J. Therm. Sci. 46, 328–341.

Zhu, X., Guo, W., Wu, X., 2012. Frequency- and temperature-dependent dielectric properties of fruit juices associated with pasteurization by dielectric heating. J. Food Eng. 109, 258–266.

Titre : Traitement thermique micro-onde de jus de fruits : modélisation multiphysique et inactivation enzymatique

Mots clés : Chauffage micro-ondes, Inactivation enzymatique, Propriétés diélectriques, Modélisation, Peroxydase

Résumé : Ce travail vise à étudier l'intérêt du chauffage micro-ondes pour l'inactivation des enzymes dans les jus de fruit, à travers des approches numériques et aussi expérimentales. En premier lieu, une étude sur les propriétés diélectriques des jus de fruits modèles est menée, démontrant leur forte sensibilité à la température, à la fréquence et à la composition du produit. Dans une seconde partie, l'inactivation de la peroxydase est étudiée par chauffage conventionnel et les données sont ajustées par un modèle cinétique du premier ordre. Dans la troisième et principale partie de ce travail, un modèle tridimensionnel, résolu par éléments finis, est proposé pour simuler le chauffage par micro-ondes du jus, en couplant électromagnétisme, transfert de chaleur et écoulement, avec la cinétique d'inactivation de la peroxydase précédemment déterminée.

Cette simulation permet de prédire la distribution spatiale de la température, le profil d'écoulement et l'inactivation de la peroxydase. L'accord entre le modèle et les expériences est très satisfaisant, ce qui confirme la pertinence de l'approche. Dans la dernière partie, les réactivations de la peroxydase après chauffage conventionnel et micro-ondes sont évaluées et comparées. Enfin, l'éventuelle existence d'effets non thermiques des micro-ondes est discutée via des expériences additionnelles. En conclusion, ces travaux montrent tout l'intérêt de la simulation numérique comme outil de compréhension du processus multiphysique du chauffage par micro-ondes pour l'inactivation des enzymes, ce qui peut être particulièrement intéressant pour la conception et l'optimisation de traitements micro-ondes.

Title : Thermal process of fruit juices using microwaves: multiphysics modelling and enzyme inactivation

Keywords : Microwave heating, Enzyme inactivation, Dielectric properties, Modeling, Peroxidase

Abstract : This work aims at studying the use of microwave heating for enzyme inactivation in fruit juices by means of numerical and experimental approaches. In the first part, a study on the dielectric properties of model fruit juices is conducted, evidencing their high dependence on the temperature, frequency and composition of the product. Then in the second part, the inactivation of peroxidase is studied using conventional heating and the data are fitted by a first order kinetic model. In the third and main part of this work, a three-dimensional finite element model is developed to simulate the microwave heating of juices, coupling electromagnetics, heat transfer and fluid flow as well as the peroxidase inactivation kinetics previously determined.

As a result, spatial temperature distribution, flow pattern and peroxidase inactivation are obtained. The model is experimentally validated and good agreement is observed, confirming the relevance of the approach. Finally, in the last part, the potential peroxidase reactivations after conventional and microwave heating are assessed and compared. Also, the possible existence of non-thermal effects of microwaves is discussed thanks to additional experimentations. In conclusion, this work shows the large interest of computer simulation as a tool for understanding the multiphysics process of microwave heating for enzyme inactivation, which can be particularly interesting for further design of optimized microwave processing.